E-Z isomerization in Suzuki cross coupling of 1, 2-dichlorovinyl phenyl ketone: Ligand effects in controlling selectivity and mechanistic studies for loss of stereochemical integrity.

by

Navneet Kaur Chehal

A Thesis submitted to the Faculty of Graduate Studies of

The University of Manitoba

in partial fulfilment of the requirements of the degree of

DOCTOR OF PHILOSOPHY

Department of Chemistry

University of Manitoba

Winnipeg, MB, R3T 2N2

List of figures

List of schemes

List of tables

Acknowledgements

I would like to take the opportunity to thank many individuals, without whom this journey would not have been possible. Firstly, I would like to thank my advisor, Dr. P.G. Hultin for his guidance, support and encouragement throughout my studies. He always had his door open for discussions pertaining to the chemistry. He always welcomed new ideas, encouraged them and always emphasized the need of the focus. I would also like to thank my advisory committee: Dr. Peter Budzelaar, Dr. John Sorensen, Dr. Geoff Tranmer and Dr. Jake Stout. I have received valuable comments and advice from all of them over the course of my project. I also appreciate guidance and help provided by Dr. Jason Hein for this project. I would also like to thank my external examiner, Dr. Jim Green (University of Windsor), for his careful reading and valuable comments on my thesis. I would also like to thank Dr. Kirk Marat for all the valuable discussions related to the NMR. I wish to express my special thanks to Dr. Peter Budzelaar. He has always been a great source of motivation, encouragement and inspiration. His enthusiasm for this project encouraged me to have discussions with him about the project.

Last but not the least, many thanks to my family and friends, who have supported me since the beginning of this challenging journey. Thank you for always being there!!

Abstract

While studying site selective palladium catalyzed Suzuki cross coupling on (***E***)-1,2-dichlorovinylphenyl ketone (***E*-1**), a loss of stereochemistry was observed in the cross coupled product. It was soon discovered that extent of the isomerized cross coupled product formed was dependent on the phosphine ligand employed in the Suzuki cross coupling reaction conditions. With the careful choice of the phosphine ligand, the reaction conditions were designed to form either retention Suzuki cross coupled product or isomerized Suzuki cross coupled product selectively. For example, the Suzuki cross coupling on ***E*-1** in the presence of DPEphos ligand gave 96% isomerized cross coupled product (***Z*-2**) whereas Suzuki cross coupling on ***E*-1** in the presence of *t*-Bu-Xantphos or no-phosphine ligand gave 94% retention cross coupled product (***E*-2**).

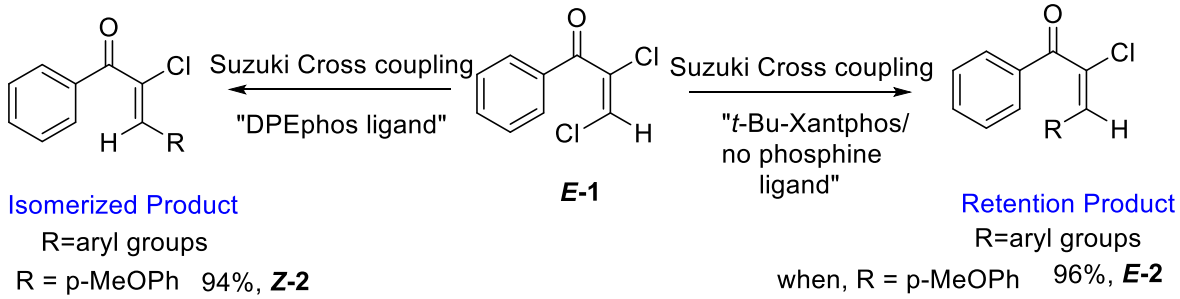

Scheme 1: Schematic representation of Suzuki cross coupling on E-1, 2-dichlorovinylphenyl ketone.

While studying the pathway by which the ***Z*-2** would form in the Suzuki cross coupling reaction, many well accepted pathways like thermal isomerization, photo-isomerization, reversible Michael addition of phosphines, isomerization due to intrinsic zwitterionic character of the vinyl palladium species, generation of palladium hydrides in the reaction conditions etc. were ruled out. It was found that ***E*-2** isomerizes to ***Z*-2** in the presence of *just* palladium catalyst. This observation along with other experimental results are well explained by a mechanism first

proposed by Canovese and Visentin for dimethyl maleate and bis(sulfonyl)ethane. According to this mechanism, an isomerization takes place by a mere coordination of the substrate to the palladium catalyst without any external promoter.

The isomerized outcome in the reactions is usually unwanted but the ability to supress or promote isomerization nearly completely is remarkable. The experimental data not only suggests that the isomerization takes place by a mere coordination of the Suzuki cross coupled product with palladium catalyst but also demonstrates that the Suzuki cross coupling reaction is indeed stereospecific in nature and that the isomerization occurs by a separate catalytic cycle. It was also observed that the presence of a single conjugated carbonyl group is sufficient to induce the isomerization. Based on this observation, one can expect isomerization in the substrates possessing an enone functionality. This is a significant observation as enone substrates are one of the important classes in the organic synthesis and prior knowledge of how these substrates can behave during Pd/phosphine catalyzed reactions is very useful.

List of Abbreviations

Pd	Palladium
[Pd]	Palladium catalyst
NaOH	Sodium Hydroxide
TBAHS	Tetrabutylammonium hydrogensulfate
TCE	Trichloroethylene
Et_2O	Diethyl ether
$CuSO_4$	Copper sulfate
THF	Tetrahydrofuran
$Pd(PPh_3)_4$	Tetrakis(triphenylphosphine)palladium(0)
aq.	Aqueous
K_2CO_3	Potassium carbonate
eq.	equivalent

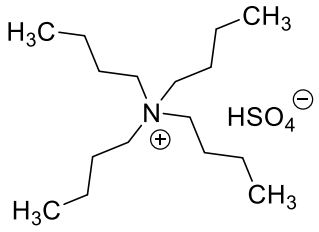

TBAHS

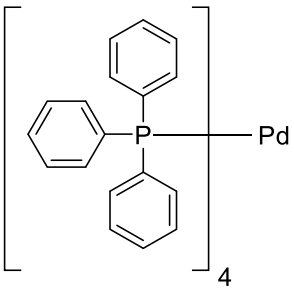

$Pd(PPh_3)_4$

M	Molar concentration (Molarity)
m/z	mass-to-charge ratio (gas chromatography)
min.	minute
h	hour
HCl	Hydrogen chloride
CO	Carbon monoxide
CH_2Cl_2	Dichloromethane (DCM)
O_3	Trioxygen (Ozone gas)
DMS	Dimethyl sulfide
NOE	Nuclear Overhauser effect
$CDCl_3$	Deuterochloroform
Ar	Aryl
ppm	parts-per-million
HMBC	Heteronuclear Multiple Bond Correlation
J	Coupling constant (NMR)
$^3J_{C,H}$	Three-bond Carbon-Proton (^{13}C-^1H) coupling
$^3J_{H,H}$	Three-bond Proton-Proton (^1H-^1H) coupling

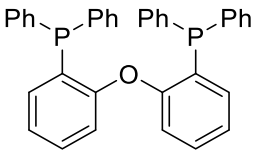

DPEphos

DPEphos	Bis[(2-diphenylphosphino)phenyl] ether
Cs_2CO_3	Cesium carbonate
CsF	Cesium fluoride
K_3PO_4	Tripotassium phosphate
$Pd_2(dba)_3$	Tris(dibenzylideneacetone)dipalladium (0)

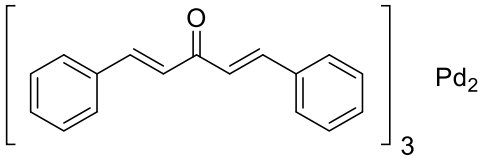

$Pd_2(dba)_3$

GC-MS	Gas chromatography – mass spectrometry

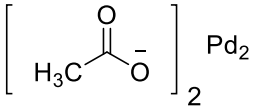

$Pd(OAc)_2$

$Pd(OAc)_2$	Palladium (II) acetate
$PdCl_2$	Palladium (II) chloride
Xantphos	4,5-Bis(diphenylphosphino)-9,9-dimethylxanthene

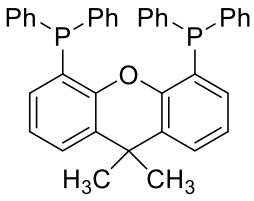

Xantphos

t-Bu-Xantphos	9,9-Dimethyl-4,5-bis(di-*tert*-phosphino)xanthene

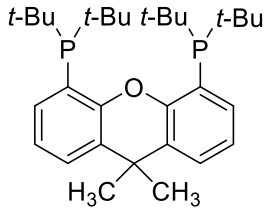

t-Bu-Xantphos

NMR	Nuclear magnetic resonance spectroscopy
HRMS	High-resolution mass spectrometry
HPLC	High performance liquid chromatography
TEMPO	2,2,6,6-Tetramethyl-1-piperidinyloxy
TMEDA	N,N,N′,N′-Tetramethylethylenediamine
DMPE	1,2-Bis(dimethylphosphino)ethane
kcal	kilocalorie
rt	room temperature
S-Phos	2-Dicyclohexylphosphino-2′,6′-dimethoxybiphenyl

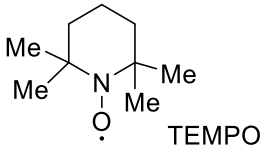

TEMPO

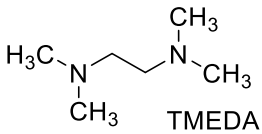

TMEDA

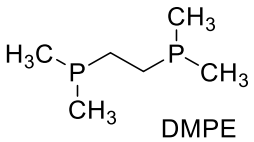

DMPE

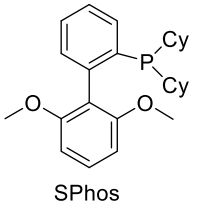

SPhos

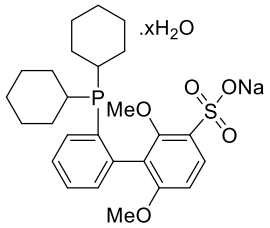

sSPhos

sSPhos	SPhos (water soluble)
K	kelvin (Temperature unit)
s	singlet
t	triplet
m	multiplet
gm	gram
mp	melting point
μL	microlitre
mL	millilitre
Hz	Hertz
δ	Chemical shift (NMR)
TLC	Thin-layer chromatography

CHAPTER-1: Background

1.1 Introduction

1.1.1. Palladium catalyzed C-C cross coupling reactions

The palladium-catalyzed cross-coupling is an indispensable tool in the formation of carbon–carbon bonds.[1] The cross-coupled product (**5**) is formed by a reaction between two components in the presence of palladium as a catalyst, an aryl/alkyl/vinyl halide (**3**) as an electrophilic component and a nucleophilic component (**4**) which depends on the specific class of cross-coupling being performed. There are some classes where the second coupling substrate is an organometallic compound, e.g. the Stille, Suzuki, Hiyama, Negishi and Kumada cross-couplings (Scheme 2), while in other classes another organic molecule is used e.g. the Heck, Sonogashira and Buchwald-Hartwig couplings.[2] (Scheme 3)

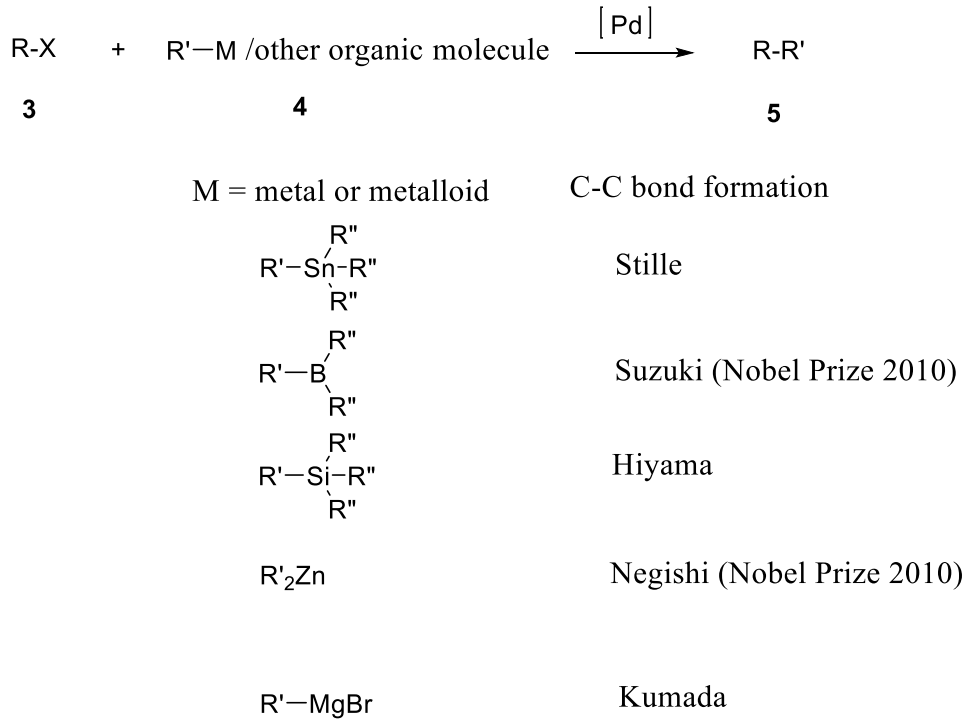

Scheme 2: Classes of palladium catalyzed cross couplings which employ organometallic reagents.

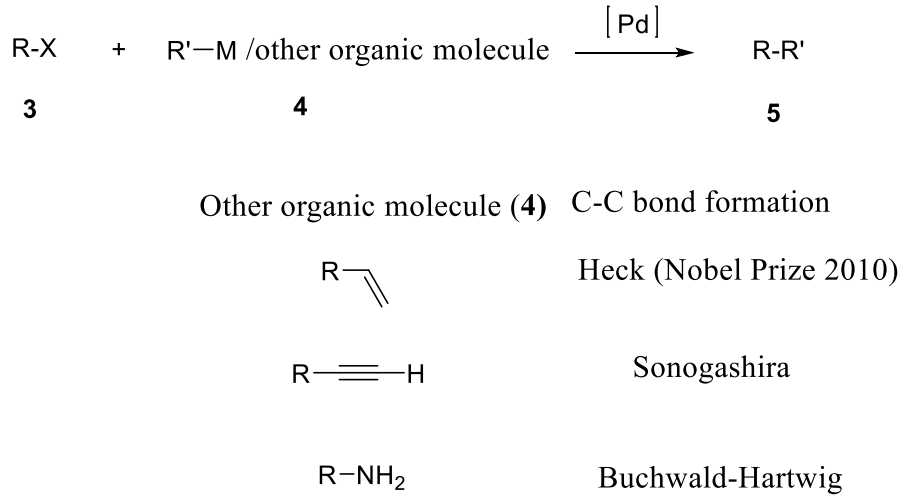

Scheme 3: Classes of palladium catalyzed cross couplings which couples two organic molecules.

The importance of these reactions is reflected by 2010 Nobel prize in Chemistry which was awarded to Akira Suzuki, Richard F. Heck and Ei-ichi Negishi for their contributions to the palladium catalyzed cross coupling reactions.[3]The general catalytic cycle for cross coupling reactions comprises of three main steps: oxidative addition, transmetallation and reductive elimination (Figure 1).[4]

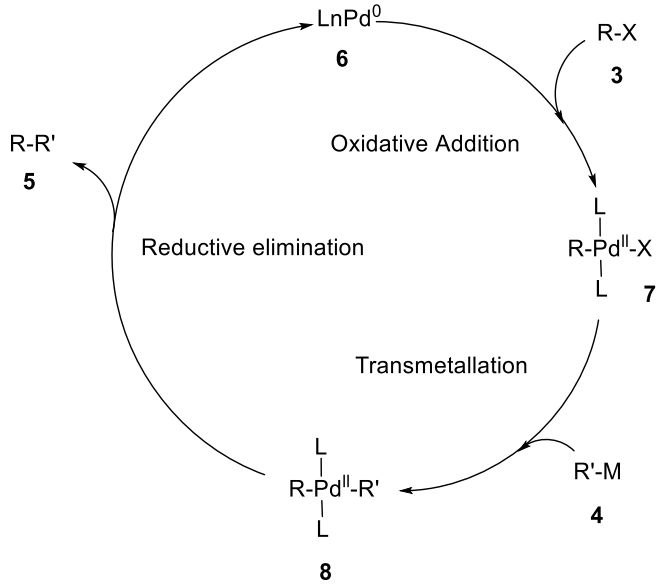

Figure 1: General catalytic cycle for a palladium catalyzed cross coupling.

General catalytic cycle goes as follows[5]: The first step is the oxidative addition of the substrate (alkyl/aryl/vinyl halide) **3** to the active catalyst $LnPd^0$ (**6**) and generates a $L_2Pd(R)(X)$ species (**7**). The valence electron, oxidation number and co-ordination number of the palladium metal increases by two in $L_2Pd(R)(X)$ (**7**). The second step of the catalytic cycle is the transmetallation. This is the step where various classes of the cross-coupling reactions differ. In this step, an organic moiety is transferred from the organometal (**4**) to **7** generating species **8**. The oxidation state, valence electrons and co-ordination number of the metal remains same in this step. The last step of the catalytic cycle is reductive elimination. The reductive elimination is reverse of the oxidative addition, where the oxidation number, co-ordination number and valence electrons of the metal decreases by two. This step is very rapid, and the C-C coupled product forms (**5**) from transmetallated species **8** in this step and **6,** Pd (0) is regenerated. The regenerated metal can undergo the catalytic cycle again.

The reactivity of the $LnPd^0$ can be varied by using phosphine ligands (Ln) with different electronic and steric properties. Phosphine ligands act as sigma donors and pi acceptors.[6] Tolman quantified an electronic parameter (ν) of mono phosphine ligands based on the stretching frequencies of CO in $LNi(CO)_3$ type complexes and invented the term "cone angle (Θ)" to describe the steric bulkiness of a mono phosphine ligand. Cone angle (Θ) is described as the angle formed at the metal vertex, when a cone is drawn from the periphery atoms of the ligands. (Figure 2).[7] Bite angle is a corresponding term describing chelating ligands (Figure 2). This can be used to determine the bulkiness of the chelating ligands (Figure 2).[8]

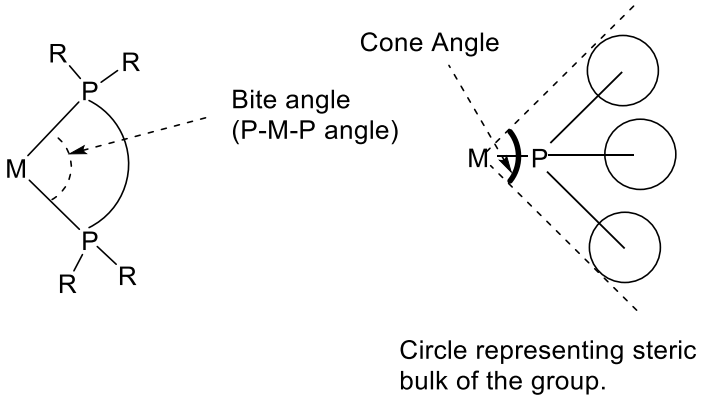

Figure 2: Pictorial representation of the cone angle and the bite angle.

The discussion below aims at the showing the overall equation of the cross-coupling reaction, highlighting the transmetallation step of the catalytic cycle.

1. Corriu-Kumada (1972)

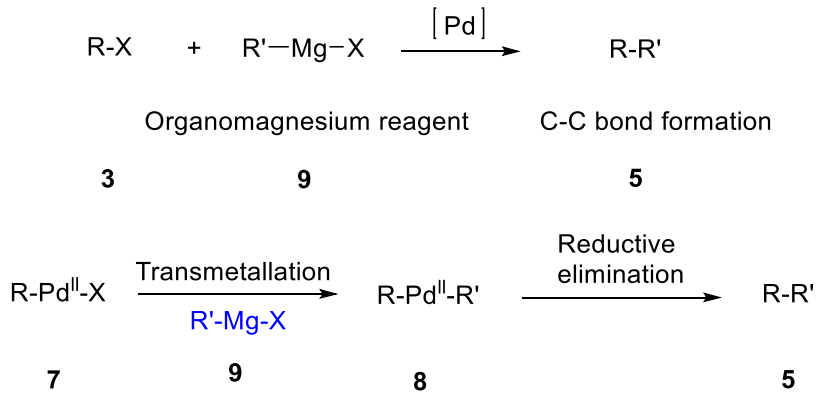

Scheme 4: Schematic representation of palladium catalyzed Kumada cross coupling.

In Corriu-Kumada cross coupling, organohalides (**3**) react with organomagnesiums (**9**, Grignard reagents) in the presence of the [Pd]. In Kumada cross coupling, the organic moiety is transferred from **9** to the oxidative addition species (**7**) generating **8** which is then followed by reductive elimination yielding cross coupled product **5** (Scheme 4).

In 1941, cross coupling of **9** with vinyl/aryl halides was demonstrated by Kharash in the presence of the catalytic amount of the cobalt chloride.[9] In 1972, Corriu[10] and Kumada[11]

performed the cross coupling of the **9** with the aryl/vinyl halide in the presence of the nickel catalyst. In 1975, this reaction was done in the presence of palladium catalyst by Murahashi et al.[12] Towards the end of the 1990, it was established that a range of **9** bearing different functional groups can be easily synthesized. This broadened the scope of these reactions.

2. Sonogashira (1975)

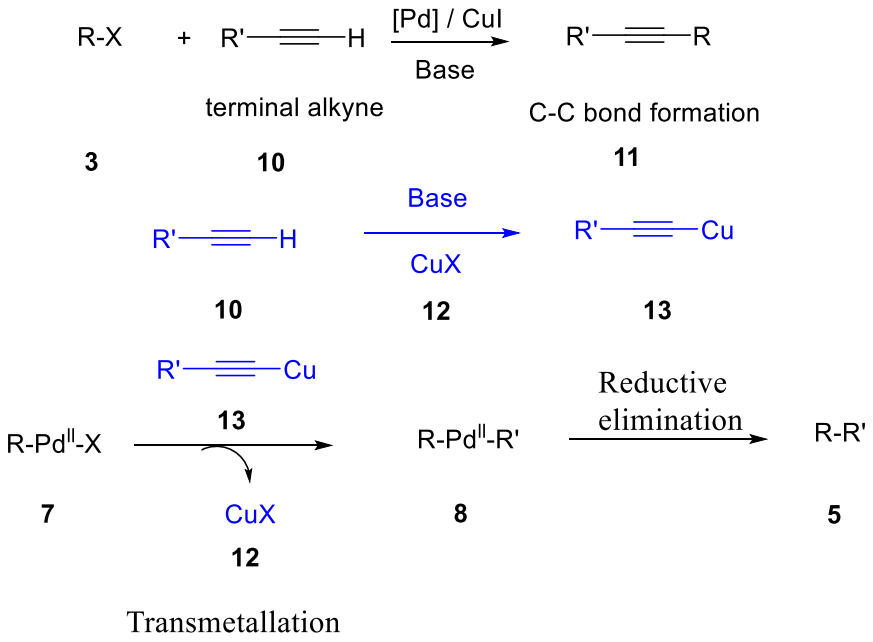

Scheme 5: Schematic representation of palladium catalyzed Sonogashira cross coupling.

In Sonogashira coupling, organohalides (**3**) react with terminal alkynes (**10**) in the presence of base, [Pd] and catalytic copper metal to form cross coupled product **11**. The catalytic cycle is comprised of three main steps: oxidative addition, transmetallation and reductive elimination (Figure 1). In the presence of the base and copper halide (**12**), the terminal alkyne (**10**) is converted to **13**. The **13** thus formed is used in the transmetallation step to transfer an alkynyl group on to the palladium metal in the species (**7**) generating **8,** which then under goes reductive

elimination generating cross coupled product (**5**). The **12** is regenerated in the transmetallation step and hence reactions require only catalytic amounts of **12** (Scheme 5).[2b]

In 1963, Stephens and Castro demonstrated first cross coupling of a cuprous acetylide (**13**) and an aryl/alkenyl halide.[13] This reaction required high temperature and stochiometric amounts of the copper in the form of cuprous acetylide (**13**). In 1975, independent efforts were made by Cassar[14], Heck[15] and Sonogashira[16] to improve the alkyne cross coupling. Of these three, Sonogashira managed to perform the reaction under mild conditions by using copper as a co-catalyst in the reaction.

3. Negishi (1966)

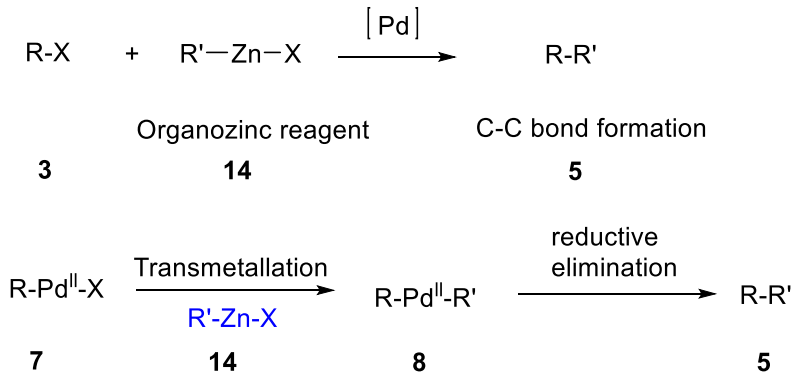

Scheme 6: Schematic representation of palladium catalyzed Negishi cross coupling.

In a Negishi coupling, organohalide (**3**) acts as an electrophilic component and organozinc reagent (**14**) acts as a nucleophilic component. This cross coupling also includes other metals of intermediate electronegativity i.e. organoaluminiums and organozirconiums.[2c] In the transmetallation step, there is a transfer of the organic moiety from organozinc (**14**) to the (**7**) leading to transmetallated species (**8**) which then under goes reductive elimination, generating the cross coupled product (**5**) (Scheme 6).

In 1976, Negishi developed a protocol for coupling organoaluminiums and aryl halides in the presence of the nickel as well as [Pd].[17] In 1977, the cross coupling with organozinc and aryl halide was reported by Negishi et. al.[18] For his efforts in the development of the cross coupling of the organozinc with organohalides, he was awarded Nobel Prize in Chemistry in 2010. Negishi cross coupling has advantages of wide substrate scope, mild conditions, by-products of the cross coupling are zinc salts and can be easily separated from the reaction via aqueous workup. The low toxicity of the zinc compounds compared to the tin compounds was also an advantage of these reactions. The organozincs **(14)** are usually air- and moisture-sensitive and care must be taken while handling them.[2c]

4. Suzuki (1979)

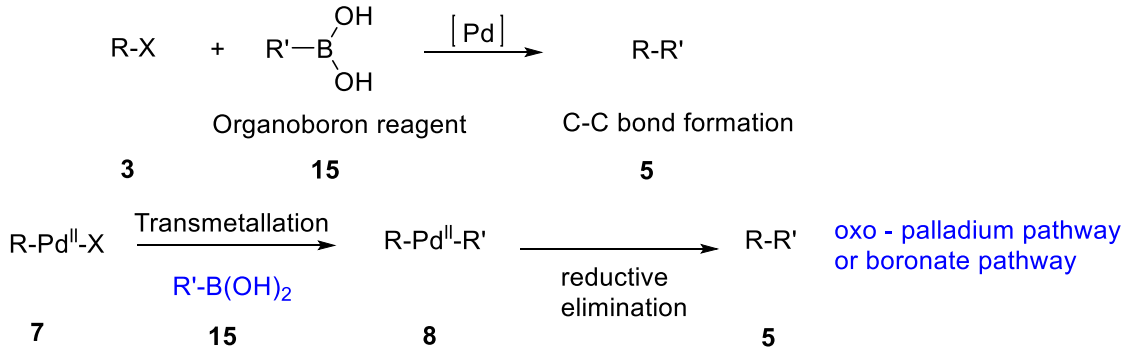

Scheme 7: Schematic representation of palladium catalyzed Suzuki cross coupling.

In Suzuki couplings, the organic moiety is transferred from an organoboron reagent (**15**) during the transmetallation step. In this reaction, the alkyl/aryl halide (**3**) acts as an electrophilic component and organoboron reagent (**15**) acts as a nucleophilic component. (Scheme 7)

The nucleophilic nature of the boron reagent is crucial.[19] The boronic reagent as such is Lewis acidic in nature since boron has three electrons in the outermost shell ($2s^2$, $2p^1$), which can engage in three sp^2 hybridized bonds and has a vacant p orbital orthogonal to the plane. The

electrophilic nature of the boron is because of this empty p orbital. The earlier attempts to cross-couple organoboron reagents (**16**) with organic halides (**17**) without the presence of the base failed, since they were not sufficiently nucleophilic and eventually a successful Suzuki cross coupled product **(18**) was accomplished by Suzuki et. al from a reaction of **16** and **17** in the presence of sodium ethoxide (NaOEt) base (Scheme 8).[17, 19-20]

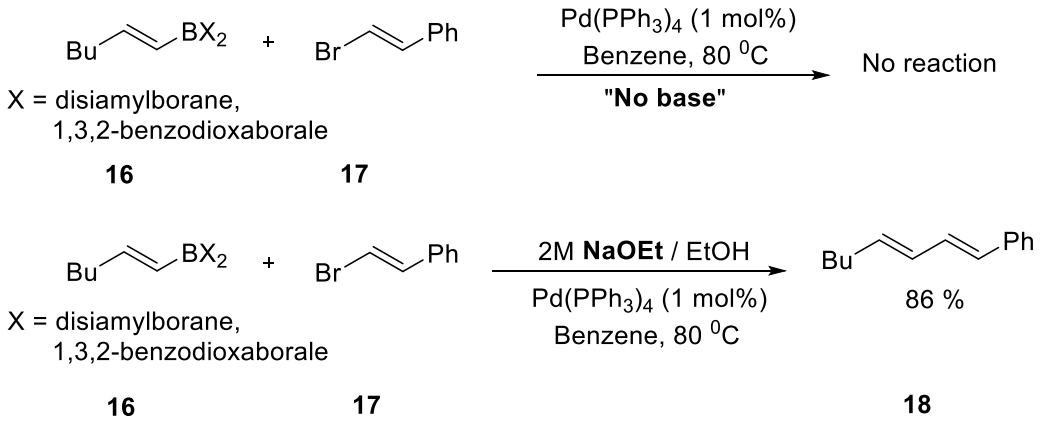

Scheme 8: Importance of presence of the base in Suzuki cross coupling reaction.

The two possible pathways have been suggested for the transmetallation step: the boronate pathway and oxo-palladium pathway (Scheme 9).[2a, 21] In the boronate pathway, boronic acid (**15**) reacts with base (**20**) and transforms to nucleophilic boronate species (**21**) which can then transfer the organic moiety to the **7**. In oxo-palladium pathway, exchange takes between oxidative addition species R-Pd-X (**7**) and a base $^{-}$OH **(20**). This generates oxo-palladium species (**19**) which can then undergo transmetallation of organoboron reagents.

The history of Suzuki cross coupling dates to 1979.[19, 22] The catalytic cycle comprises of three key steps i.e. oxidative addition, transmetallation and reductive elimination. The relative reactivity order of electrophiles is R-I > R-Br > R-OTf > R-Cl.[2a] There are different kinds of organoborons that can be used e.g. boronic esters, boronic acids, trifluoroboronates, N-

coordinated boronates, boronamides and organo boranes.[23] Mayr has developed a nucleophilicity scale for relative comparison of the nucleophilicity of boron reagents.[23-24]

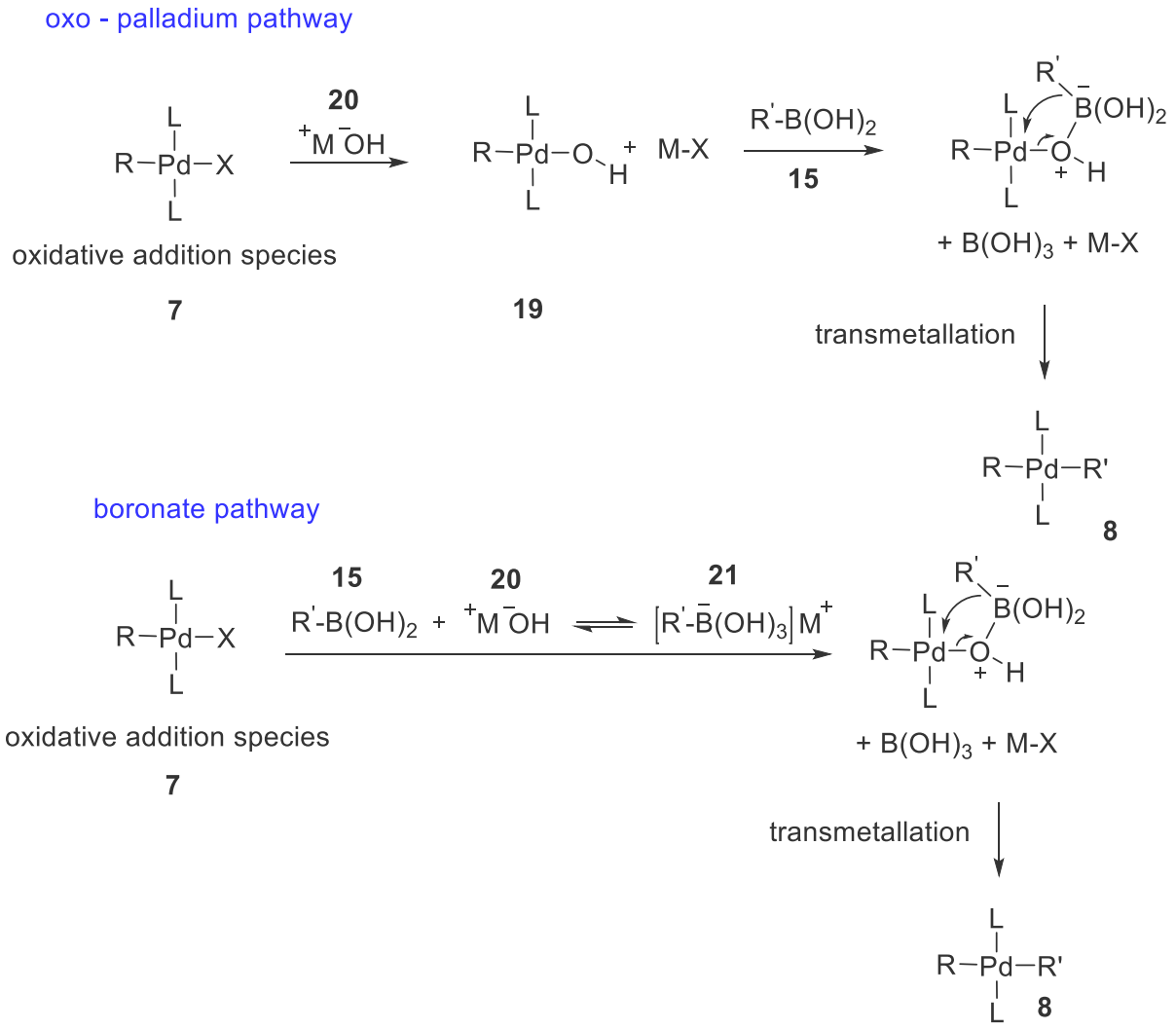

Scheme 9: Suggested pathways for transmetallation in Suzuki cross coupling reaction.

Suzuki cross couplings suffer from the side reactions like protodeboronation, oxidation and palladium catalyzed homocoupling (Scheme 10).[2a] Usually these side reactions can be controlled by doing Suzuki cross coupling reaction in anhydrous conditions and by careful optimization of reaction conditions.

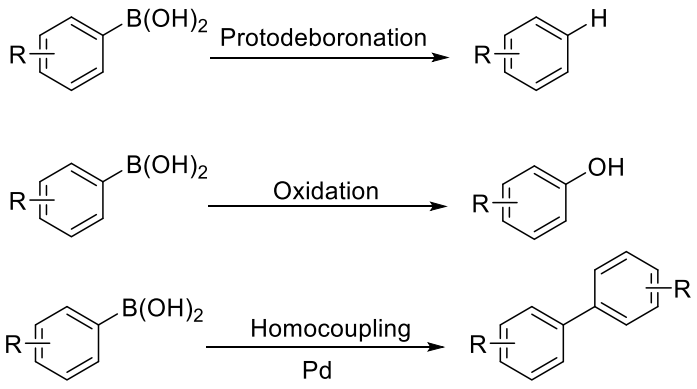

Scheme 10: Observed side reactions during Suzuki cross coupling.

5. Stille (1977)

In Stille coupling, the alkyl/aryl halide (**3**) acts as an electrophilic component and organotin reagent (**22**) acts as a nucleophilic component. In the transmetallation step, there is a transfer of the organic moiety from organotin reagent (**22**) to (**7**) leading to transmetallated species (**8**) which then goes under reductive elimination generating cross coupled product (**5**) (Scheme 11).

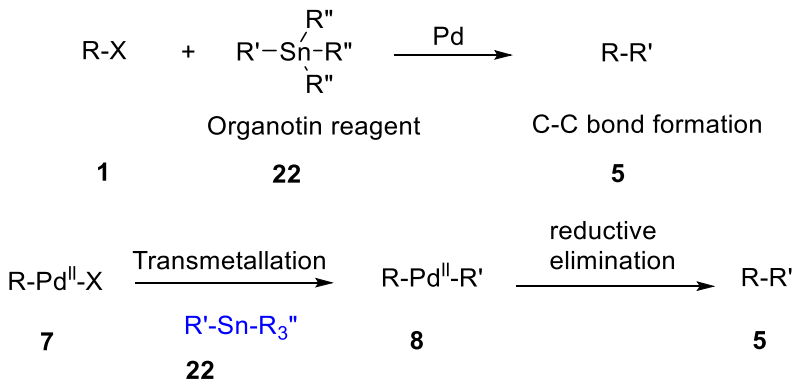

Scheme 11: Schematic representation of palladium catalyzed Stille cross coupling.

The history of Stille coupling dates back in 1977 when Kosugi et al. published allylation of aromatic halides by allyl tin compounds in the presence of the palladium catalyst.[25] In 1978, Milstein and Stille synthesized ketones from palladium catalyzed reaction of acid chlorides with

22.[26] The breakthrough was made in 1978 with Stille's mechanistic studies on coupling of **22** with aryl and benzyl halides, which helped in understanding mechanism of the reactions.[27]

Organotin reagents offer advantage of various functional groups tolerance but suffer from huge disadvantage of toxicity.[1, 28]

6. Hiyama (1988)

In Hiyama coupling, the organic moiety is transferred from organosilicon reagents (**23**) during the transmetallation step. In the transmetallation step, the organic moiety is transferred from the pentacoordinated silicates (**24**) rather than **23** to the oxidative addition species (**7**) leading to transmetallated species (**8**) which then goes under reductive elimination generating cross coupled product (**5**) (Scheme 12).

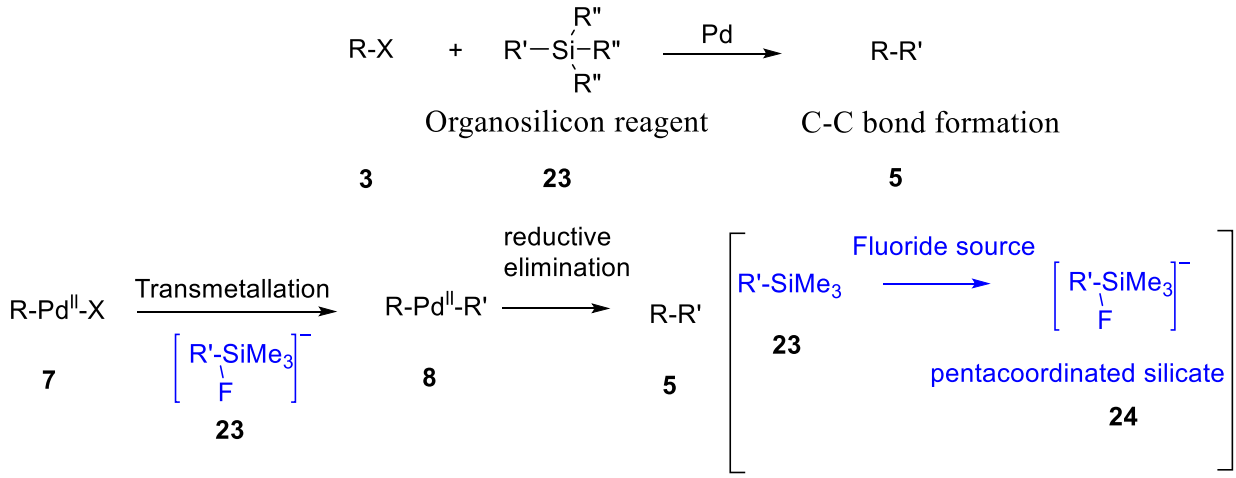

Scheme 12: Schematic representation of palladium catalyzed Hiyama cross coupling

Cross coupling of organopentafluorosilicates and aryl halides in the presence of palladium was first demonstrated by Kumada et. al in 1982.[29] Drastic conditions were employed in this reaction and a mixture of regioisomers was observed. In 1988, Hiyama et. al cross coupled alkyl, allyl and alkenyl halides with **23**, which were activated by the fluoride source like tris (diethylamino)sulfonium difluorotri - methylsilicate (TASF), in the presence of the palladium

catalyst.[30] Hiyama cross coupling employed mild reaction conditions, showed wide functional group tolerance and gave high yields.

7. Mizoroki - Heck (1972)

In Mizoroki-Heck cross coupling, an aryl/ alkenyl halide (**3**) couples with an alkene (**25**) (Scheme 13). Heck and Mizoroki was awarded Nobel Prize, 2010 for their efforts in developing this cross-coupling reactions.

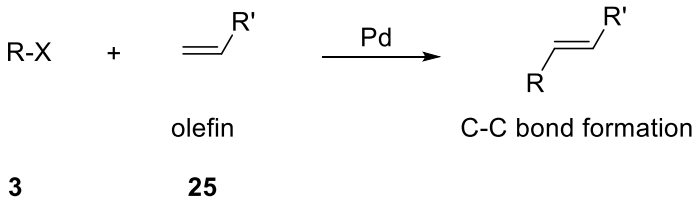

Scheme 13: Schematic representation of palladium catalyzed Heck cross coupling.

As shown in Figure 3, there are some additional steps in the catalytic cycle for Heck-Mizoroki reaction. This catalytic cycle involves consists of following steps:[5a] a) oxidative addition takes place to the Pd^0 (**6**) generating species **7**; b) 1,2 insertion – In this reaction, the **26** inserts into the Pd-R bond of **7** generating **27**. In general, the term "*1, n-insertion*" refers to reactions of the type [M]-X + Y → [M]-Y-X (X=H, alkyl, aryl) where *n* indicates the number of atoms between M and X in the product;[5a] c) β-Hydride elimination - In this reaction, there is elimination of Pd(II)-H (H at the β carbon) from **27** generating **28** and **29**. In general, elimination reactions are the reverse of the insertion reaction i.e. these are reactions of the type [M]-Y-X → [M]-X, and when X = H then these reactions are termed as hydride elimination. These reactions are designated by Greek letters like α, β, δ.... instead of numbers and Greek letters denote the position of H to be eliminated. In this case, the H is at β position in **27** and

hence this reaction is known as β-Hydride elimination.[5a, 6] d) Pd(0) species, **6** is generated in this step with the help of a base from **29**, which can be used again in the catalytic cycle.

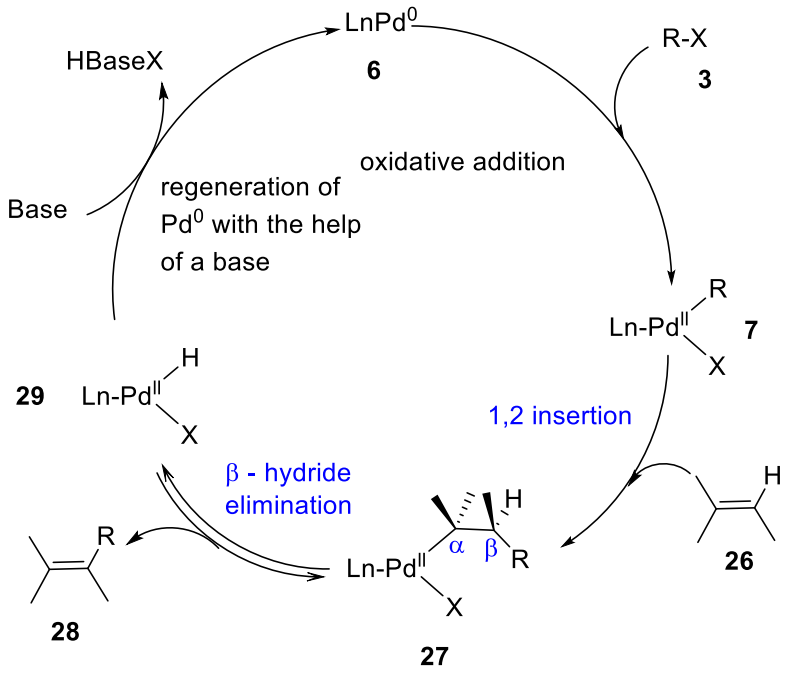

Figure 3: General palladium catalyzed catalytic cycle for Heck cross coupling.

In 1968, Heck et al. demonstrated the coupling of the organomercury compounds with alkenes in the presence of palladium catalyst.[31] The toxic organomercury compounds were soon replaced by aryl halides with the discovery by Heck and Mizoroki in 1970s. In 1971, Mizoroki demonstrated the coupling of the aryl iodide with **28** in the presence of palladium catalyst.[32] In 1972, Heck demonstrated the coupling between similar functionalities.[33] Both discoveries were independently done around the same time.

The Heck reaction can tolerate various functionalities, is known for mild condition, regioselectivity and stereoselectivity.

1.1.1. Stereoselectivity in palladium catalyzed cross coupling reactions

The question of stereochemistry does not arise when coupling partners are aromatic substrates but when one of the coupling partners is vinylic, *E*-*Z* stereochemistry needs to be considered. Maintenance of the stereochemistry is crucial when aiming for the target molecules.[34] Some examples from literature displaying retention of a specific stereochemistry are palladium catalyzed synthesis of chalcones (**32**) from benzoyl chloride (**31**) and *E*-potassium styryltrifluroborates (**30**) by Masum et al.(Scheme 14),[35] palladium catalyzed formylation of vinyl halides (**33**) in the presence of carbon monoxide and tin hydride (**34**) by Stille et al. (Scheme 15),[36] cross coupling of aryl fluorosulphonates (**37**) with organotin reagent (**36**) by Roth et al. (Scheme 16),[37] palladium catalyzed cross coupling of chloroarene (**40**) with organochlorosilane (**39**) by Hiyama et al. (Scheme 17),[38] palladium catalyzed Negishi cross coupling of organozinc (**42**) with *E* or *Z* alkoxy-vinyliodide (**43**) gave the respective **44** and **45** isomer as demonstrated by Normant et al.[39] (Scheme 18)

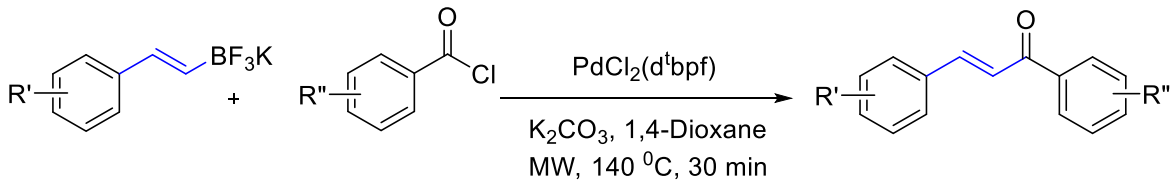

30 **31** **32**

Scheme 14*: Retention of stereochemistry during palladium catalyzed synthesis of chalchones.*[35]

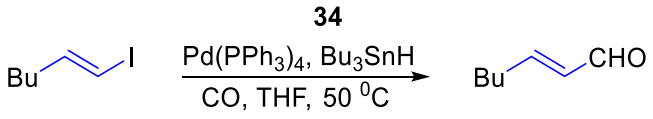

33 **35**

Scheme 15*: Retention of stereochemistry during palladium catalyzed formylation of organohalide.*[36]

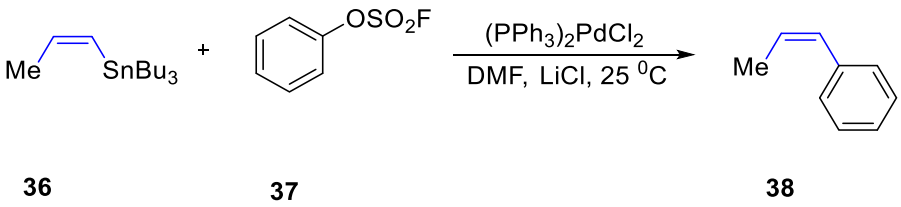

Scheme 16: Retention of stereochemistry during palladium catalyzed cross coupling of aryl fluorosulphonate with organotin reagent.[37]

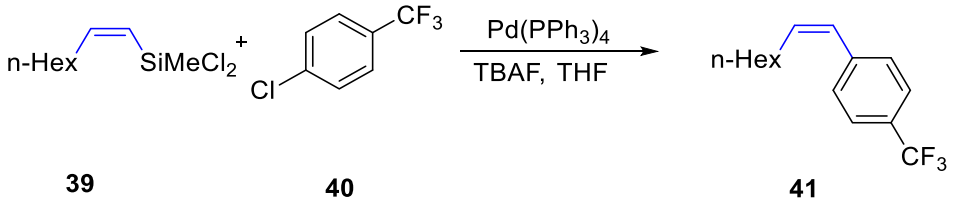

Scheme 17: Retention of stereochemistry during palladium catalyzed cross coupling of chloroarene with organochlorosilane.[38]

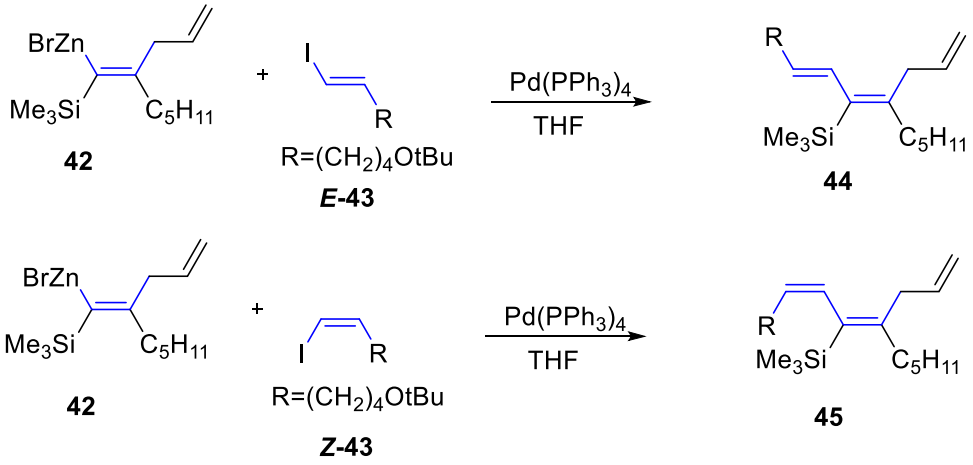

Scheme 18: Retention of stereochemistry during palladium catalyzed cross coupling of organozinc with alkoxy-vinyliodide.[39]

1.1.3. Loss of stereochemistry in cross coupling reactions

Discussed below are the examples of cross coupling reaction where the loss of stereochemistry during palladium catalyzed reactions has been reported. Different reasons have been proposed for the isomerization. During the study of stereochemistry of transmetallation in

Stille coupling of vinyl trialkyltin reagents (**47**) and benzoyl chloride (**46**) in the presence of benzylchlorobis(triphenylphosphine) (**48**) as a palladium catalyst, formation of *E*-chalchones (***E*-49**) product was dominant (Scheme 19).[40]

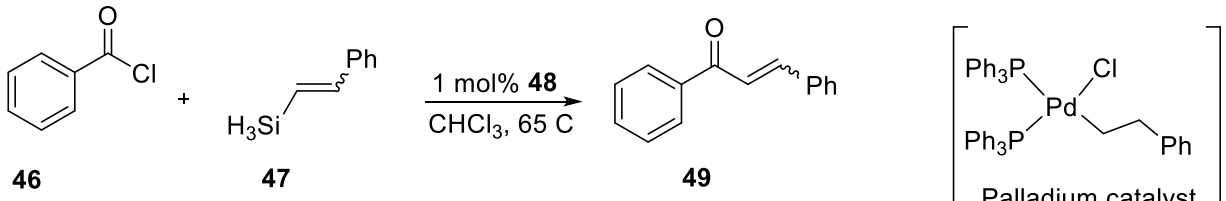

Entry	47 (*E*/*Z*)	49 (*E*/*Z*)	
1	95/5	100/0	
2	15/85	100/0	
3	15/85	33/66	(Reaction done in dark, in presence of 10% 2,6-di-tert-butylphenol.)

Scheme 19: Stereochemistry studies in palladium coupling of benzoyl chloride and styryltrimethyltin.[40]

As shown in Scheme 19 in entry 1 and entry 2, ***E*-49** was formed predominantly despite the ratios of *E* and *Z* ratios of **47**. It was verified that ***Z*-49** does not isomerize under reaction conditions. This ruled out the isomerization taking place at the product stage. The authors have mentioned that isomerization of **47** takes place under radical conditions. The mechanism explaining how radicals may form in the reaction conditions and how they can isomerize **47** has not been mentioned. But the use of 10% 2,6 -di-tert-butylphenol (radical quencher, entry 3, Scheme 19) has been shown to predominantly form ***Z*-49**. The *E*-*Z* equilibrium lies towards the thermodynamically stable ***Z*-49** product.

The reasons for erosion of stereochemistry were different on changing the organotin substrate from **47** to **37** (Scheme 20). The cross coupling of **46** and **37** yielded 50:50 (*E: Z*)

mixture of **50**. It was found that in this isomerization of ***Z*-50** takes place in the presence of reaction conditions and it eventually changes to ***E*-50** (Scheme 20).

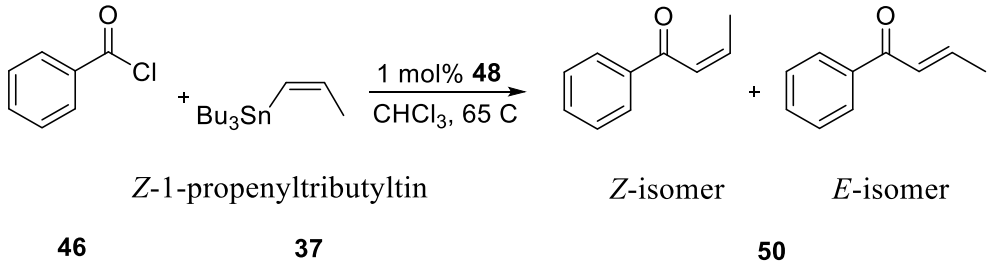

Scheme 20: Stereochemistry studies in palladium catalyzed coupling of benzoyl chloride and (Z)-propenyltributyltin.[40]

When *Z* - benzyl 3-(tributylstannyl)propenoate (**51**) was used as an organotin substrate, a mixture of 62:38 (*E*:*Z*) **52** was formed under the reaction conditions. It was observed that the ***Z*-52** isomerizes under the reaction conditions (Scheme 21).

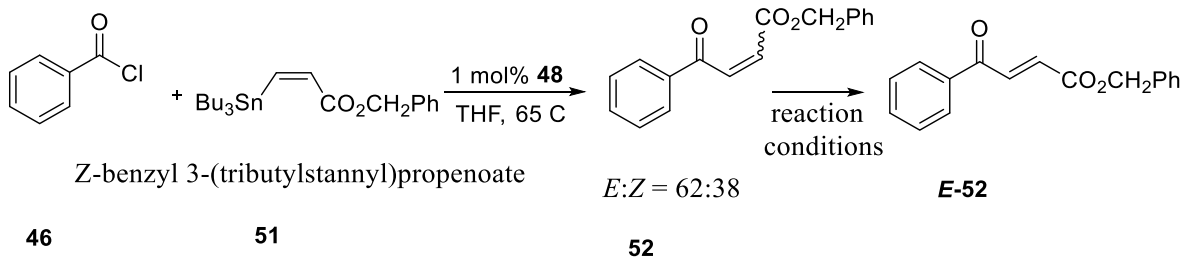

Scheme 21: Stereochemistry studies in palladium catalyzed coupling of benzoyl chloride and (Z)-benzyl 3-(tributylstannyl)propenoate.[40]

In the above-mentioned study by Stille et al., no explanation has been given to support why ***Z*-49** does not isomerize under reaction conditions whereas ***Z*-50** and ***Z*-52** does. Further, no plausible mechanism was proposed for the isomerization.

Further ligand effects were studied on the rates of Stille coupling reactions employing triphenylphosphine (**53**), tri-2-furylphosphine (**54**) and triphenylarsine (**55**).[41] While studying

the ligand's effects on the coupling between **46** and **37**, it was observed that the different ligands gave different extent of isomerization in **50** (Scheme 22).

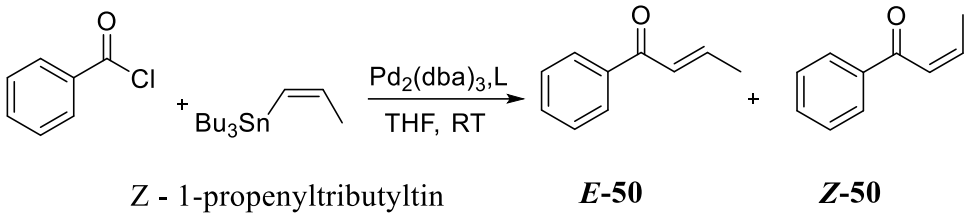

46 **37**

Entry	Ligand	**(*E*:*Z*) 50**
1.	PPh_3 (**53**)	30:70
2.	$(2\text{-furyl})_3P$ (**54**)	4.5:95.5
3.	$AsPh_3$ (**55**)	30:70

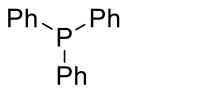

Triphenylphosphine

53

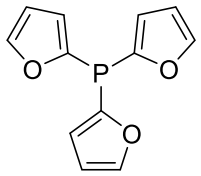

Tri(2-furyl)phosphine

54

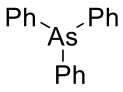

Triphenylarsine

55

Scheme 22: Ligand effect in Stille coupling of benzoyl chloride and (Z)-1-propenyltributyltin.[41]

The reaction was screened with three different ligands and reactions were monitored by NMR. The loss of stereospecificity in the presence of triphenylphosphine (**53**) and triphenyl arsine (**55**) was substantial but there was no loss of stereospecificity in the presence of trifurylphosphine (**54**) (Scheme 22). With the reference of their work,[42] it has been mentioned that the enone **50** isomerizes but further studies explaining how the product isomerizes and why different ligands give different isomerization ratios has not been mentioned.

Isomerization was also observed during the palladium catalyzed Stille coupling of vinyl iodides and vinyl tin reagents in the presence of carbon monoxide (Scheme 23).[43] Following are the examples where isomerization was observed:

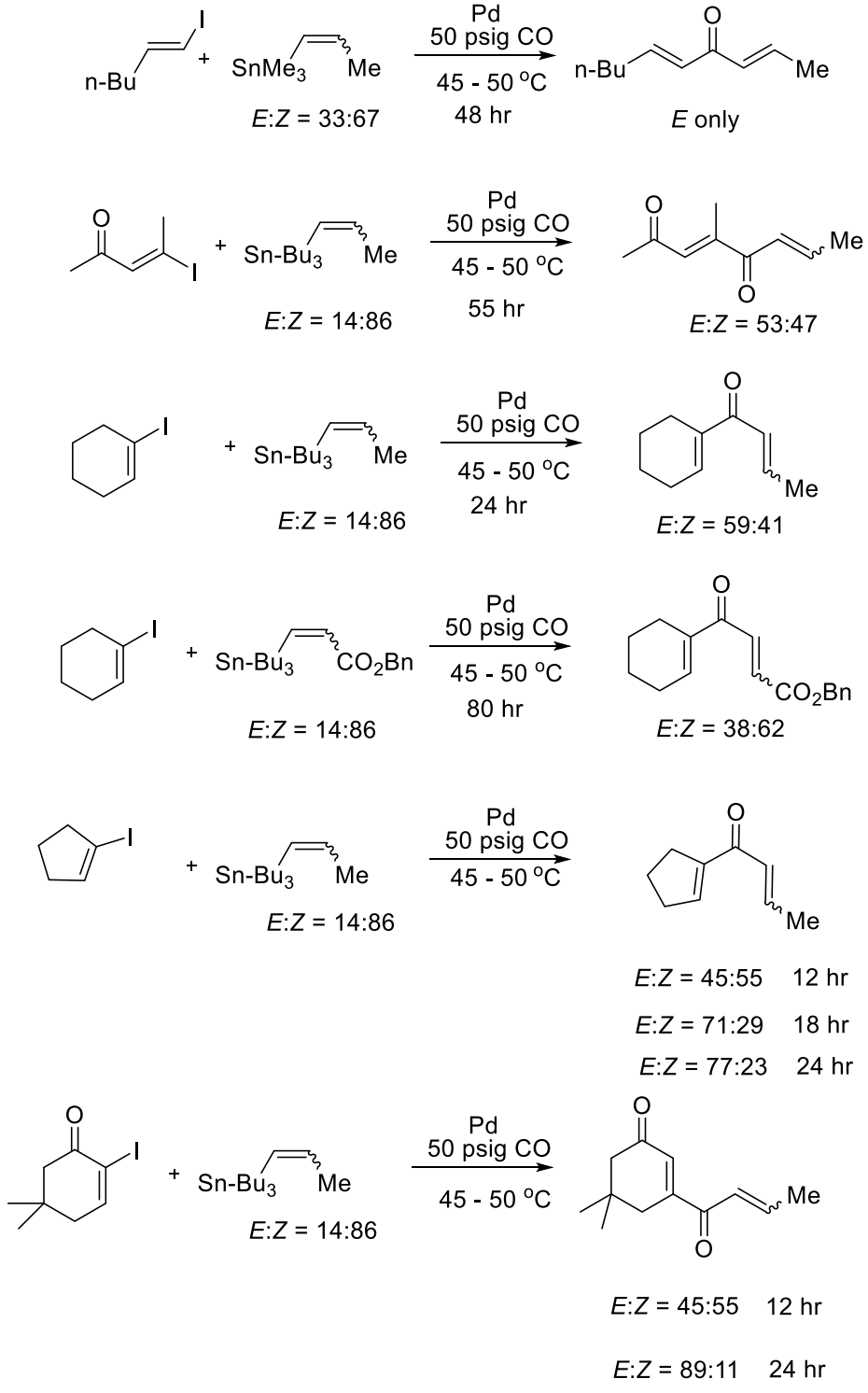

Scheme 23: Loss of stereospecificity during palladium catalyzed carbonylative cross coupling of vinyl iodide and organotin reagents.[43]

As shown in Scheme 24, after oxidative addition of vinyl halide to the palladium (**56**), CO inserts into palladium vinyl bond (**57**). Insertion of CO into the palladium carbon is known as a carbonylation reaction. This is followed by transmetallation with vinylorganotin substrate to give (**58**) and eventual reductive elimination yields divinyl ketones (**59**). Isomerization was observed when *Z*-vinyl substrates were used, and the loss of stereochemistry was observed in the product.

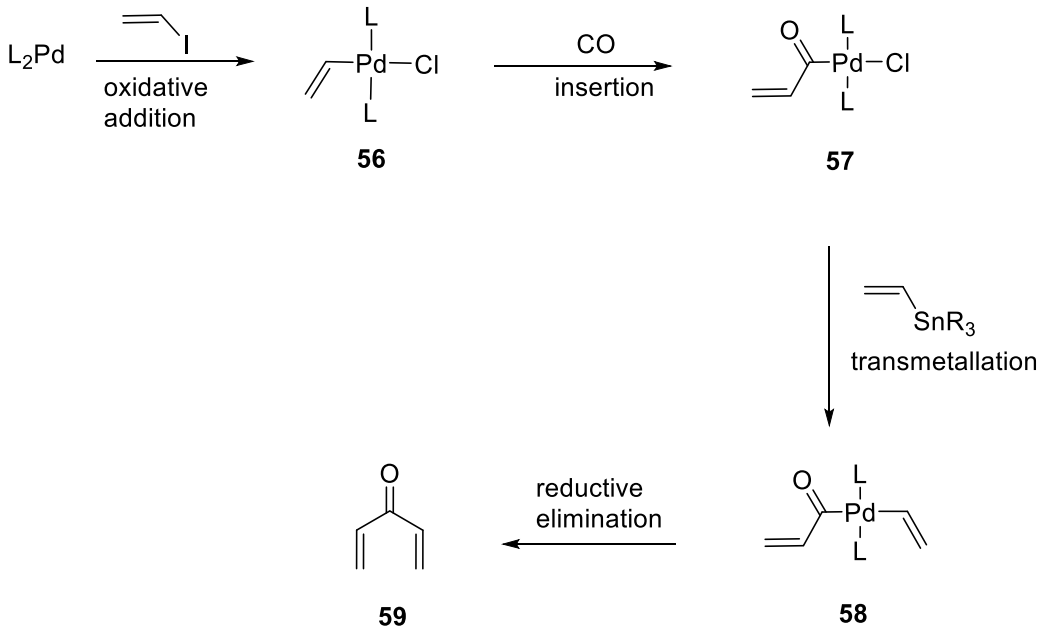

Scheme 24: Insertion of CO during palladium catalyzed Stille coupling.

To find the reason for the isomerization, detailed studies were performed on the carbonylative cross coupling of cyclohexenyl iodide (**60**) with benzyl-(*Z*)-3-(tributylstannyl)propenoate (**51**).[43] After 80 h, the *E*:*Z* ratio of the **61** obtained was 80:20 (Scheme 25). It was observed that **51** did not isomerize under reaction conditions. Based on this observation, it was suggested that the loss of stereochemistry was at the product stage or in the transmetallation step.

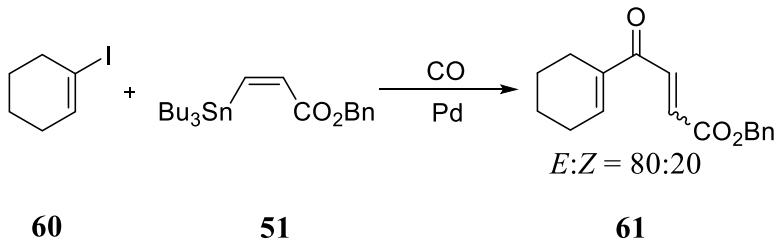

Scheme 25: Palladium catalyzed carbonylative cross coupling of cyclohexenyl iodide and benzyl Z-3-(tributylstannyl)propenoate.[43]

In another coupling reaction between (*E*)-1-iodohexene (**33**) and predominantly (*Z*)-1-(tributylstannyl)propene (**37**), product ***Z*-62** was formed predominantly after 24 hr. As shown in Scheme 26, it was observed that ***Z*-62** continued to isomerize under reaction condition and transformed to ***E*-62** after 48 hr. Based on this, authors emphasized on the loss of stereochemistry at the product stage. Photoisomerization has been suggested as the part reason for loss of stereochemistry in the product as Stille et al. observed formation of 20% ***Z*-62** after 48 hr (suppression of isomerization) in the reaction shown in Scheme 26, when done in the dark.[43] Further studies for how the loss of stereochemistry takes place in the product has not been mentioned by authors.

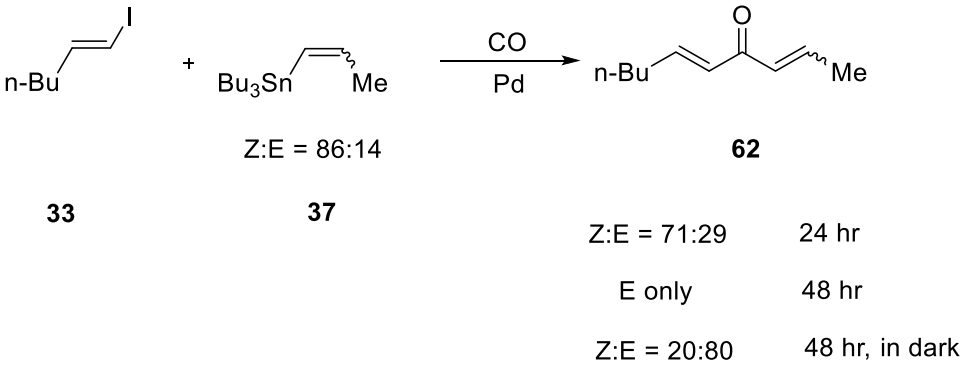

Scheme 26: Stereochemistry studies on palladium catalyzed carbonylative cross coupling of vinyl iodide and 1-(tributylstannyl)propene.[43]

Erosion in stereochemistry was also observed during palladium catalyzed formylation of cis-iodohexene (**63**) with carbon monoxide and tin hydride.[36] The reason for the loss of stereochemistry has not been suggested by the authors (Scheme 27).

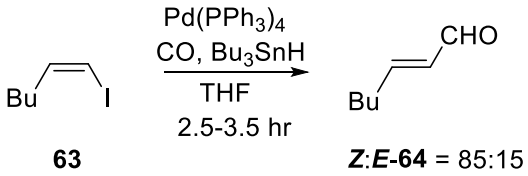

Scheme 27: Isomerization during formylation of vinyliodide and tributyltinhydride.[36]

1.1.4. Pathways for isomerization

Some pathways have appeared in the literature very frequently. These pathways are discussed below.

Phosphine mediated *E-Z* isomerization

The *E, Z* isomerization has been observed to be catalyzed by the phosphine present in the reaction. Brien et al. observed the *E, Z* isomerization of the α,β unsaturated product (**68**) from the catalytic Wittig reaction between **65** and **66** in the presence of the catalyst **67**. (Scheme 28).[44]

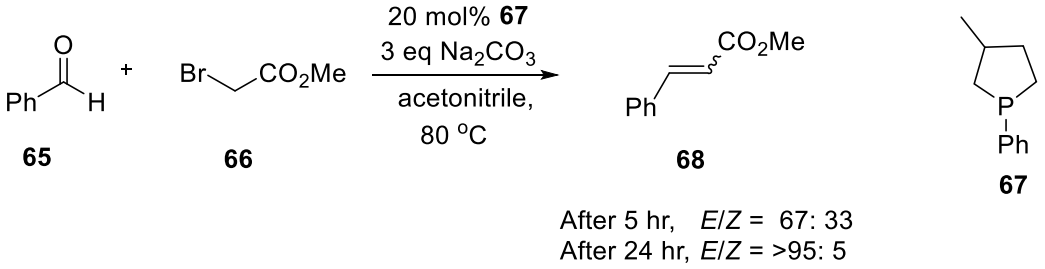

Scheme 28: E-Z isomerization observed during catalytic witting reaction.

Brien et al. observed that 67% ***E*-68** and 33% ***Z*-68** was formed after 5 hr and 95% ***E*-68** and 5% ***Z*-68** was obtained after 24 hr (Scheme 28). They postulated that the isomerization could

be phosphine mediated. As shown in Scheme 29, phosphine ligands were envisioned to promote the isomerization of ***Z*-68** via Michael addition to the conjugated double bond, bond rotation (**70**) followed by the elimination of the phosphine from **70** to yield ***E*-68**.

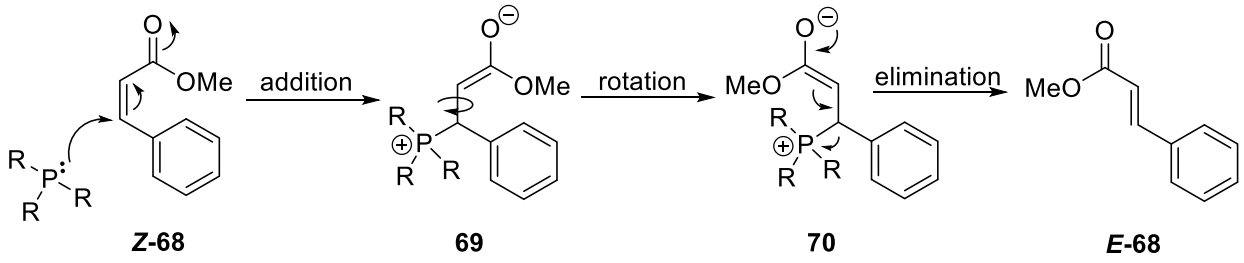

Scheme 29: Mechanism for E-Z isomerization in the presence of phosphine.

They further verified the isomerization of the ***Z*-68** to ***E*-68** by monitoring the reaction of ***Z*-68** in the presence of the **67** in d_8-toluene at 100 °C. The complete isomerization of ***E*-68** to ***Z*-68** was achieved in 10.5 hr (Scheme 30).

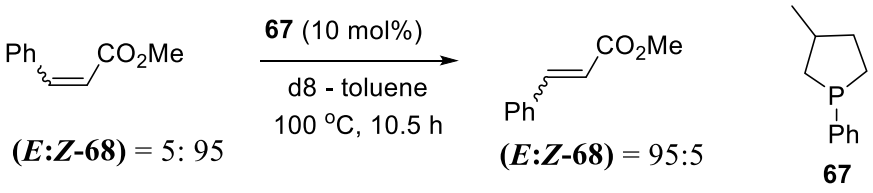

Scheme 30: E-Z isomerization of an enone in the presence of phosphine.

The phosphine mediated isomerization pathway has also been proposed by Yamamoto et al. for the observed isomerization of the oxindole (**74**), synthesized from 2-(alkynyl)phenylisocyanate (**71**) and terminal alkynes (**72**) via intramolecular nucleophilic vinylpalladation of isocyanates.[45] The formation of mixture of ***E*-74** and ***Z*-74** isomer was observed on complete completion of the reaction. It was observed that 99% ***E*-74** was formed when reaction was let go for additional time (Scheme 31).

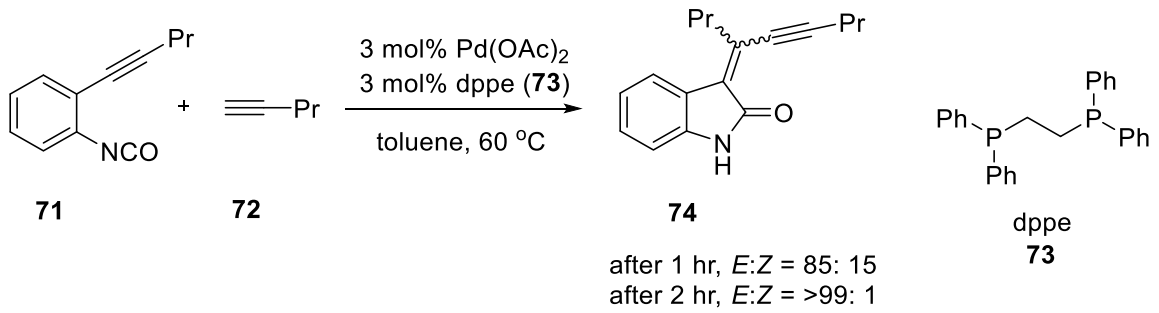

Scheme 31: Isomerization observed during synthesis of oxindole.

It was postulated that ***Z*-74** isomerizes to ***E*-74** in the presence of dppe (**73**) phosphine in the reaction conditions. They verify their postulated mechanism by exposing ***Z*-74** to 3 mol% dppe (**73**) in deuterated toluene at 60 °C (Scheme 32). They observed that ***Z*-74** changed to ***E*-74** within 2 hr.

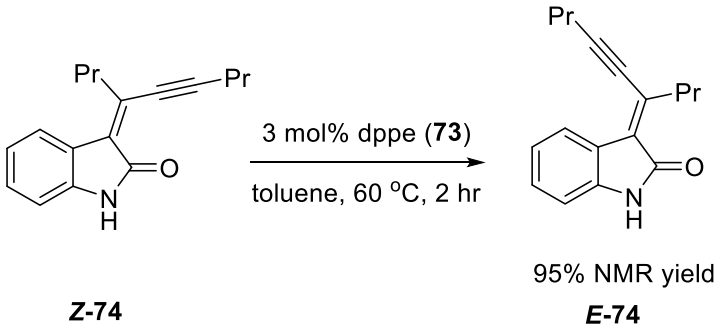

Scheme 32: E-Z isomerization of oxindole in the presence of a phosphine ligand "dppe".

Palladium hydride

Palladium hydrides (**76**) has been known to be responsible for the isomerization in olefins[46] (***Z*-75** to ***E*-75**) , migration of double bond/chain walking[46a, 47] (**77** to ***iso*-77**) and formation of isomerized cross coupled product[48] (**80**) (Scheme 33).

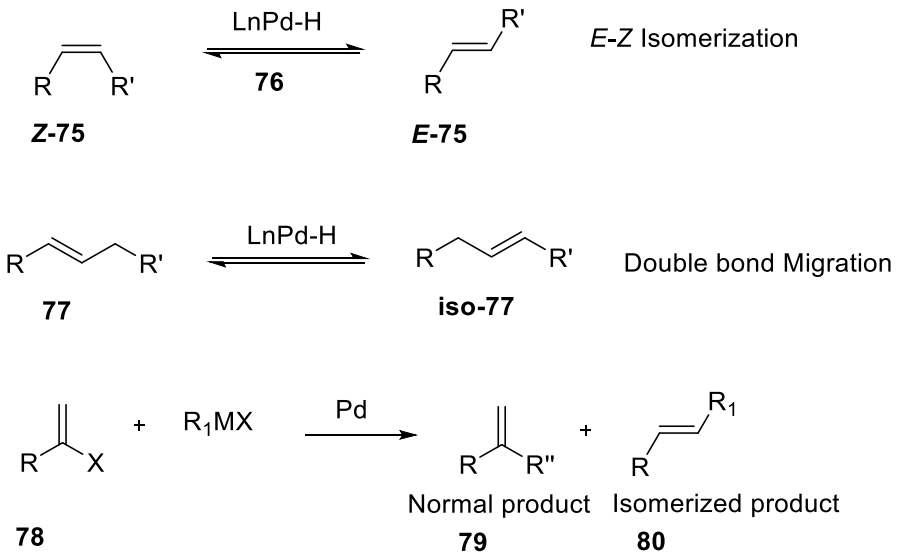

Scheme 33: Palladium hydride species catalyzed olefin isomerization, double bond migration and formation of migrated cross coupled product.

Formation of isomerized product

In the palladium catalyzed Heck coupling of **81** or **82** with **83**, the expected product would be **84** but the formation of **85** has also been observed (Scheme 34).

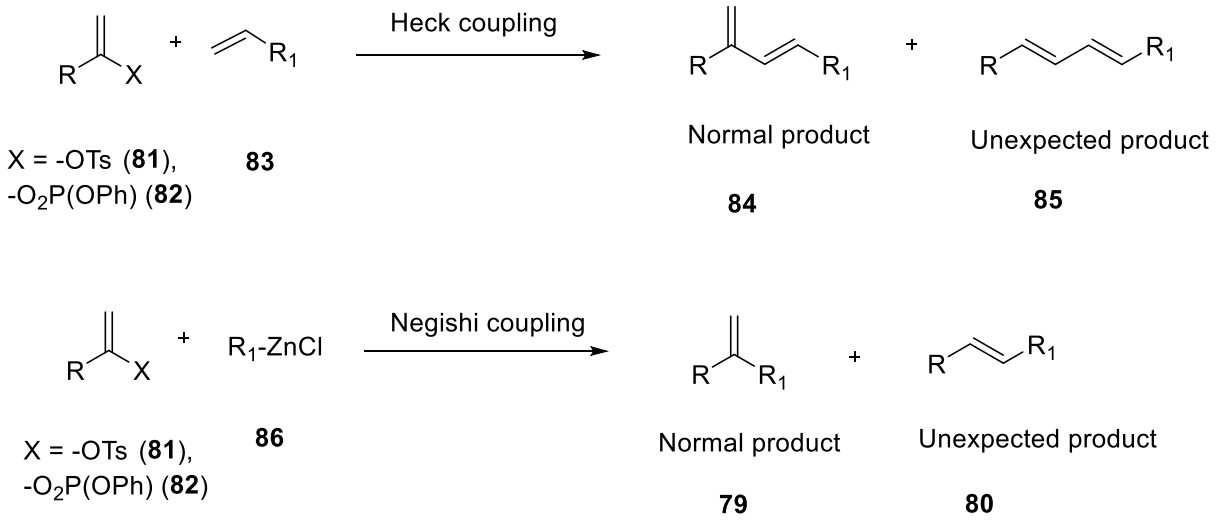

Scheme 34: Normal and rearranged product from palladium catalyzed Heck and Negishi coupling.

Similarly, in the palladium catalyzed Negishi coupling of **81** or **82** with **86**, the expected product would be **79** but the formation of **80** has also been observed (Scheme 34). The palladium hydride species formed in the reaction conditions has been proposed as the root cause of the unexpected product formation **85** and **80**.

Skrydstrup et al. reported the formation of the unexpected product from Mizoroki Heck[48] and Negishi[49] of non activated tosylates (**87**) and phosphates (**90**). (Scheme 35)

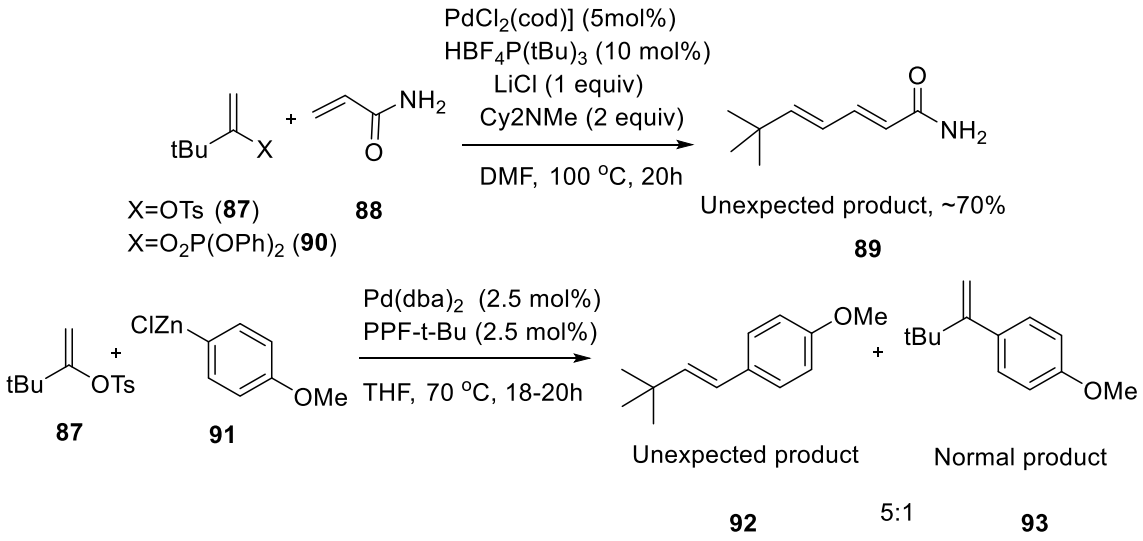

Scheme 35: Normal product and 1,2- migration product from heck reaction with alkenyl phosphates and tosylates.[48b]

To understand the formation of the isomerized product, Skrydstrup et al. performed DFT studies on tert-butyl vinyl substrates (Scheme 36).[48a]

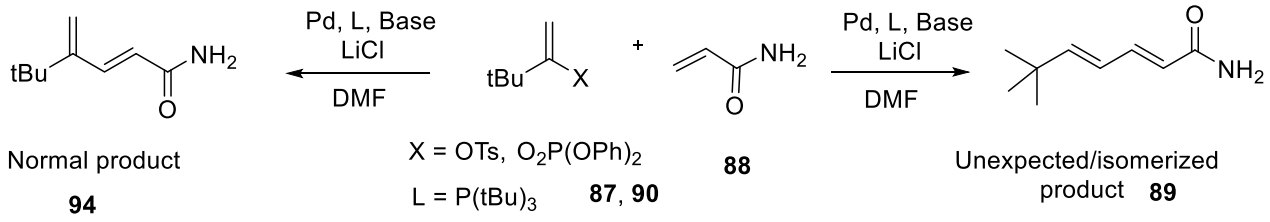

Scheme 36: Normal and rearranged product formation from Heck coupling on tert-butyl vinyl substrate.

The Scheme 37 shows a pathway for the formation of **94**. For the normal product formation, oxidative addition of tert butyl vinyl substrate (**87** or **90**) to the palladium takes place. It has been suggested by authors that chloride ions, which are present in the reaction conditions, are likely to displace tosylate or phosphate in oxidative addition species leading to the formation of **95**. Then, another alkene substrate (**88**) would coordinate to **95** species and form **96**. This will be followed by migratory insertion of the olefin (**97**) and then eventually β-Hydride elimination taking place to yield the expected (**94**) coupled product.

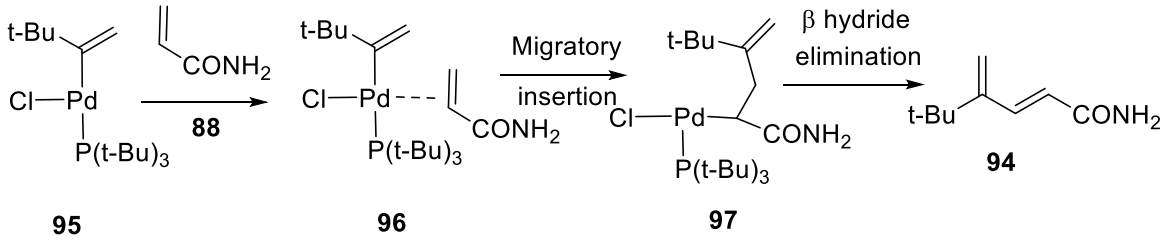

Scheme 37: Mechanism of Heck cross coupling demonstrating the formation of the expected product.

The proposed mechanism for the isomerized product (**89**) is represented in Scheme 38. It involves the β-Hydride elimination of the olefin in oxidative addition species **95** which leads to the alkyne coordinated **98** species. This mechanism would require the presence of H in the olefin. The insertion of tert-butyl acetylene to the palladium hydride takes place leading to the formation of isomeric tert-butyl vinylpalladium (II) species (**99**). This is followed by the coordination of another olefin substrate (**88**) yielding species **100**, migratory insertion of the olefin to form **101** and eventual β-Hydride elimination leading to the formation of the isomerized (**89**) coupled product.

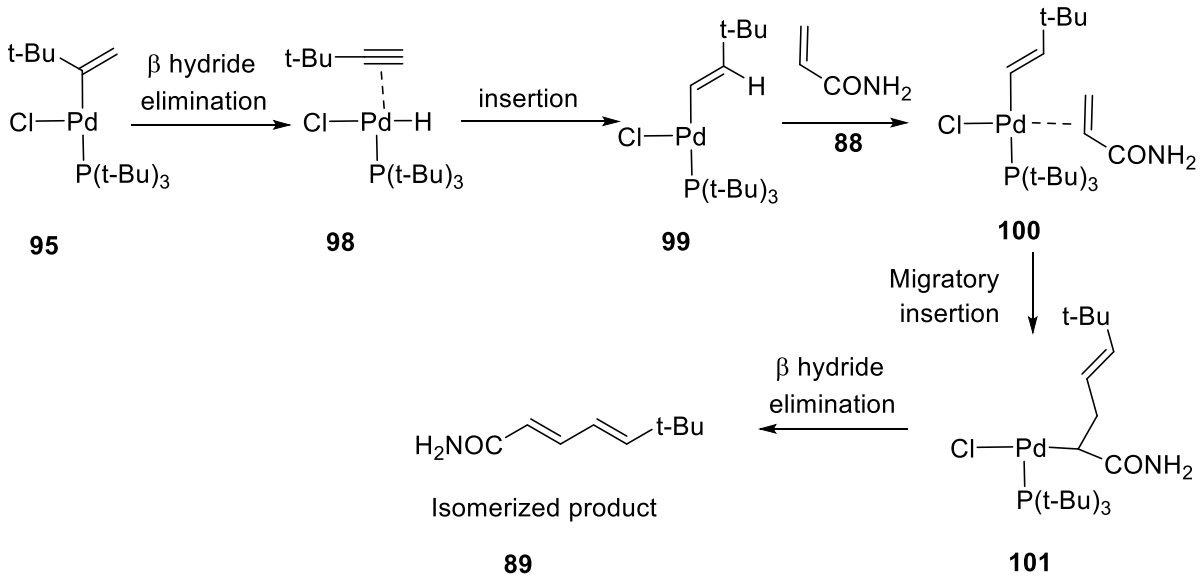

Scheme 38: Proposed mechanism for the generation of the migrated product.[48]

Olefin isomerization

Skrydstrup et al. has shown the isomerization in double bonds and migration of double bond by palladium hydride species, generated in situ.[46a] Wide range of alkenes has been shown to isomerize by palladium hydride and some examples are shown in Scheme 39.

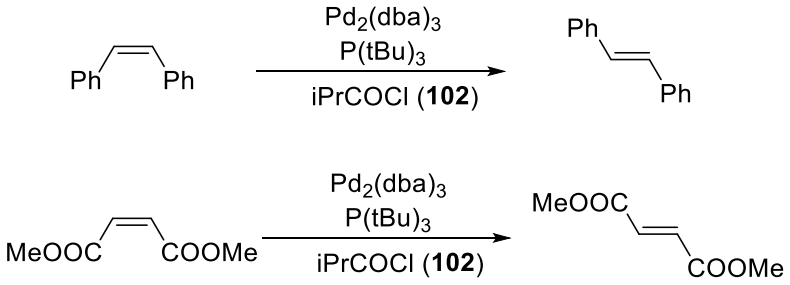

Scheme 39: Examples of E-Z isomerization catalyzed by palladium hydride.[46a]

A mixture in the ratio of 1:1:1 of $Pd_2(dba)_3$, $P(tBu)_3$ and iPrCOCl (isobutyryl chloride, **102**) has been used as a reaction conditions. The palladium hydride species can be easily generated from these conditions (Scheme 40). In this, **102** is acting as a hydride source.[46a] Skrydstrup et a. monitored the mixture of $Pd_2(dba)_3$, $P(tBu)_3$ and **102** by ^{31}P NMR. They observed **103** and

105 via NMR. Based on the observed species, they proposed (Scheme 40) that the oxidative addition of **102** to the palladium catalyst (**6**) takes place, which generates a tri-coordinated complex **103**. A vacant site in **103** allows the β-Hydride elimination to take place, which leads to the formation of palladium hydride species (**105**) and ketene (**104**) as a side product.[46a] The **105** species formed in situ can catalyze the *E-Z* isomerization of the olefins.

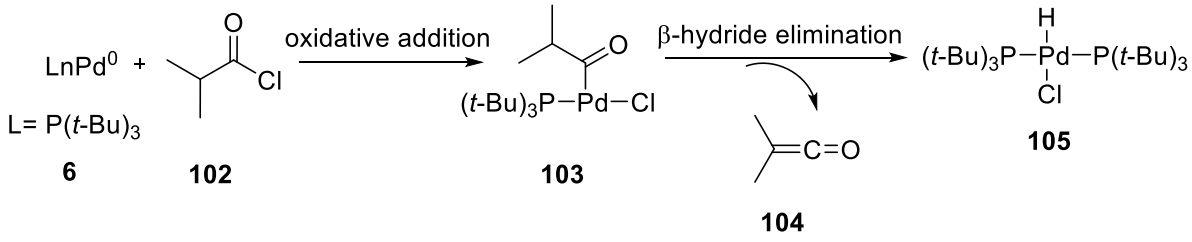

Scheme 40: Mechanism proposed by Skrydstrup et al. for the formation of palladium hydride species.[46a]

As shown in Scheme 41 for *E-Z* isomerization, palladium hydride (**76**) adds to the olefin (***Z*-75**). In **106,** the double bond of the olefin now becomes a single bond, permitting the rotation around the single bond followed by loss of palladium hydride species from **107** via β-Hydride elimination, leading to the isomerized (***E*-75**) olefin. With this, there is a regeneration of the palladium hydride species and hence it acts as a catalyst for *E-Z* isomerization.[50]

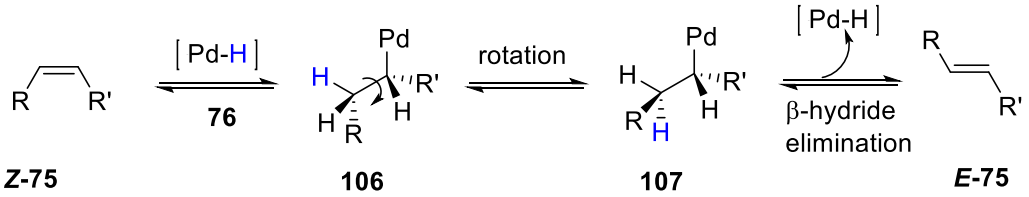

Scheme 41: General mechanism for E-Z isomerization by palladium hydride species.[46a, 50]

Double bond migration

As shown in Scheme 42, migration of double bond in the presence of palladium hydride takes place by sequential migratory insertion of palladium hydride species and β-Hydride elimination. [46a, 47]

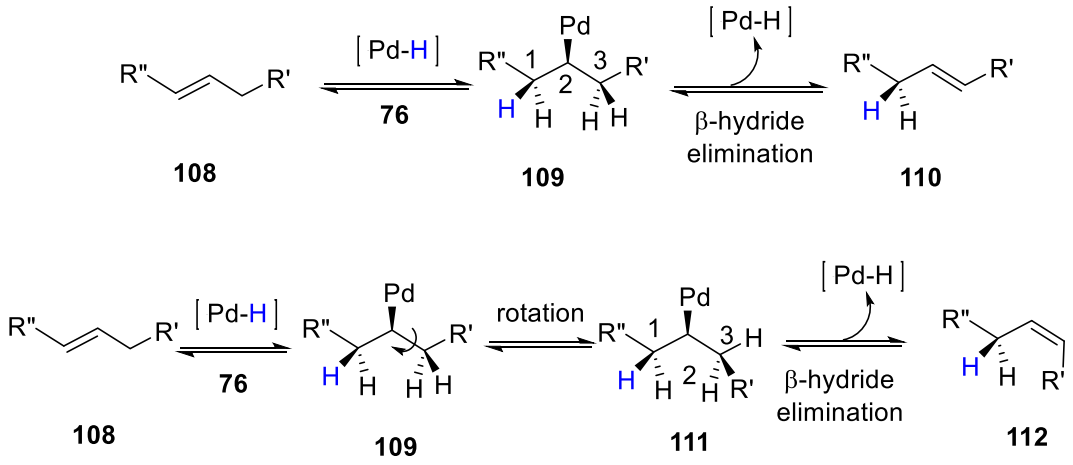

Scheme 42: General mechanism for Double bond migration catalyzed by palladium hydride.

For double bond migration, the palladium hydride species (**76**) adds to the olefin (**108**). This is followed by the β-Hydride elimination with the hydrogen from the adjacent carbon (C_3 in **109**) for the regeneration of the palladium hydride species. If it abstracts hydrogen from C_1 in **109**, then there will be no double bond migration (*E-Z* isomerization could be plausible, Scheme 41) but if the abstraction is from C_3, then there will be double bond migration. If the rotation around the single bond (**111**) takes place prior β-Hydride elimination, then there will be double bond migration as well the *E-Z* isomerization in the outcome (**112**).

The Scheme 43 shows some examples of migration of such a bond. Along with the migration there is some loss in stereochemical integrity, depending on whether the rotation around the single bond takes place prior β-Hydride elimination.

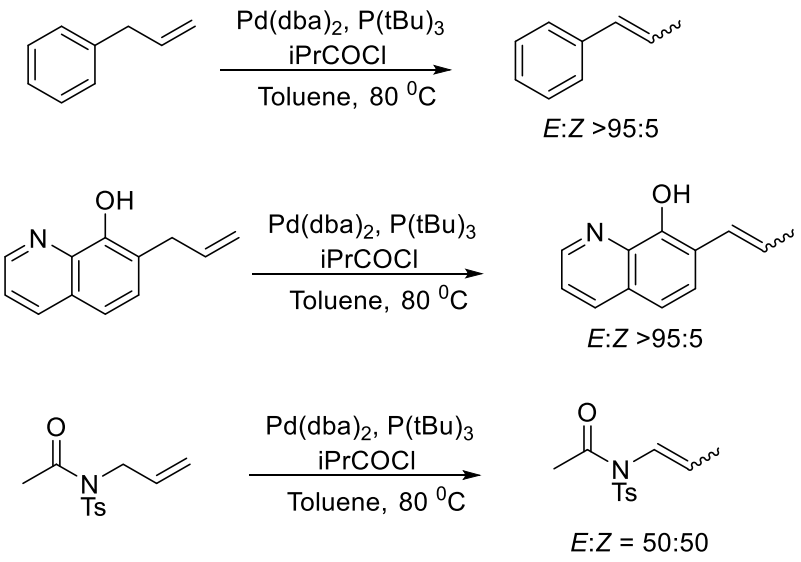

Scheme 43: Examples of migration of double bond catalyzed by palladium hydride species.[46a]

Lipshutz et al. studied the ligand effects on the Negishi, Suzuki and Stille cross coupling of ***Z*-113** (Scheme 44).[51] These three reports highlight the loss of stereochemistry in olefins during the palladium catalyzed cross coupling reactions. They observed that the extent of an isomerization in the reactions depended on the ligand used and synthesized both *E* and *Z* cross coupled product selectivity.

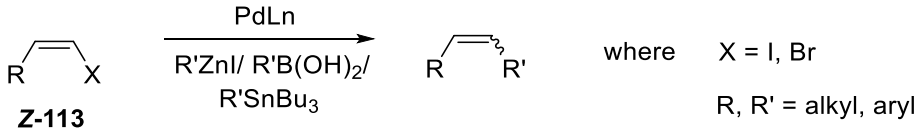

Scheme 44: Loss of stereochemistry in cross coupling at Z olefin centre.

Although the studies primarily targeted the studies of *Z* vinyl halides (***Z*-113**), the isomerization was observed in enone (**114** and **117**) species too (Scheme 45). While studying Stille coupling on enone, almost complete loss of stereochemistry was observed by Lipshutz et. al.[51a] Almost 95% of the isomerized cross coupled product ***E*-116** was observed in Stille cross

coupling of **114** and **115**. Isomerization in enone was also observed in 1991 by Roth et al. while studying Stille coupling on vinyl triflates.[52]

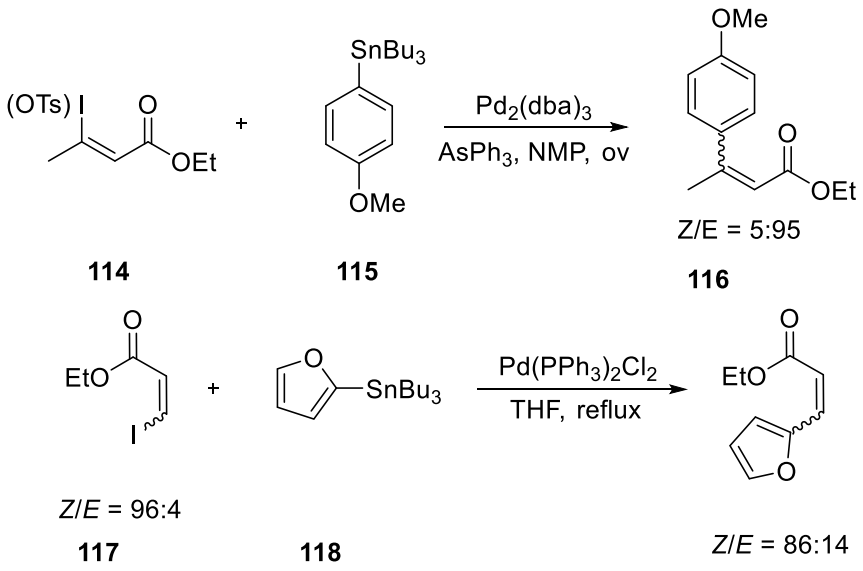

Scheme 45: Loss of stereochemistry during Stille coupling of enone.[51a, 52]

Some isomerization was also observed while performing Suzuki cross coupling on **117** (Scheme 46).[51c]

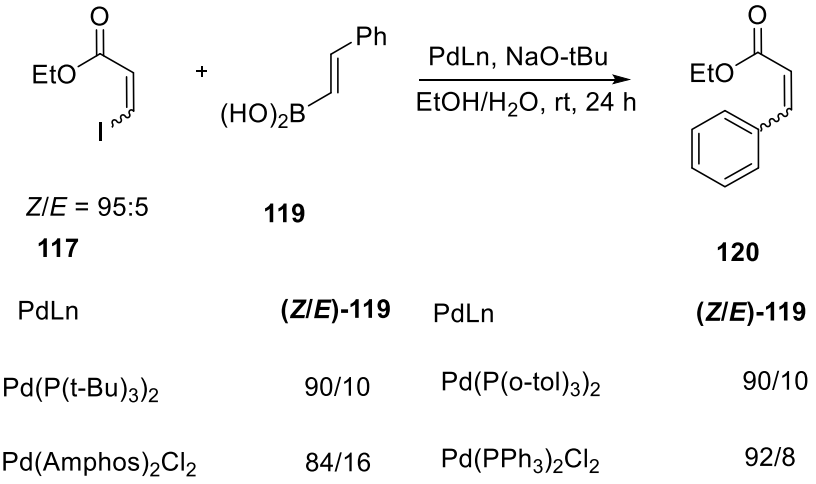

Scheme 46: Ligand effect on the stereochemistry of enone cross coupling.[51c]

Lipshutz et al. observed that the isomerization during Negishi and Stille coupling did not stop with completion of the cross-coupling reaction. To support this observation, they proposed a pathway involving the palladium hydride species responsible for the isomerization (Scheme 47, for mechanism see Scheme 41). This would mean that the palladium hydride species (**76**) are formed in the reaction conditions and can catalyze the isomerization of the ***Z*-75** even after the completion of the cross-coupling reaction. The further discussion of how palladium hydride species may form in the reaction was not mentioned.

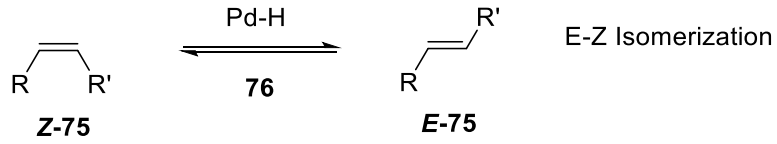

Scheme 47: Loss of stereochemistry via palladium hydride pathway.[51a, 51b]

In yet another report by Jung et al., isomerization of olefin has been observed in the presence of a palladium hydride.[46b] (Scheme 48).

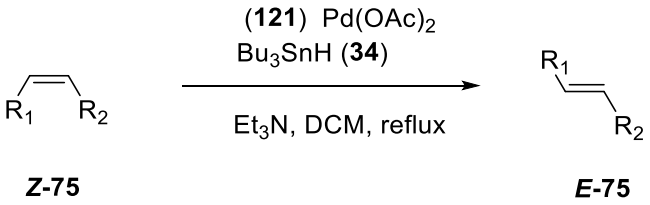

Scheme 48: E-Z isomerization of olefin by Pd-H.

As shown in Scheme 49, in the first step palladium acetate catalyst (**121**) reacts with tributyltin hydride (**34**) and get reduced to Pd(0) species (**6**). Compound **34** does oxidative addition to Pd(0) generating **123**. This is followed by the co-ordination of the *Z*-olefin (***Z*-75**) to the **123** forming **124**. This is followed by insertion of the ***Z*-75** to the palladium hydride species leading to the formation of **125**. After insertion, the double bond of the olefin becomes

a single bond (**126**) permitting the rotation around the single bond. This is followed by β-Hydride elimination leading to the thermodynamically stable *E* alkene (***E*-75**).

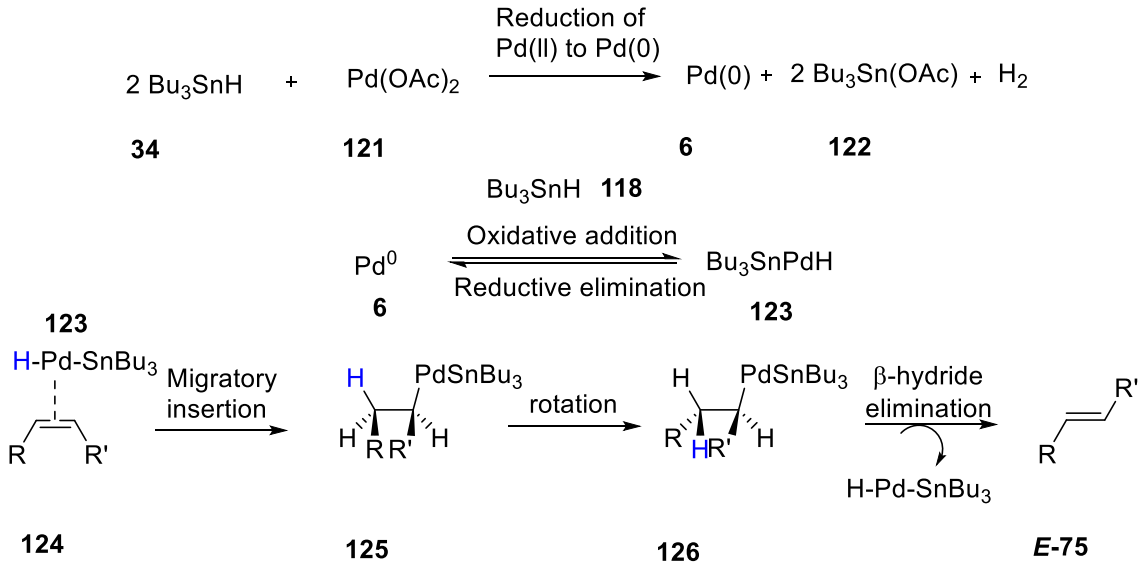

Scheme 49: Proposed mechanism for isomerization by tributyltin hydride.[46b]

Examples of *E*-*Z* isomerization in the presence of tributyltin hydride are shown below in Scheme 50. In all these examples, there is complete conversion of *Z* olefin to thermodynamically stable *E* olefin.

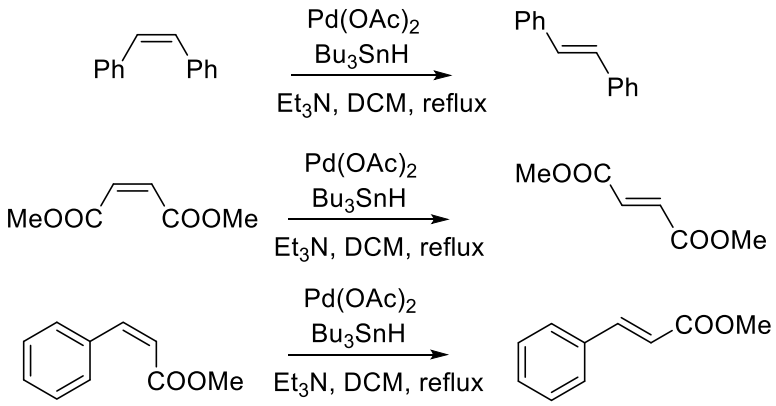

Scheme 50: Examples of E-Z isomerization in the presence of tributyltin hydride.[46b]

Zwitterionic pathway

Mixture of *cis* (**128**) and *trans* (**130**) adducts have been observed during the carbopalladation of alkynes (Scheme 51).[53] Insertion of alkenes and alkynes to M-H or M-C are known as hydrometallation or carbopalladation respectively. In Scheme 51, insertion of alkyne to M-C in **127** generating **128** is a carbopalladation reaction. From stereochemical point of view, insertions are syn.[53a],[53c] This would mean only *cis* adducts (**128**) should form but there have been literature precedents to support the formation of *trans* adducts (**130**).[53-54]

The formation of the *trans* product (**130**) during the carbopalladation has been attributed to the intrinsic zwitterionic character of the vinylmetal intermediate (**129 a, b**) by these authors. This would be expected to weaken a C=C bond, which might allow rotation to occur. The **128** formed from syn insertion transforms to a **130** via **129a, b**.

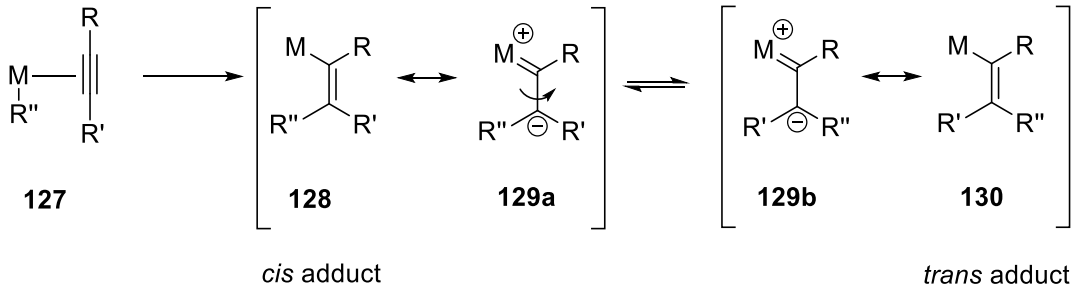

Scheme 51: Formation of trans products during carbopalladation via proposed zwitterionic pathway.[53a]

Jutand et. al studied the mechanism of carbopalladation reaction of alkynes to aryl palladium complexes. As mentioned above, carbopalladation is a reaction between alkyne (**132**) and palladium (II) species (**131**), formed after oxidative addition of aryl/alkyl halide to the palladium. They observed the formation of the **133** along with expected **134**.[53a] (Scheme 52)

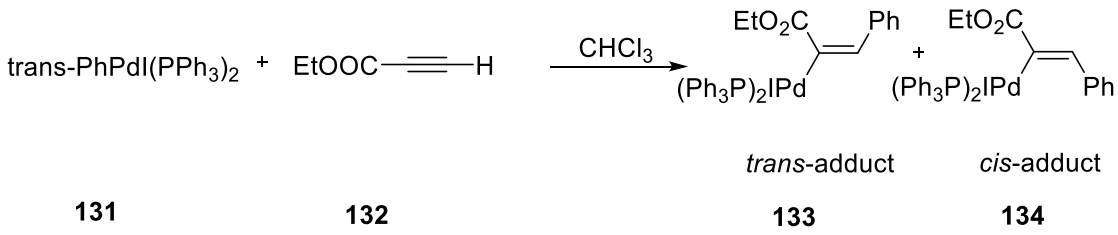

Scheme 52: Carbopalladation of terminal alkyne.[53a]

To probe the mechanism, Jutand et al. synthesized **133** and **134** by an oxidative addition of a mixture of *E* and *Z* vinyl iodides (**135** and **136**) to the palladium catalyst in $CDCl_3$ at room temperature (Scheme 53).

On monitoring the reaction by ^{31}P NMR, it was found that the **134** forms first and then **133** appears. After the completion of the oxidative addition, the ratio of the mixture stabilizes at 64% **133** and 36% **134**. The ratio of the mixture ideally should be 34% **133** and 66% **134** as oxidative addition is stereospecific. To explain the isomerization observed in Scheme 53, Jutand et al. proposed that the isomerization of **134** leads to the formation of the **133** via zwitterionic pathway explained in Scheme 51.

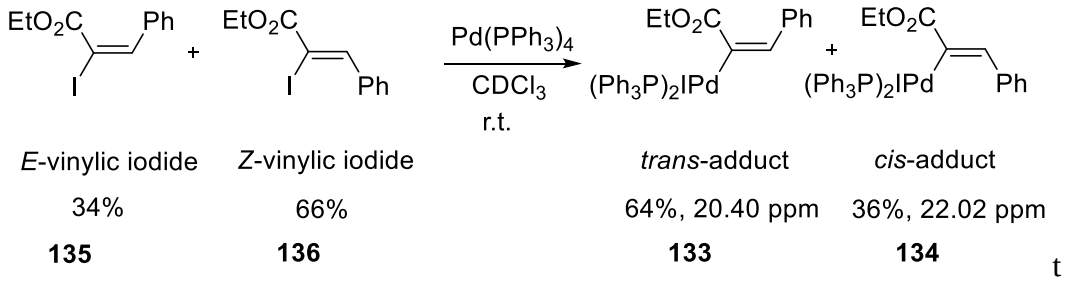

Scheme 53: Synthesis of oxidative addition species from vinyl halides.

As mentioned above, Lipshutz et al. observed isomerization during cross coupling reactions on *Z*-olefins. Some isomerization was also observed while performing Suzuki cross coupling on *Z* vinyl halides and they demonstrated that different ligands gave different extent of isomerization (Scheme 54).[51c]

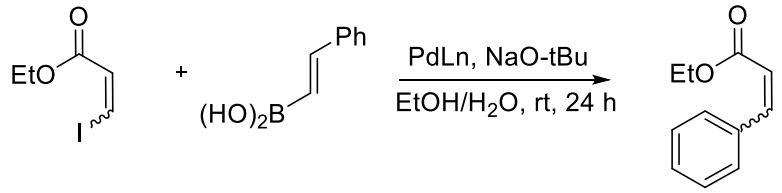

Z/*E* = 95:5

117

120

119

PdLn	(*E*/*Z*)-119	PdLn	(*E*/*Z*)-119
$Pd(P(t\text{-}Bu)_3)_2$	10/90	$Pd(P(o\text{-}tol)_3)_2$	10/90
$Pd(Amphos)_2Cl_2$	16/84	$Pd(PPh_3)_2Cl_2$	8/92

Scheme 54: Ligand effect on the stereochemistry of enone cross coupling.[51c]

For the loss of stereochemistry during Negishi and Stille coupling, Lipshutz et al. have proposed two plausible pathways.[51a, 51b]

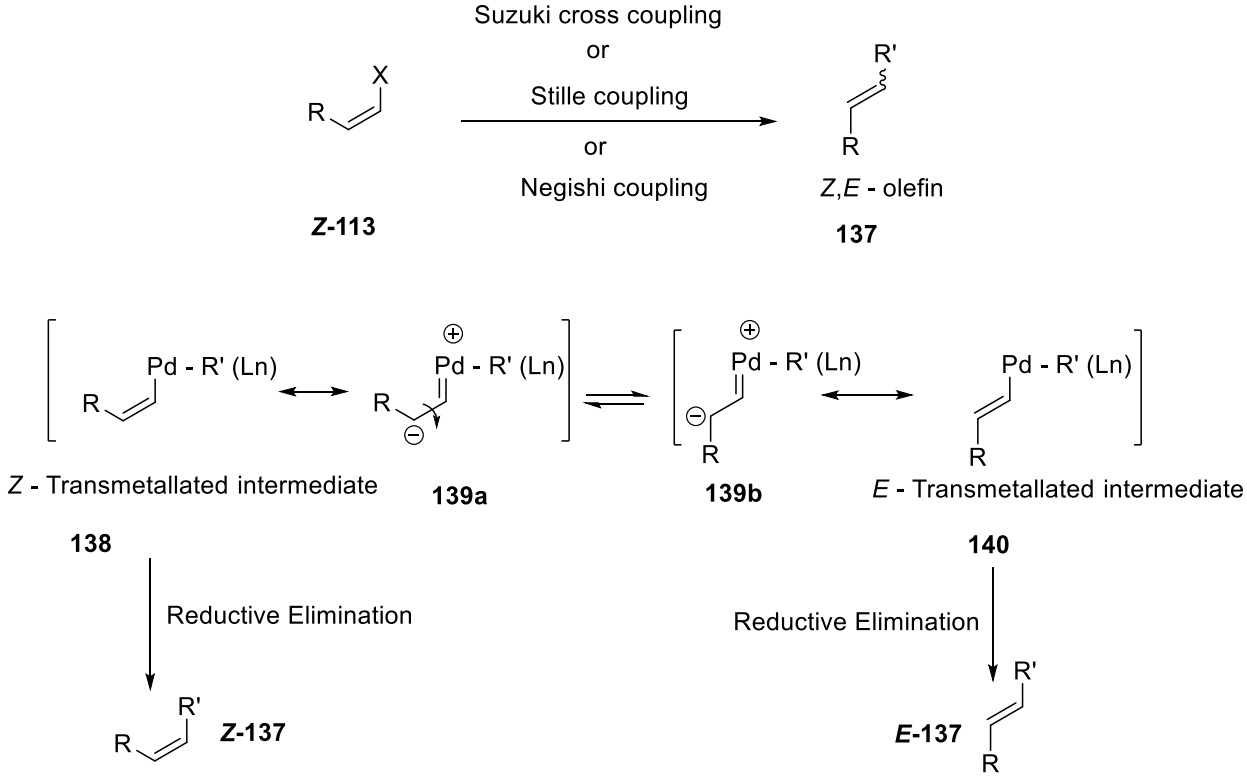

Scheme 55: E-Z isomerization via zwitterionic palladium carbene pathway.

One pathway is the palladium hydride mediated one, which has been discussed above. Another pathway proposed by authors is via zwitterionic palladium carbene **139a, b** (in the transmetallation step) after stereospecific oxidative addition of ***Z*-113** to Pd (0) (Scheme 55). This is the only pathway that has been suggested to be responsible for loss of stereochemistry during Suzuki cross coupling on ***Z*-113**.[51c] According to this mechanism (Scheme 55), either reductive elimination takes place on **138** (formed by the transmetallation of the stereospecific oxidative addition species) leading to the cross coupled product with retention, ***Z*-137** or *Z*-transmetallated intermediate, or **138** can transform to **140** (formed via zwitterionic palladium carbene species **139a, b**) which would eventually lead to the formation of isomerized cross coupled product ***E*-137** by reductive elimination of the **140**.

Seo et al. synthesized 3-(Diarylmethylene)oxindoles (**141**) using Songashira, Heck and Suzuki-Miyaura reactions in one pot (Scheme 56).[55],[56] No issues related to stereochemistry arised when Ar_1 and Ar_2 were the same but when Ar_1 and Ar_2 were different, mixtures of ***E*** and ***Z*-142** were formed.

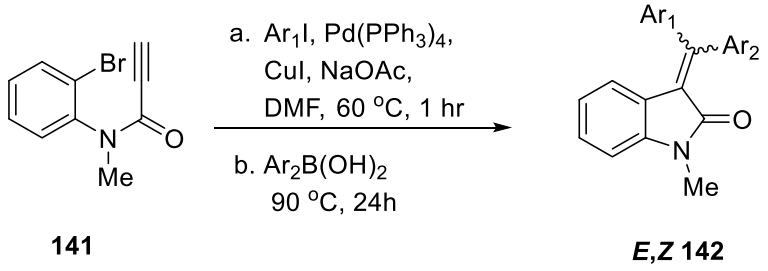

141 ***E*,*Z* 142**

Scheme 56: Synthesis of 3-(Diarylmethylene)oxindoles.

Experimentation was designed to find out whether the isomerization was taking after the product formation or during the reaction. Both pure ***E*** and ***Z*-143** (Scheme 57) were exposed to the reaction conditions and less than 20% isomerization was observed.

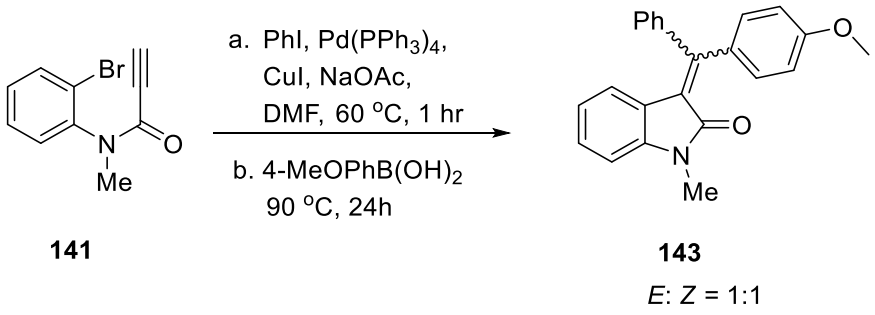

141 **143**

E: *Z* = 1:1

Scheme 57: E-Z isomerization during synthesis of 3-(Diarylmethylene)oxindoles.

After ruling out the isomerization after the product formation, Seo et al. proposed isomerization during the Heck and Suzuki Miyaura reaction via zwitterionic palladium carbene pathway (Scheme 58). According to this interpretation, the vinylpalladium intermediate ***E*-144** is undergoing *E*/*Z* isomerization, which authors justified by proposing that it has the same kind of zwitterionic character as discussed above. The transmetallated intermediate ***E*-145** (formed from the transmetallation on ***E*-144**) leads to the formation of the retention product ***E*-143** and if ***E*-144** transforms to ***Z*-144** via zwitterionic vinyl palladium carbene (**146a, b**) it can lead to the formation of the isomerized product ***Z*-143** (formed from the transmetallation on ***Z*-145**).

Based on this mechanism, Seo et al. further proposed that using the silver additives in the reactions can improve the selectivity of the outcome. Silver additives are known for changing a neutral palladium catalytic cycle to the cationic pathway.[57] They proposed that in the cationic pathway for the Heck reaction[58], palladium metal possesses the positive charge (**147**, Scheme 59) and with this positively charged species in the catalytic cycle, the formation of the zwitterionic species (**146**) will become difficult and hence the isomerization pathway (Scheme 58) will get suppressed.

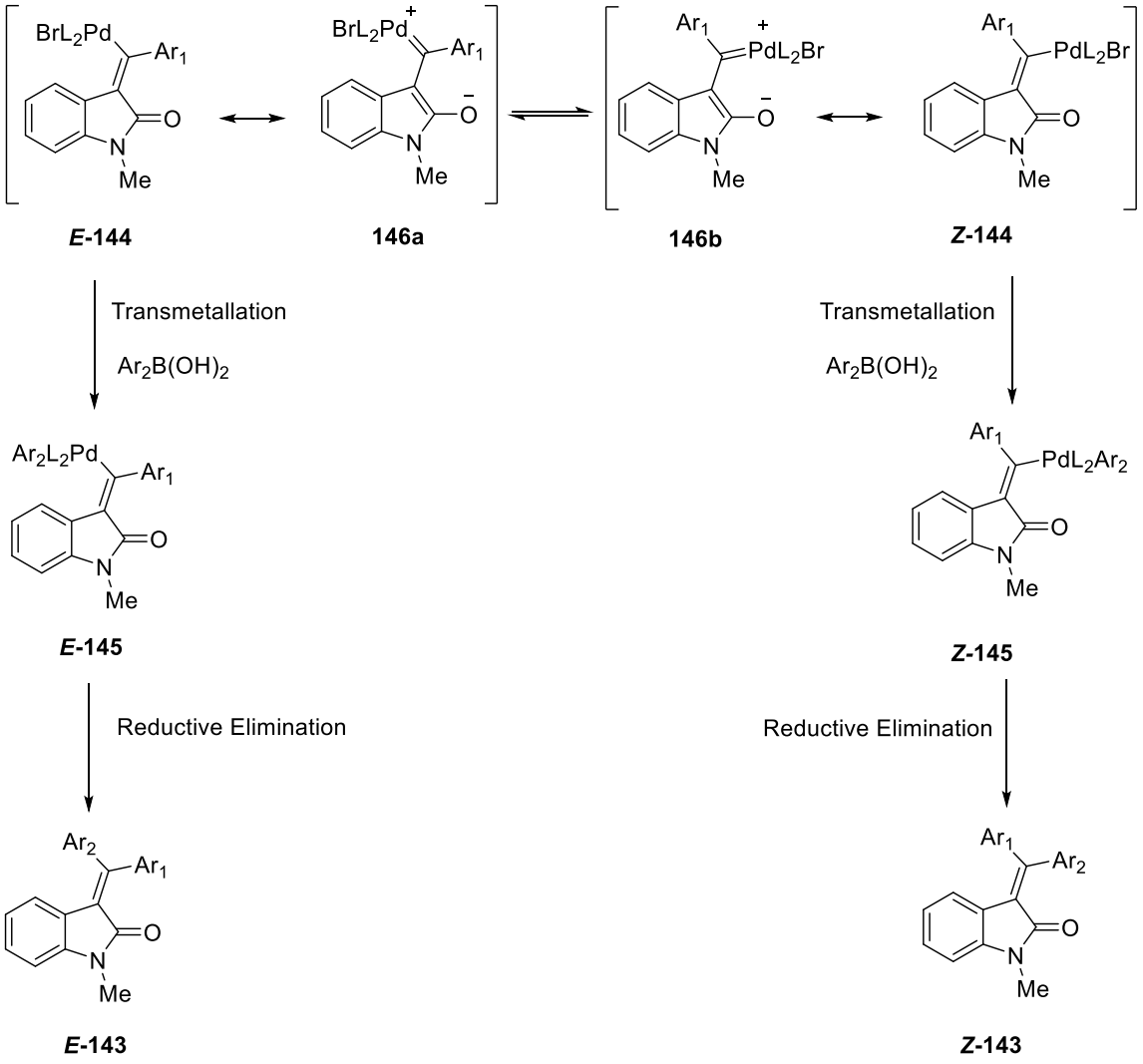

Scheme 58: Proposed mechanism for loss of stereochemistry in 3-(Diarylmethylene)oxindoles.

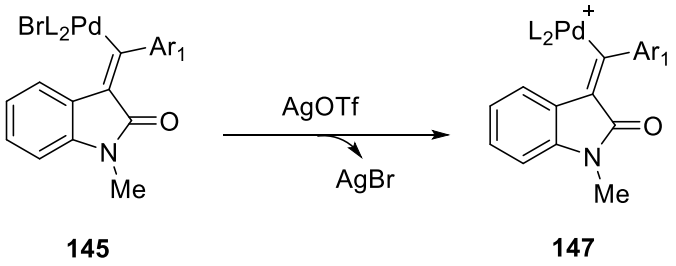

Scheme 59: Positively charged palladium species during cationic Heck coupling pathway.

To test this hypothesis, they added a silver additive in the reaction (Scheme 60). It was observed that the selectivity of the outcome improved, and it yielded expected ***E*-143** isomer selectively. This experiment strengthened the mechanistic pathway proposed by Seo et al.

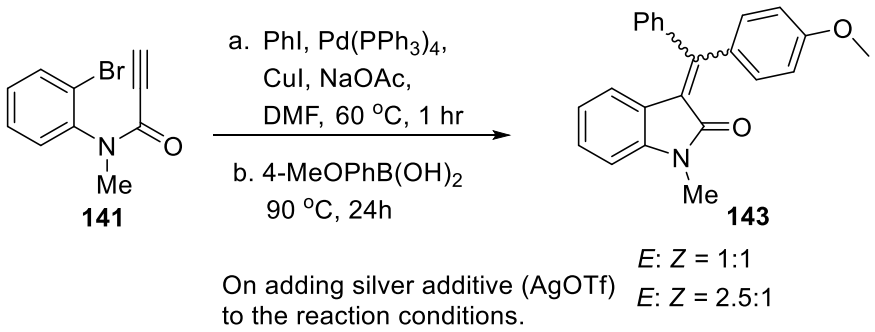

Scheme 60: Addition of silver additives in synthesis of 3-(Diarylmethylene)oxindoles.

This mechanism has been proposed for other metals like rhodium, nickel and ruthenium. This mechanism was proposed by Bergmann et al. to support the formation of the trans insertion product while studying the reaction of alkynes in the presence of the nickel catalyst (Scheme 61).[59] Schwartz et al. proposed the zwitterionic pathway to explain isomerization in vinylic rhodium complexes (Scheme 62).[54a] Trost et al. explained anti addition product during ruthenium catalyzed hydrosilylation (Scheme 63).[54b]

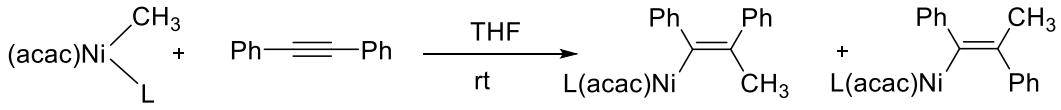

Scheme 61: Nickel catalyzed carbopalladation of alkynes.[59]

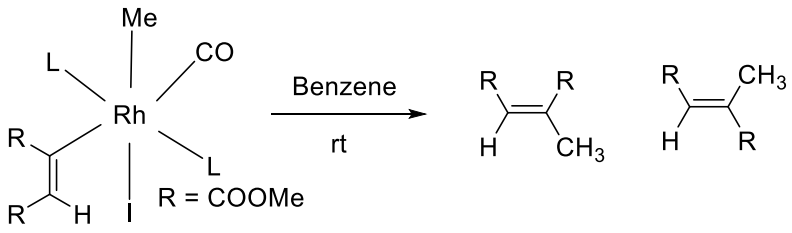

Scheme 62: Isomerization in vinylic rhodium complexes.

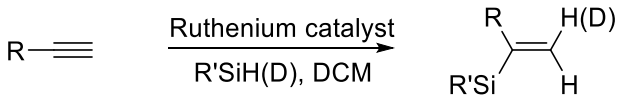

Scheme 63: Loss of stereochemistry during hydrosilylation catalyzed by ruthenium complexes.[54b]

Co-ordination pathway

The *E*-*Z* isomerization of the olefins by coordination to the [Pd] was proposed by Visentin et al.[60] They observed that dimethyl maleate (***Z*-148**) isomerizes to dimethyl fumarate (***E*-148**) in the presence of catalytic amount of the palladium catalyst (**149**) in deuterated chloroform at room temperature (Scheme 64).

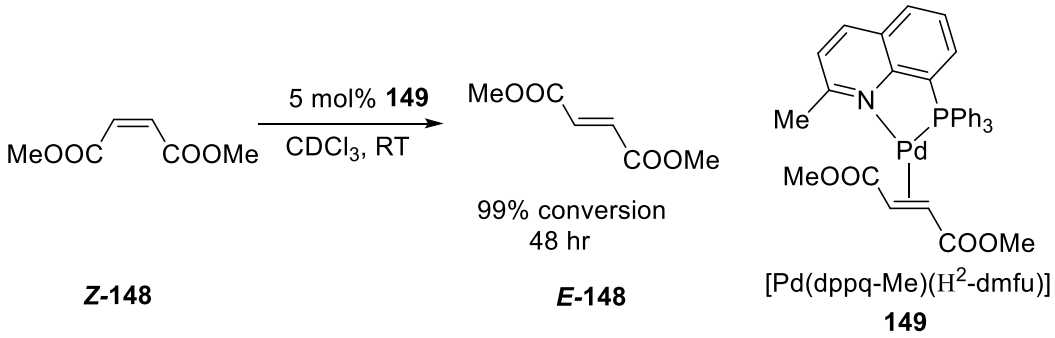

Scheme 64: Isomerization of dimethyl maleate to dimethyl fumarate.

To propose their observation, authors suggested a pathway that involves just the olefin and the palladium catalyst. (Scheme 65).

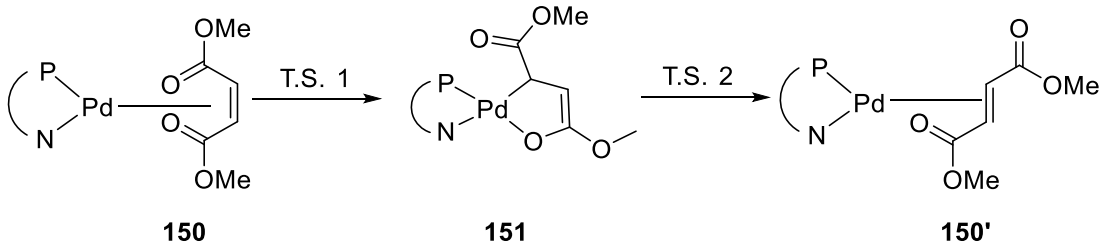

Scheme 65: E-Z isomerization of Z-alkene in the presence of the [Pd].[60]

According to this mechanism, the electron poor olefin (in this case ***Z*-148**) coordinates to the palladium metal (**150**). This leads to the five membered metallacycle intermediate (**151**) via transition state TS 1. It converts to the thermodynamically stable dimethyl fumarate coordinated to the palladium (**150'**) via TS 2 and finally dissociates into ***E*-148** and regenerates the palladium catalyst (Scheme 65).

This mechanism has been proposed as a pathway for the observed isomerization during the palladium catalyzed stereoselective synthesis of diarylallylidene oxindoles (**154**) by Seo et. al.[61] They synthesized **154** from propiolamide (**141**), aryl iodide (**152**) and styrylboronic acid (**153**) by using three different reactions i.e. Sonogashira, Heck and Suzuki in one pot (Scheme 66). It was observed that *E-Z* isomerization can be controlled by selective use of the ligands which led them to stereoselectively synthesize both ***E*** and ***Z*-154** isomers. The ***Z*-154** isomer was synthesized by using *t*-Bu-Xantphos as a ligand and ***E*-154** isomer was synthesized by using PPh_3 as a ligand.

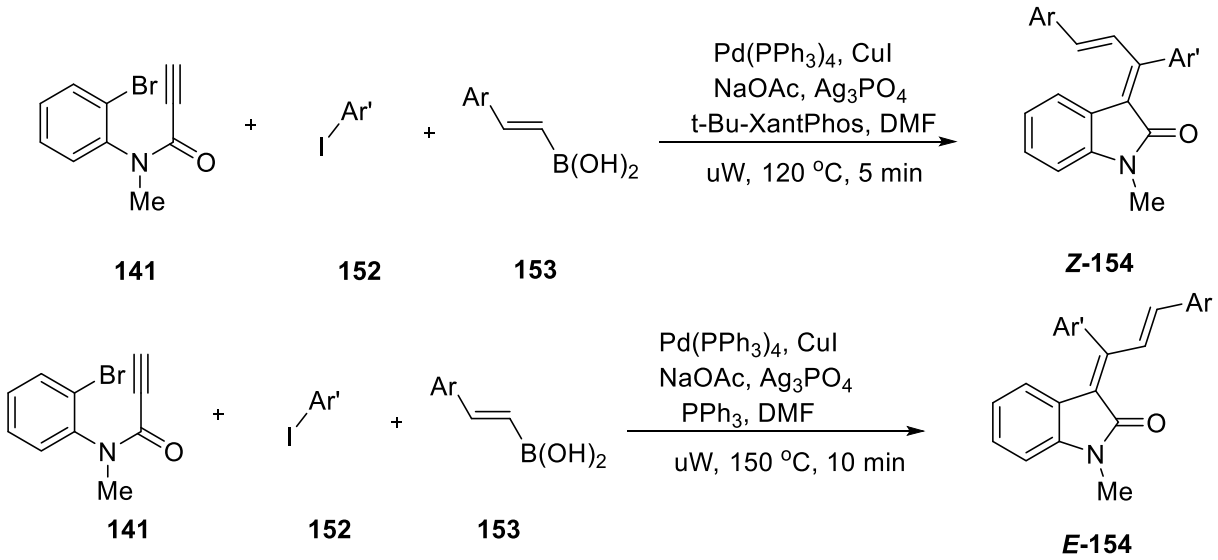

Scheme 66: Ligand controlled stereoselective synthesis of Z and E-oxindoles.

To understand the isomerization mechanism, the ***Z*-154** and ***E* -154** products were exposed to all the reagents used in the reaction conditions. It was found that when ***Z*-154** was exposed to the reagents (Scheme 67), 66% formation of ***E*-154** was observed, whereas when ***E*-154** isomer was exposed to the reagents used in Scheme 67, only 2% formation of ***Z*-154** was observed. This experiment clarified that ***Z*-154** isomer forms first in the reaction and then it isomerizes to the ***E*-154**.

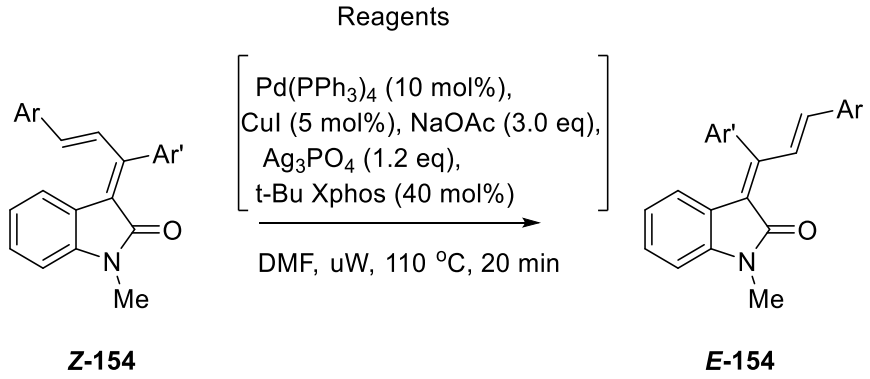

Scheme 67: Isomerization studies on Z-isomer.

Further, the individual reagent studies were performed on the ***Z*-154** (Scheme 68). Without any reagent only 14% isomerization was observed, which remained the same in the presence of phosphine ligands, triphenyl phosphine (40 mol%) and t-Bu Xantphos (40 mol%). This ruled out the isomerization by phosphine ligands. It was observed that 98% isomerization of ***Z*-154** to ***E*-154** takes place in the presence of $Pd(PPh_3)_4$ and 58% isomerization of ***Z*-154** to ***E*-154** was observed in the presence of the 5 mol% CuI. This experiment suggested that $Pd(PPh_3)_4$ and CuI are the major contributors in the isomerization of ***Z*-154** to ***E*-154**.

To support the observation, it has been suggested by the authors that the isomerization can take place via coordination of metal (both metals palladium and copper) to the pi-system of the ***Z*-154** which can then proceed via pathway suggested by Visentin et al. in Scheme 65.[60] No

suggestions has been made to why the presence of PPh_3 would selectively lead to the formation of ***E*-154** and *t*-Bu-XPhos would selectively lead to the formation of ***Z*-154**.

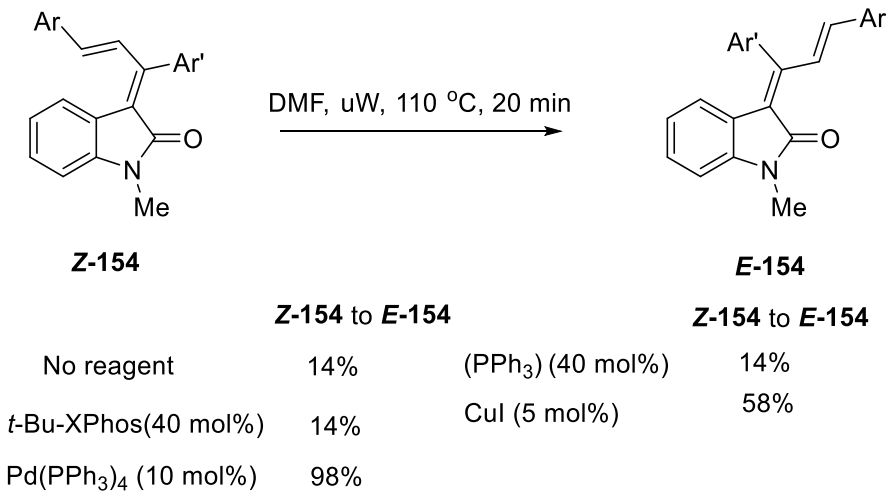

Scheme 68: Individual studies on (***Z*-154**).

Poisson et. al synthesized trifluoromethylated 1,3-butadienes (**157**) by palladium catalyzed directed C-H functionalization of acrylamides **155** with **156**.[62] The ***Z*-157** isomers were formed when R was any aryl group in acrylamide substrate (Scheme 69) but ***E*-157** isomers were formed when simple acrylamide substrates were used i.e. R = H (Scheme 70).

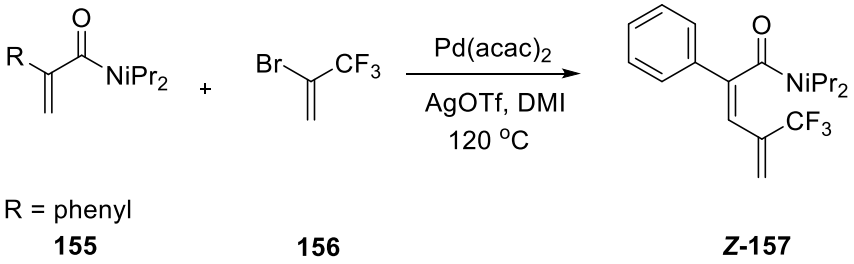

Scheme 69: Stereoselective synthesis of trifluoromethylated 1,3-butadienes by palladium catalyzed directed C-H functionalization.

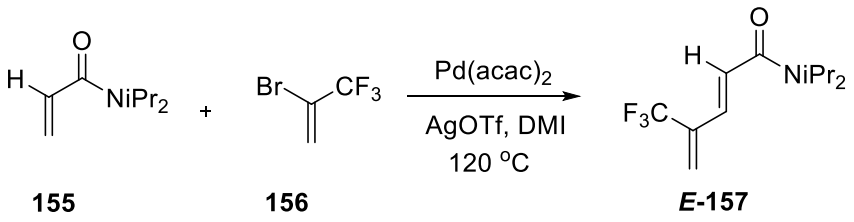

155 **156** ***E*-157**

Scheme 70: Palladium catalyzed directed C-H functionalization of simple acrylamides results in E isomer.

The authors suggested the formation of the opposite isomer i.e. ***E*-157** could arise from the palladium catalyzed isomerization of the ***Z*-157** via mechanism proposed Visentin et al. in Scheme 65. No further isomerization studies have been presented by the authors.

Moran et. al synthesized *E* and *Z* olefins by nickel catalyzed selective reduction of alkynes in the presence of zinc metal and formic acid.[63] They discovered that ***Z*-160** olefins can be selectively synthesized by exposing **158** to the nickel catalyst, zinc and formic acid in dioxane whereas the presence of triphos ligand (**159**) along with nickel catalyst, zinc and formic acid in dioxane allowed them the access to the ***E*-160** (Scheme 71).

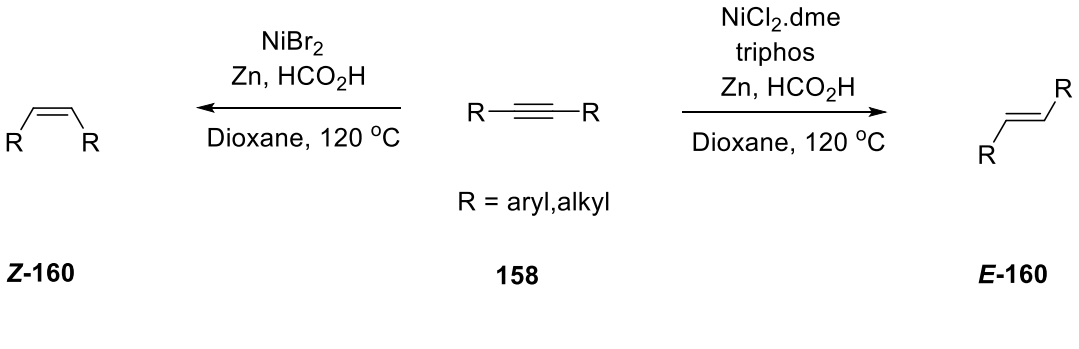

***Z*-160** **158** ***E*-160**

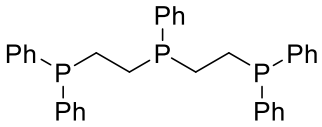

Triphos

159

Scheme 71: Ligand controlled synthesis of E and Z olefins by nickel catalyzed transfer hydrogenative alkyne semireduction.

To study the role of the triphos ligand, authors exposed *Z*-stilbene (***Z*-161**) to both the reaction conditions. It was found that no isomerization took place in the absence of the phosphine ligand whereas complete isomerization took place in one hour at 120 °C in the presence of the triphos ligand (Scheme 72).

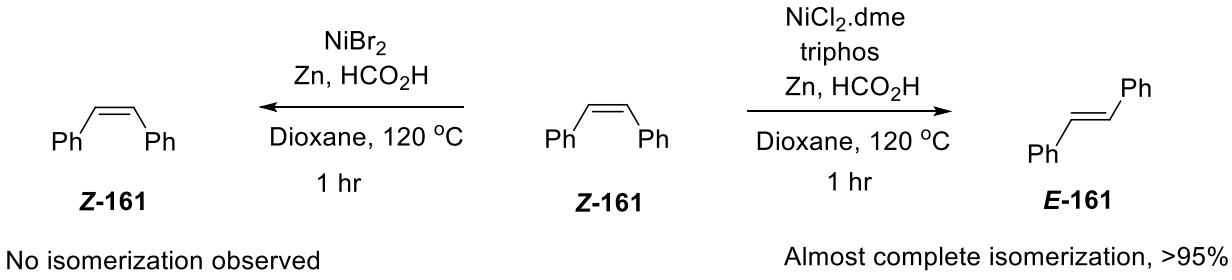

Scheme 72: Isomerization studies on stilbene.

Based on this observation, the authors suggested the formation of ***Z*-161** takes place first which is then followed by the rapid Ni-triphos complex catalyzed isomerization. They have referenced metal hydride pathways and the pathway suggested by Visentin et al. to support a rapid isomerization process. Further studies regarding isomerization have not been mentioned by the authors. This does not seem to take into account the Visentin's emphasis of the critical role of enone for the mechanism as stilbene does not have any enone functionality in them.[60] Metal hydrides pathway could be reasonable for these olefins as plethora of alkenes have been demonstrated to isomerize in the presence of the metal hydride.[46a]

CHAPTER-2: Results and discussions

2.1. Initial plan

In recent years, our research group has focussed on the cross-coupling reactions of substrates possessing the dichlorovinyl functionality. The previous graduate student from our research lab studied Suzuki cross coupling reactions on 1,2-dichlorovinylphenyl ether substrate (***E*-162**).[64] It was found that first Suzuki cross coupling exclusively took place on the α carbon-chlorine bond. Different tetra-substituted alkenes were synthesized by doing a second cross coupling on the β C-Cl bond and different α-substituted benzofurans were synthesized by C-H activation. On the same lines, I chose to study Suzuki cross coupling reactions on 1,2-dichlorovinylphenyl ketone (***E*-1**).

***E*-1** ***E*-162**

Figure 4: The structure of 1,2-dichlorovinylphenyl ether.

This seemed interesting because the electronic environment of the vinyl halide groups in ***E*-1** is quite different from that in ***E*-162** and this gives the opportunity to study the reactivity of two electronically different substrates under the Suzuki cross coupling conditions. To study how electronic differences can affect the regioselectivity of the substrate, the first step of the plan was to study whether the first Suzuki cross coupling selectively takes place at α C-Cl bond or it takes place at β C-Cl bond in ***E*-1**. A plan was made to extend this project (Scheme 73). This depended on the site of the first cross coupling. If the cross coupling took place at α carbon first, then it could be followed by C-H activation to close the ring. This two-step reaction (Path

B) can result in the synthesis of the 2-substituted indenones (**165)**. If cross coupling took place at the β position, then instead of doing cross coupling first, C-H activation could be used in the first step to close the ring and then cross coupling could be done to synthesize **165** (Path A).

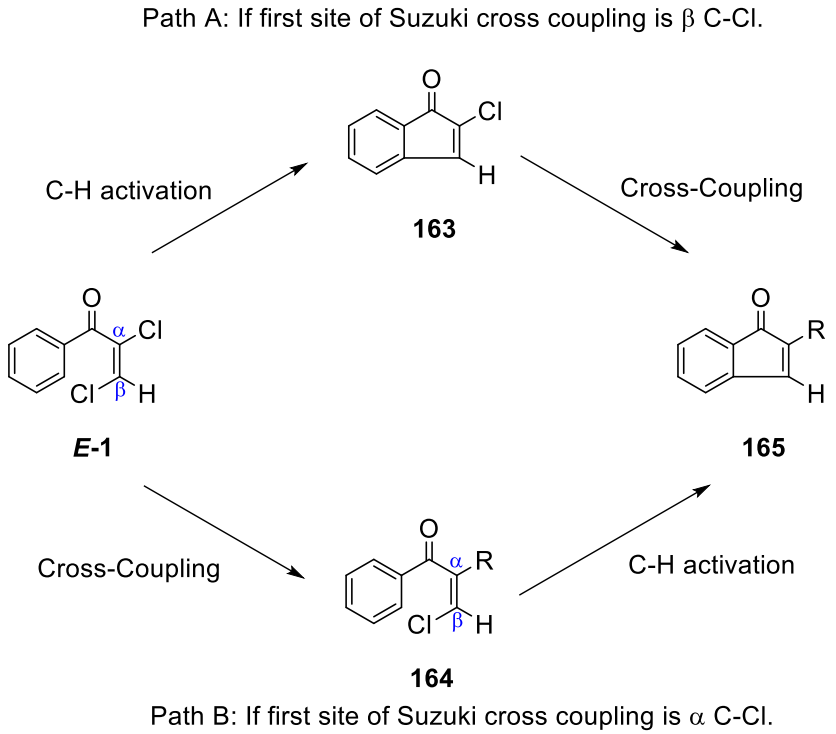

Scheme 73: Schematic representation of the plan for the synthesis of 2-substituted indanones.

While doing experimentation, it was observed that the Suzuki cross coupling on ***E*-1** was regioselective at the β C-Cl bond. This clearly suggests that there will never be a formation of **164** and hence the path B can not be continued for the synthesis of the **165**. Following path A, an attempt was made to synthesize α-chloro indenone **163**. For this ***E*-1** was reacted with palladium catalyst and base in the presence of dioxane at reflux conditions. No formation of indenone (**163**) was observed and after this no further attempts were made to synthesize **163**.

Along the studies, it was found that the Suzuki cross coupling were not only regioselective at β position but also led to the loss of stereochemistry in the Suzuki cross coupled product

(Scheme 74). I found the loss of stereochemistry very intriguing and decided to concentrate on the stereoselectivity of the cross-coupling reaction rather than synthesizing 2-substituted indenones (**165**).

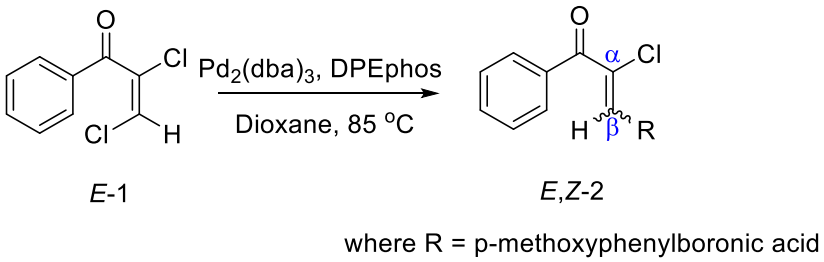

Scheme 74: Loss of stereochemistry in the Suzuki cross coupled product.

2.2. Synthesis of 1, 2-dichlorovinylphenyl ketone

The synthesis of the 1,2-dichlorovinylphenyl ketone (***E*-1**) was done by using two step procedure mentioned in the literature.[65] The schematic representation is shown below in Scheme 75. Step 1 of the reaction was done by using the procedure from Jonczyk et al.[65] The synthetic procedure described in the same paper for compound ***E*-1** did not give complete conversion. However, another procedure from the same laboratory for methyl 2-formylphenylacetate gave full conversion and was used for the synthesis of ***E*-1** from ***E*-167**.[66]

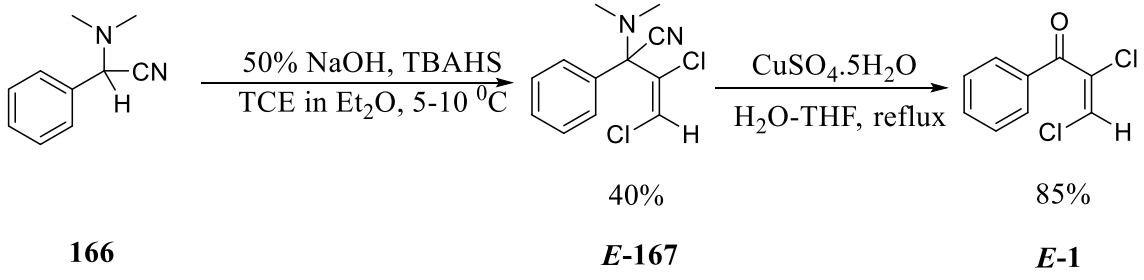

Scheme 75: Two step synthesis of 1,2- dichlorovinylphenyl ketone.[65]

The two-step procedure employs an Umpolung approach[67] as there is an inversion of polarity at the carbon. This is a nucleophilic acylation with α-aminonitrile functionality acting

as an acyl anion equivalent.[68] It was discovered by Hauser et al. in 1960 that compound **166** can be alkylated, followed by unmasking the α-aminonitrile functionality to yield carbonyl compounds.[69] This discovery encouraged this class of compounds to be used as latent acyl carbanions.[66, 70]

In the first step, **166** reacts with trichloroethylene (**168**) in the presence of base, 50% and phase transfer reagent, tetrabutylammonium hydrogen sulfate (TBAHS) (Scheme 75).[65]

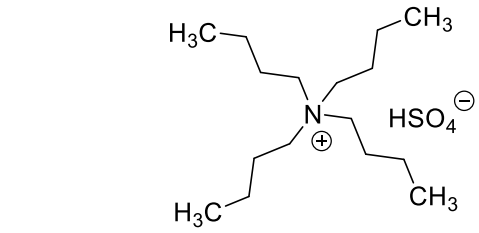

TBAHS (tetrabutylammonium hydrogen sulfate)

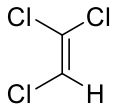

TCE (tetrachloroethylene)
165

Scheme 76: Structures of tetrabutylammonium hydrogen sulfate (TBAHS) and tetrachloro ethylene (TCE).

The mechanism postulated by Jonczyk et al. is as follows (Scheme 77). In the first step, **166** is deprotonated using sodium hydroxide under phase transfer conditions and the carbanion thus generated (**170**) acts as a nucleophile and adds to the electrophilic dichloroacetylene (**169**) leading to the formation of the **167**. The dichloroacetylene (**169**) is generated by the elimination of hydrogen chloride from trichloroethylene (**168**) in the presence of the base via an E1cb mechanism.[65, 71]

It was postulated that the carbanion (**170**) adds to the dichloroacetylene (**169**) in a trans fashion giving rise to *E* stereochemistry in **167**.[65, 72] The trans addition of the carbanion disfavours the further elimination of hydrogen chloride, so that the reaction stops at **167**. The ***Z*-167** was never observed in these experiments. The stereochemistry of the compounds **167** and **1** have been assumed to be *E* in the literature.

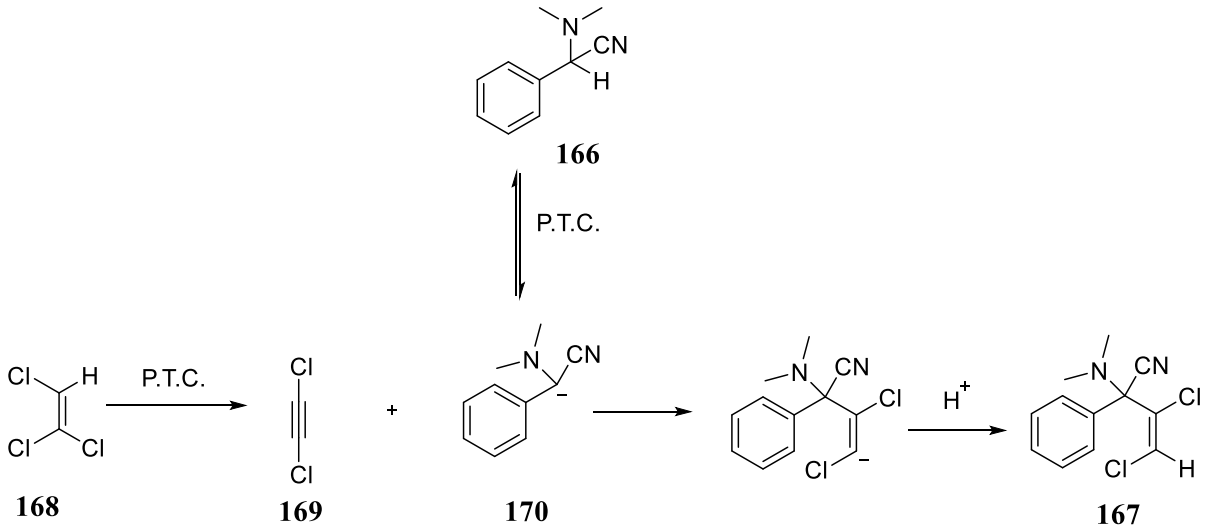

Scheme 77: Mechanism proposed by Jonczyk for the synthesis of (***E-164***)**.**

As mentioned above, in the second step the carbonyl functionality is unmasked by the hydrolysis of the dimethylamino functionality of **167**. This mode of reactivity of α-amino nitriles is extremely useful as in this the aminonitrile functionality behaves as masked acyl anion equivalent and is used to convert α-aminonitrile to carbonyl compounds.[68] The second step of the reaction was carried out in the presence of copper sulfate following the procedure described in the literature.[66] It was observed by Buchi et al. in 1978 that copper sulfateμμ accelerates the hydrolysis of aminonitriles.[70d] They reasoned that copper removes cyanide from the aminonitrile-iminium cyanide equilibrium as shown in Scheme 78.

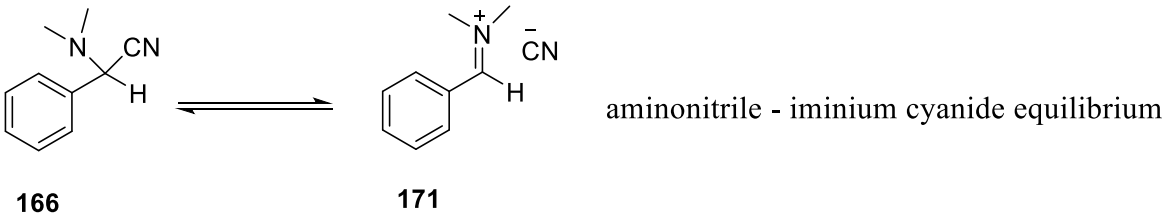

Scheme 78: Aminonitrile - iminium cyanide equilibrium and role of copper sulfate.

2.3. Determination of the regioselectivity of Pd catalyzed Suzuki cross coupling

The general catalytic cycle of Suzuki cross-coupling is comprised of three steps: oxidative addition, transmetallation and reductive elimination (Figure 5).[73] Site selectivity in cross-coupling reactions is governed by the insertion of palladium in the carbon-halogen bond during the oxidative addition step.[74]

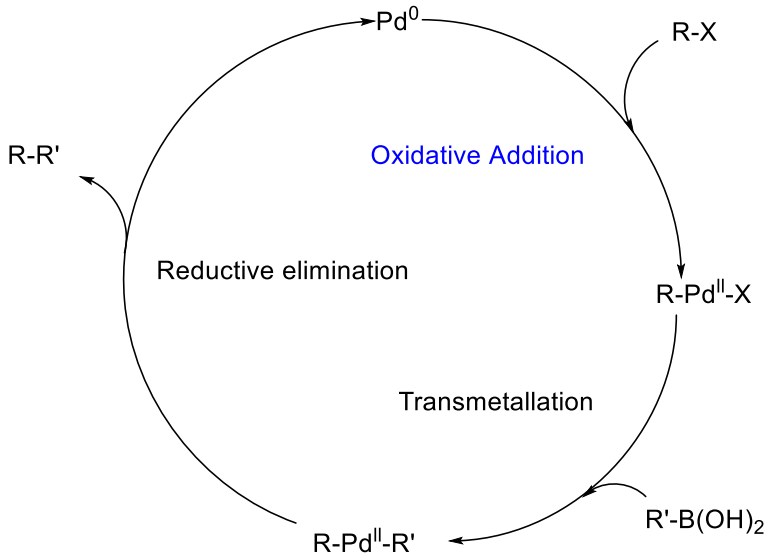

Figure 5: General catalytic cycle for Suzuki cross coupling reaction.

The palladium inserts in the more electrophilic C-X bond.[74] In compounds possessing enone functionality, it can be easily predicted that the β position is more electrophilic than the α position and hence it should be the first site of cross-coupling. Also, it has been reported previously that the β position is the first site of Suzuki cross-coupling in 2,3-dibromo-1*H*-inden-1-one (**172**)[75] and 3,4-dibromo-2(5*H*)-furanone (**173**)[76]. Based on our predictions and literature support, the β site was the predicted site of first cross coupling in ***E*-1**.

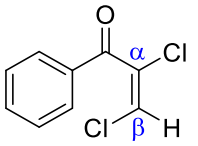

1,2- dichloro vinyl phenyl ketone

1

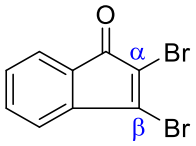

2,3 - dibromo-1H-inden-1-one

172

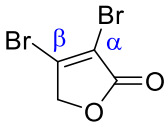

173

Figure 6: Structures of 1,2- dichloro vinyl phenyl ketone, 2,3- dibromo-1H-indenone-1-one[75] and 2,3-dibromofuranone[76].

Experimental studies verified the site of the attack. The very first Suzuki cross coupling was performed on ***E*-2** with 6 mol% $Pd(PPh_3)_4$, 2 M aqueous K_2CO_3 and 1 equivalent of *p*-methoxyphenyl boronic acid in dioxane at 65 °C (Scheme 79).[75]

The reaction was analyzed after 25 min with GC-MS. The complete consumption of ***E*-2** with formation of two new peaks of the same m/z i.e. 272 were observed in the chromatogram. The two peaks in the ratio of 24: 76 for the same mass suggested the formation of the isomers in the reaction (Figure 7).

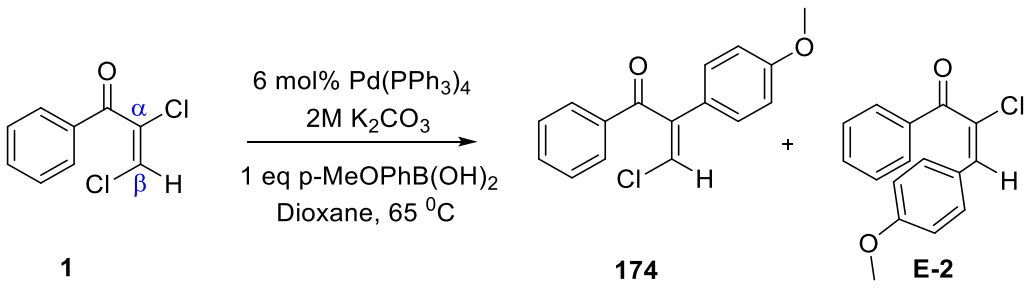

1 **174** **E-2**

Presumed Regioisomers

Scheme 79: Presumed synthesis of isomers during first Suzuki cross coupling.

With two possible sites of cross coupling in **1**, it was *presumed* that this cross-coupling was not regioselective and had formed regioisomers **174** and ***E*-2**.

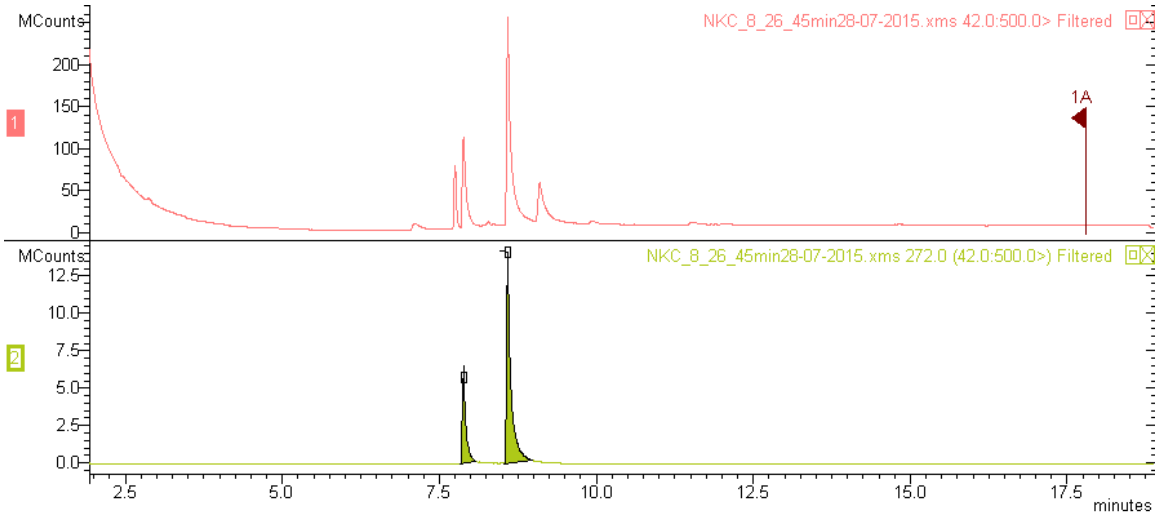

Figure 7: Two peaks of m/z 272 observed by GC-MS.

2.4 Identification of the unexpected product: Losing stereocontrol instead of regiocontrol

The first challenge was to identify the two product isomers. The lack of protons in **174** and ***E*-2** posed a restriction in identifying two compounds solely by routine NMR. To overcome this challenge, ozonolysis was performed on the presumed regioisomers (**174** and ***E*-2**). The isomers were isolated and exposed to the ozonolysis conditions (Scheme 80).

As shown below, regioisomer ***E*-2** would lead to the formation of the **175** and 4-methoxybenzaldehyde (**176**) whereas regioisomer **174** would lead to the formation of the diketone (**177**) and formyl chloride (**178**), which would further decompose into HCl and CO. With this approach, the formation of the 4-methoxybenzaldehyde (**176**) would indicate regioisomer ***E*-2** and absence of 4-methoxybenzaldehyde (**176**) would mean regioisomer **174**.

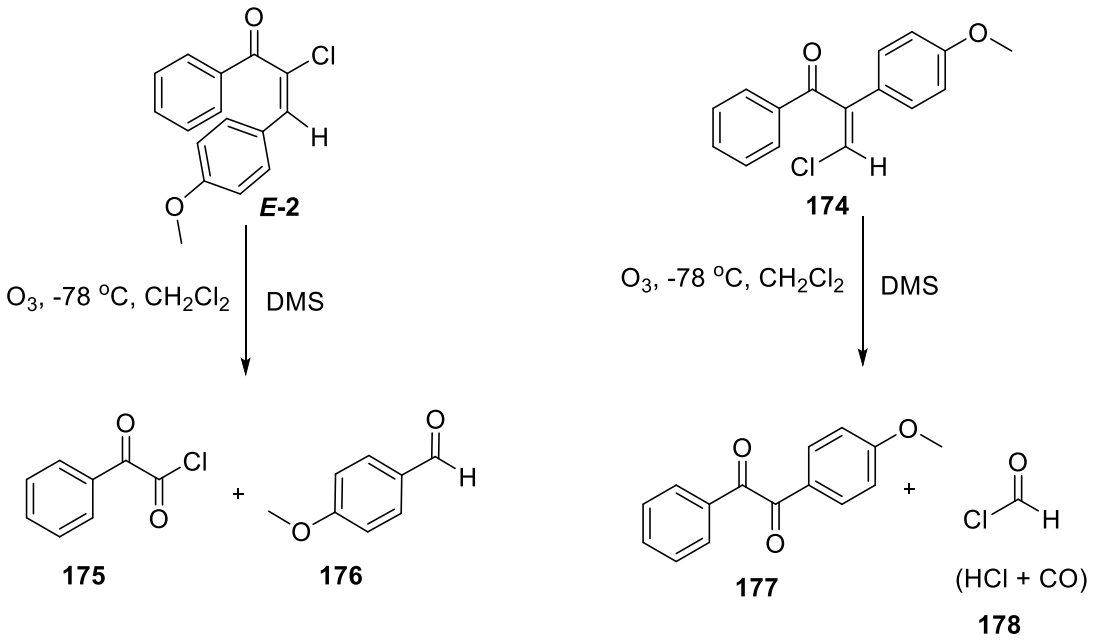

Scheme 80: Expected product from the Ozonolysis on regioisomers.

On experimentation, it was observed that both the isolated isomers gave 4-methoxy benzaldehyde (**176**). The only plausible way for both the isomers to give 4-methoxy benzaldehyde (**176**) on ozonolysis is if they are stereoisomers (***E*-2** and **Z-2**) and not regioisomers (***E*-2** and **174**) (Figure 8).

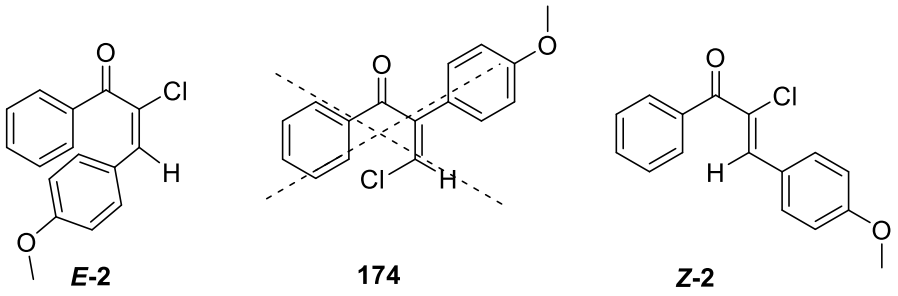

Figure 8: Stereoisomers (instead of Regio isomers) formation during Suzuki cross coupling on 1,2-dichlorovinylphenylketone.

This experiment helped in verifying that stereoisomers (***E*-2** and ***Z*-2**) were formed instead of regioisomers (***E*-2** and **174**) but did not give any information about the major isomer. It was

presumed that the major isomer would be ***E*-2** since the retention of configuration is normally formed during Suzuki cross coupling reactions.[2a]

To identify the major and minor isomer, a second cross coupling with methyl boronic acid was performed on an 80:20 mixture of isomers (***Z*-2** and ***E*-2**). The second cross coupling with methyl boronic acid was performed with the aim of doing NOE studies on the resulting α-methylated Suzuki cross coupled product (***E*-179** and ***Z*-179**) (Figure 9). The magnitude of the NOE enhancement between methyl and vinylic protons by irradiating either methyl or vinylic protons could help in elucidating the isomers.

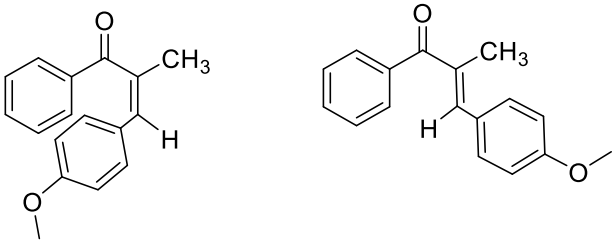

Isolated minor isomer
***Z*-179**

Isolated major isomer
***E*-179**

*Figure 9: Stereoisomers formed after second cross coupling on mixture of isomers, (**Z/E-2**).*

On experimentation, the mixture of isomers (***E*** and ***Z*-179**) was formed in the ratio 89:11 in 74% yield. The NOE studies were performed on the mixture of isomers (Figure 10).

On irradiating the methyl protons of the isolated major isomer, it was found that the magnitude of the signal enhancement between methyl protons and the vinylic proton is only 0.23% whereas the magnitude of the signal enhancement between methyl protons and the ortho aromatic proton is 2.70%. Further, on irradiating methyl protons of the minor isomer, it was found that the magnitude of the signal enhancement between methyl protons and the vinylic proton is only 2.64% whereas the magnitude of the signal enhancement between methyl protons

and the ortho aromatic proton is negligible. This study implied that the major isomer is ***E*-179** instead of the predicted ***Z*-179** isomer.

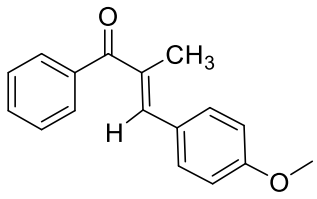

Isolated major isomer

***E*-176**

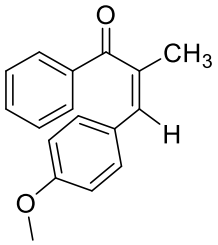

Isolated minor isomer

***Z*-176**

NOE (500 MHz, $CDCl_3$) - irradiating methyl protons

CH_3 ↔ vinylic proton = 0.23% CH_3 ↔ vinylic proton = 2.64 %

CH_3 ↔ aromatic ortho proton = 2.70% CH_3 ↔ aromatic ortho proton = negligible

NOE (500 MHz, $CDCl_3$) - hitting vinylic protons

Vinylic proton ↔ methyl proton=0.18% Vinylic proton ↔ methyl proton = 2.06%

Vinylic proton↔ ortho Ar proton=3.08% Vinylic proton ↔ ortho Ar proton= 1.72 %

*Figure 10: NOE studies on (**E/ Z-179**).*

This was further confirmed by irradiating vinylic protons in the major and minor isomer. It was found that the magnitude of the signal enhancement between methyl protons and the vinylic proton of major isomer is only 0.18% whereas the magnitude of the signal enhancement between vinyl protons and the ortho aromatic proton is 3.08%. Further, on irradiating vinylic proton of the minor isomer, it was found that the magnitude of the nuclear enhancement between methyl protons and the vinylic proton is only 2.06% whereas the magnitude between methyl protons and the ortho aromatic proton is 1.72%. The nuclear enhancement magnitude

values of methyl and vinylic protons clearly imply that the major isomer is ***Z*-179** instead of the predicted ***E*-179** isomer.

This experiment suggested that the major isomer is the one with inversion of stereochemistry i.e. ***E*-179**. This came as a surprise since Suzuki cross coupling usually proceed retention of the stereochemistry.[64] The next question was to find the origin of the loss of stereochemistry: Is this happening during first cross coupling or the second cross coupling (Scheme 81)?

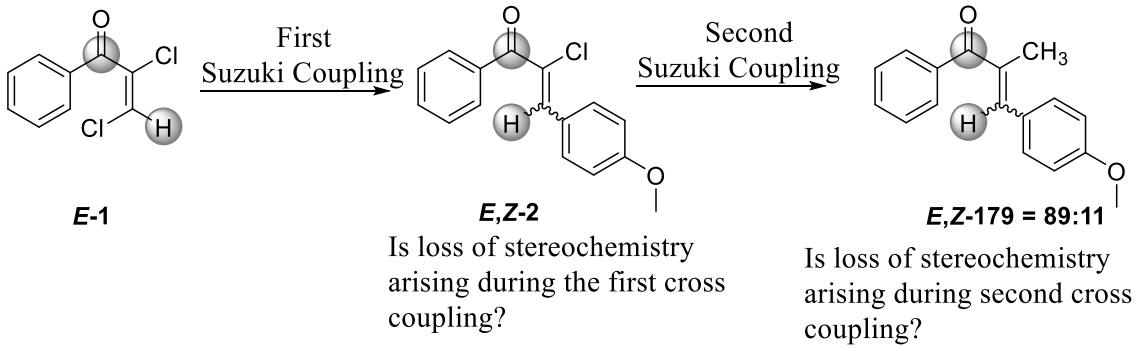

Scheme 81: Possible places for loss of stereochemistry.

Coupling constant studies between three bonds away ^{1}H and ^{13}C were further done on the isomers to finally establish the stereochemistry (Figure 11). For this the coupling constant between the carbonyl carbon and the vinylic proton three bonds away was measured. The values can be easily measured using HMBC shows the coupling of the vinylic proton at 7.49 ppm and carbonyl carbon at 191.75 ppm.

It is known that magnitude of the coupling between the vinylic proton and the allylic carbon separated from it by three bonds for an *trans* (strictly according to the relation of vinylic proton with carbonyl carbon) isomer is greater than that for a *cis* isomer i.e. *trans* $^{3}J_{C,H} > cis\ ^{3}J_{C,H}$.[77]

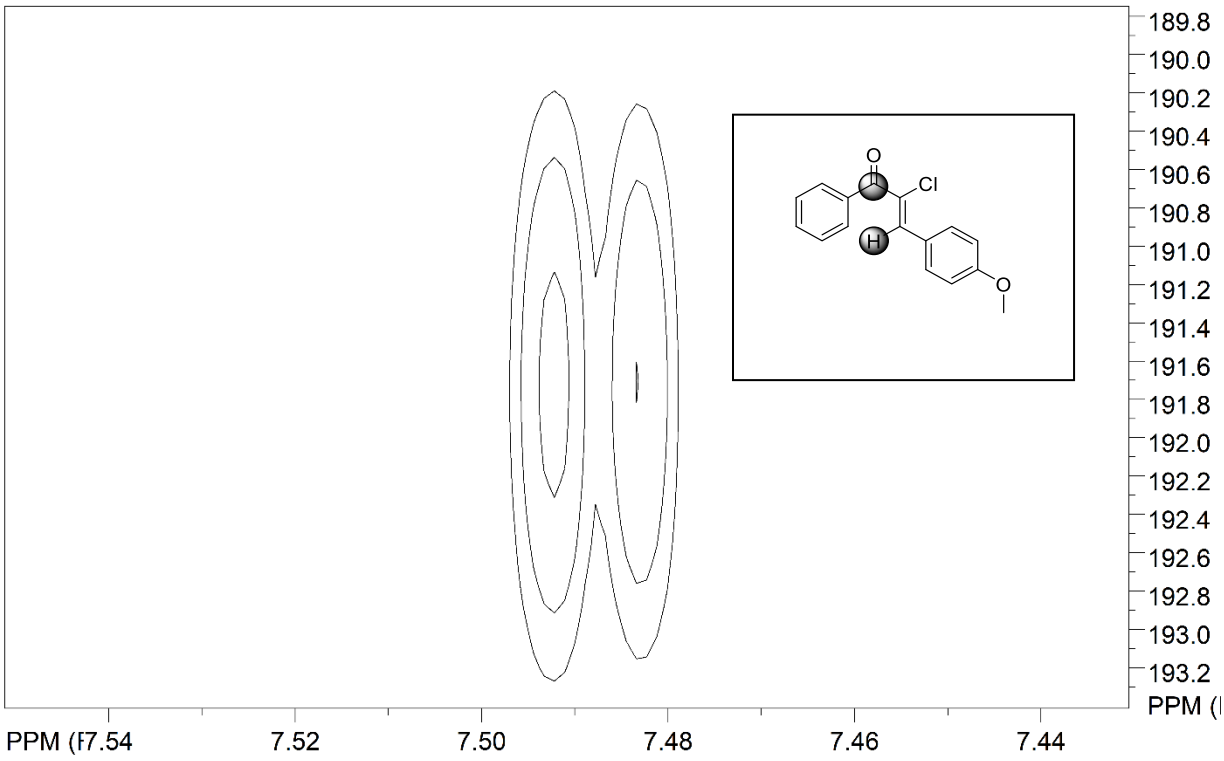

Figure 11: Three bond coupling constant measurement via HMBC.

The $^{3}J_{C,H}$ was measured for all the isomers and it was found that the major isomer formed in the first cross coupling had the *Z* configuration. The ***Z*-2** and ***E*-2** were further characterized by their crystal structures (Figure 12). Evidently, there is a loss of stereochemical integrity during the first cross-coupling reaction.

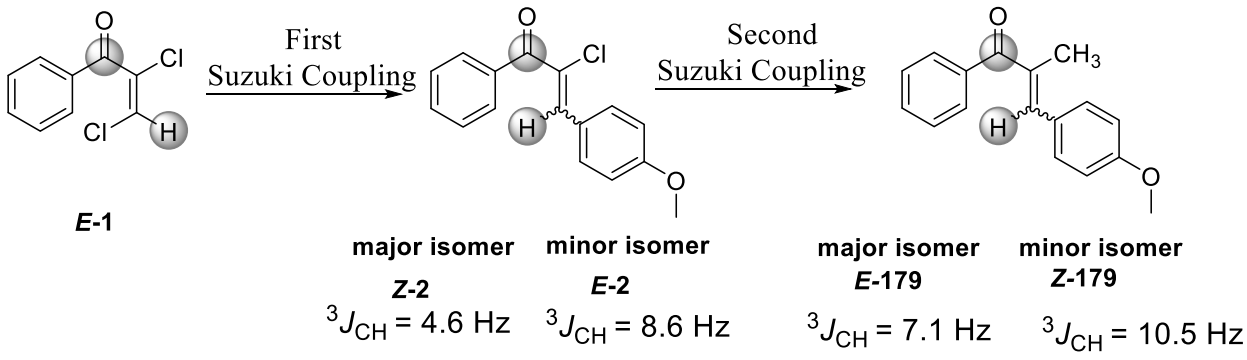

Scheme 82: The identification of stereochemistry with three bond (C-H) coupling constant values.

As shown above in Scheme 82, the $^{3}J_{C,H}$ value of the major isomer after first cross coupling was 4.6 Hz and the value of $^{3}J_{C,H}$ for minor isomer was 8.6 Hz. Since *trans* $^{3}J_{C,H}$ > *cis* $^{3}J_{C,H}$, therefore it was concluded that major isomer is ***Z*-2** and minor isomer is ***E*-2**.

Further crystal structures were obtained for ***Z*-2** and ***E*-2** isomers. The availability of the structures further verified that there is a loss of stereochemistry in the cross-coupling reaction and that ***Z*-2** is the major isomer being formed in the reaction.

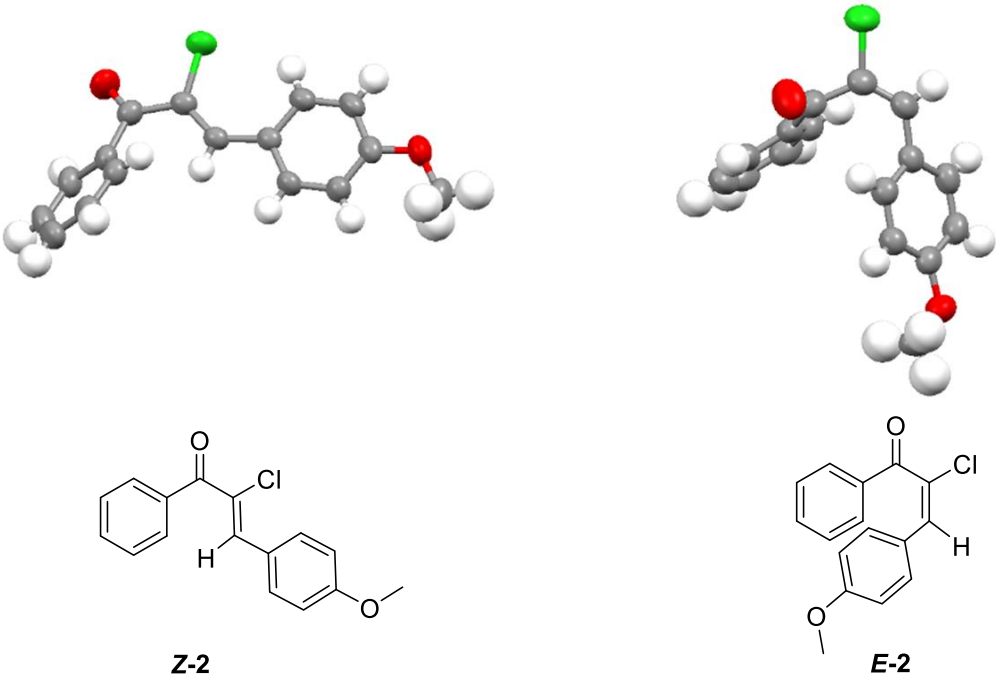

Figure 12: Crystal structures of (***Z*-2**) *and* (***E*-2**).

At this point it was evident that the major Suzuki cross coupled is formed with the inversion of stereochemistry (***Z*-2**). It was proposed that either the loss of stereochemistry is taking place during the cross-coupling reaction or the Suzuki cross coupling is taking place on the ***Z*-1**. It could be possible that the two-step synthesis of **1** (Scheme 75) was leading to the *Z* stereochemistry. So, it was critical to verify the stereochemistry of **1** and **167** at this point. The

recrystallization of **167** was possible and *E* stereochemistry of **167** was verified by crystal structure (Figure 13).

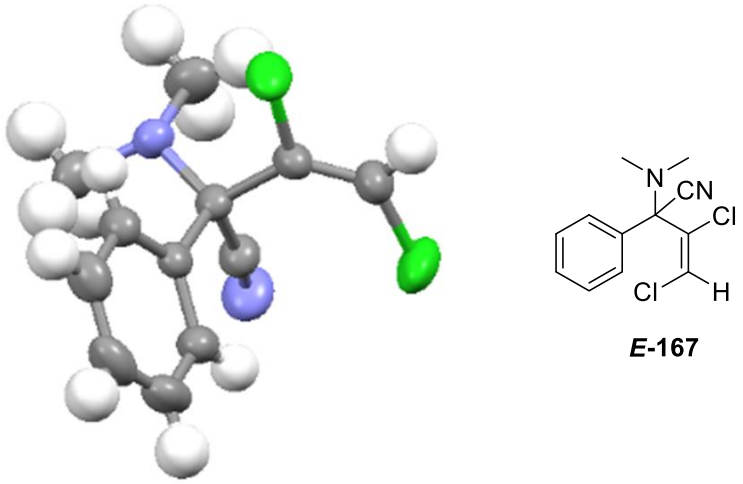

Figure 13: Crystal structure of (***E-167***).

The compound **1** was an oil and because of the liquid state, the crystal structure of the compound **1** could not be obtained. The only way to determine the stereochemistry of the compound **1** was to synthesize its isomer and then establish stereochemistry using $^{3}J_{C,H}$.

Phosphines have been known to promote isomerization in enone type compounds.[44] The mechanism for this process could be the potential addition of the phosphine in a Michael fashion, rotation around the single bond and then elimination of the phosphine as discussed in chapter 1.[44]

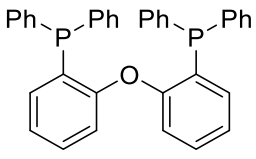

Figure 14: Structure of DPEphos.

On the same lines the ***E*-1** was reacted with 5 mol% DPEphos **(180**) in dioxane at reflux**.** It was observed that after 24 h, ***E*-1** isomerized to ***Z*-1** in the presence of catalytic amount of DPEphos (**180**) (Scheme 83). After synthesizing the ***Z*-1**, three bond coupling constant values were measured using HMBC. It was found that the $^{3}J_{C,H}$ for ***E*-1** is 7.0 Hz and ***Z*-1** is 2.9 Hz. The isomers gave different retention times, when analyzed by GC-MS (Figure 15).

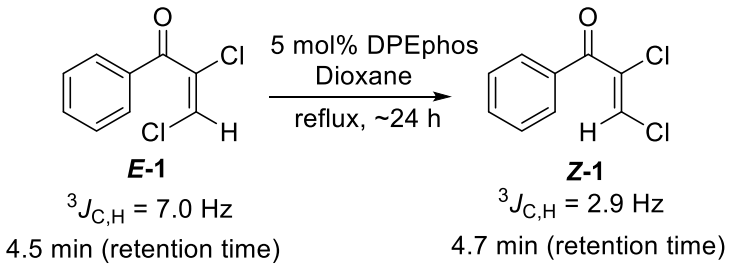

*Scheme 83: Isomerization of (**E-1**) to (**Z-1**) in the presence of DPEphos.*

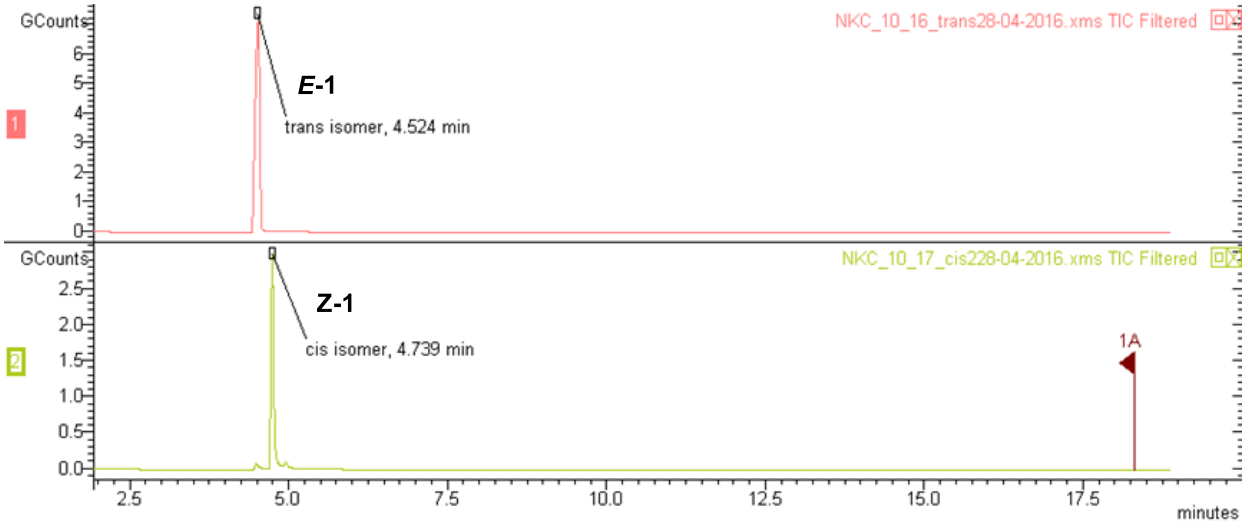

Figure 15: Chromatogram showing E-1 and Z-1 retention times.

These studies elucidated that loss of stereochemistry is taking place during Suzuki cross coupling conditions (Scheme 84).

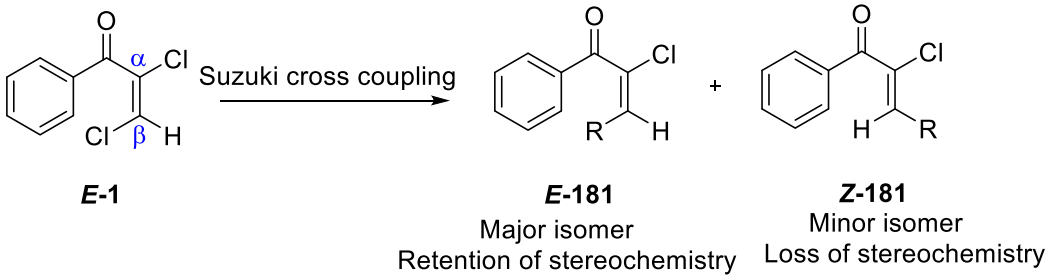

*Scheme 84: Schematic representation of the Suzuki cross coupling outcome on (**E-1**).*

2.5. Control over inversion and retention of configuration

After identifying the loss of the stereocontrol in these reactions, the challenge was to find the reaction conditions that would enable the synthesis of both the retention product and the isomerization product selectively. To attain the control, optimization studies were carried out with different palladium sources, ligands, bases, solvents.

2.5.1 Base and solvent screening

Bases play a crucial role in the Suzuki cross coupling reactions.[19] The bases used for the screening were Cs_2CO_3, CsF, K_2CO_3 and K_3PO_4. The solvents chosen for this study were aprotic polar dioxane and non-polar toluene. The reactions were performed on ***E*-1** with 2.5 mol% $Pd_2(dba)_3$, 1 eq 4-methoxyphenylboronic acid, 3 equivalents base in solvent at 85 °C (Scheme 85). These reactions were run for one hour and without phosphine ligand in them.

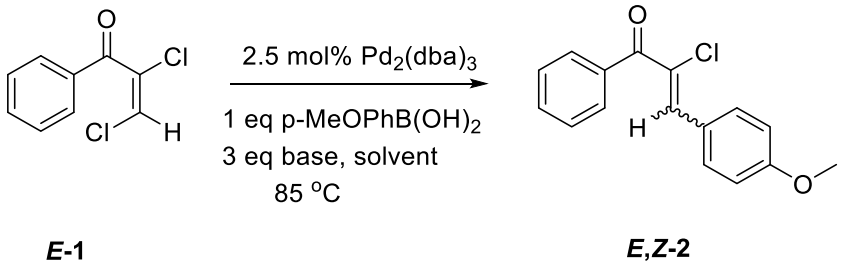

*Scheme 85: Base and solvent screening on (**E-1**) for Suzuki cross coupling.*

All the reactions were analyzed by GC-MS. The retention of stereochemistry (***E*-2**) was observed in the absence of the phosphine ligands (for details, see section 2.5.3.). It was observed that Cs_2CO_3 in dioxane gave 100% conversion with 94% selectivity for ***E*-2**. This was followed by CsF in dioxane, which gave 98% conversion with 87% selectivity for ***E*-2**, and the reactions with other combinations of bases and solvents were very slow (Figure 16). The results obtained using Cs_2CO_3 were slightly better than those obtained using CsF and hence, Cs_2CO_3 was used as a base for the rest of our studies.

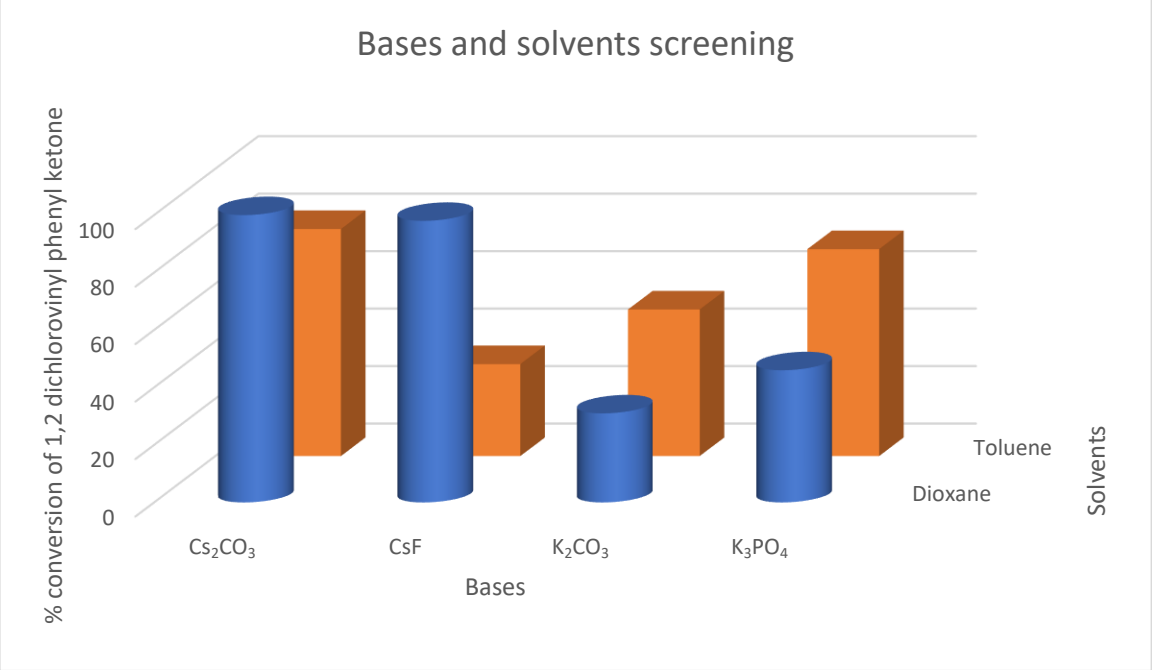

Figure 16: Base and solvent screening.

2.5.2 Palladium catalyst screening

For palladium catalyst screening, various Pd (0) and Pd (II) precursors were used. The reactions performed on ***E*-1** with 2.5 mol% of different palladium sources (Scheme 86). All the reactions were analyzed by GC-MS after one hour.

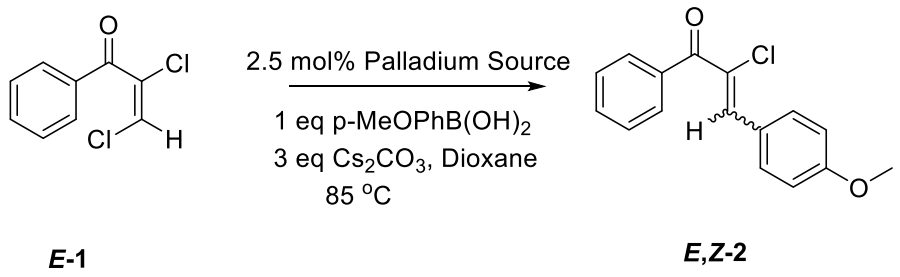

***E*-1** **E,Z-2**

*Scheme 86: Screening of different palladium sources on (**E-1**) for Suzuki cross coupling.*

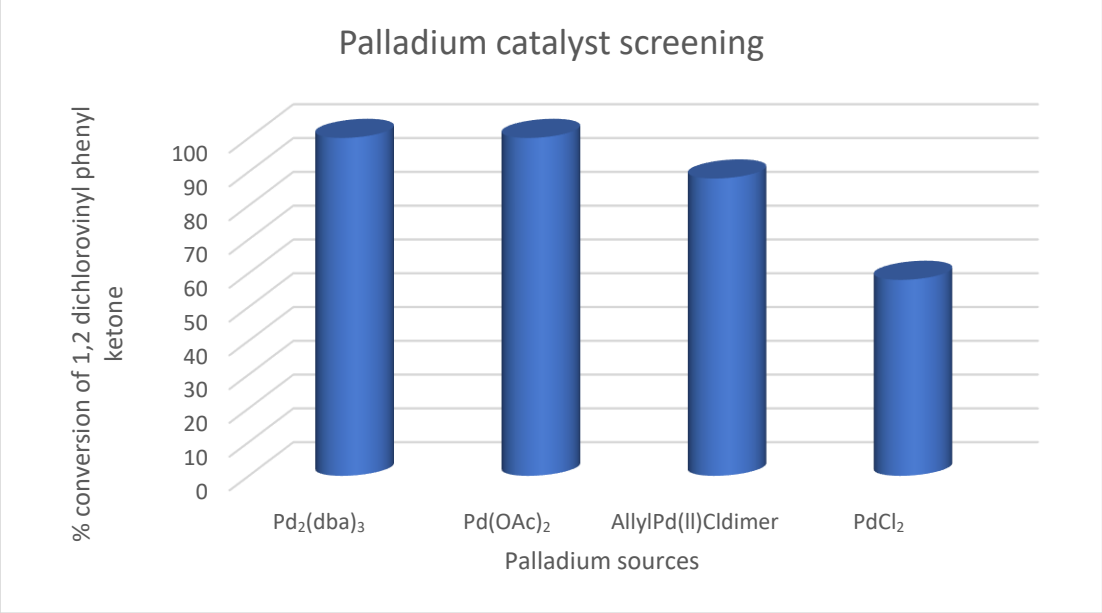

*Figure 17: Palladium catalyst screening in Suzuki cross coupling of (**E-1**).*

As shown in Figure 17, $Pd_2(dba)_3$ in dioxane gave 100% conversion with 94% ***E*-2**. This was followed by $Pd(OAc)_2$ in dioxane, which also gave 100% conversion but with 91% ***E*-2**, whereas other palladium catalysts i.e. $PdCl_2$ and AllylPd(II)Cl dimer were slower than both $Pd_2(dba)_3$ and $Pd(OAc)_2$. Based on the screening results, $Pd_2(dba)_3$ was selected. for reactions.

5.3 Phosphine ligand screening

After finding the best combination of the palladium source, base and solvent, the reactions were screened with the different phosphine ligands. The wide variety of monophosphine and

bisphosphine ligands screened for Suzuki cross coupling on ***E*-1** are shown in Figure 18. For screening purposes, Suzuki cross coupling reaction was performed on ***E*-1**.

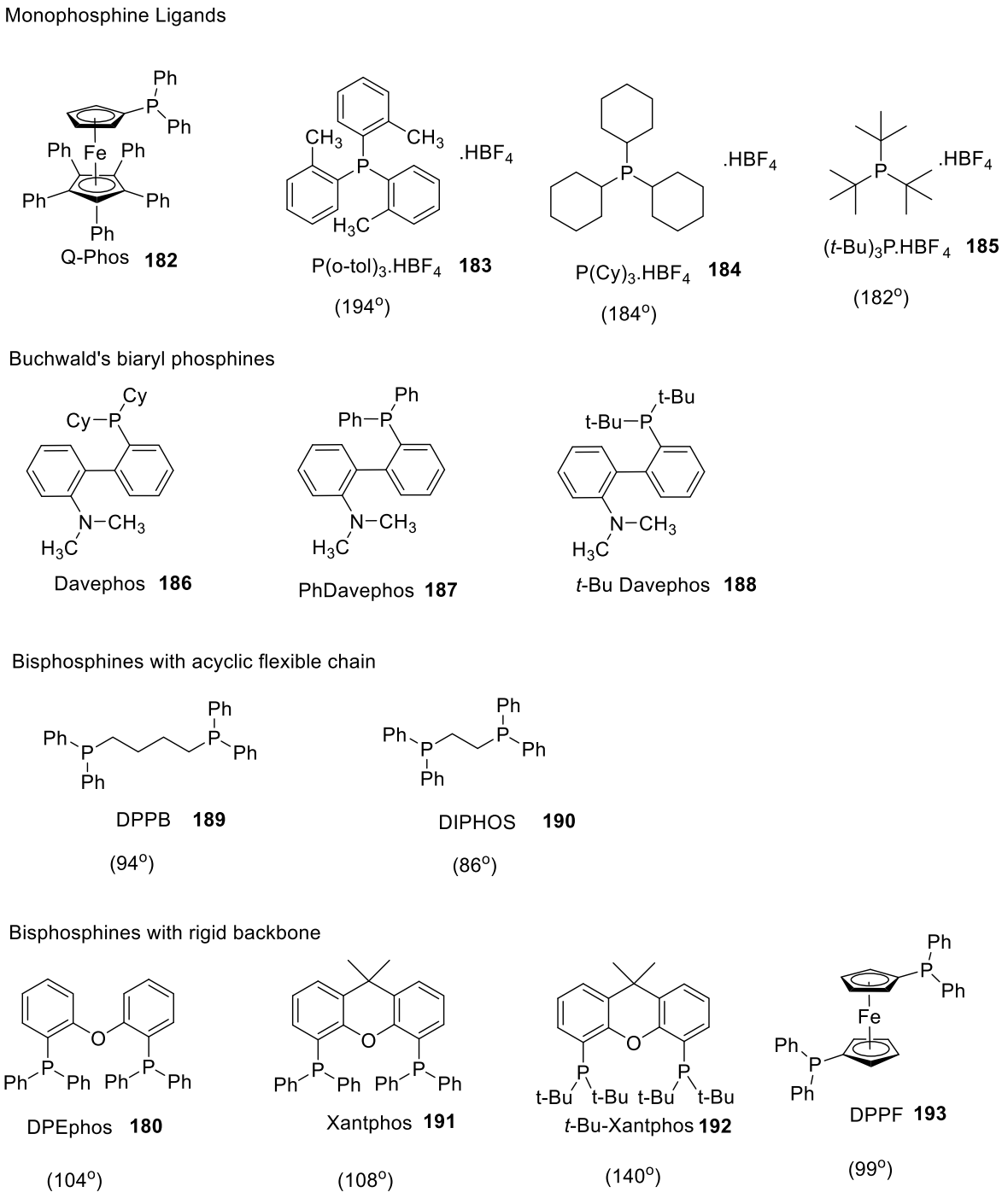

Figure 18: Different phosphine ligands used in screening. The cone angles/ bite angles of some ligands mentions in brackets.[78]

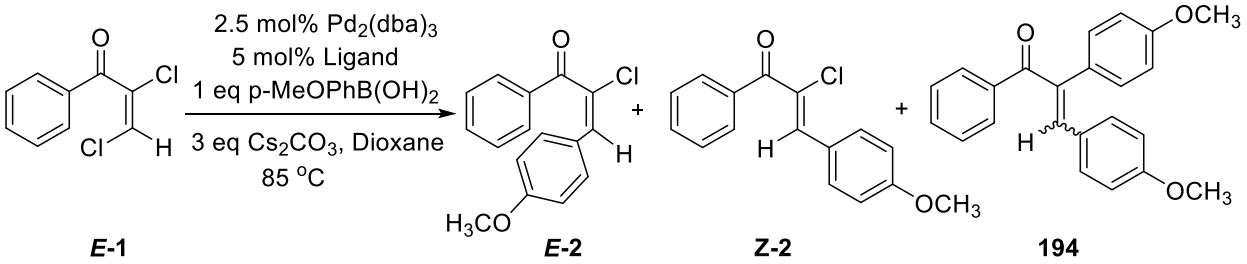

Entry	Ligand	After 1 hour ***E*-2: *Z*-2: 194**	After 24 hours ***E*-2: *Z*-2: 194**
1.	DPEphos (**180**)	4:96:0	4:96:0
2.	Xantphos (**191**)	6.5:93:0.5	4:96:0
3.	Davephos (**186**)	18:76:6	6:88:6
4.	PhDavePhos (**187**)	30:68:2	21:76:3
5.	$P(o\text{-}tol)_3$ (**183**)	35:64:1	5:93:2
6.	DIPHOS (**190**)	43:57:0	11:88:1
7.	$(Cy)_3P{\cdot}HBF_4$ (**184**)	50:50:0	7:93:0
8.	DPPF (**193**)	51:49:0	15:85:0
9.	$(t\text{-}Bu)_3P{\cdot}HBF_4$ (**185**)	70%; 44:23:3	100%; 10:80:10
10.	DPPB (**189**)	75:23:2	10:89:1
11.	Q-Phos (**182**)	81:19:0	29:67:4
12.	*t*-BuDavephos (**188**)	74:17:9	12:79:9
13.	*t*-Bu-Xantphos (**192**)	93:5:2	5:89:4
14.	No ligand	94:5:1	55:43:2

Table 1: Suzuki cross coupling outcome from different phosphine ligand screening. The quantitative studies were done using GC-MS.

As shown in Table 1, the fascinating difference in the Suzuki cross coupling outcome was observed when bidentate ligands DPEphos (**180**) or Xantphos (**191**) or *t*-Bu-Xantphos (**192**) were used. The best selectivity for the isomerized Suzuki cross coupled product (***Z*-2**) was

achieved using either **180** or **191** (96% selectivity). The product with retention of configuration (***E*-2**) was best prepared using **192** (93% selectivity) or by using no phosphine ligand (94% selectivity) (entry 14).

The bite angle of the **180** and the **191** ligand, leading to the isomerized Suzuki cross coupled product (entry 1 and 2, Table 1) is 104° and 108° respectively whereas the bite angle of the **192** ligand (entry 13) which leads to the Suzuki cross coupled product with retention is 140°.[78c] This suggests that steric bulk of the ligand plays a role in the retention of stereochemistry. The results of all other monophosphine and bisphosphine ligands fall in between the extremes of the **180** and **192**. It is intriguing that other bulky monophosphate ligands like **183** [$P(o\text{-}tol)_3.HBF_4$ (194°)], **184** [$P(Cy)_3$.HBF4 (184°)] and **185 [**$P(t\text{-}Bu)_3.HBF_4$ (182°)] do not show as much selectivity as **192** (Figure 18).

As shown in Table 1, it is very interesting that the ***E*-2** is also formed selectively when no-phosphine (entry 14) ligand is used in the Suzuki cross coupling reaction conditions. The only difference between the conditions under which the ***Z*-2** is formed (entry 1, Table 1) and the ***E*-2** (entry 14, Table 1) is the presence of the phosphine ligand. This clearly suggests that the phosphine ligand does play a role in the isomerization. The question that arises from this is how can phosphine induce isomerization? One way in which phosphine can induce isomerization is via Michael addition of phosphine to the conjugated double bond, bond rotation around the single bond and then followed by the elimination of the phosphine. Other plausible ways for the isomerization could be via palladium hydride species formation in the reaction, rotation in the transmetallated intermediate because of the zwitterionic character of the vinylpalladium species or via coordination of the conjugated enone to the palladium metal. All these pathways

require phosphine ligand. The detailed studies of these pathways have been discussed in Pathways for isomerization.

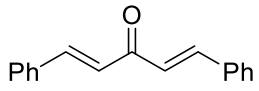

dibenzylideneacetone

195

Figure 19: Structure of compound dibenzylideneacetone

In the no phosphine conditions (entry 14, Table 1), dibenzylideneacetone (**195**) present in the $Pd_2(dba)_3$ acts as a ligand. The selectivity achieved by **195** is same as that achieved by *t*-Bu-Xantphos. (entry 13 and 14, Table 1). The electronics of dba are very different from that of *t*-Bu-Xantphos. The ligand **195** is electron poor and *t*-Bu-Xantphos is electron rich. This suggests that electronics of the ligands solely can not explain the stereoselectivity achieved by the two ligands. Perhaps, an isomerization pathway is more complex and there is an involvement of some other intermediate. There is a need to find a plausible pathway for an isomerization which might then explain the reason for the less effectiveness of *t*-Bu-Xantphos (**192**) and no phosphine ligand in isomerization (see 2.7. Mechanistic Insight).

It has been observed that Suzuki cross coupled ***E*-2** changes to the thermodynamically more stable ***Z*-2** isomer. Since the isomerization continues after the completion of the Suzuki cross coupling reaction, this suggests that the isomerization is taking place outside the catalytic cycle. Although no strong conclusion can be made whether the sole pathway of the isomerization lies outside the catalytic cycle. There is a possibility of two simultaneous isomerization pathways (inside the catalytic cycle and outside the catalytic cycle) in the reaction (see discussion 2.7. Mechanistic Insight).

To summarize, the optimization studies successfully provided the route for the selective synthesis of *E* or *Z* isomer. Using the DPEphos (**180**) in the reaction conditions, the isomerized product ***Z*-2** was synthesized with 96% selectivity in 25 mins, while use of *t*-Bu-Xantphos (**192**)/ no phosphine led to the retention product ***E*-2** with 94% selectively in an hour. These studies also suggested that the phosphine ligand plays a major role in the isomerization and there is at least one separate isomerization pathway that operates outside the catalytic cycle.

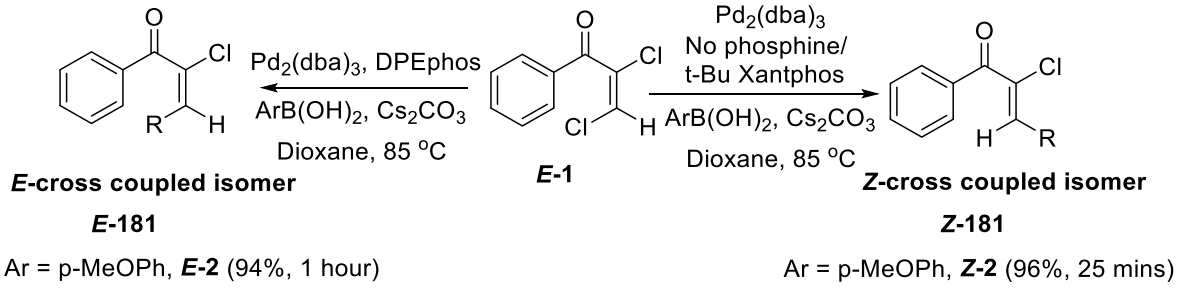

*Scheme 87: Retention and isomerized from Suzuki cross coupling outcome on (**E-2**).*

2.6. Synthesis of *E* and *Z* isomers

With the strategy to synthesize either the retention or the isomerized product isomer, the substrate scope was explored by using wide range of aryl boronic acids (**196**). Out of different boronic reagents,[23] boronic acids were used for this work. Boronic acids were first employed in Suzuki cross coupling in 1981 and since then they have been a very useful class of boron reagents.[20]

The phosphine ligand DPEphos in the presence of $Pd_2(dba)_3$, $ArB(OH)_2$ (**196**) and Cs_2CO_3 at 85 °C was used to synthesize isomers with inversion in stereochemistry (***Z*-181**) selectively (Table 2 and Table 3).

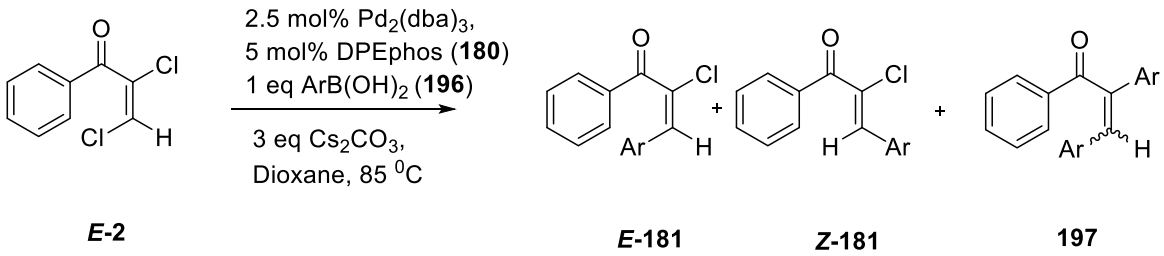

Entry	Boronic acid	Product	Time(h)/*E-181*: *Z*-181: 197	Yield (*Z* isomer)	$^3J_{C,H}$
1.	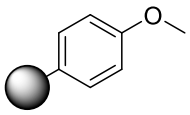	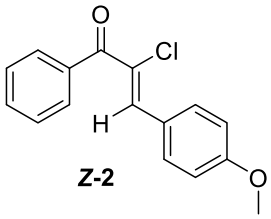 ***Z*-2**	0.5/ 4:96:0	80%	4.90
2.	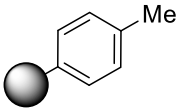	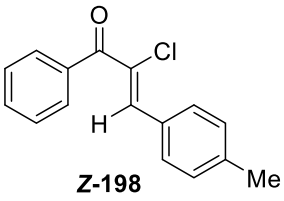 ***Z*-198**	0.5/ 5:92:3	76%	4.65
3.	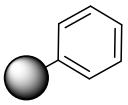	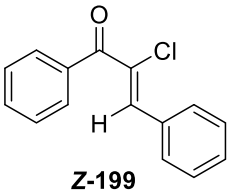 ***Z*-199**	2.0/ 8:90:2	70%	4.66
4.	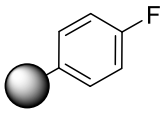	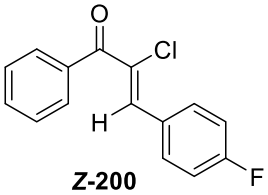 ***Z*-200**	5.0/ 6:94:0	78%	4.63

Table 2: Substrate scope for Z-Suzuki cross coupled isomers.

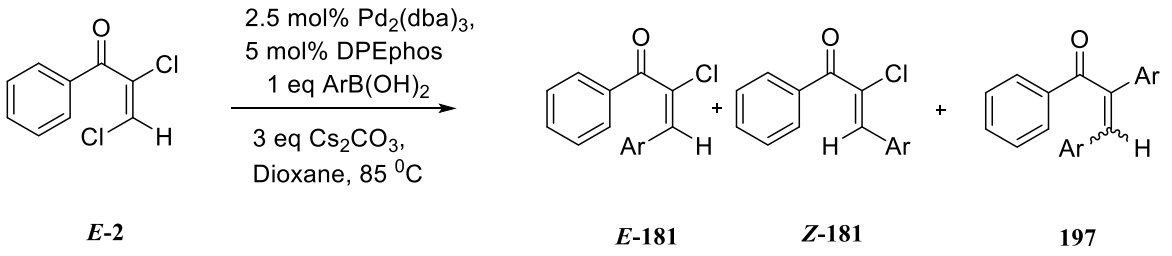

Entry	Boronic acid	Product	Time(h)/*E*-181: *Z*-181: 197	Yield (*Z* isomer)	$^3J_{C,H}$
5.	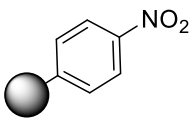	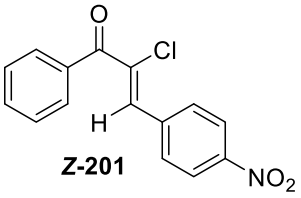 ***Z*-201**	24/ no product observed	-	-
6.	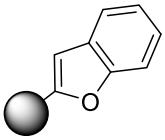	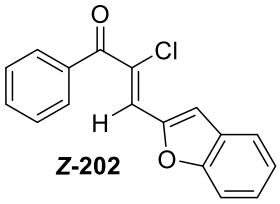 ***Z*-202**	2.0/ 3:91:0	74%	4.51
7.	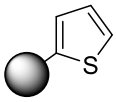	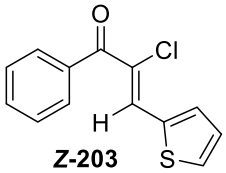 ***Z*-203**	24/ 16:80:4	62%	4.95
8.	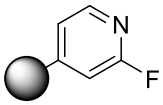	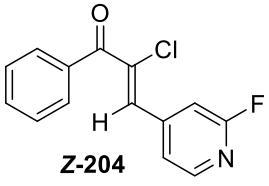 ***Z*-204**	24/ 4:95:1	69%	4.42

Table 3: Substrate scope for Z-Suzuki cross coupled isomers (continued)

The phosphine ligand *t*-Bu-Xantphos in the presence of $Pd_2(dba)_3$ or no phosphine ligand i.e. just $Pd_2(dba)_3$, $ArB(OH)_2$ (**200**) and Cs_2CO_3 at 85 °C was used to synthesize isomers with retention of stereochemistry (Table 4 and Table 5).

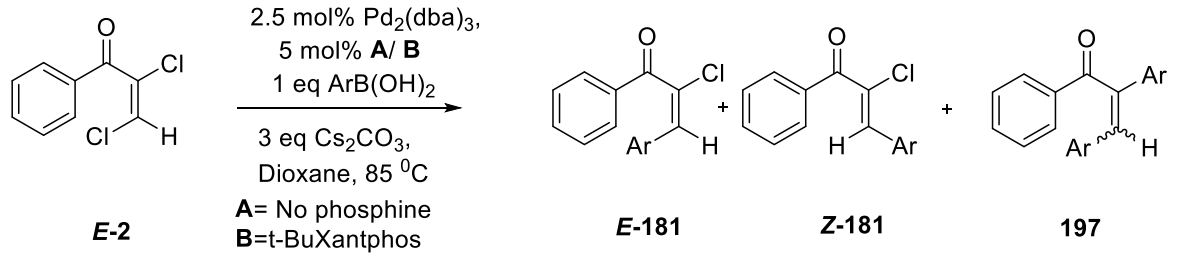

Entry	Boronic acid	Product	Conditions	Time(h)/ *E*-181:*Z*-181:197	Yield (*E* isomer)	$^3J_{C,H}$
1.	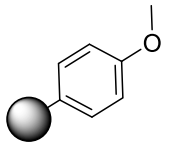	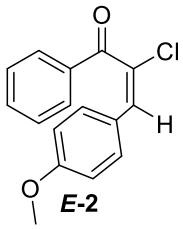 ***E*-2**	A	1.5/ 94:5:1	78%	8.56
			B	1.0/ 93:5:2	73%	8.56
2.	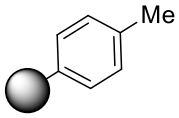	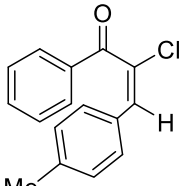 ***E*-198**	A	2.0/ 90:6:4	75%	8.79
3.	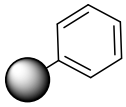	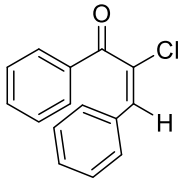 ***E*-199**	A	3.5/ 94:4:2	69%	8.60
4.	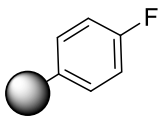	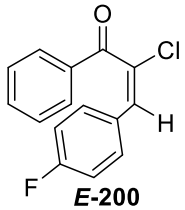 ***E*-200**	A	7.0/ 91:9:0	72%	8.27

Table 4: Substrate scope for E-Suzuki cross coupled isomers.

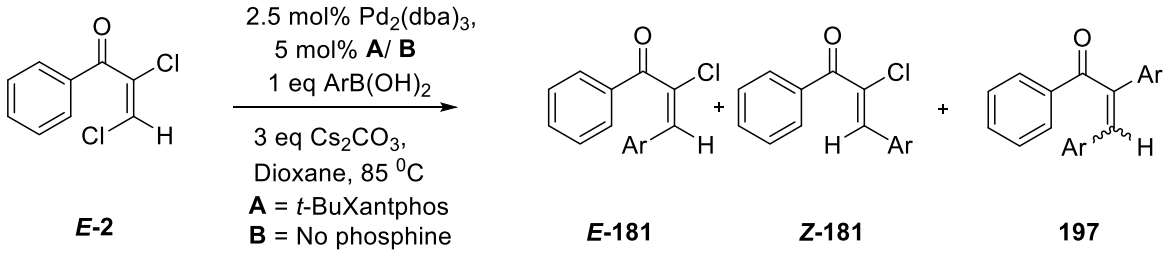

Entry	Boronic acid	Product	Conditions	Time(h)/ *E*-181:*Z*-181:197	Yield (*E* isomer)	$^3J_{C,H}$
5.	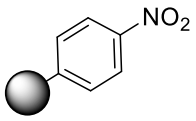	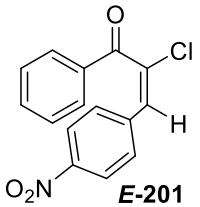 ***E*-201**	A, B	24/ no product observed	-	-
6.	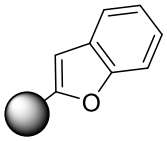	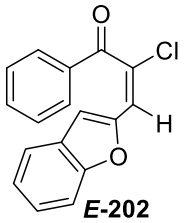 ***E*-202**	A	8.0/ 90:10:0	76%	8.11
7.	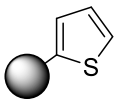	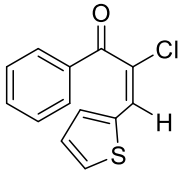 ***E*-203**	A	24/ 95:5:0	77%	8.11
8.	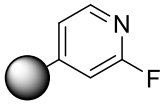	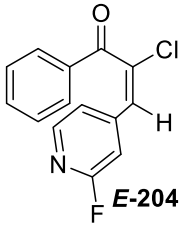 ***E*-204**	A B	24/ no product observed 24/ 13% conversion (83:17:0)	– –	– –

Table 5: Substrate scope for E-Suzuki cross coupled isomers (continued).

It was observed that the reaction conditions for either *E* or *Z* isomer were stereo-selective for all the aryl boronic acids (**196**) used. The characterization of the products was done by NMR spectroscopy and HRMS. The configuration in all the compounds was established by $^3J_{C,H}$ measurements.

The crystal structures for some Suzuki cross coupled product were obtained to further elucidate the stereochemistry of the isomers synthesized. The recrystallization attempts were successful for ***E*-2** (Table 4), **Z-2** (Table 2), ***Z*-198** (Table 2), ***E*-202** (Table 5) and ***Z*-202** (Table 3)**.** The ***E*** and ***Z*** isomers of **202**, ***Z*-2**and ***Z*-198** were recrystallized by using the mixture of hexanes and ethyl acetate. ***E*-2** was recrystallized using acetone.

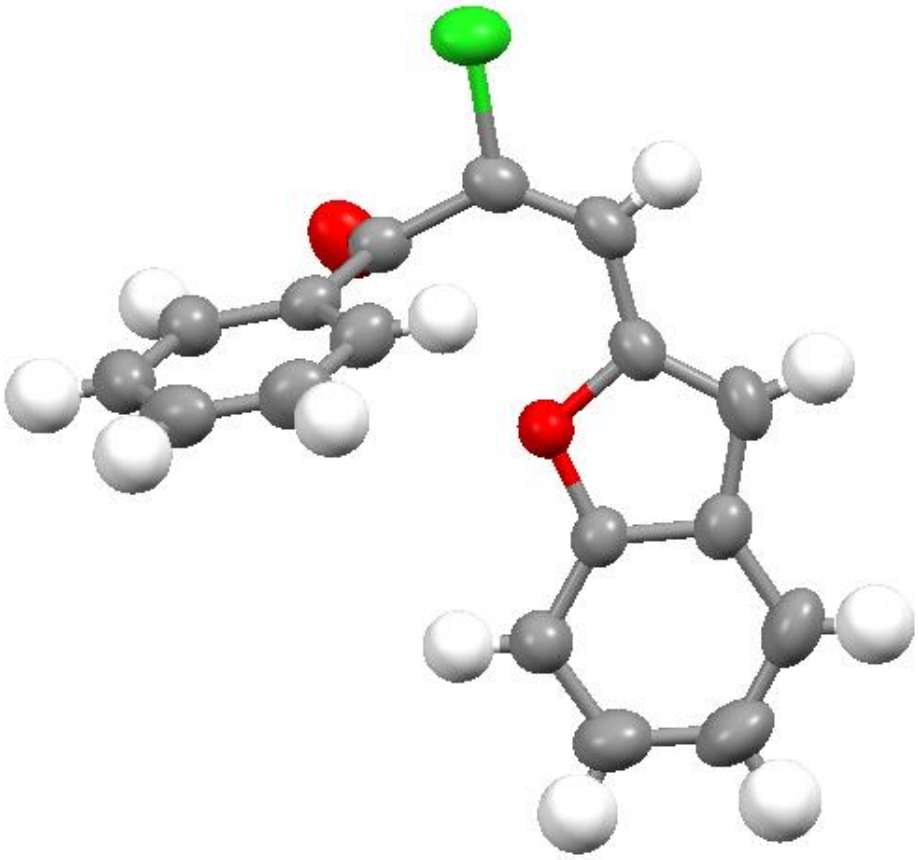

Figure 20: Crystal structure of (***E*-202**).

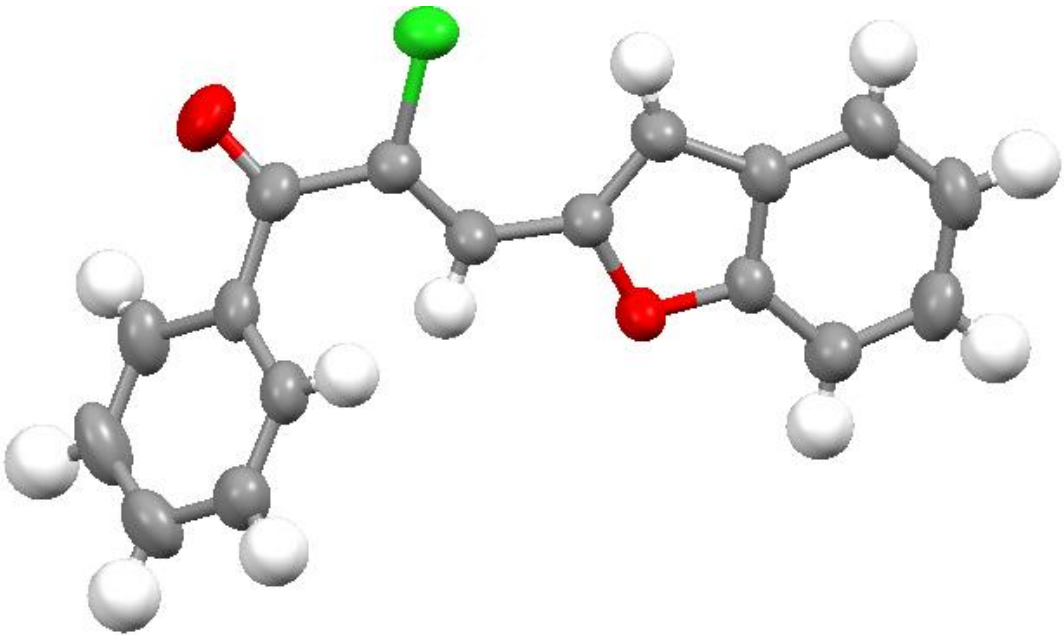

Figure 21: Crystal structure of (***Z*-202**)*.*

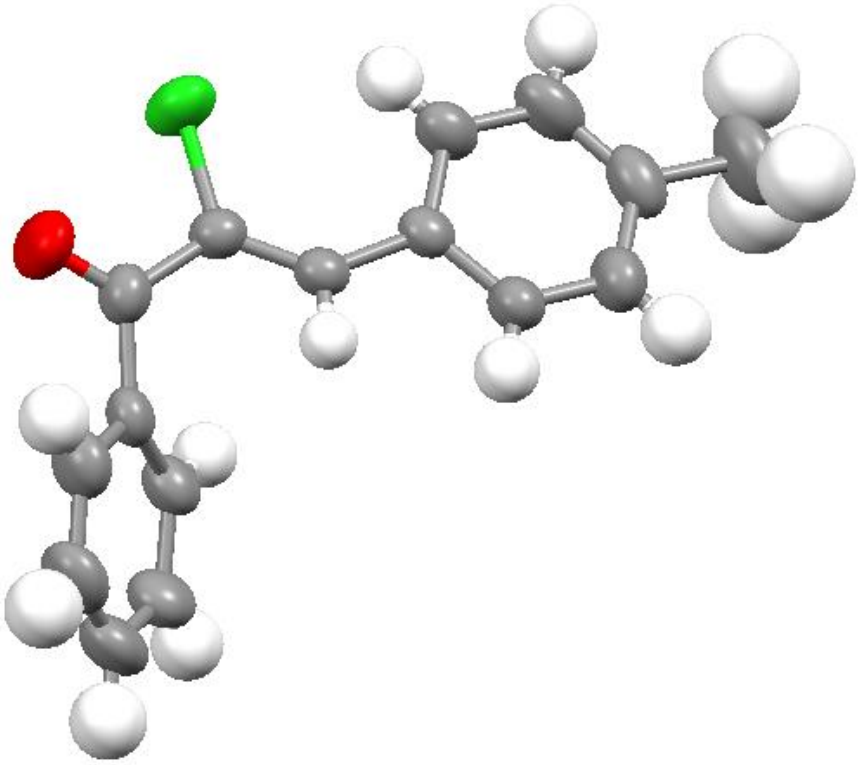

Figure 22: Crystal structure of (**Z-198**)*.*

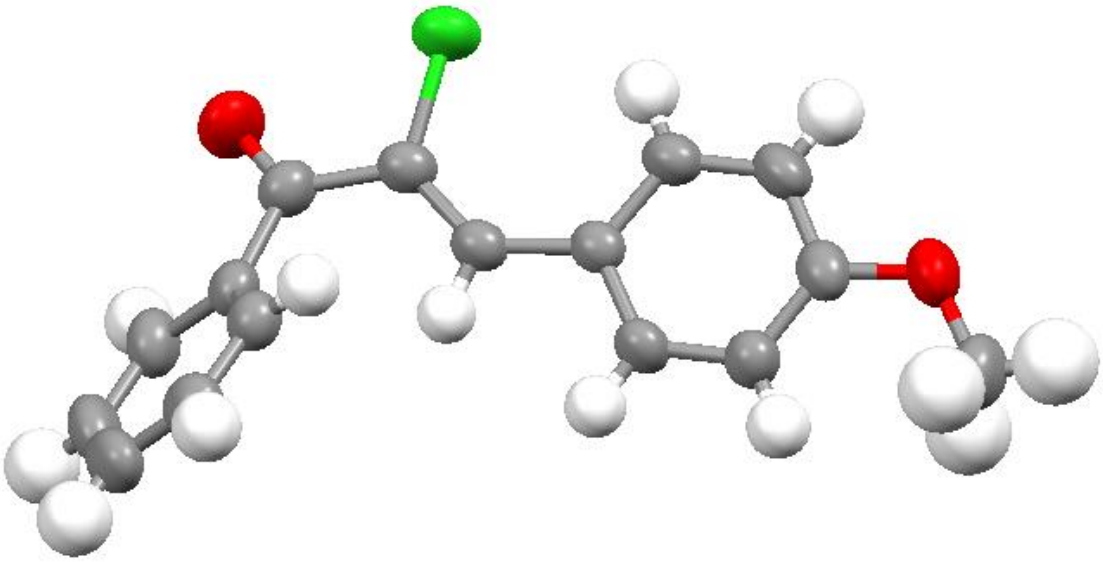

Figure 23: Crystal structure of (***Z-2***)*. This picture is also shown in figure 12.*

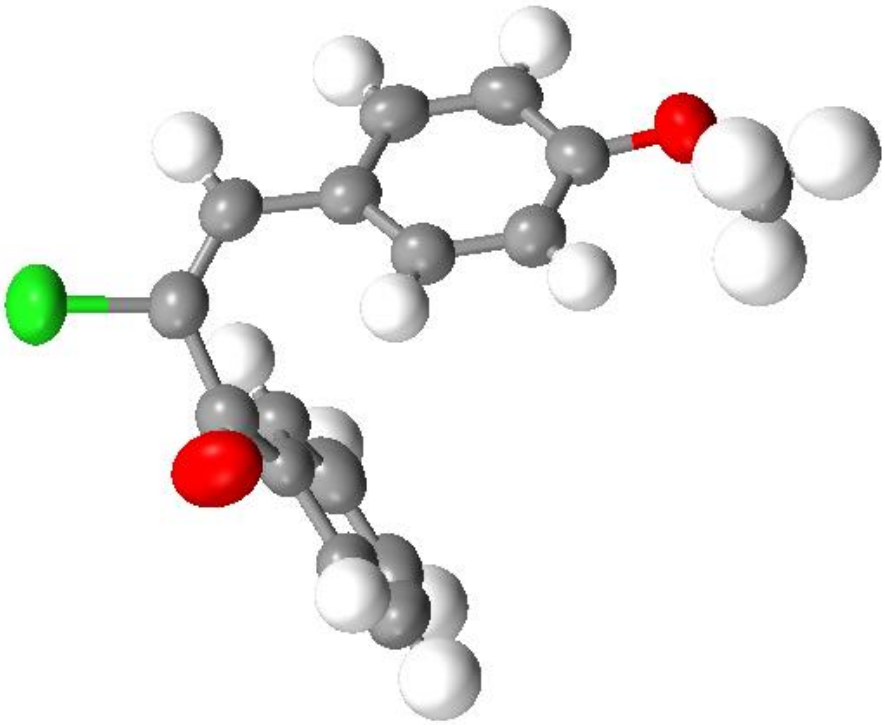

Figure 24: Crystal structure of (***E-2***)*. This picture is also shown in figure 12.*

It was observed that the *E* isomer isomerizes to the thermodynamically stable *Z* isomer upon prolonged stirring of the reaction mixture. For excellent selectivity of the kinetic product, i.e. *E*

isomer, the reactions were carefully monitored and quenched as soon as the 100% conversion of the starting material was achieved.

For both the isomers, the reactions proceeded as anticipated. As shown in Table 2 and Table 4, the reactions with electron rich boronic acid like p-methoxyphenylboronic acid (entry 1) and p-methylphenylboronic acids (entry 2) finished faster than phenyl boronic acid (entry 3) while reaction with p-nitrophenyl boronic acid (entry 5, Table 3 and Table 5) gave no or little conversion. Since the substrate i.e. **1** and palladium catalyst remains same for all the aryl boronic acids, the oxidative addition step of the catalytic cycle can not be held responsible for the rate difference with different substrates. This difference in the rates is in the good correlation with the fact that the boron reagent acts as an nucleophilic component in the transmetallation step of the Suzuki cross coupling reactions.[19] The more electron rich the nucleophilic center is, the faster is the rate of the reaction, as observed in the case of p-methoxy phenyl boronic acid/ p-methyl phenyl boronic acid and the electron poor (p-nitrophenyl) the nucleophilic center, the slower is the rate of the reaction.

The common side product observed with all the aryl boronic acids was the Suzuki dicoupled product (**194**), i.e., the cross coupling took place at both α and β C-Cl bonds in ***E*-2**. The formation of **194** was observed during synthesis of both *E* (Table 2 and Table 4) and *Z* isomers (Table 3 and Table 5).[2a] [23]

2.7. Mechanistic Insight

An extensive isomerization observed in the presence of some phosphine ligands was very intriguing. Detailed studies were done to find a plausible pathway responsible for the isomerization. The pathways tested for the isomerization are follows:

1. Thermal Isomerization
2. Photo-isomerization
3. Isomerization by Phosphine ligands
4. Individual reagents and their combination studies to find out whether the isomerization is taking outside or inside the catalytic cycle.
5. Palladium Hydride
6. Coordination to the transition metal

2.7.1 Thermal isomerization

The thermal stabilities of ***E*-1** and ***E*-2** were confirmed by heating ***E*-1** and ***E*-2** in dioxane at 85 °C. Compound ***E*-1** did not show any isomerization after 24 hr whereas ***E*-2** only showed no isomerization after one hour and only 3% isomerization after 3 hr, when analyzed by GC-MS (Scheme 88). This experimental data clearly does not justify the observed level of the isomerization in the Suzuki cross-coupling on ***E*-1**.

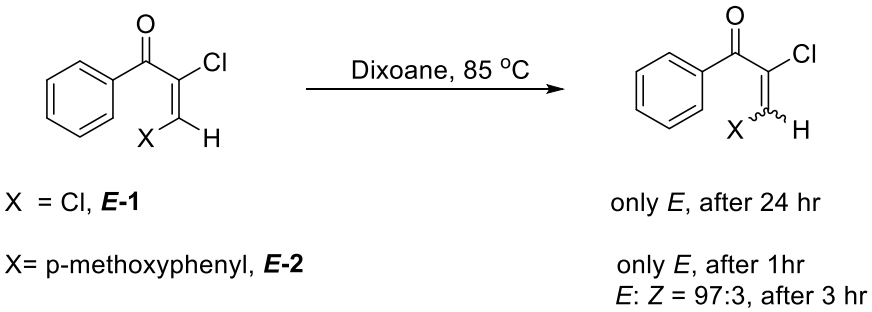

*Scheme 88: Reaction for thermal stability of (**E-1**) and (**E-2**).*

2.7.2. Photo-isomerization

Cis-trans isomerization has been observed in olefins and enone functionalities in the presence of light.[40, 43, 79] To confirm whether or not the isomerization is taking place in the presence of the light, the Suzuki cross coupling reaction was run on ***E*-1** in a test tube wrapped with an aluminium foil (Scheme 89).

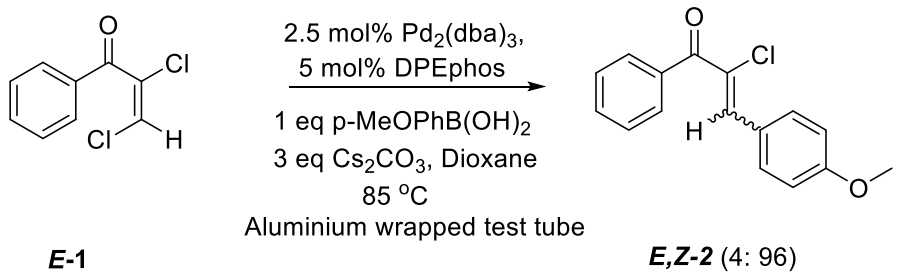

*Scheme 89: Photo-isomerization test for Suzuki cross coupling on (**E-1**).*

The same extent of isomerization was observed in Suzuki cross coupled product as would be observed without the aluminium foil wrapped test tube. This experiment suggests that the light is not responsible for the fast isomerization observed in the Suzuki cross coupling reaction. This being said, it has been observed that ***E*-2** changes to ***Z*-2** after prolong sitting on the bench (~7-10 days).

2.7.3. Phosphine ligands

Phosphine ligands were envisioned to promote the isomerization of ***E*-1** or ***E*-2** via Michael addition of phosphine to the conjugated double bond of ***E*-2**. This is followed by bond rotation in **205** and then an elimination of the phosphine in **206** yielding ***Z*-2** (Scheme 90).[44-45]

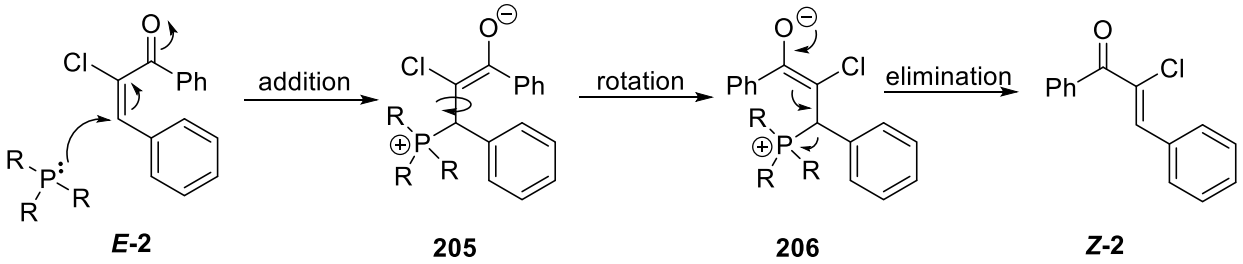

*Scheme 90: Mechanism for E-Z isomerization of (**E-2**) to (**Z-2**) by phosphine ligands.*

To verify this ***E*-1** and ***E*-2** were heated with the 5 mol % DPEphos in the presence of dioxane at 85 ℃ separately (Scheme 91). Compound ***E*-1** gave only 8% isomerization and compound ***E*-2** led to only 3% formation of ***Z*-2** in 1 hr.

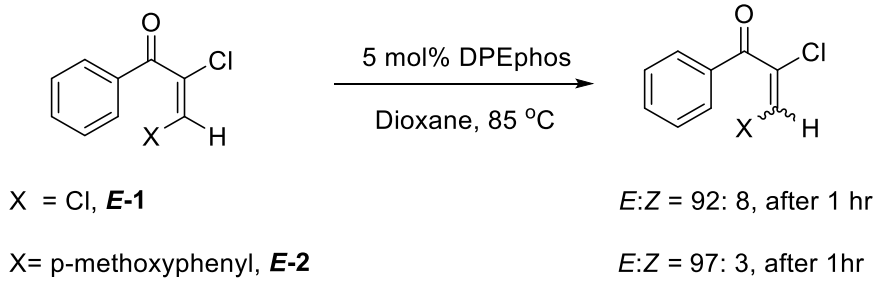

*Scheme 91: Experimentation to verify the isomerization of (**E-1**) and (**E-2**) takes place via phosphine ligands*

It was observed that ***E*-1** led to the formation of 95% ***Z*-1** when heated for 24 hr with 5 mol% DPEphos at 85 °C whereas only 6% ***Z*-2** was observed when ***E*-2** was heated for 24 hr with 5 mol% DPEphos at 85 °C. This concludes that DPEphos phosphine ligand can isomerize compound ***E*-1** but only when heated for an extended period. Using this observation ***Z*-1** was synthesized to establish the stereochemistry of ***E*-1** in section 2.4.

The complete conversion of ***E*-1** under DPEphos Suzuki cross coupling conditions is observed in 25 min and hence, the isomerization induced via only phosphine does not serve as a satisfactory explanation for stereoselective formation of ***Z*-2** in 25 minutes.

2.7.4. Isomerization arising inside/outside the catalytic cycle

After ruling out the simple pathways, some more detailed studies were performed. It was envisioned that the isomerization could take place either during Suzuki cross coupling process, i.e., inside the catalytic cycle, or it can take place outside the catalytic cycle (Figure 25). For isomerization to take place outside the catalytic cycle, it would mean that either the ***E*-1** isomerizes before entering the catalytic cycle (Path A) or Suzuki cross coupled retention product (***E*-2**) isomerizes after leaving the catalytic cycle (Path C). For isomerization to take place inside the catalytic cycle (Path B) would possibly imply that it is taking place between one of the steps in the catalytic cycle.

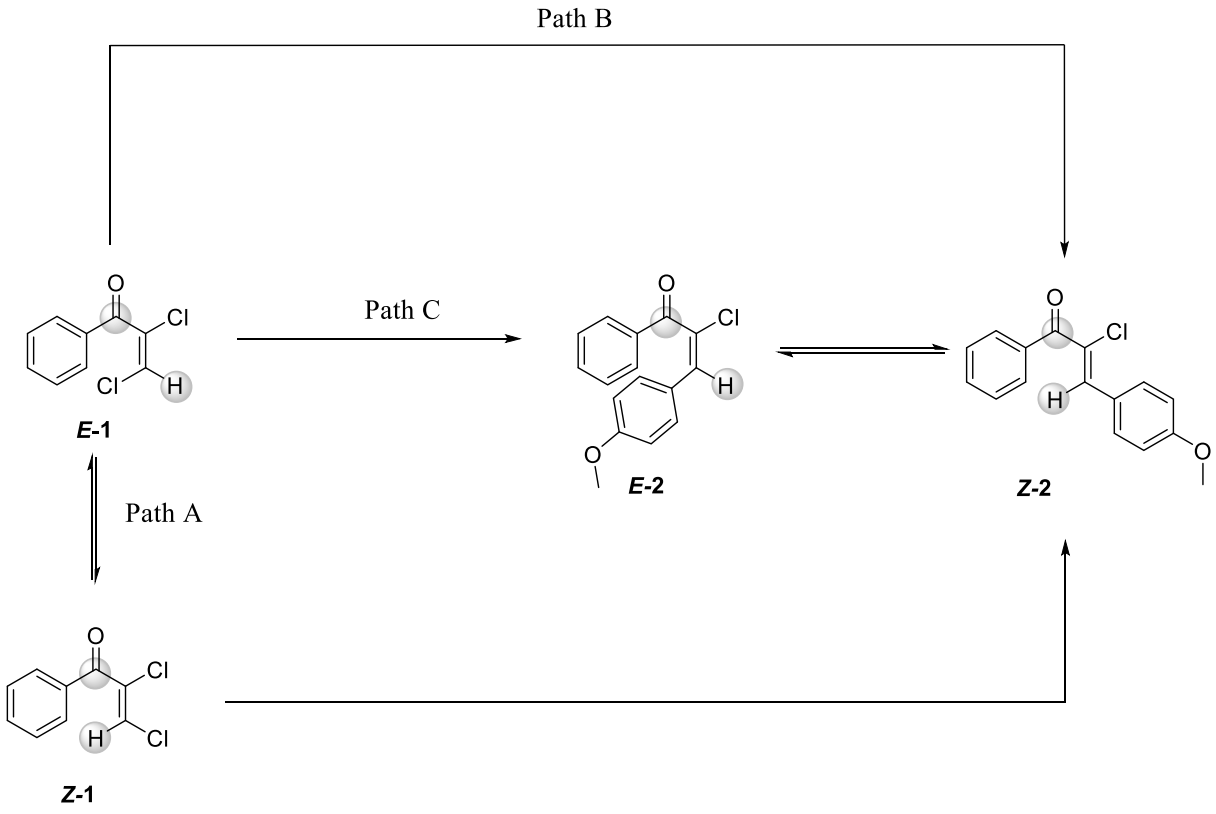

Figure 25: Pictorial representation of three plausible pathways leading to the isomerized Suzuki cross coupling product.

If the isomerization takes place via Path A or C, then Suzuki cross coupling reactions would be considered stereospecific, whereas if it takes place via Path B, then there would be loss of stereospecificity in the Suzuki cross coupling reaction. The simplest way to know this would be to monitor the entire reaction. The first choice to monitor the entire process was with the easily accessible NMR instrument. Reaction monitoring by NMR spectroscopy can provide detailed insights, but because of the presence of the solid base i.e. cesium carbonate in the reaction, this technique could not be used to monitor the entire cross coupling reaction. For this, we collaborated with Dr. Jason Hein (University of British Columbia). He mentioned about the availability of an automated analytical set up in his laboratory that combines automated reaction sampling from the reaction mixture, quenches the aliquot and performs real time analysis via HPLC. These reactions were of interest to him as he could demonstrate the ability of his instrument to monitor the heterogenous reactions.

With a hope of monitoring reaction progress and eventually acquiring some kinetic data, the Suzuki cross coupling on ***E*-1** with $Pd_2(dba)_3$ (0.25 mol%), DPEphos (0.5 mol%), p-methoxyphenylboronic acid and cesium carbonate in dioxane at 40 °C was run on the automated platform (Scheme 92).

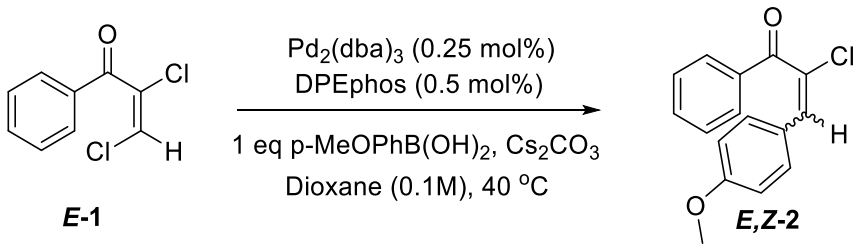

*Scheme 92: Suzuki cross coupling on (**E-1**) monitored via HPLC.*

The formation of ***Z*-2** was observed in the very first data point (Figure 26) and hence whether ***E*-2** forms first and then isomerizes to ***Z*-2** could not be answered. The aim of finding whether

the Suzuki cross coupling on ***E*-1** is stereospecific or not could not be accomplished by using this instrument.

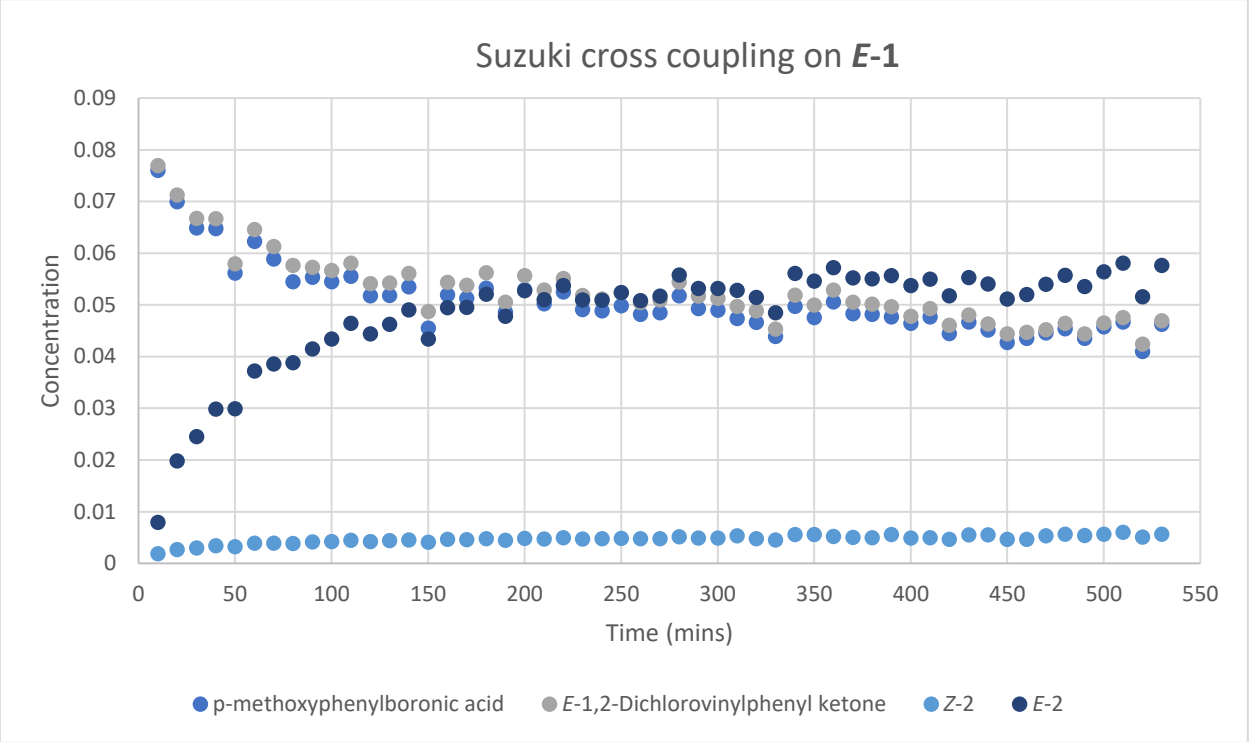

*Figure 26: Suzuki cross coupling on **E-1**.*

The instrument monitored the reactions very well but the higher degree of scatter in the plot raised the concerns of the reproducibility.[80] The lack of reproducibility could be because of the presence of the heterogenous base in the reaction which can lead to the variation in the concentration of each aliquot. This experiment suggested that the instrument still needs development to perform kinetic analysis of the heterogenous reactions. Owing to the lack of reproducibility, the kinetic studies were not continued for this project.

Attempt was made to use organic base, triethylamine instead of the heterogenous base. The Suzuki cross coupling on ***E*-1** did not take place in the presence of the triethylamine.

Standalone studies on ***E*-1** and ***E*-2** - Individual reagents and their combinations

We proposed that isomerization could take place inside the catalytic cycle or outside the catalytic cycle. The isomerization taking place inside the catalytic cycle would mean that it takes place during one of the three steps, i.e., oxidative addition, transmetallation or reductive elimination. The isomerization taking place during the catalytic cycle would simply imply Suzuki cross-coupling is not stereospecific in nature. If ***E*-1** isomerizes before entering the catalytic cycle or ***E*-2** isomerizes after leaving the catalytic cycle, then the isomerization process can be envisioned as taking place outside the catalytic cycle. This would mean that Suzuki cross-coupling reactions are stereospecific in nature and there is an independent mechanism for the isomerization.

After ruling out the accepted mechanisms, detailed studies with individual reagents and their combinations were performed on ***E*-1** and ***E*-2**. Both ***E*-1** and ***E*-2** were heated with individual reagents and their combinations in dioxane at 85 °C. The aim was to find the combination that gives the significant isomerization. These reactions were analyzed by GC-MS after 1 h, 2 h, 3h and 24h.

2.7.4.1. Outside the catalytic cycle: Path A

The Table 6 shows the extent of isomerization of ***E*-1** when exposed to the individual/ combination of the reagents used in the Suzuki cross coupling of ***E*-1**. Although the reactions were monitored for 24 h, the first hour time window results are crucial. This is because, 96% selectivity of the isomerized product was observed in about 25 mins as an outcome of Suzuki cross coupling on ***E*-1**.

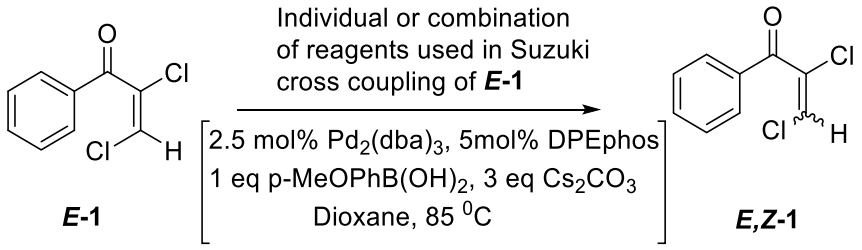

***E*-1** ***E,Z*-1**

S.No.	Component	*E*: *Z* (1) After 1h	*E*: *Z* (1) After 2h	*E*: *Z* (1) After 3h	*E*: *Z* (1) After 24 h
1.	$Pd_2(dba)_3$	100:0	100:0	100:0	91:9
2.	DPEphos	92:8	73:27	57:43	5:95
3.	Cs_2CO_3	100:0	N/P	-	-
4.	Dioxane	100:0	100:0	100:0	100:0
5.	p-MeOPhB$(OH)_2$	100:0	100:0	100:0	100:0
6.	$Pd_2(dba)_3$ + DPEphos	100:0	100:0	100:0	100:0
7.	$Pd_2(dba)_3$ + Cs_2CO_3	100:0	100:0	N/P	-
8.	$Pd_2(dba)_3$ + p-MeOPhB$(OH)_2$	100:0	99:1	99:1	96:4
9.	DPEphos + Cs_2CO_3	99:1	99:1	N/P	-
10.	DPEphos + p-MeOPhB$(OH)_2$	98:2	93:7	89:11	20:80
11.	Cs_2CO_3 + p-MeOPhB$(OH)_2$	N/P	-	-	-
12.	$Pd_2(dba)_3$ + DPEphos + Cs_2CO_3	100:0	100:0	100:0	N/P
13.	$Pd_2(dba)_3$ + DPEphos + p-MeOPhB$(OH)_2$	100:0	100:0	100:0	100:0
14.	DPEphos + Cs_2CO_3 +	N/P	-	-	-

	p-MeOPhB(OH)$_2$				

*N/P = No product observed

*Table 6: E-Z isomerization results when **E-1** is exposed to individual or combination of the Suzuki cross coupling reaction conditions.*

Compound ***E*-1** only isomerized in the presence of 5 mol% DPEphos. It was observed that ***E*-1** led to the formation of 8% ***Z*-1** when heated for 1 hr and 95% ***Z*-1** when heated for 24 hr with 5 mol% DPEphos in dioxane at 85 °C. This would imply phosphines are inducing the isomerization but as discussed in the section 2.7.3., the isomerization via this pathway has been ruled out. These studies suggested that ***E*-1** does not isomerize before entering the catalytic cycle and therefore Path A (Figure 25) is too slow to be the main isomerization process. The other combination that led to 80% of the isomerization of ***E*-1** after 24 hr is 5 mol% DPEphos and p-MeOPhB(OH)$_2$. This combination gave only 2% isomerization after an hour, so isomerization with this combination can not be responsible for the loss of the stereochemistry in the Suzuki cross coupling reaction. Also, no isomerization of ***E*-1** was observed in the presence of the $Pd_2(dba)_3$ and DPEphos which suggests that the oxidative addition is stereospecific.

2.7.4.2: Inside the catalytic cycle: Zwitterionic character of vinyl palladium species-Path B

It has been proposed in the literature that the vinylpalladium intermediate (**207**) has a significant zwitterionic character as indicated by resonance structures **208** and **208′**. This would be expected to correspond to a weakening of the C=C bond, which might allow rotation to occur. This pathway can explain the transformation of **207** to **209** (Scheme 93).

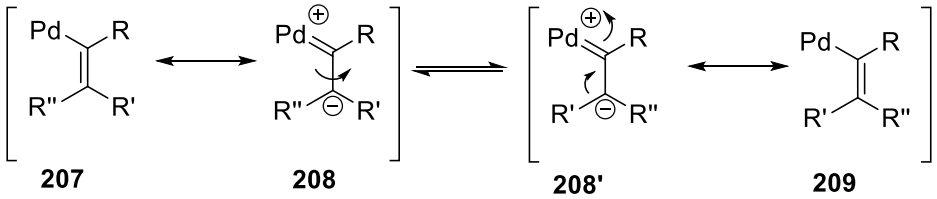

Scheme 93: E-Z isomerization via vinylpalladium intermediate.

This pathway can be envisioned to take place on ***E*-1** after oxidative addition (but before the transmetallation step) as shown in Scheme 94. There is a formation of vinylpalladium species **210** after oxidative addition.

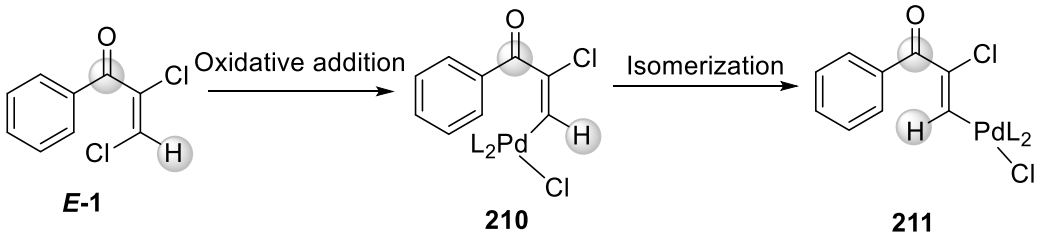

*Scheme 94: E-Z isomerization after oxidative addition on (**E-1**).*

This pathway can also be envisioned to take place on the transmetallated species during the transmetallation step (**212**) (Scheme 95).

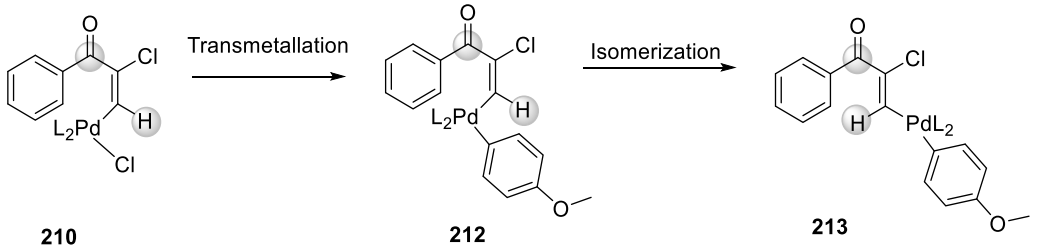

Scheme 95: E-Z isomerization during transmetallation step

The isomerization of ***E*-1** during the oxidative addition was ruled out based on the experimentation done in section 2.7.4.1. No isomerization was observed when ***E*-1** was heated with $Pd_2(dba)_3$ and DPEphos (**180**) at 85 °C (see section 2.7.4.1).

Isomerization during the transmetallation step is one of the accepted mechanisms in the literature.[51b, 53a, 53c, 53d, 60, 81] Lipshutz et al. proposed this pathway for the loss of stereochemistry during Suzuki, Negishi and Stille cross couplings on *Z* alkenyl halides, as mentioned in Chapter 1. If loss of the stereochemistry is taking place in the transmetallation step, it would mean that there is stereospecific insertion of palladium in the oxidative step followed by the isomerization in the transmetallated intermediate, which is proposed to possess zwitterionic character.

To test this pathway, Suzuki cross coupling was done on ***E*-1** with different concentrations of the catalyst. The reactions were let go for 1 hr and then analyzed by GC-MS. It was proposed that changing the catalyst concentration in the Suzuki cross coupling reaction would change the rate of the Suzuki cross coupling reaction but should not change the ratios of the isomers.

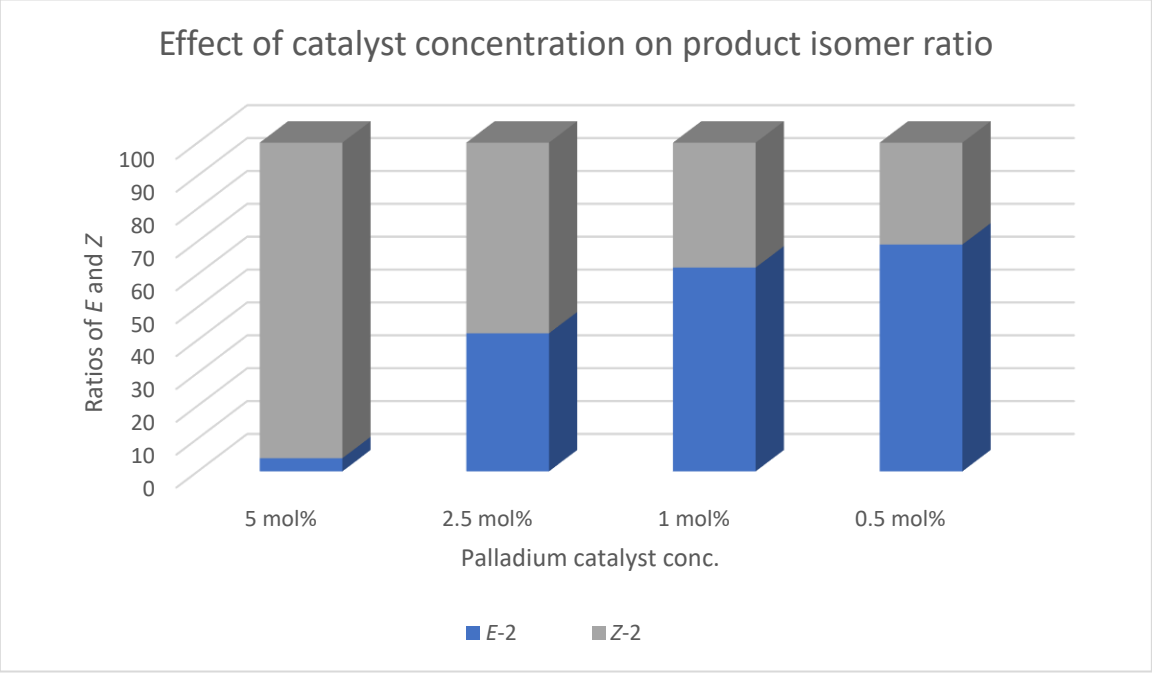

*Figure 27: Reaction outcome by varying palladium catalyst concentration in Suzuki cross coupling on (**E-1**).*

As shown above in Figure 27, when a Suzuki cross coupling on ***E*-1** with 5 mol% and 2.5 mol% was analyzed after one hour with GC-MS, it was observed that both the reactions has achieved 100% conversion but the *E*/*Z* ratios from the two reactions were vastly different. The reaction with 5 mol% gave 96% *E* isomer whereas the reaction with 2.5 mol% gave only 42% *E* isomer. The rate of the isomerization further decreased by lowering the catalyst loading. This ruled out isomerization taking place in the transmetallation step via zwitterionic vinylpalladium species.

The proposal of the isomerization taking place inside the catalytic cycle arising is contrary to the observation that the *E*/*Z* ratio is not constant. As discussed in the section 2.6., it has been observed that the isomerization continues even after the completion of the Suzuki cross coupling reaction. If this is the sole pathway then the ratios of *E* and *Z* isomers established during the Suzuki cross coupling reactions should be final, but this is contrary to the observation.

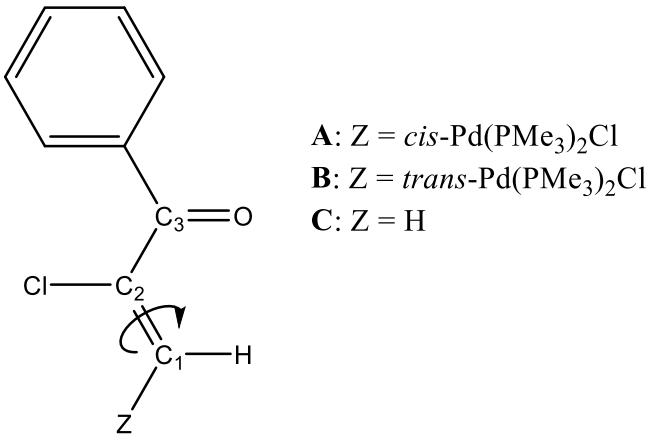

Figure 28: Model compounds for DFT studies.

From the DFT calculations of the forced rotation around C_1=C_2 bond (in model compounds A, B and C, Figure 28) done by Dr. Peter Budzelaar, it was revealed that the palladium atom

does not facilitate rotation (see Appendix). The barrier for the rotation around C=C bond in model compounds A and B was similar to when there is hydrogen atom at the position of the palladium (model compound C).

If the vinylpalladium compound **207** has a zwitterionic character as displayed by resonance form **208**, then it would be expected that C_1=C_2 bond length would be elongated and C_2-Pd bond would be shortened (Scheme 96). In the DFT studies done by Dr. Peter Budzelaar, it was revealed that the lengths of the C=C and C-Pd were not perturbed. On the basis of this study, the isomerization via vinylpalladium carbene **208** was completely ruled out.

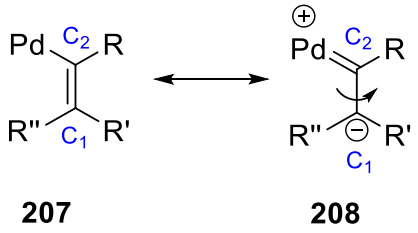

Scheme 96: Zwitterionic structure for vinylpalladium species.

2.7.4.3: Outside the catalytic cycle: Path C

Similarly, compound ***E*-2** was heated with all individual reagents and their combination in dioxane at 85 °C and reactions were analyzed by GC-MS. The reactions were analyzed after 1h, 2h, 3h and 24h. The results after 1hr are crucial because 96% loss of stereochemistry was observed in 25 mins during Suzuki cross coupling on ***E*-1**. The results below in Table 7, shows the extent of isomerization of ***E*-2** when exposed to the individual/ combination of the reagents used in the Suzuki cross coupling of ***E*-1**.

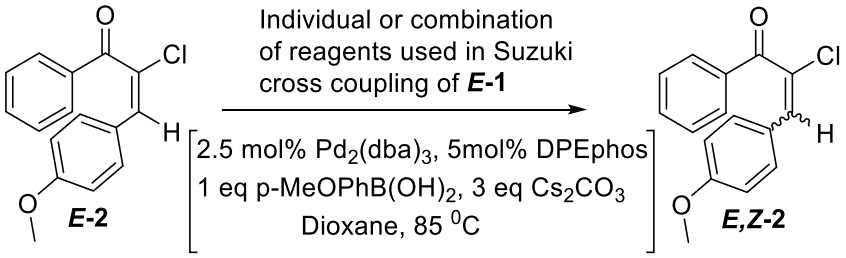

S.No.	Component	*E*: *Z* (2) After 1h	*E*: *Z* (2) After 2h	*E*: *Z* (2) After 3h	*E*: *Z* (2) After 24 h
1.	$Pd_2(dba)_3$	98:2	98:2	98:2	98:2
2.	DPEphos	97:3	97:3	96:4	94:6
3.	Cs_2CO_3	99:1	95:5	91:9	80:20
4.	Dioxane	100:0	97:3	97:3	94:6
5.	p-MeOPhB$(OH)_2$	99:1	98:2	98:2	92:8
6.	$Pd_2(dba)_3$ + DPEphos	13:87	4:96	4:96	4:96
7.	$Pd_2(dba)_3$ + Cs_2CO_3	92:8	89:11	91:9	83:17
8.	$Pd_2(dba)_3$ + p-MeOPhB$(OH)_2$	93:7	93:7	88:12	77:23
9.	DPEphos + Cs_2CO_3	82:18	89:11	89:11	80:20
10.	DPEphos + p-MeOPhB$(OH)_2$	89:11	87:13	86:14	85:15
11.	Cs_2CO_3 + p-MeOPhB$(OH)_2$	82:18	53:47	31:69	17:83
12.	Pd2$(dba)_3$ + DPEphos + Cs_2CO_3	36:64	34:66	25:75	23:77
13.	$Pd_2(dba)_3$ + DPEphos + p-MeOPhB$(OH)_2$	10:90	4:96	4:96	4:96
14.	DPEphos + Cs_2CO_3 +	63:37	36:64	15:85	6:94

	p-MeOPhB(OH)$_2$				

*N/P = No product observed

*Table 7: E-Z isomerization results when **E-2** is exposed to individual or combination of the Suzuki cross coupling reaction conditions*

The results in Table 7 clearly showed that there were some combinations that gave minor isomerization of ***E*-2**, i.e., the combination of DPEphos and Cs_2CO_3 led to 18% isomerization in an hour, the combination of DPEphos and p-MeOPhB(OH)$_2$ led to 11% isomerization of ***E*-2** in an hour, presence of both cesium carbonate and p-MeOPhB(OH)$_2$ led to 18% isomerization, the combination of DPEphos, Cs_2CO_3 and p-MeOPhB(OH)$_2$ led to 40% isomerization in an hour. All these combinations did not answer the extensive isomerization (96% in 25 mins) observed in Suzuki cross coupling of ***E*-1**, hence efforts were not made to study these combinations.

When ***E*-2** was heated with the combination of $Pd_2(dba)_3$ and DPEphos in dioxane at 85 °C, it led to the formation of ~ 87 % ***Z*-2** after an hour. It was interesting to observe that ***E*-2** does not isomerize in the presence of the $Pd_2(dba)_3$ by itself and DPEphos by itself (see Chapter 6: NMR spectra). It was further observed that the combination of p-MeOPhB(OH)$_2$, DPEphos and $Pd_2(dba)_3$ led to ~ 90 % isomerization of ***E*-2** in 1 hour. The combination of $Pd_2(dba)_3$, DPEphos and Cs_2CO_3 led to ~ 60% isomerization after an hour. Since the presence of $Pd_2(dba)_3$ and DPEphos is common in all these combinations, efforts were made to probe a pathway that would involve the presence of both the components i.e. $Pd_2(dba)_3$ and DPEphos.

The further attempt that were made to observe the isomerization of ***E*-2** in the presence of $Pd_2(dba)_3$ and DPEphos used the NMR instrument. This was done to verify the results obtained from GC-MS and to make sure that no decomposition of the materials is taking place. Initial attempts were made to imitate the reaction conditions. For this the reaction was done in a NMR

tube using ***E*-2**, 2.5mol% $Pd_2(dba)_3$ and 5mol% DPEphos in dioxane as solvent at 77 °C. Since the deuterated dioxane is expensive, d_{12}-cyclohexane was used as to provide the NMR field lock and dioxane as a reaction solvent. Owing to the concentration of the dioxane in the reaction mixture, the dioxane peaks needed to be suppressed in the NMR spectra. This way of monitoring the reactions did not prove to be useful because the methoxy characteristic peaks that could be used for analysis hid under the dioxane peak. The efforts were made to suppress the dioxane peaks but that affected the methoxy peaks too.

To overcome this problem, toluene was used as a reaction solvent instead of the dioxane. During the screening studies toluene/cesium carbonate combination gave same result as dioxane/ cesium carbonate combination. The other advantage of using toluene as a reaction solvent is that the deuterated toluene is much cheaper than deuterated dioxane and hence deuterated toluene can act both as reaction solvent and provide NMR field lock.

To observe the isomerization using NMR spectroscopy, the reaction with ***E*-2**, 2.5 mol% $Pd_2(dba)_3$ and 5 mol% DPEphos (**180**) in d_8-toluene at 77 ^{0}C in the NMR tube was performed. After data processing, the -OCH_3 signals of ***E*-2**and ***Z*-2** were integrated. The first scan was taken just with ***E*-2** in d_8-toluene. This was done to verify the purity of the ***E*-2** before adding the palladium catalyst. As shown in Figure 29, the ***E*-2** isomer is 99% pure. The peak at 3.2 ppm is the methoxy proton of ***E*-2** and peak at 3.4 ppm is from the methoxy proton of ***Z*-2**.

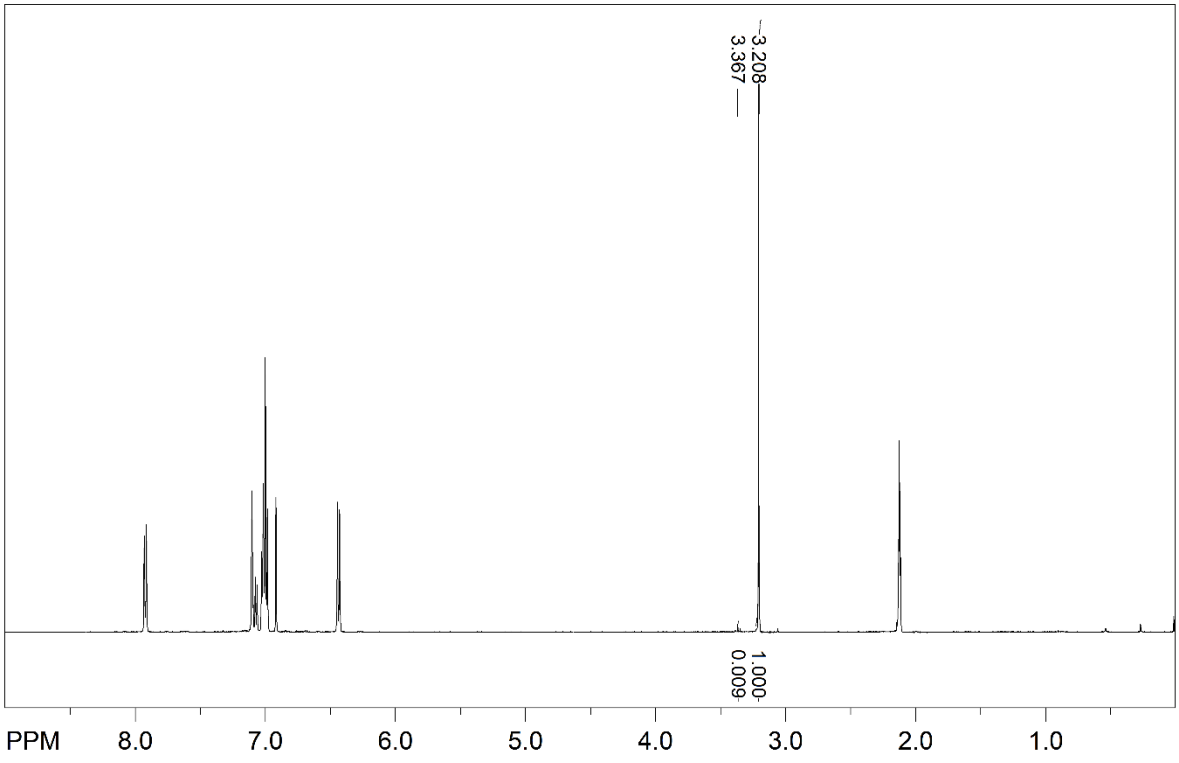

*Figure 29: NMR spectrum of (**E-2**) in d_8-toluene.*

To the 99:1 (***E*-2**: ***Z*-2**) mixture of isomers in d_8-toluene, 2.5 mol% $Pd_2(dba)_3$ and 5 mol% DPEphos was added. For this, the NMR tube was taken out from the NMR instrument and the palladium catalyst was added to the NMR tube. The tube was placed back in the NMR instrument**.** The experiment was set to acquire an array of NMR spectra for 3.5 hr after every 3 min. As shown in Figure 30, the ratio of the isomers changed to 47:53 (***E*-2**: ***Z*-2**) from 99:1 (***E*-2**: ***Z*-2**) in the very first spectrum acquired. This implied that the isomerization was very fast. The ratios changed from 99:1 (***E*-2**: ***Z*-2**) to 47:53 (***E*-2**: ***Z*-2**) during the time spent in ejecting NMR tube from the instrument, injecting palladium catalyst and placing the NMR tube back in instrument (~ 5 min).

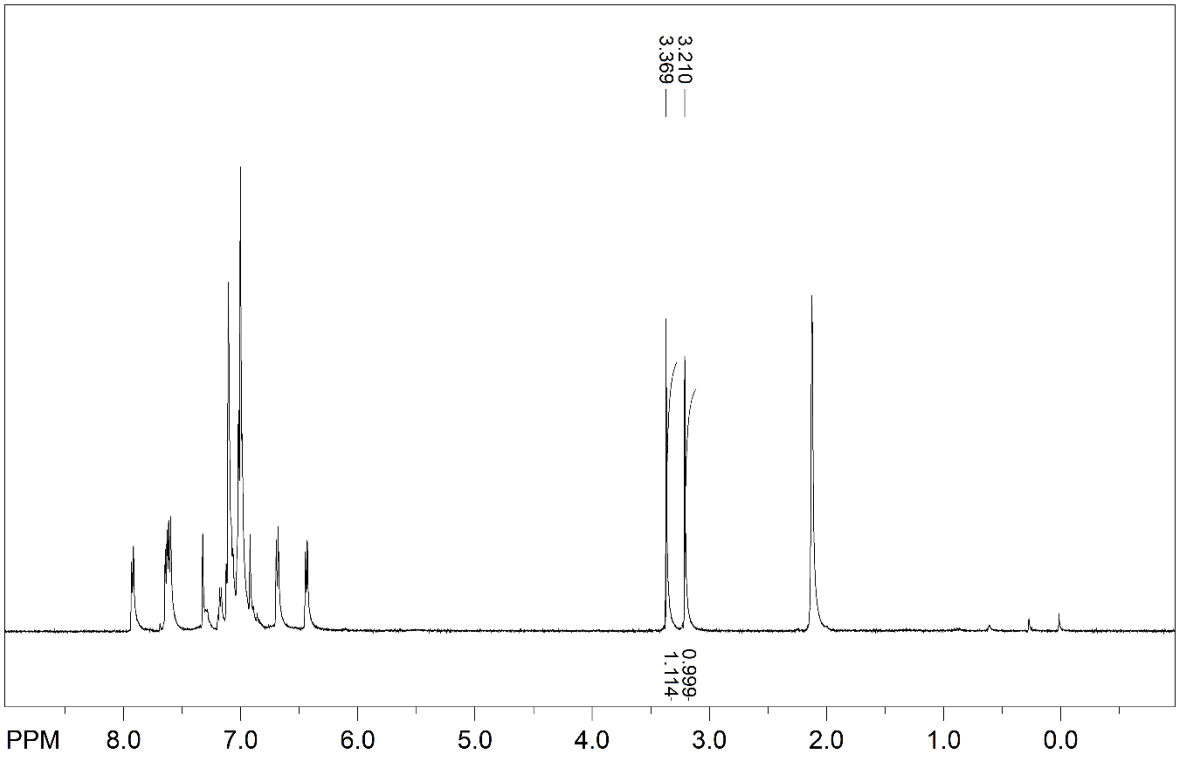

*Figure 30: The NMR spectrum of (**E-2**) in d_8-toluene after adding palladium catalyst.*

The ratios further changed to 4:96 (***E*-2**: ***Z*-2**) in about 25 minutes as showed in Figure 31. The reaction was monitored for 1.5 hr. It was observed that the ratio 4:96 (***E*-2**: ***Z*-2**) did not change further (Figure 32). It was further observed that ***E*-2** *does not* isomerize when $Pd_2(dba)_3$ and DPEphos (**177**) were used by themselves (see Chapter 6: NMR spectra).

The array of the first 20 scans acquired from the above experiment is shown below in Figure 32. It clearly shows that ***Z*-2** changes to ***E*-2** rapidly at 77 °C in the presence of the palladium catalyst. The ratio of the methoxy integrals calculated from the processed data was plotted against the time and the graph was acquired (Figure 33).

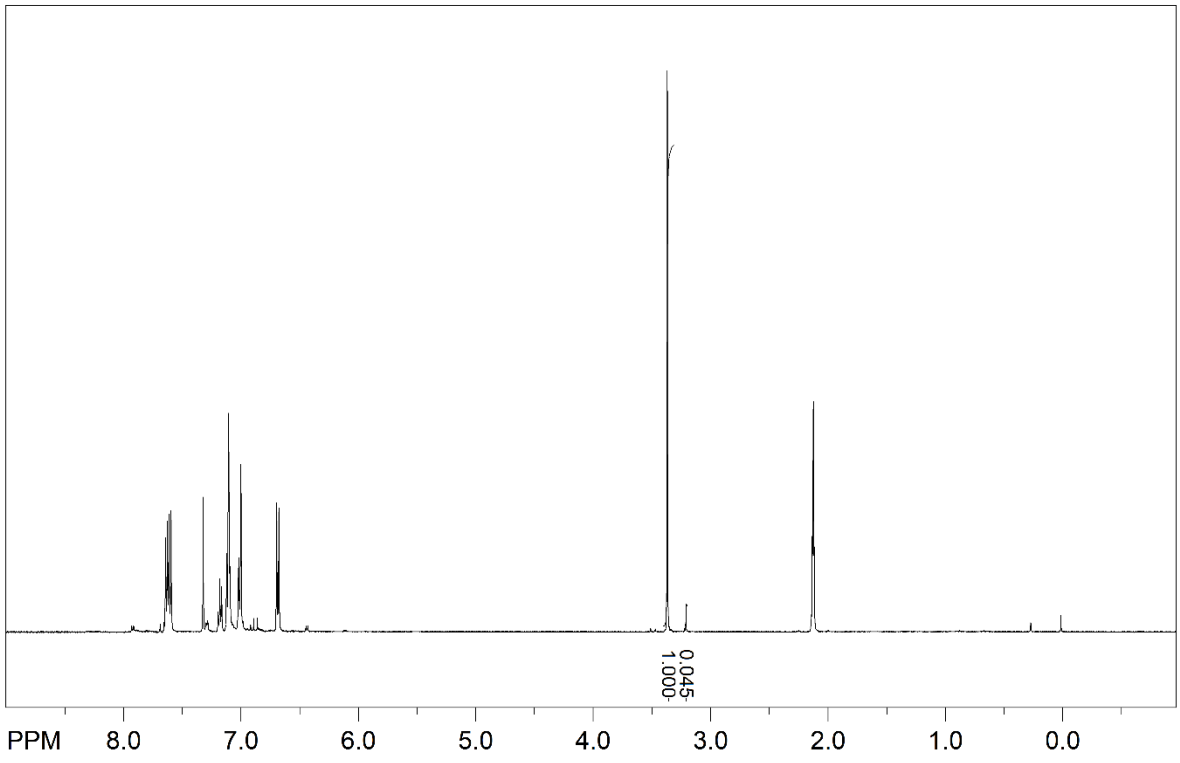

*Figure 31: The NMR spectrum of (**E-2**) in d_8-toluene after 25 min of adding 5 mol% Pd/DPEphos.*

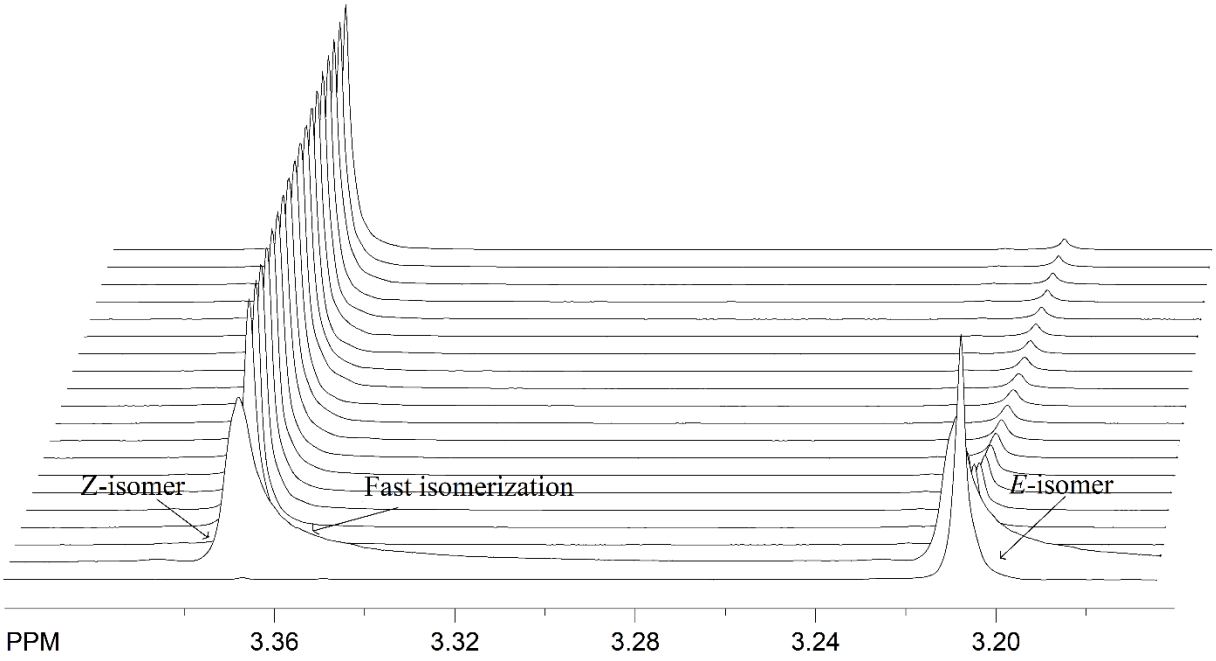

*Figure 32: Isomerization of (**E-2**) to (**Z-2**) in the presence of a 5 mol% Pd/DPEphos.*

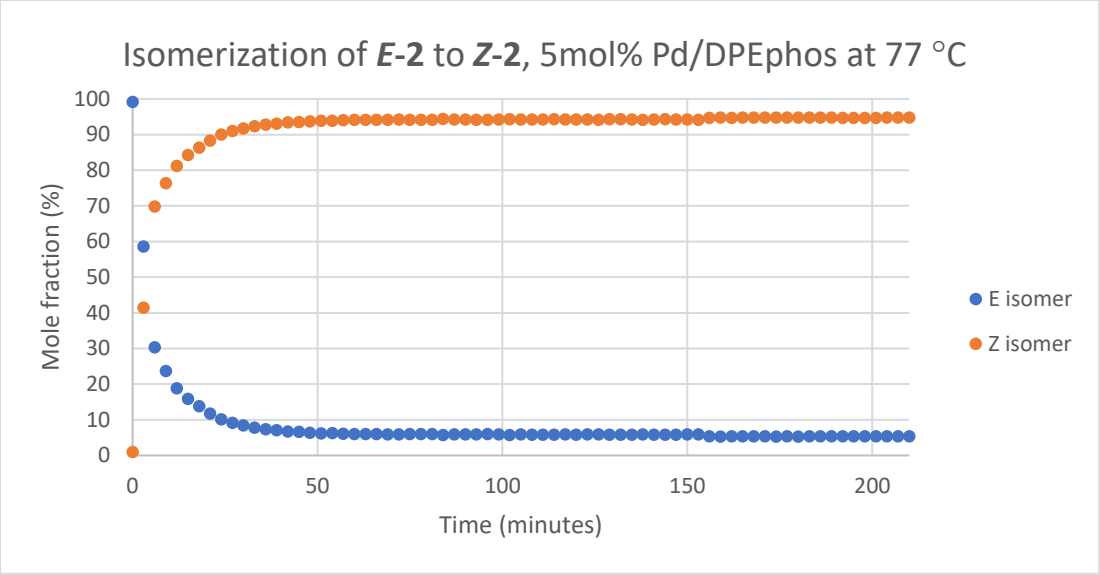

*Figure 33: Graph representing the ratios of (**E-2**) and (**Z-2**) with time in presence of a palladium catalyst at 77 ℃.*

The efforts were also made to study isomerization of ***Z*-2** to ***E*-2** at 40 ℃. As shown in Figure 34, the isomerization slows down as expected at the lower temperature.

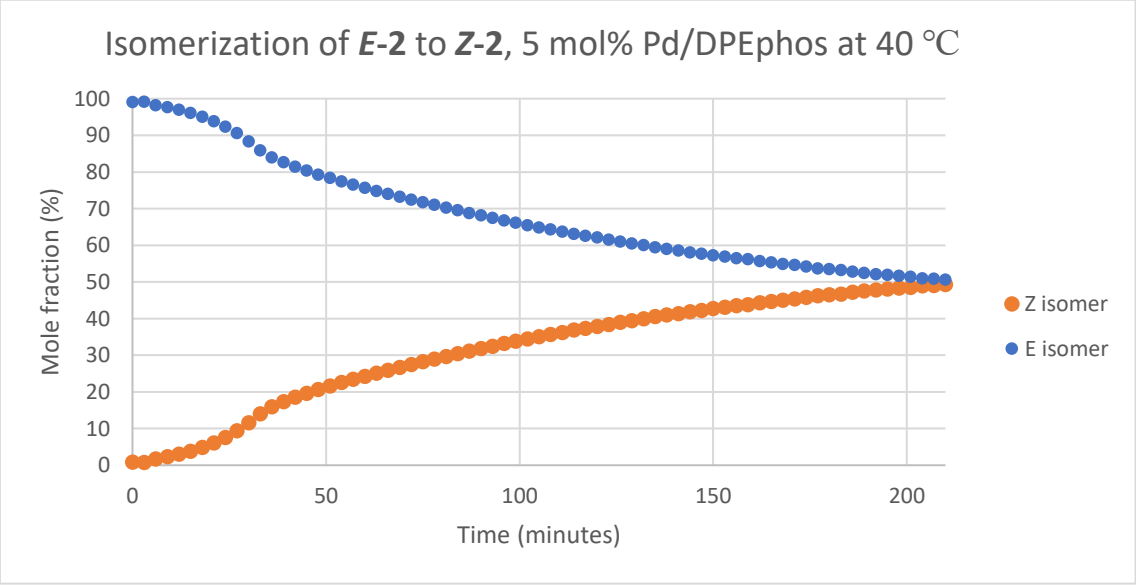

*Figure 34: Graph representing the ratios of (**E-2**) and (**Z-2**) with time in presence of a palladium catalyst at 40 ℃.*

The experimental data suggested that the presence of both palladium and ligand (DPEphos) is the minimum requirement for the isomerization of ***E*-2**. Also, these studies justified that the isomerization is taking place outside the Suzuki cross coupling catalytic cycle (Path C, Figure 25) and substantiated that Suzuki cross coupling reactions on ***E*-1** are stereospecific.

2.7.5. Palladium Hydride

Palladium hydride has been known to show isomerization in olefins.[46a] Formation of a palladium hydride species requires at least the presence of a palladium catalyst (precursor) and a ligand. One plausible pathway responsible for isomerization of ***E*-2** could be the in-situ generation of a palladium hydride species. Isomerization of various alkenes in the presence of a palladium hydride has been illustrated by Skydstrup et al. on various alkenes.[46a]

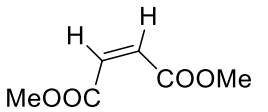

Dimethyl maleate
***Z*-148**

Figure 35: Structure of a dimethyl maleate.

Dimethyl maleate (***Z*-148**) has been shown to isomerize in the presence of palladium hydride species.[46a]

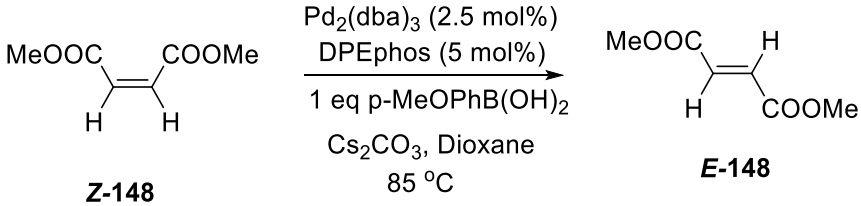

***Z*-148**
1 equivalent

***E*-148**

80% NMR conversion of ***Z*-148** to ***E*-148**

Scheme 97: Isomerization of dimethyl maleate under DPEphos Suzuki cross coupling conditions

To test whether palladium hydride species are being formed in the reaction conditions, dimethyl maleate (***Z*-148**) was added to the DPEphos Suzuki cross coupling conditions without ***E*-2** (Scheme 97). The reaction was let go for 1 hour at 85 ℃ and it was observed that ***Z*-148** isomerized to the 80% dimethyl fumarate ***E*-148**. The crude NMR spectrum (Figure 36) of the reaction clearly shows the formation of dimethyl fumarate (***E*-148**).

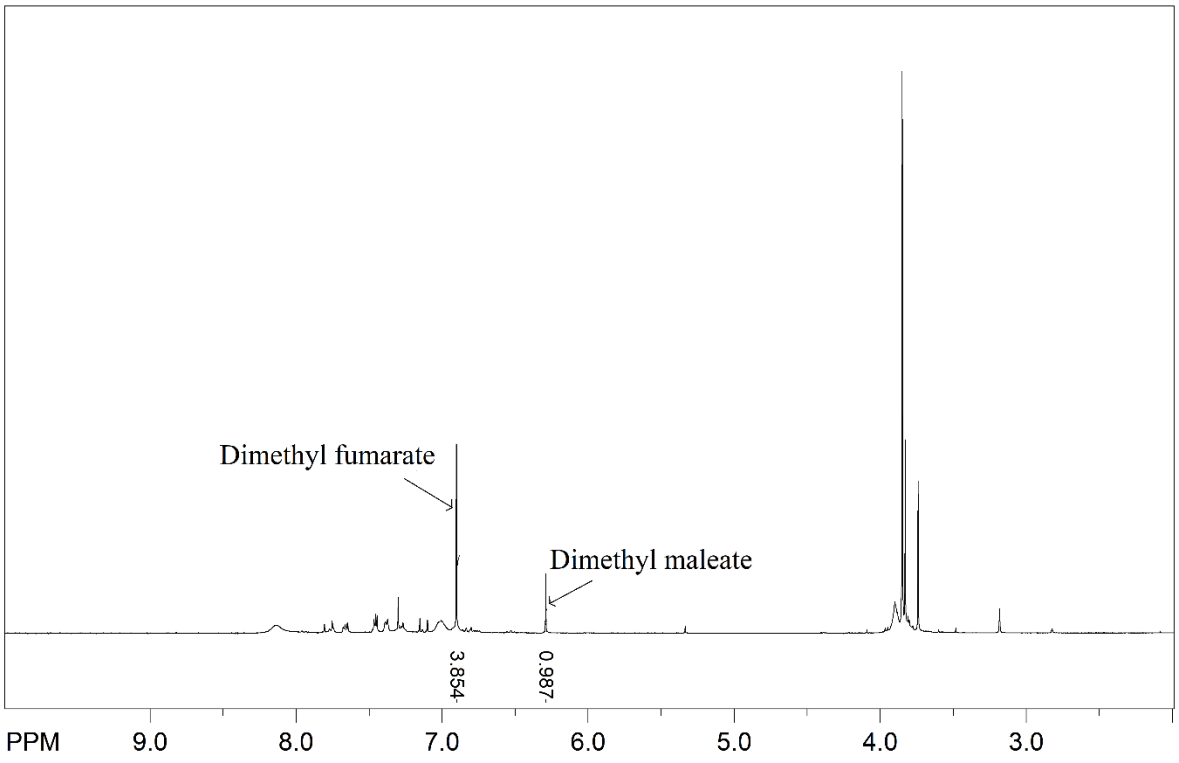

Figure 36: Crude NMR spectrum showing dimethyl maleate isomerization to dimethyl fumarate.

Further it was hypothesized that if ***Z*-148** is added to the Suzuki cross coupling of ***E*-1** under DPEphos Suzuki cross coupling reaction conditions (Scheme 98), then dimethyl maleate (***Z*-148**) could act as an inhibitor and can quench palladium hydride. As a result, addition of dimethyl maleate can result in more Suzuki cross coupled retention product. For this, different concentrations of ***Z*-148** were added the Suzuki cross coupling of ***E*-1** as shown in Scheme 98.

The reactions were analyzed by GC-MS after one hour. The concentrations of the dimethyl maleate used were 0%, 10 mol%, 100 mol% and 500 mol%.

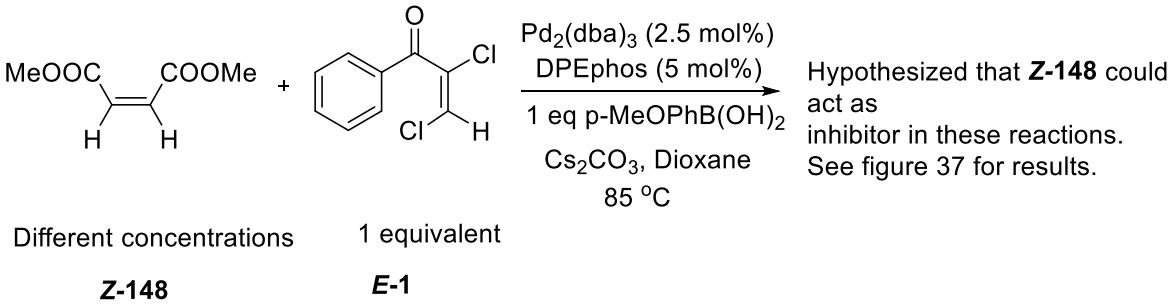

Scheme 98: Experiment designed to verify whether dimethyl maleate acts as an inhibitor.

It was noted that the ratios of retention Suzuki cross coupled product (***E*-2**) and isomerized Suzuki cross coupled product (***Z*-2**) depended on the concentration of dimethyl maleate, with a higher concentration of dimethyl maleate favouring the Suzuki cross coupled product with retention (Figure 37).

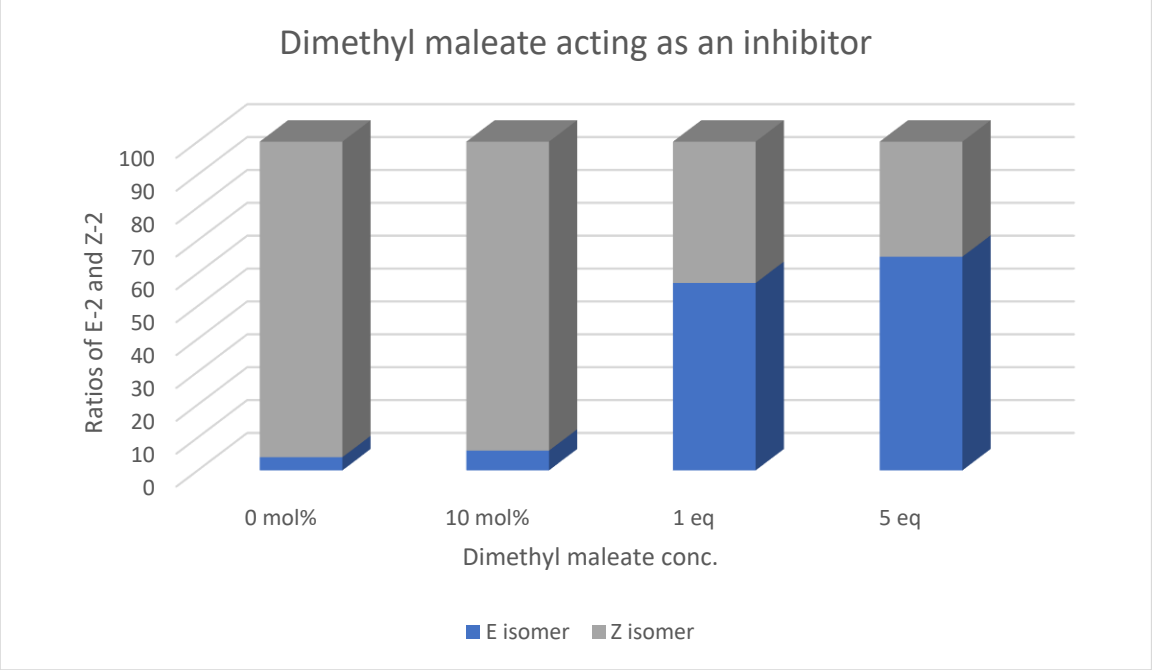

*Figure 37: Chart depicting ratios of (**E-2**) and (**Z-2**) affected by different dimethyl maleate concentrations.*

These two dimethyl maleate experiments strengthened the assumption of the presence of palladium hydride species in the reaction conditions.

As discussed in 2.7.4.3, the minimum requirement for the isomerization is the presence of $Pd_2(dba)_3$ and DPEphos (**180**). It would make sense to assume that if palladium hydride species is responsible for the isomerization then they are being formed in the presence of $Pd_2(dba)_3$ and DPEphos. For this the reaction of dimethyl maleate, $Pd_2(dba)_3$ and DPEphos in the presence of deuterated toluene was run in NMR tube for 1.5 hr at 77 °C and the reaction was monitored by the NMR instrument (Scheme 99). No isomerization was observed in the reaction shown in Scheme 99 after 1.5 hr (Figure 38).

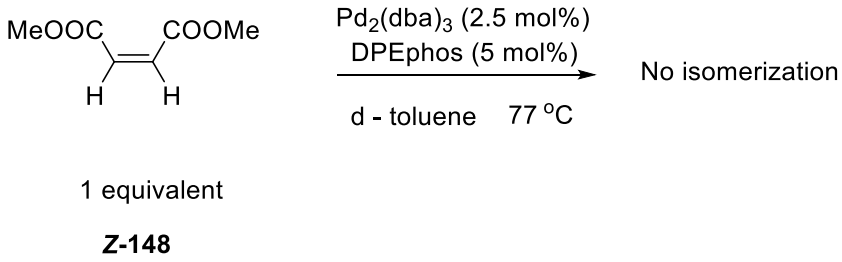

Scheme 99: Experiment designed to verify the presence of the palladium hydride species.

The array of spectra was acquired for the reaction for 1.5 hr. The first spectrum (from below) shown is Figure 38 was acquired after adding palladium catalyst to dimethyl maleate in d_8-toluene at 77 °C. The second spectrum was the last spectrum acquired i.e. after 1.5 hr for the reaction. The third spectrum is a reference spectrum for pure dimethyl fumarate. Since no change was observed between the first and the second spectra, it can be concluded that the palladium hydrides are not generated in the minimum required conditions for isomerization i.e. combination of $Pd_2(dba)_3$ and DPEphos. This experiment argued against a palladium hydride mechanism.

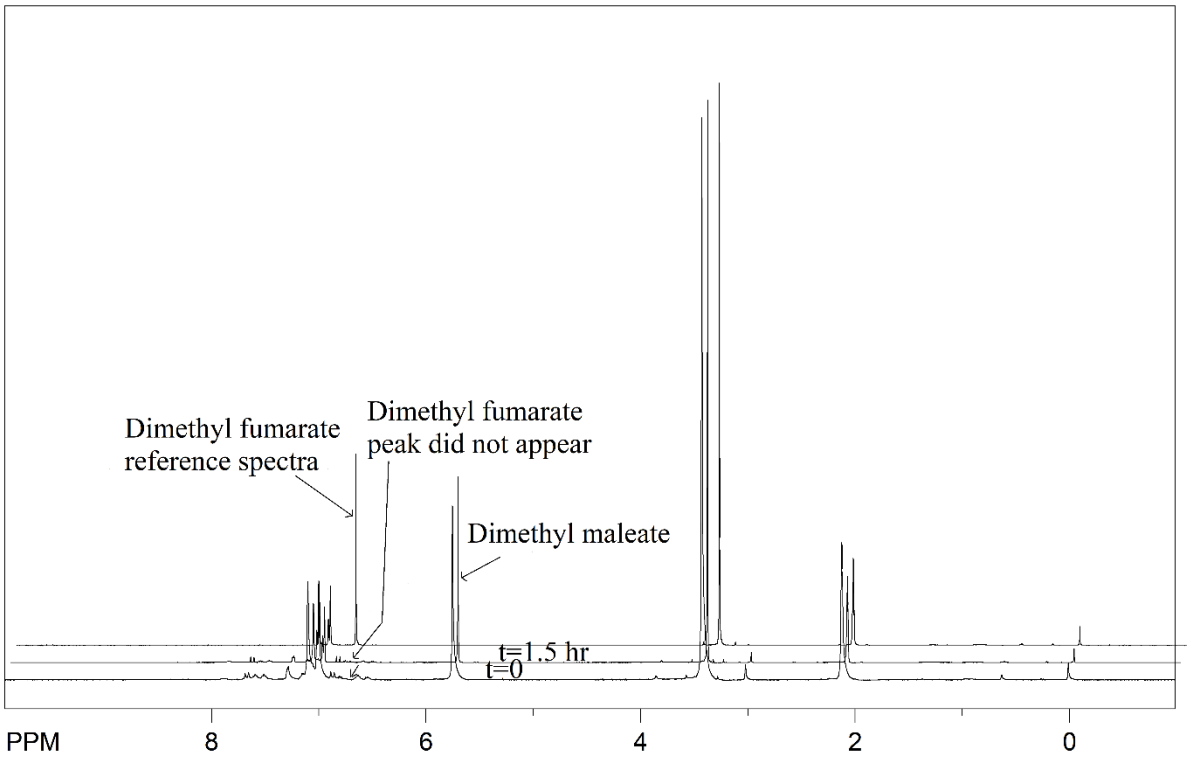

Figure 38: NMR spectra of dimethyl maleate in presence of the palladium catalyst stacked with dimethyl fumarate NMR spectrum.

To further test the presence of a palladium hydride species in the minimal isomerization conditions, a different alkene i.e. cis stilbene was chosen. Cis-stilbene (***Z*-161**) has also been shown to isomerize like dimethyl maleate by Skrydstrup et al.[46a]

For this the reaction of cis-stilbene, $Pd_2(dba)_3$ and DPEphos in the presence of deuterated toluene was run in NMR tube for 1.5 hr at 77 °C (Scheme 100). The reaction was monitored by NMR spectroscopy.

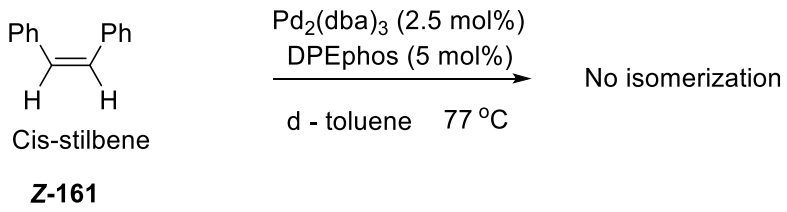

Scheme 100: Testing the isomerization of cis stilbene in the presence of a [Pd].

No isomerization was observed in the reaction shown in Scheme 100 after 1.5 hr. The series of spectra was acquired for the reaction for 1.5 hr.

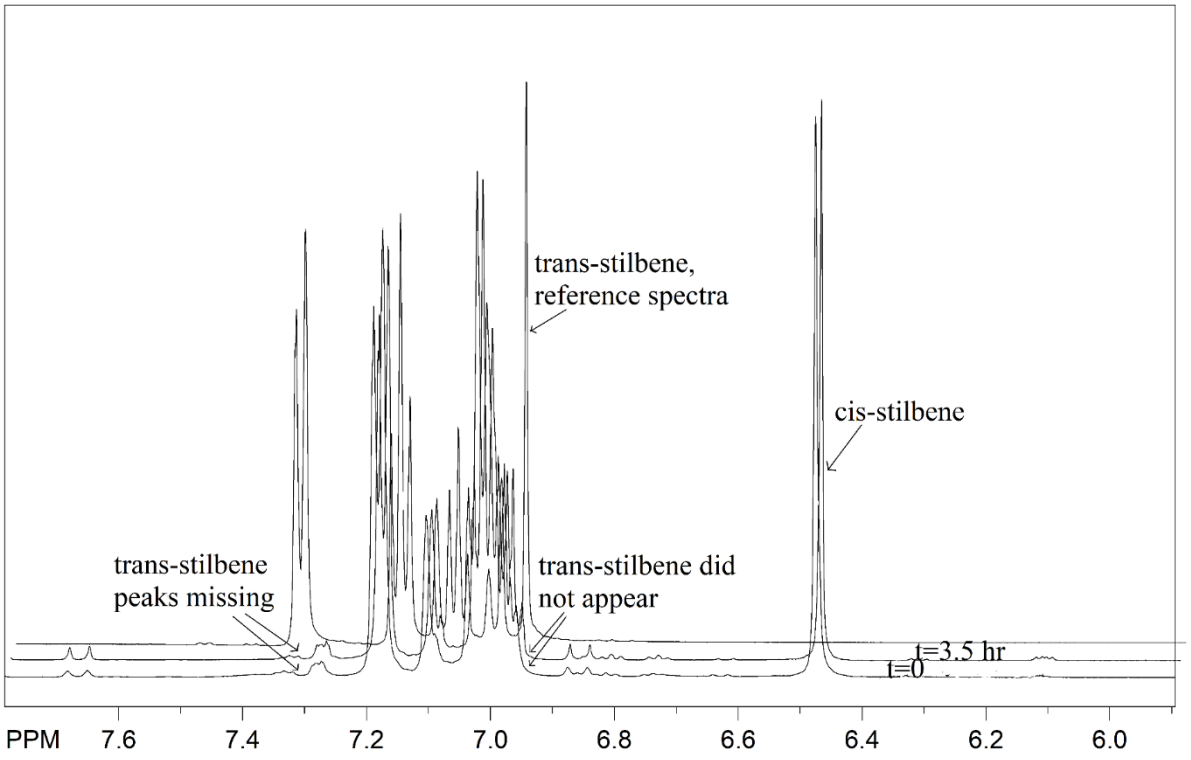

Figure 39: NMR spectra showing no isomerization of cis-stilbene after 1.5 hr

The first spectrum (t=0) shown is Figure 39 was acquired after adding palladium catalyst to cis-stilbene at 77 °C. The second spectrum was the last spectrum acquired i.e. after 1.5 hr for the reaction. The third spectrum is the reference spectrum for pure trans-stilbene.

Since no change was observed between the first and the second spectrum, it can be concluded that the palladium hydride is not generated in the minimum required conditions for isomerization i.e. combination of $Pd_2(dba)_3$ and DPEphos. This experimentation also argued against a palladium hydride mechanism.

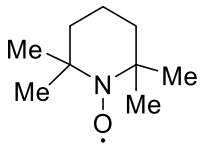

TEMPO
209

Figure 40: Structure of TEMPO.

Palladium hydride traps are compounds known to decompose or quench the palladium hydride species.[82] The palladium hydride trap TEMPO (Figure 40) was used in Suzuki cross coupling reaction. To further verify the presence of the palladium hydride species in the minimal conditions of isomerization, palladium hydride trap TEMPO (**209**) was used.[82] A Suzuki cross coupling reaction of ***E*-1** was run with TEMPO (Scheme 101). The reaction was analyzed by GC-MS and 96% isomerization of ***E*-2** to ***Z*-2** was observed.

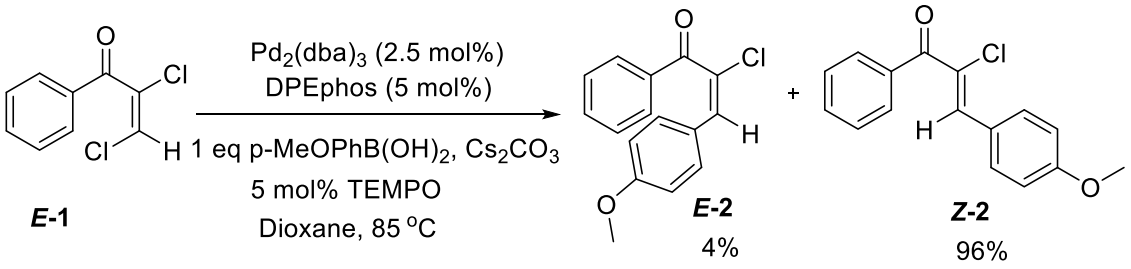

Scheme 101: Use of palladium hydride trap in Suzuki cross coupling of (***E*-1**).

Further, 5 mol% TEMPO (**209**) was added to the reaction mixture of ***E*-2**, 2.5 mol% $Pd_2(dba)_3$, 5 mol% DPEphos in d_8-toluene at 40 °C (Scheme 102). The reaction with 5 mol% TEMPO (**209**) was monitored by NMR for 1.5 hr. The spectrum acquired at the end of 1.5 hr still showed the isomerization (see Chapter 6: NMR spectra). These experiments negate the presence of the palladium hydride species in the isomerization reaction conditions.

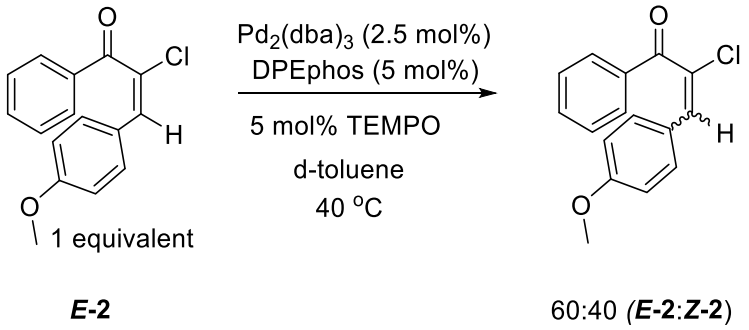

Scheme 102: Palladium hydride trap in the isomerization reaction condition.

Fu et al. demonstrated the use of an amine base Cy_2NMe in regeneration of Pd (0) from Pd (Ⅱ) hydride species.[83] Lipshutz et al. also demonstrated the use amine bases like of TMEDA **(210**) and triethylamine (**211**) in retention of configuration during the Negishi cross coupling.[51b]

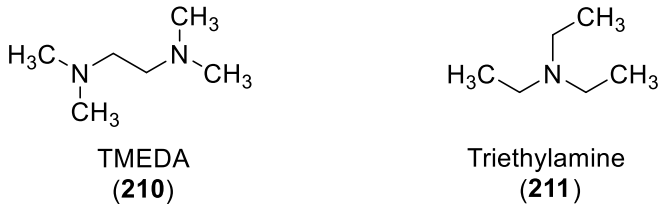

Figure 41: Structures of TMEDA and triethylamine.

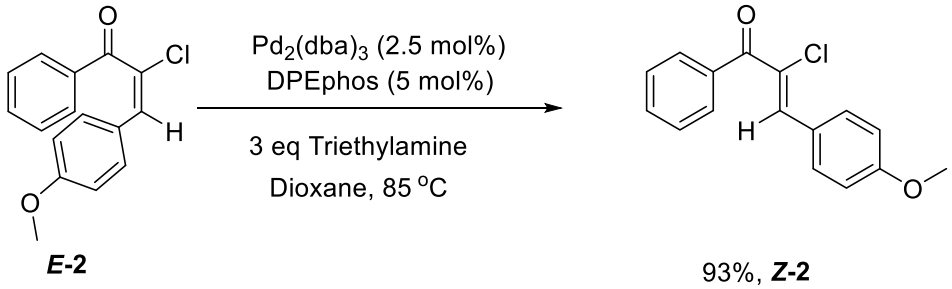

Scheme 103*: The addition of triethylamine to the isomerization reaction conditions.*

On the same lines, the triethylamine was added to the reaction mixture of ***E*-2**, $Pd_2(dba)_3$ and DPEphos in dioxane at 85 °C (Scheme 103). No significant suppression in isomerization was observed after one hour (analyzed by GC-MS).

Further, if palladium hydride can be hypothesized to form in the reaction conditions for Suzuki cross coupling of ***E*-1**, then palladium hydride species should also be expected to form in the reaction conditions of the Suzuki cross coupling of ***E*-162** (Scheme 104).

Further, the responsibility of the palladium hydride species for the isomerization observed during Suzuki cross coupling of ***E*-1** is ruled out on the basis that no isomerization was observed when the cross couplings were performed on the ***E*-162** by the previous graduate student.[64]

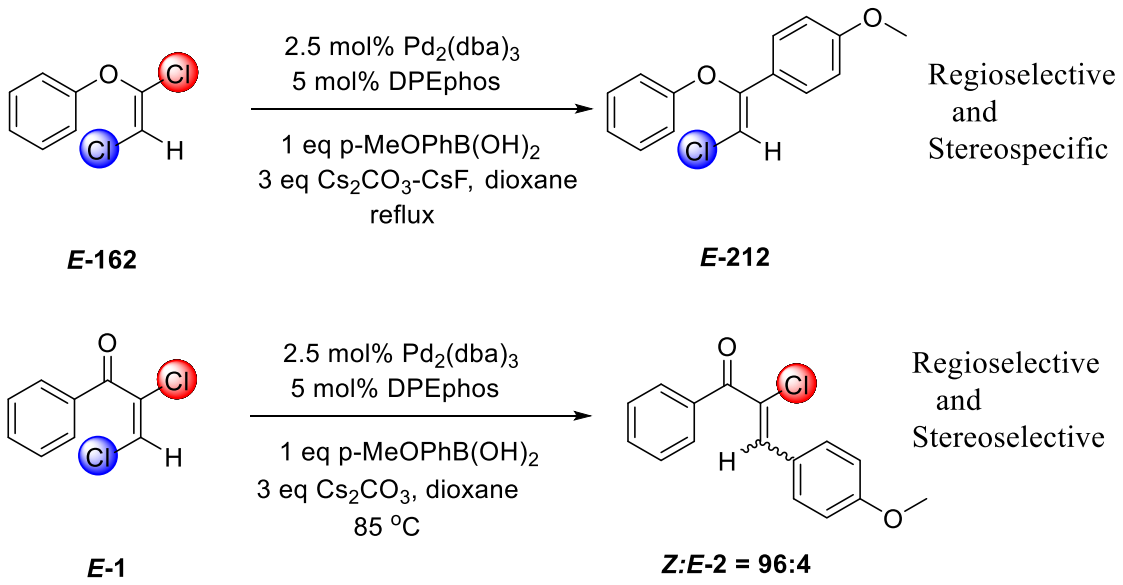

*Scheme 104: Suzuki cross coupling on (**E-162**) and (**E-1**) for comparison.*

It should be noted that reaction conditions for the Suzuki cross coupling of ***E*-162** were very similar to that employed for the Suzuki cross coupling of ***E*-1**. The cross coupling on ***E*-162** were regioselective and stereospecific whereas Suzuki cross coupling on ***E*-1** were regioselective and stereoselective (Scheme 104).

Based on the above arguments it seems very unlikely that a palladium hydride is responsible for the fast isomerization observed with Pd/phosphine combination.

2.7.6. Co-ordination of the substrate to the transition metal

Another pathway that necessitates the presence of a metal catalyst and a ligand is by direct co-ordination of the substrate with the transition metal. This pathway was proposed by Visentin et al. for isomerization of dimethyl maleate in the presence of palladium and P, N ligands.[60]

Visentin et al. proposed the metal coordination pathway, when they observed that dimethyl maleate (***Z*-148**) isomerizes to dimethyl fumarate (***E*-148**) in the presence of palladium complexes [Pd(dppq)(η^2-dmfu)] and [Pd(dppq-Me) (η^2-dmfu)] without any external promoter (mentioned in Chapter 1, Pathways for isomerization). The fact that ***E*-2** undergoes isomerization in the presence of just $Pd_2(dba)_3$ and P, P ligand combination emphasizes this pathway (section 2.7.4.3).

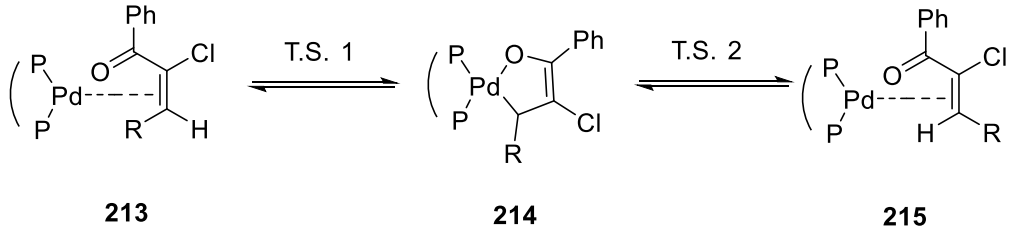

213 **214** **215**

*Scheme 105: Envisioned E-Z isomerization by coordination of (**E-2**) to the palladium catalyst.*

This pathway was envisioned for the observed isomerization of ***E*-2** to ***Z*-2**, with the π co-ordinated complex of ***E*-2** and palladium metal center stabilized by the phosphine ligands, subsequently goes to a relatively low energy five-membered metallacycle intermediate (**213**). This eventually leads to the thermodynamically more stable π coordinated complex of ***Z*-2**. (Scheme 105).

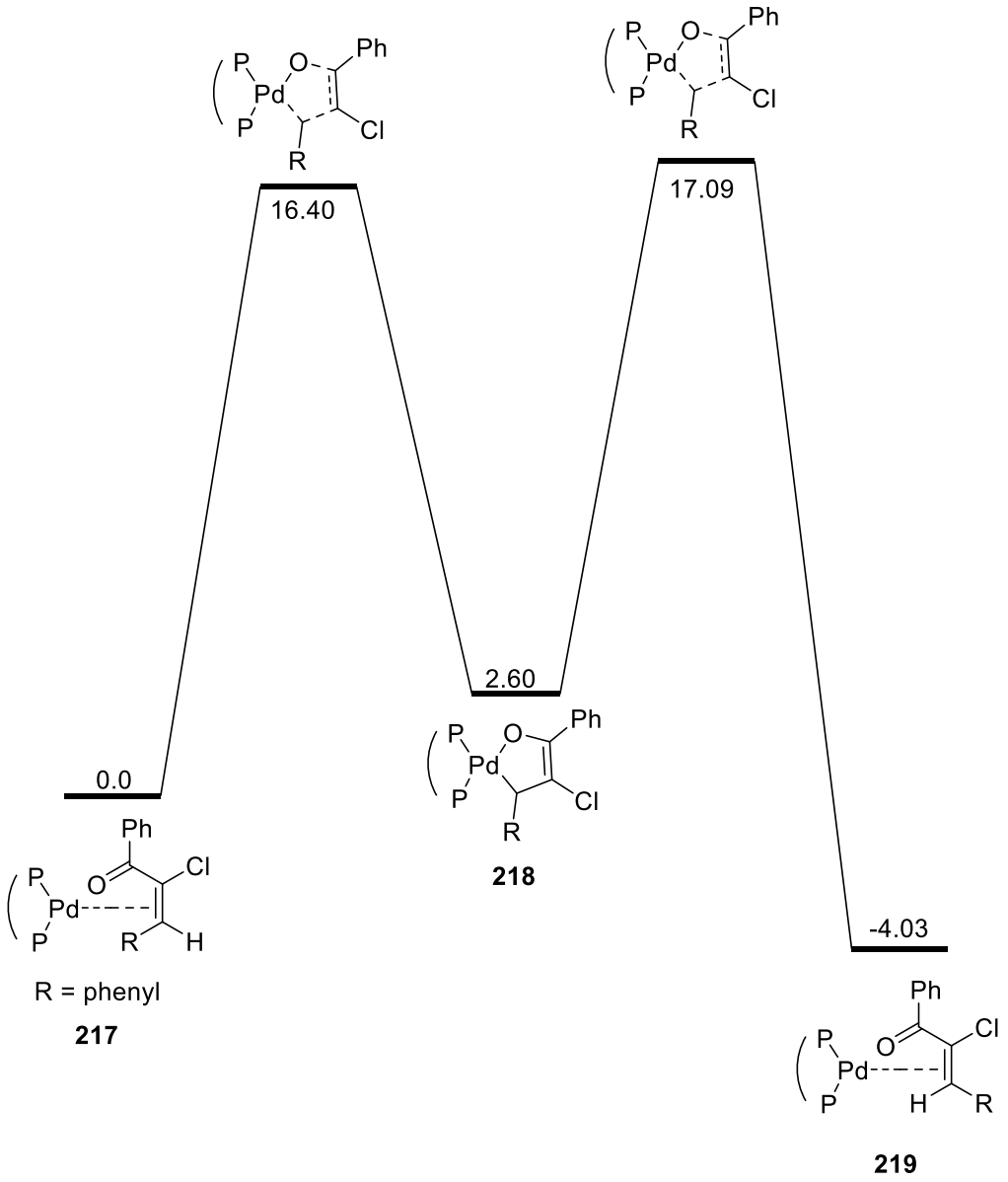

*Figure 42: Two transition states and three minima located for (**E-199**) via DFT studies. Energies (kcal mol^{-1}) relative to **217** are indicated for each calculated stationary state.*

DFT calculations were done by Dr. P.H.M. Budzelaar to calculate the energetics of an enone system. The calculations were done with simple DMPE (**216**) ligand. This ligand was chosen as a generic bisphosphine ligand model but not intended to model any specific ligand used in the experimental work.

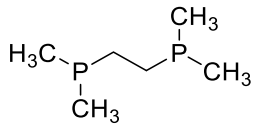

216

Figure 43: Structure of DMPE ligand.

The three minima and two transition states were located for ***E*-199**/ ***Z*-199**. The kinetic barrier for the entire process was ~ 17 kcal (Figure 42).

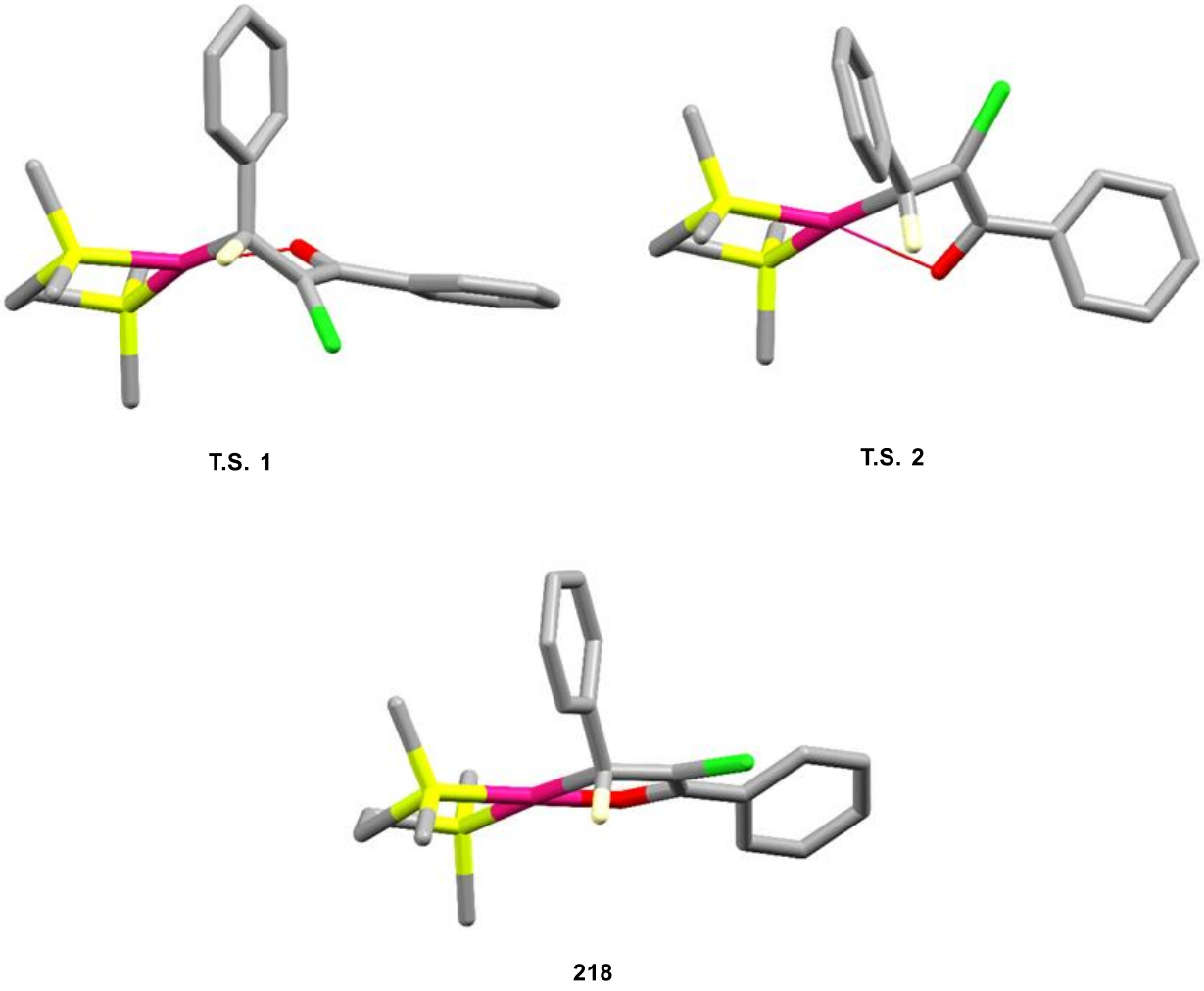

Figure 44: Pictures for two transition states and an intermediate shown in Figure 42.

The formation of 5-membered metallacycle (**218**) can be described as a rapid nucleophilic attack of palladium at 1,4 olefinic site leading to the shift of the double bond and eventually a

forming a bond between Pd and oxygen. The pictures in Figure 44, shows that the two transition states (Figure 42) go via flat five membered metallacycle (**218**) and there is a ring flipping between two transition states.

As discussed in the Section 2.5.3, the outcome of the Suzuki cross coupling can be tuned by the nature of the ligand. The presence of the DPEphos ligand led to the ***Z*-2** and presence of *t*-Bu-Xantphos or "no phosphine ligand" led to the formation of ***E*-2**. It has been made clear in section 2.7.4.3 that the presence of $Pd_2(dba)_3$ and DPEphos (phosphine ligand) is the requirement of the isomerization. To demonstrate the effect of ligands on the isomerization, the reactions showed in Scheme 106 and Scheme 107 were monitored by NMR spectroscopy. In first reaction, ***E*-2** was run with $Pd_2(dba)_3$ and DPEphos in d_8-toluene at 77 °C (Scheme 106). The fast isomerization in presence of DPEphos is clearly demonstrated in Figure 45. Although the reaction was let go for 5 hr but the formation of 96% ***Z*-2** was observed in about half an hour.

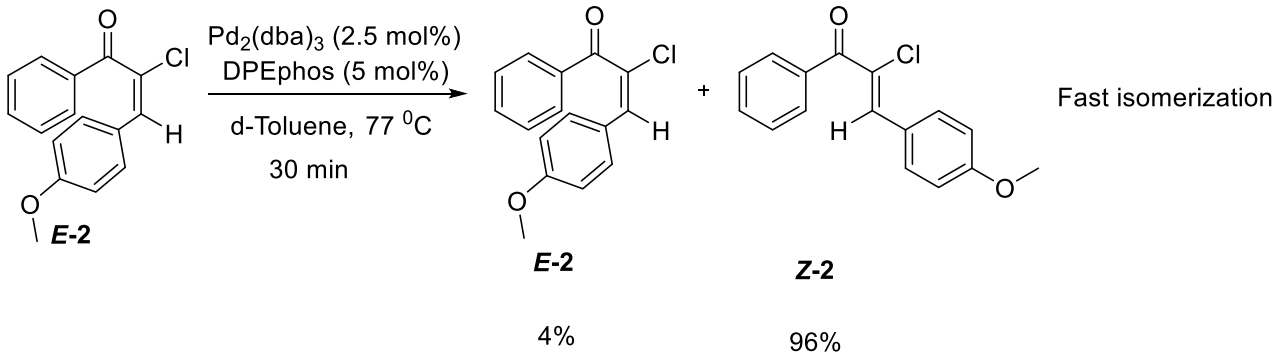

*Scheme 106: (**E-2**) to (**Z-2**) isomerization in the presence of the DPEphos phosphine.*

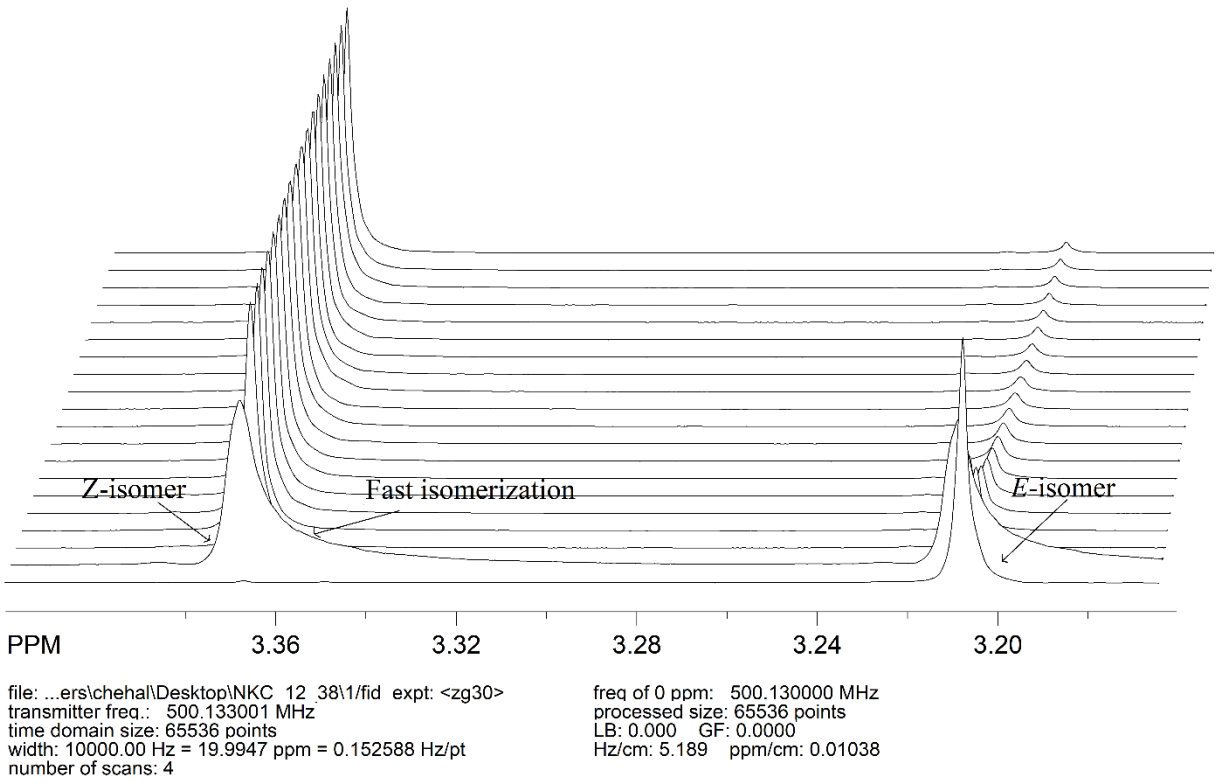

*Figure 45: Isomerization of (**E-2**) in 5 mol% Pd/DPEphos monitored by NMR. This figure is same as figure 34.*

In second reaction, ***E*-2** was run with $Pd_2(dba)_3$ and *t*-Bu-Xantphos in d_8-toluene at 77 °C (Scheme 107). The slow isomerization in the presence of *t*-Bu-Xantphos are clearly demonstrated in Figure 46. Only 4% of the isomerization was achieved after four hours.

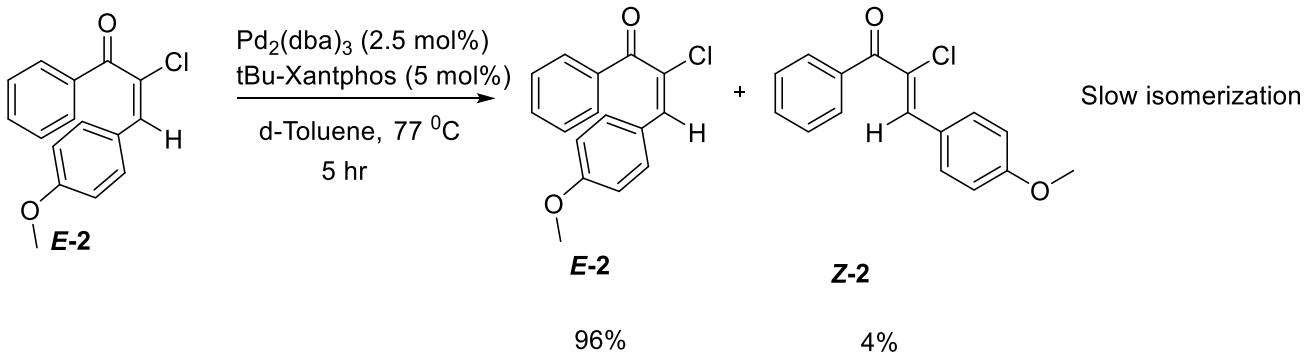

*Scheme 107: (**E-2**) to (**Z-2**) isomerization in the presence of the t-Bu-Xantphos phosphine*

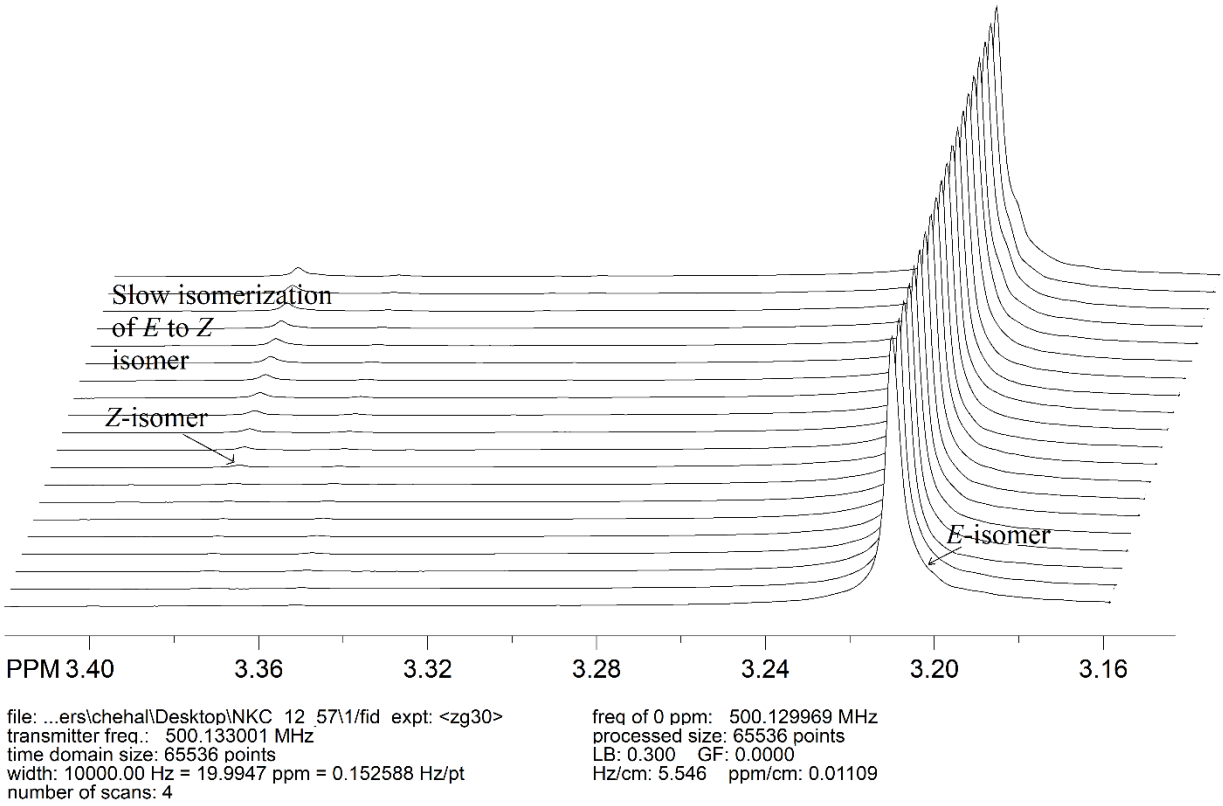

*Figure 46: Isomerization of (**E-2**) in 5 mol% Pd/ t-Bu-Xantphos phosphine monitored by NMR.*

According to the proposal, isomerization goes via five membered intermediate **218** (Figure 42). It can be suggested that there could potentially be a difficulty in the formation of the five membered metallacycle **218** due to the steric hindrance from the *t*-Bu-Xantphos, and hence the isomerization in the presence of the *t*-Bu-Xantphos is slow. Whereas the fast isomerization taking place in the presence of the DPEphos could be suggestive of easier formation of five membered metallacycle which eventually leads to ***Z*-2**.

The compound ***E*-2** possessing enone functionality isomerizes in the presence of $Pd_2(dba)_3$ and DPEphos. To test whether the enone functionality is important, the ketone functionality in ***E*-2** was reduced. No isomerization was observed when compound **220**, obtained by reduction of C=O in ***E*-2** to C-OH, was exposed to $Pd_2(dba)_3$ and DPEphos. Further, cis stilbene (***Z*-161**)

did not isomerize in the presence of the isomerization reaction conditions $Pd_2(dba)_3$ and DPEphos (Scheme 108).

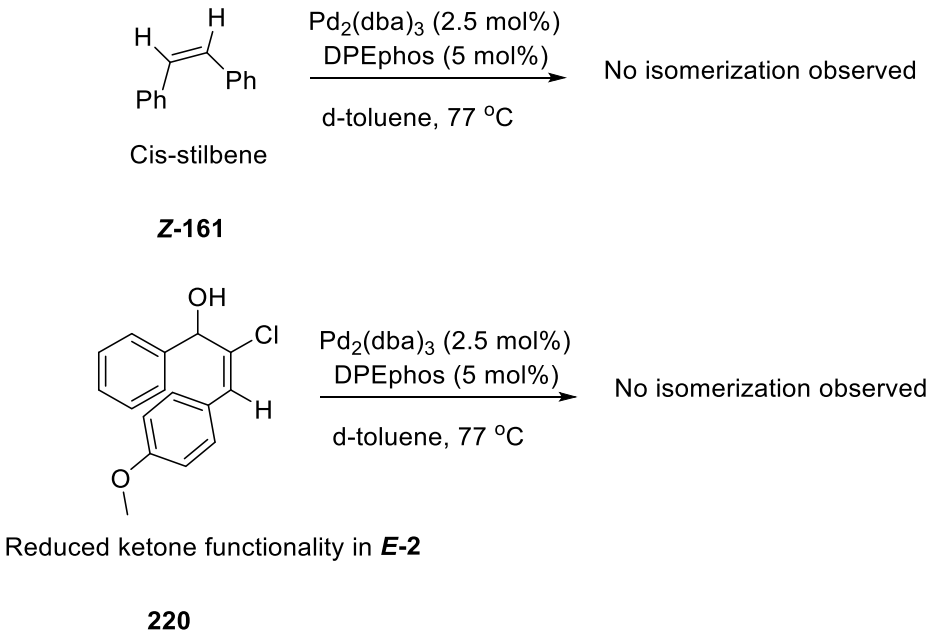

*Scheme 108: Cis-stilbene and (**E-2**) with reduced ketone functionality in isomerization conditions.*

The Suzuki cross coupling on ***E*-159** was stereospecific[64] whereas Suzuki cross coupling outcome of ***E*-1** was overall stereoselective.

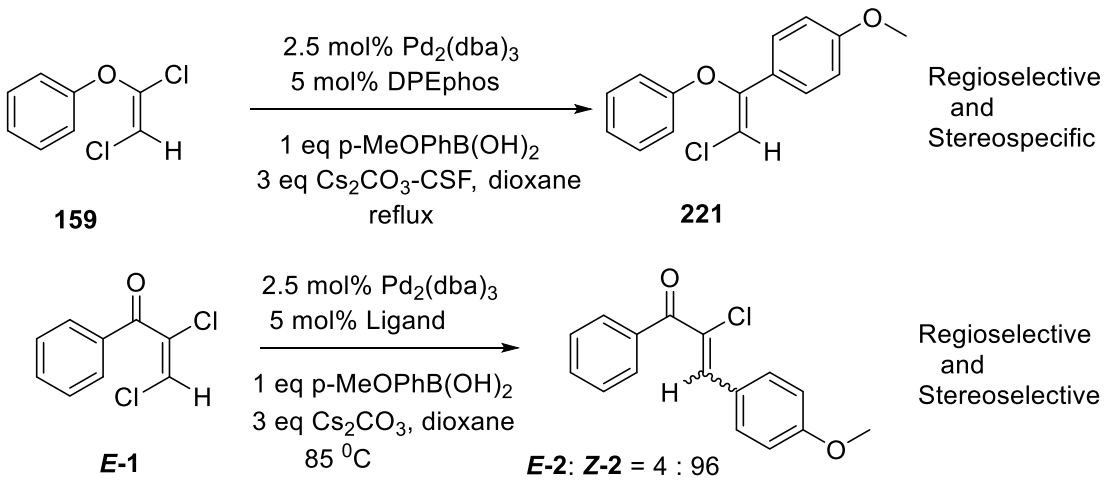

Scheme 109: Suzuki cross coupling outcome on (E-159) and (E-1).

The reaction conditions for both the substrates for cross coupling were very similar (see section 2.7.5). These studies show that the presence of one conjugated carbonyl functionality is sufficient for isomerization. This pathway can be also envisioned for dienes. That being said, the ligand effects might be different. No dienes were used in this project and hence not tested for isomerization in the presence of the Pd/P catalyst.

It was observed experimentally that dimethyl maleate (***Z*-148**) isomerizes in the reaction conditions (Scheme 97) but no isomerization was observed when reaction of ***Z*-148** was run with just $Pd_2(dba)_3$ and DPEphos in d_8-toluene at 77 °C (Scheme 99). Visentin et al. also observed no isomerization of the dimethyl maleate in the presence of a P, P ligand.[60] The slow isomerization of ***Z*-148** could be because of the calculated ~ 23 kcal/mol kinetic barrier (Figure 47) which is ~ 6 kcal/mol more than the barrier for ***E*-2** (Figure 42).

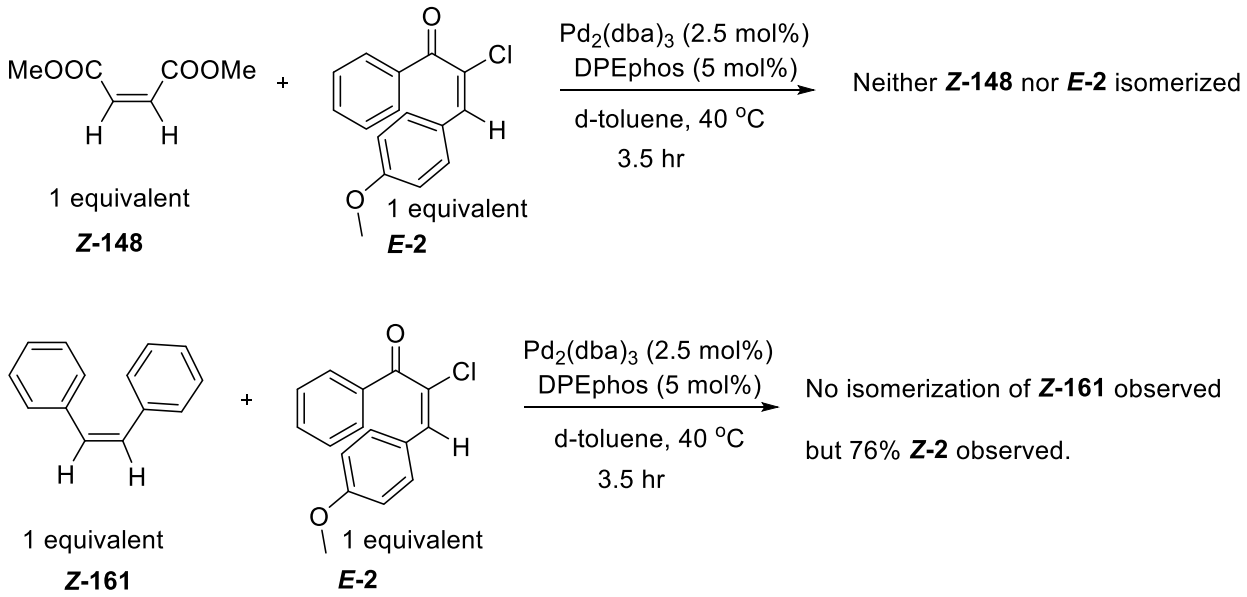

*Scheme 110: Experiment to verify whether (**E-2**) isomerizes in the presence of (**Z-148/ Z-161**) in the isomerization conditions.*

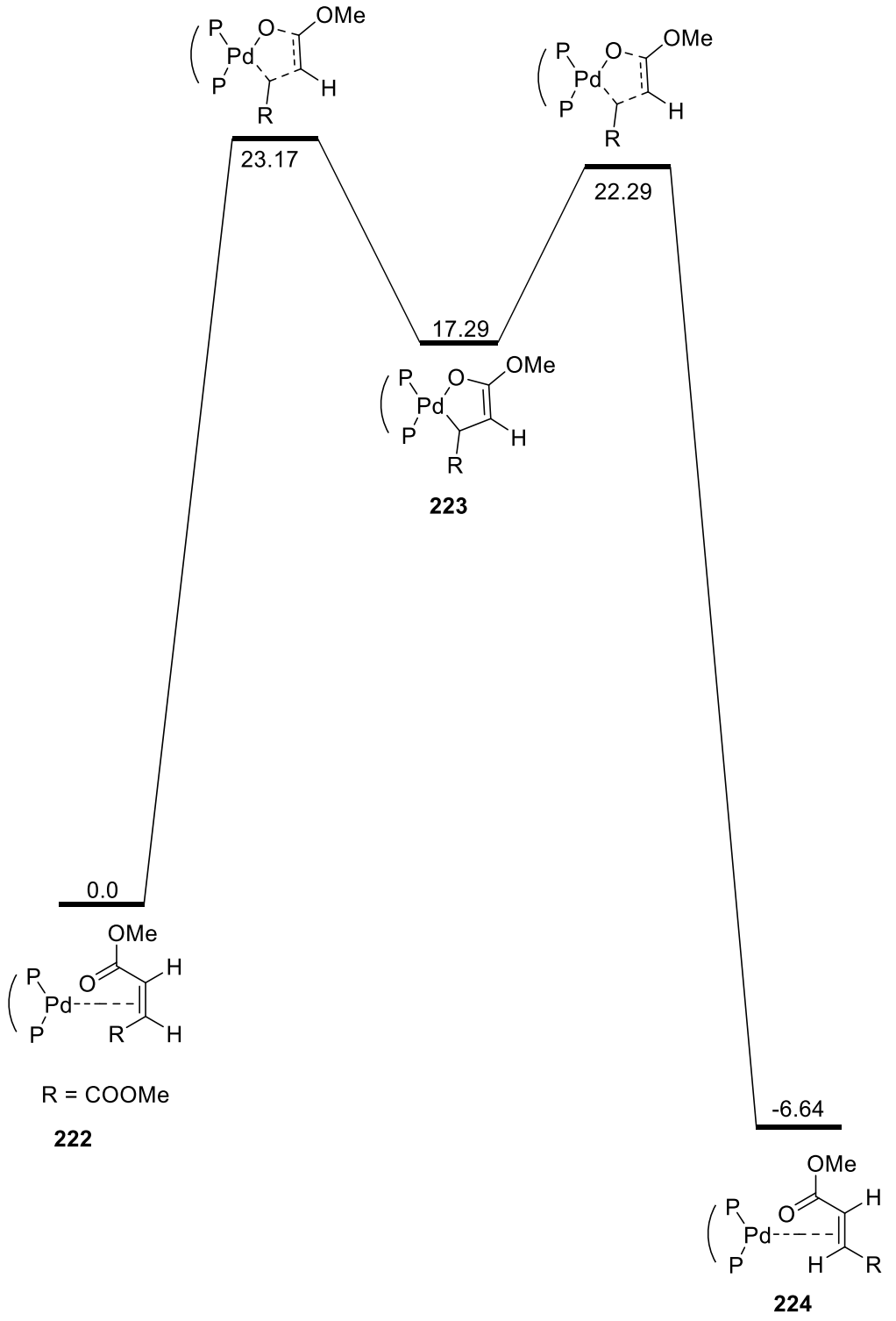

*Figure 47: Two transition states and three minima located for (**Z-148**) via DFT studies. Energies (kcal mol^{-1}) relative to **213** are indicated for each calculated stationary state.*

As shown in Scheme 110, an experiment was performed where the mixture of ***Z*-148** (1 equivalent) and ***E*-2** (1 equivalent) was run with $Pd_2(dba)_3$ and DPEphos in d_8-toluene at 40 °C. In the similar experiment, a mixture of ***Z*-161** (1 equivalent) and ***E*-2** (1 equivalent) was run with $Pd_2(dba)_3$ and DPEphos in d_8-toluene at 40 °C. It was observed neither ***Z*-148** nor ***E*-2** isomerizes under the isomerization conditions. Conversely, ***Z*-161** does not isomerize but ***E*-2** isomerizes under isomerization condition (Scheme 110). This experiment suggests dimethyl maleate (***Z*-148**) binds catalyst strongly with metal catalyst and no isomerization of ***E*-2** takes place. Further, calculations (done by Dr. Peter Budzelaar) also suggested that the pi complexes from the dimethyl maleate (***Z*-148**) would be more tightly bound to the palladium that ***E*-2**. This was consistent with our observation from the competition experiment above in Scheme 110.

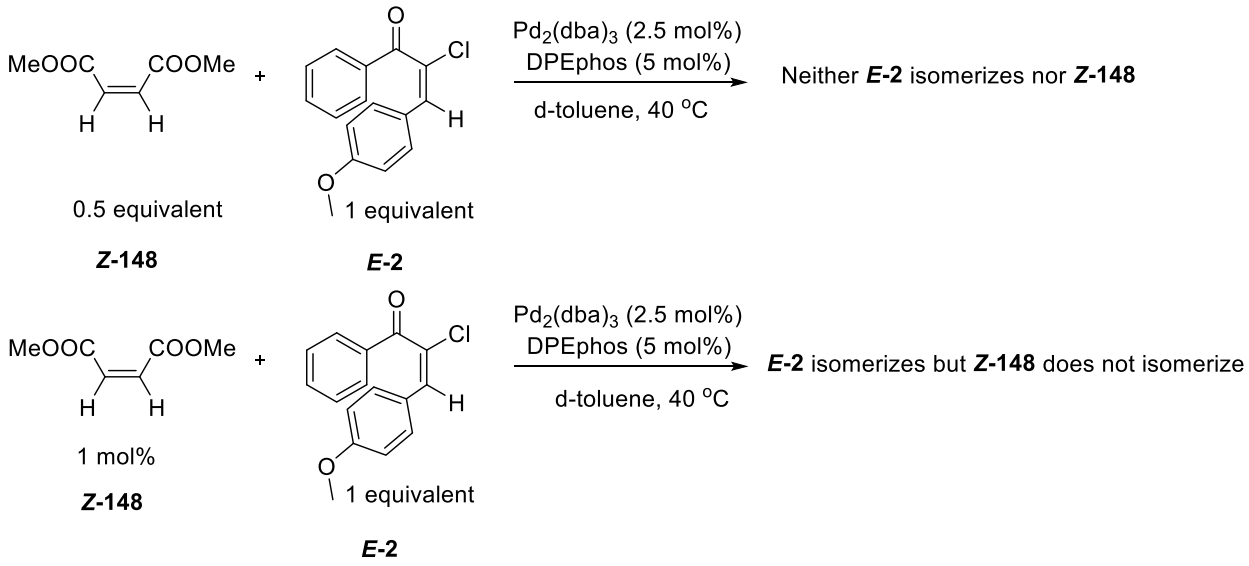

*Scheme 111: Experiment to verify whether (**E-2**) isomerizes in the presence of in the isomerization conditions by varying concentration of (**Z-148**) in the reaction conditions.*

Further it was hypothesized that if ***E*-2** does not isomerize under isomerization conditions due to ***Z*-148** binding to the palladium then if the concentration of ***Z*-148** is lowered i.e. less than 2.5 mol% (since 2.5 mol% of palladium source is used in the reaction) then ***E*-2** should isomerize again. To verify this, an experiment was performed where the mixture of ***Z*-148** (0.5

equivalent) and ***E*-2** (1 equivalent) was run with $Pd_2(dba)_3$ and DPEphos in d_8-toluene at 40 °C (Scheme 111). In the similar experiment, a mixture of ***Z*-148** (1 mol%) and ***E*-2** (1 equivalent) was run with $Pd_2(dba)_3$ and DPEphos in d_8-toluene at 40 °C (Scheme 111). It was observed that ***E*-2** does not isomerize (and nor does ***Z*-148**) in the reaction (Figure 48) whereas ***Z*-148** does not isomerize but ***E*-2** isomerizes in the reaction shown in Figure 49 and Figure 50. This suggests that dimethyl maleate binds to the catalyst or in other words poisons the catalyst preventing the isomerization of ***E*-2**.

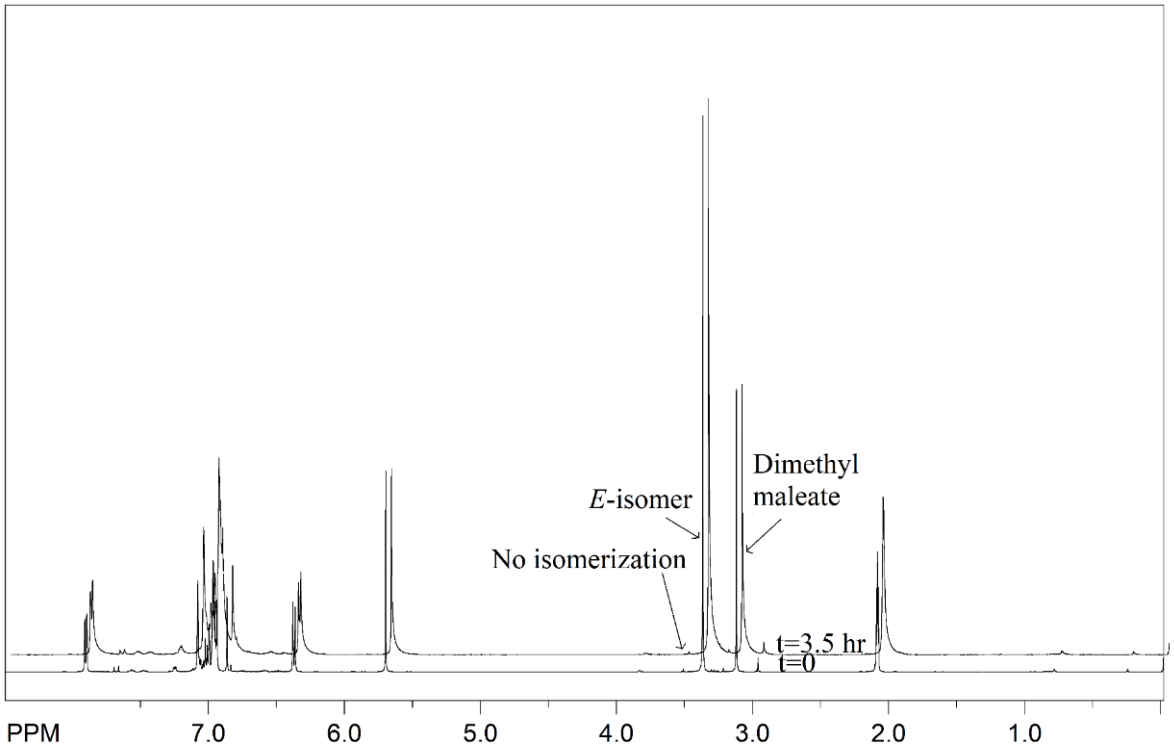

*Figure 48: No isomerization of (**E-2**) observed in the presence of 1 equivalent of dimethyl maleate.*

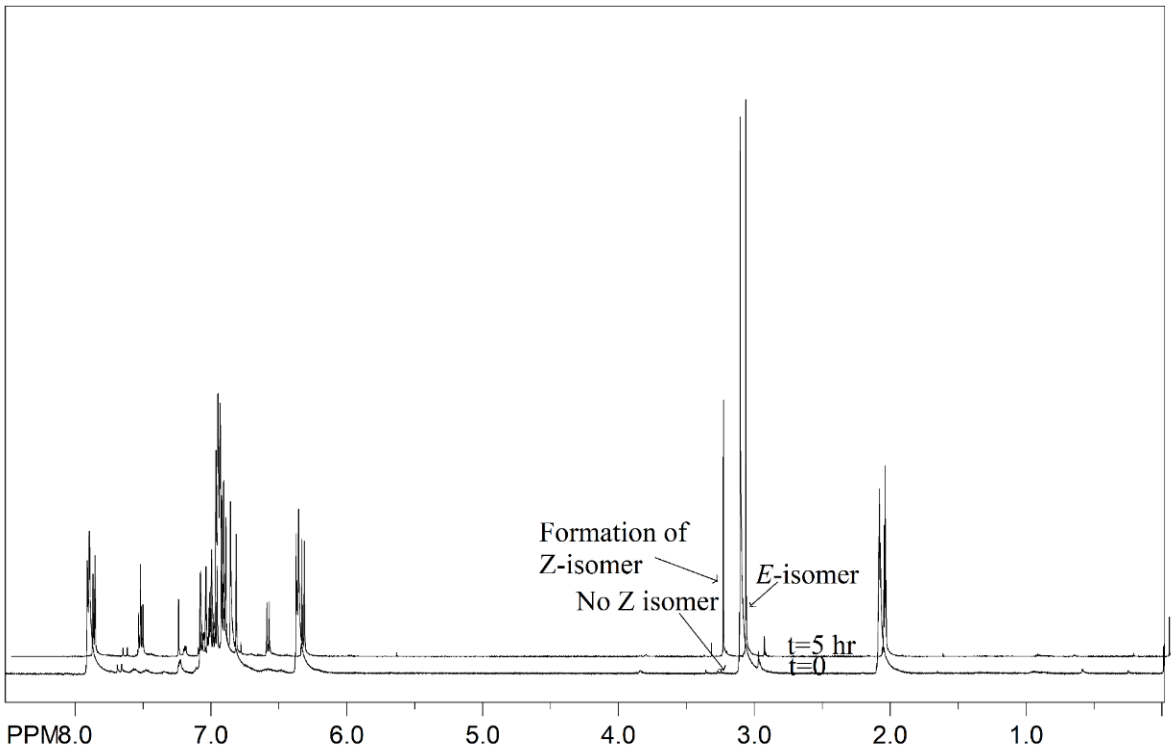

*Figure 49: Isomerization of (**E-2**) observed in the presence of cis-stilbene reaction.*

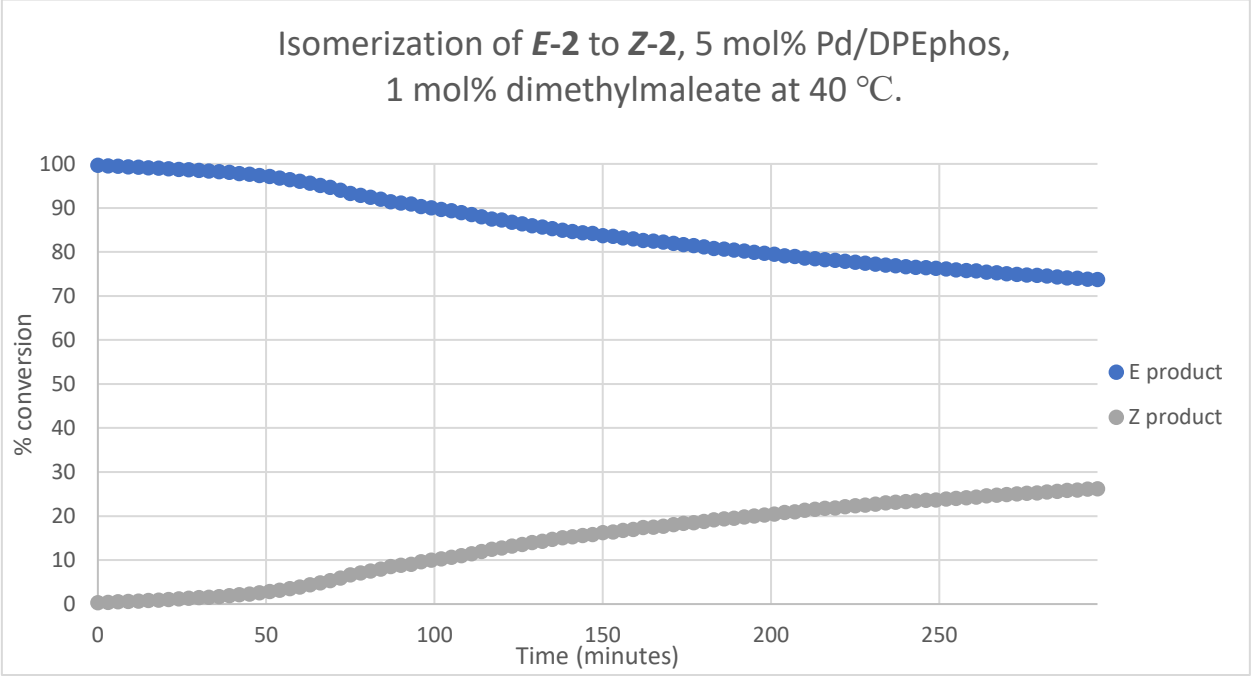

*Figure 50: Graph showing the isomerization of (**E-2**) to (**Z-2**) in the presence of the 1 mol% dimethyl maleate.*

So far, our experimental studies demonstrated that dimethyl maleate (***Z*-148**) does isomerize in the presence of the reaction conditions (Scheme 97) but not when exposed to the minimal isomerization conditions i.e. Pd/P catalyst system (Scheme 99). While studying *E-Z* isomerization of dimethyl maleate, Visentin et al. observed that isomerization was found to be particularly easy with a "soft/hard" P/N ligand at Pd compared to "soft/soft" P/P ligand.[60] Along the same lines, the formation of a "soft/hard" P/O ligand from "hard/hard" P/P ligand in the reaction conditions was hypothesized as one of the possibilities for the observed isomerization of the dimethyl maleate (***Z*-148**) in the reaction conditions (Figure 51). The phosphine present in the ligands can easily oxidise to phosphine oxide in the presence of oxygen.[84]

216 **225**

Figure 51: Plausible formation of P, O ligand by oxidation of P, P ligand.

The computational studies were carried to find how much difference P, O ligand can make in the energies instead of P, P ligand. The calculations were carried out with DMPE ligand (**216**) instead of the ligands used in the reactions. The calculations suggested that the barriers of both the transition states reduced for isomerization of ***Z*-148** and ***E*-199** for the P, O ligand The kinetic barrier for ***E*-199** in the presence of P, P phosphine was ~17 kcal/mol (Figure 42) and it reduced to ~13 kcal/mol (Figure 53) in the presence of P,O ligands. The kinetic barrier of ***Z*-148** in the presence of P, P ligand was ~ 23 kcal/mol (Figure 47) and it reduced to ~ 21 kcal/mol (Figure 52) in the presence of the P, O ligands. Although this is a crude model for the real system, but it does suggest that barriers do get reduced for P, O ligand.

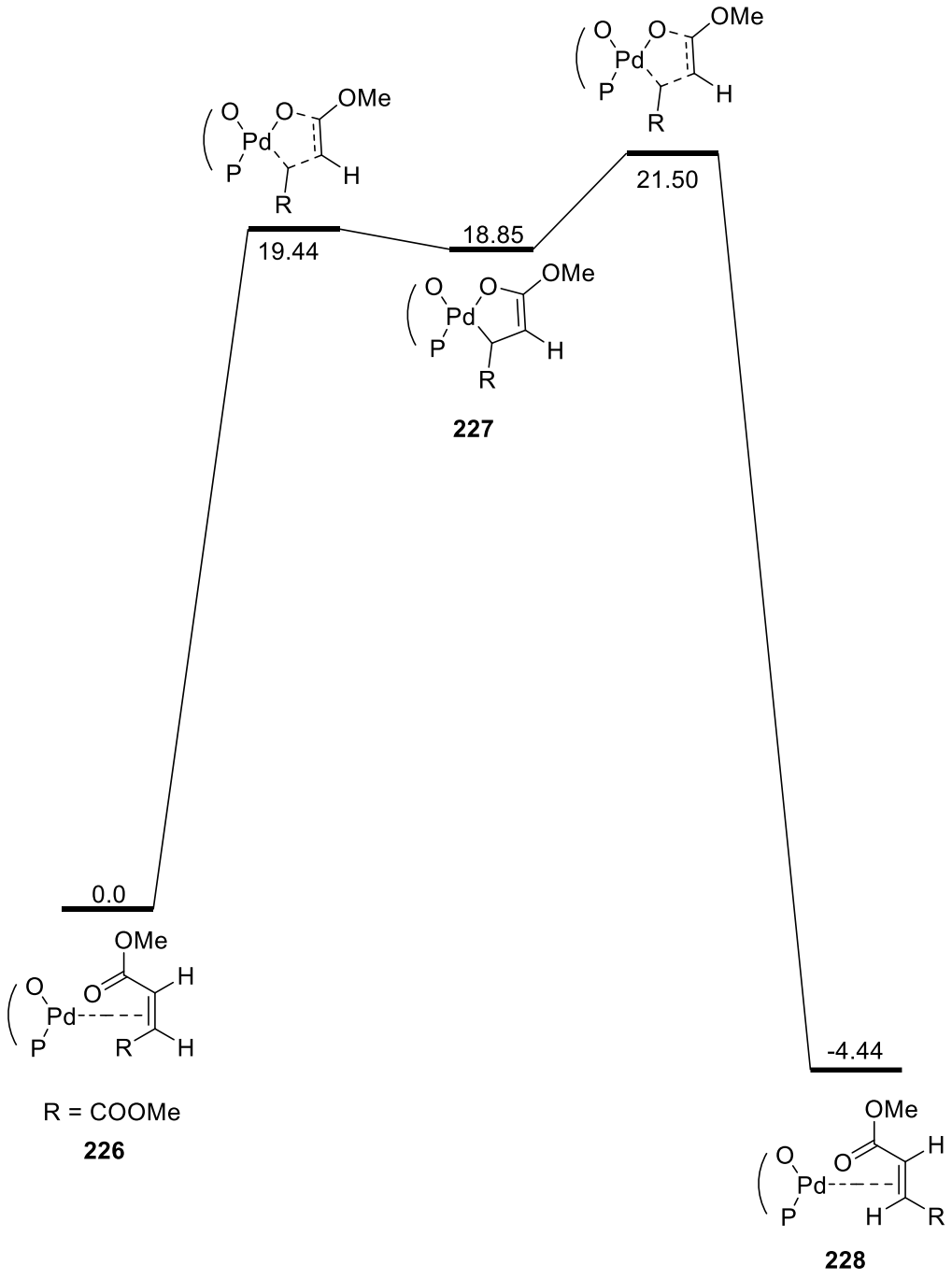

*Figure 52: Schematic representation of isomerization pathway of (**Z-148**) with P, O ligand. Energies (kcal mol^{-1}) relative to **226** are indicated for each calculated stationary state.*

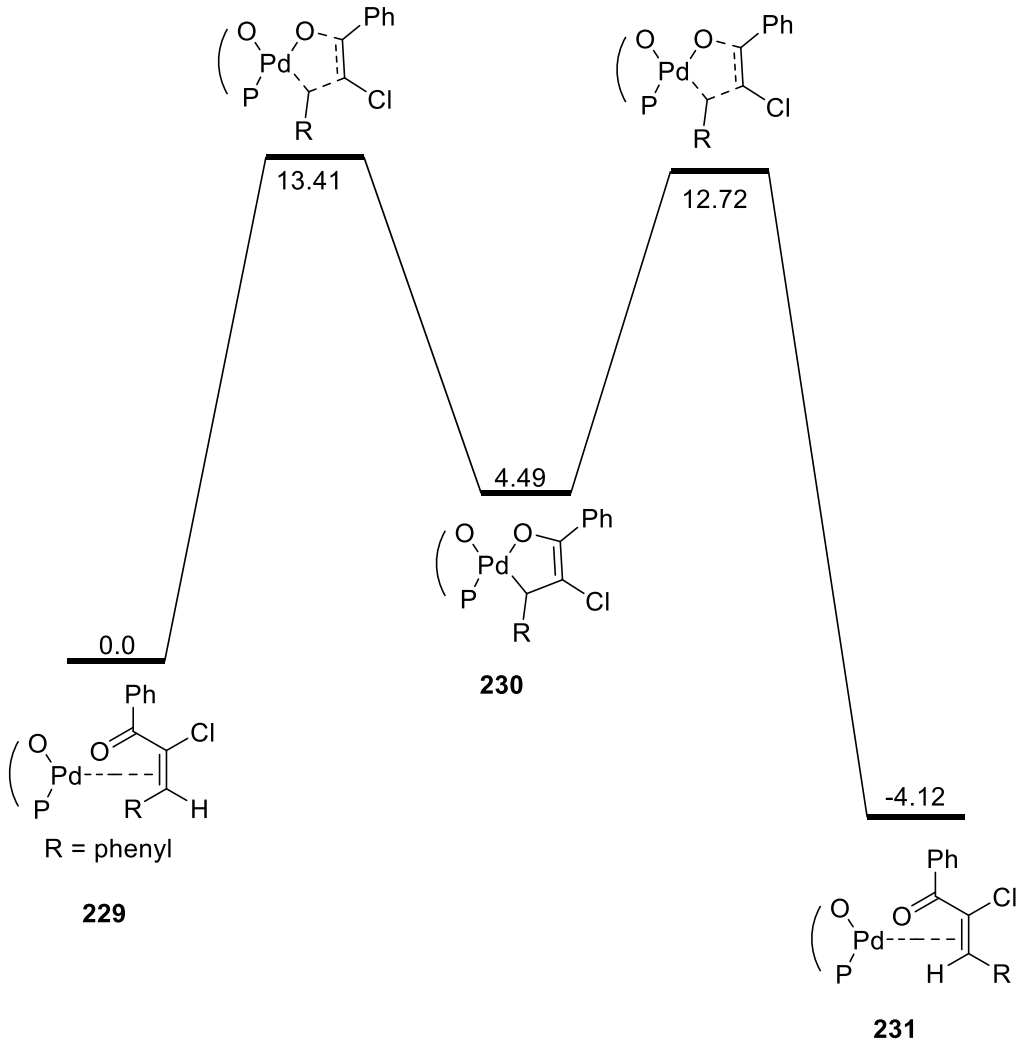

*Figure 53: Schematic representation of isomerization pathway of (**E-199**) with P, O ligand. Energies (kcal mol^{-1}) relative to **229** are indicated for each calculated stationary state.*

No isomerization was observed when ***E*-1** (which also possesses enone functionality) was reacted with $Pd_2(dba)_3$ and DPEphos in dioxane at 85 °C.

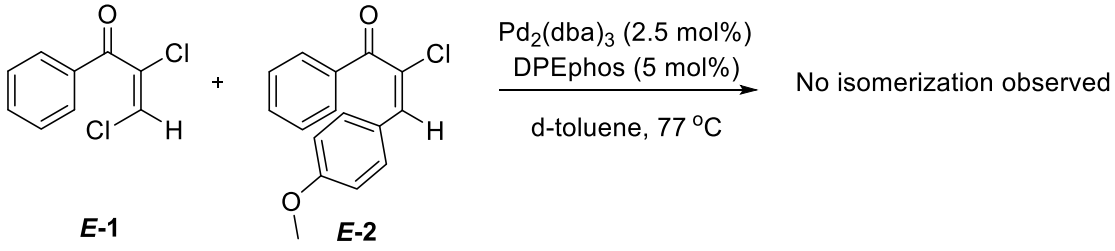

*Scheme 112: Verifying the isomerization of (**E-2**) in presence of the (**E-1**).*

Further, when ***E*-2** was exposed to $Pd_2(dba)_3$ and DPEphos in the presence of ***E*-1** (Scheme 112), the isomerization of neither ***E*-2** nor ***E*-1** was not observed. It was proposed that palladium catalyst participates in oxidative addition when ***E*-1** is present.

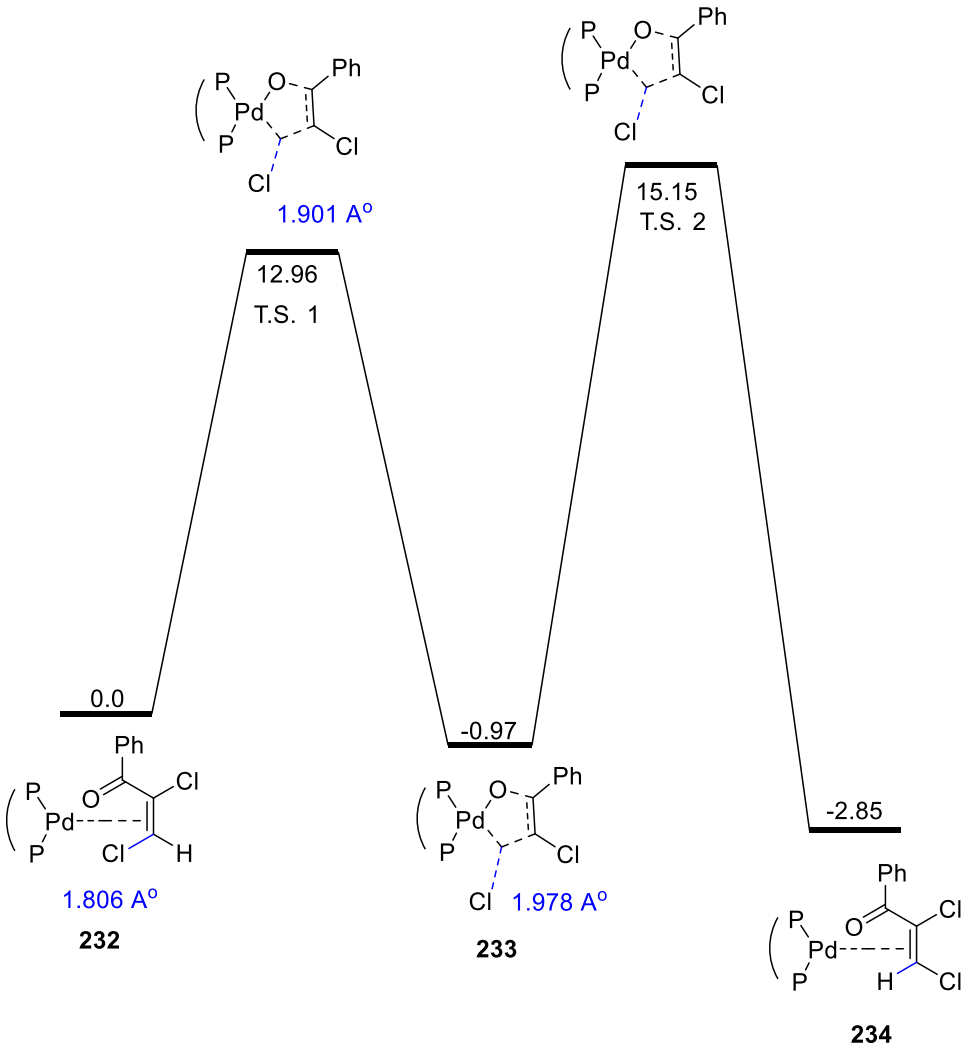

*Figure 54: Two transition states and three minima located via DFT studies for (**E-1**).*

The computational studies suggest that the kinetic barrier for ***E*-1** to ***Z*-1** is 15.15 kcal/mol (Figure 54). It should be noted that this barrier is 1.94 kcal/mol lower than that of ***E*-199** (17.09 kcal/mol, Figure 42). Despite the lower kinetic barrier, the compound ***E*-1** does not isomerize in the presence of the palladium catalyst. The computational studies suggest that the bond length

of β C-Cl bond increases when ***E*-1** interacts with the palladium catalyst. The bond length of β carbon chloro bond increases from 1.806 A° to 1.901A° in T.S. 1, which further increases to 1.978 A° in the five membered metallacycle (Figure 54). No such lengthening of the bonds was observed for ***E*-2**. It is suggestive from the observation of an extreme lengthening of the β C-Cl bond from the computational calculations (Figure 54), that β C-Cl bond that there is a possibility of Cl^- directly getting eliminated generating **235**, which could be an alternative way of oxidative addition. Exploration of this reaction path further would require inclusion of solvation in the geometry optimization, which goes beyond the scope of this work (Scheme 113).

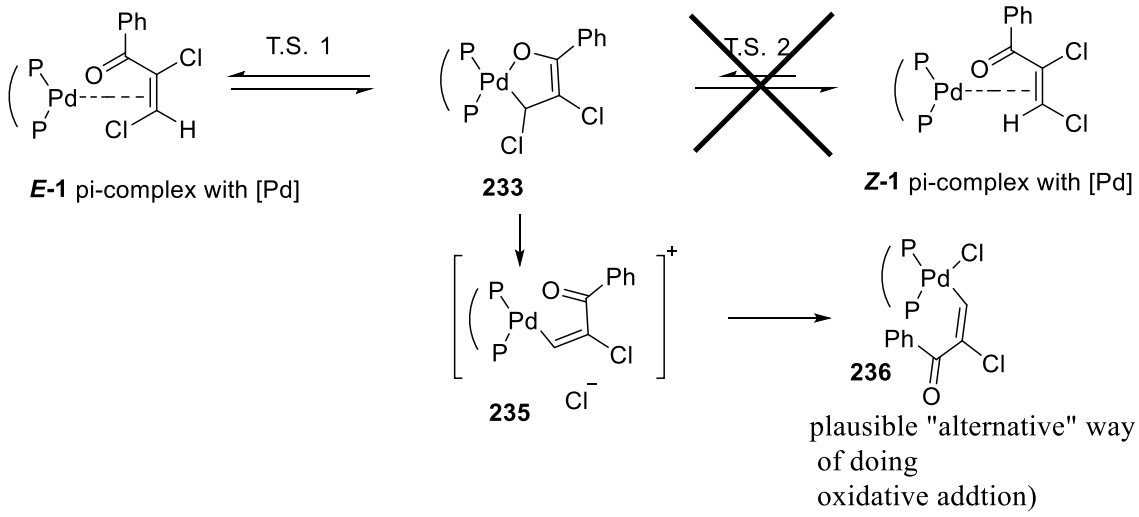

Scheme 113: Plausible alternative oxidative addition pathway instead of isomerization in (***E*-1**).

2.8. Summary

We have successfully demonstrated that Suzuki cross coupling reactions on ***E*-1** are regioselective at β C-Cl bond and there is a loss of stereochemistry in Suzuki cross coupling outcome. We also have demonstrated that the isomerization is dependent on the phosphine ligand used. Depending on the ligand used in the reaction conditions, either Suzuki cross coupled product with retention or isomerized Suzuki cross coupled product could be selectively formed. The isomerized cross coupled product is formed selectively when DPEphos is used and retention of stereochemistry in the cross coupled product is achieved when *t*-Bu-Xantphos or no phosphine ligand is used.

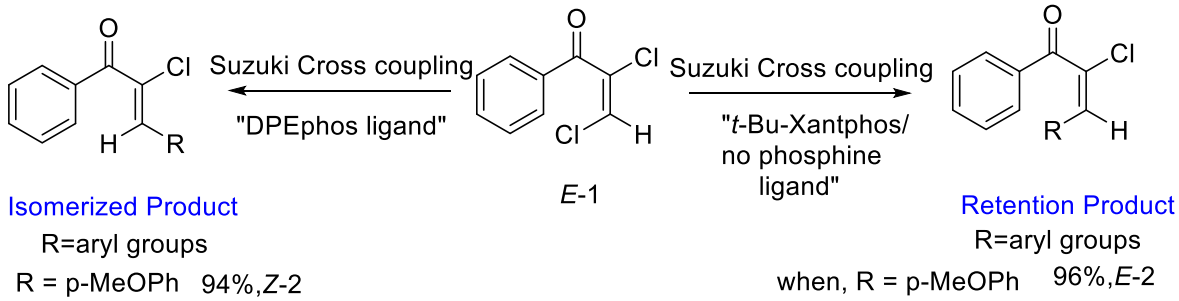

Scheme 114: Isomerization and retention in the product during Suzuki cross coupling on (***E*-1**).

We have also demonstrated that the isomerization takes place on the ***E*-2** (and not on ***E*-1**) in the presence of Pd_2dba_3 and DPEphos, whereas $Pd_2(dba)_3$ and DPEphos by themselves were ineffective in isomerization. This work has ruled out the simple mechanisms like thermal isomerization, photo-isomerization, Michael type addition-elimination of the phosphine ligands, palladium hydride or the zwitterionic pathway that could be responsible for an isomerization. Isomerization takes place outside the catalytic cycle and the Suzuki cross coupling reactions themselves are stereospecific with isomerization taking place in the separate

catalytic cycle. The pathway responsible for the isomerization is proposed to involve the formation of the five-membered metallacycle intermediate (Scheme 115).

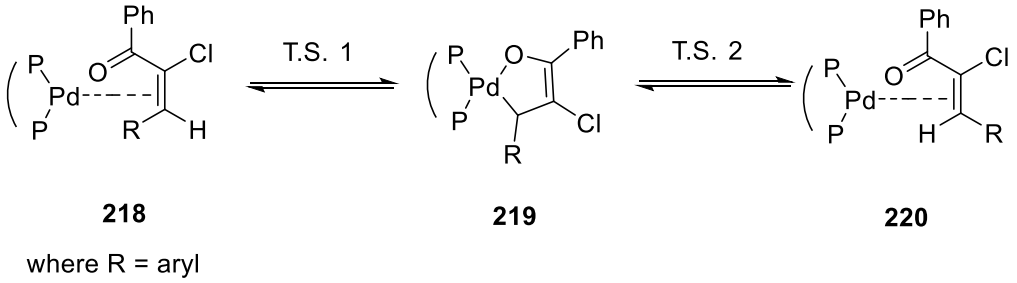

Scheme 115: Postulated pathway for isomerization of the Suzuki cross coupling product.

Chapter 3: Recent Progress And Future Directions

Second cross coupling

My Ph.D. focussed on the Suzuki cross coupling at the β position. This can be extended to the second cross coupling at α position. The Nazarov cyclization can be performed on the cross coupled product at β position and cross coupled product at both α and β position to yield 2,3 – diarylindanones. The reaction shown in Scheme 116 demonstrates the Nazarov cyclization performed on 2-arylchalcones by Zhu et al.[85] On the same lines, this project can be envisioned for the synthesis of 2-substituted indanones via Nazarov cyclization on Suzuki cross coupled products.

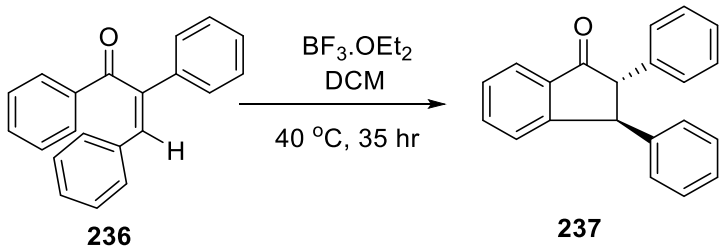

Scheme 116: Synthesis of 2-substitued indanones via Nazarov cyclization of 2-arylchalcones by Zhu et al.[85]

During this project, a second Suzuki cross coupling with methyl boronic acid was performed on ***Z*-2**. It was observed that ***E*: *Z*-2** = 20: 80 led to ***E*: *Z*-179** = 89: 11.

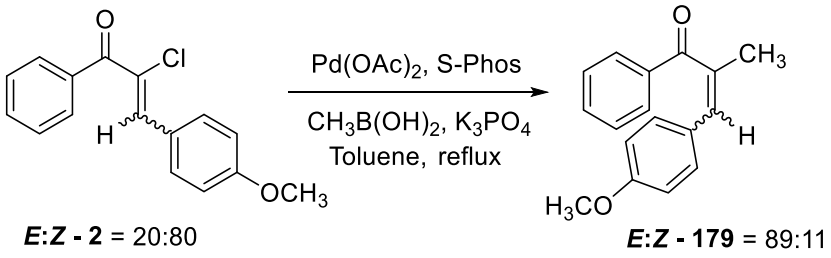

*Scheme 117: Suzuki cross coupling on (**E/Z-2**) with methylboronic acid.*

A second cross coupling was tried on ***E*-2** with p- methoxyphenylboronic acid in the presence of *t*-Bu-Xantphos. It should be noted that *t*-Bu-Xantphos phosphine ligand has yielded retention of stereochemistry when Suzuki cross coupling was done on the β C-Cl bond. It was expected that reaction in Scheme 118 would lead to only formation of **238** with retention of stereochemistry. When the reaction was analyzed by GC-MS, the mixture of products, 17% ***Z*-2** and 51% ***E/Z*-238** was observed after one hour. The reaction was let run for 72 hours and 28% ***Z*-2** and 71% ***E/Z*-238** was observed.

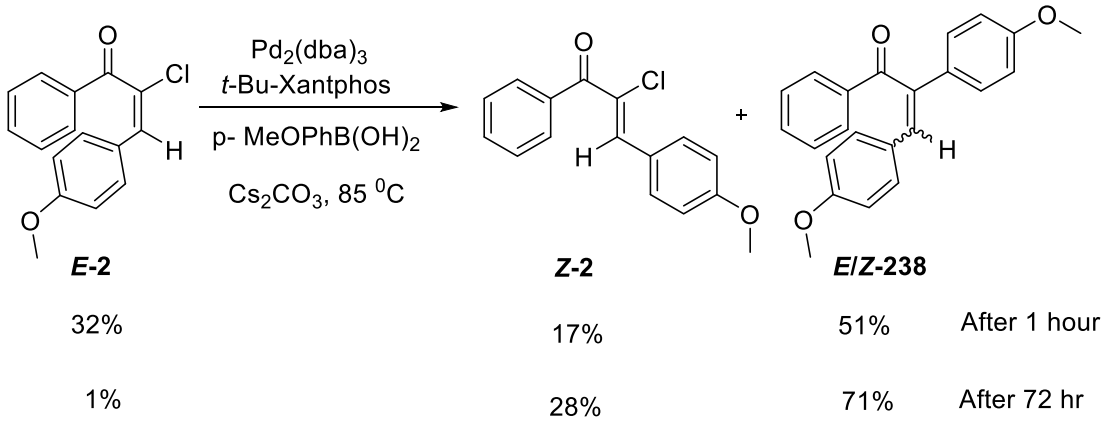

Scheme 118: Suzuki cross coupling on (***E*-2**) *with p-methoxyphenylboronic acid.*

It is apparent from these results that second cross coupling is much slower than the first cross coupling at β C-Cl bond. Also, these studies suggest that the synthesis of dicoupled product with retention of chemistry could be difficult since the isomerization of ***E*-2** to **Z-2** does also take place. Further studies to modify the reaction conditions were not done due to the lack of the time.

Suzuki cross coupling reaction in presence of water

The Suzuki cross coupling reaction at β position was also successful in the presence of water Scheme 119. This eliminated the use of organic solvents in the reaction conditions. The reaction conditions were optimized for both retention and isomerization Suzuki cross coupled product.

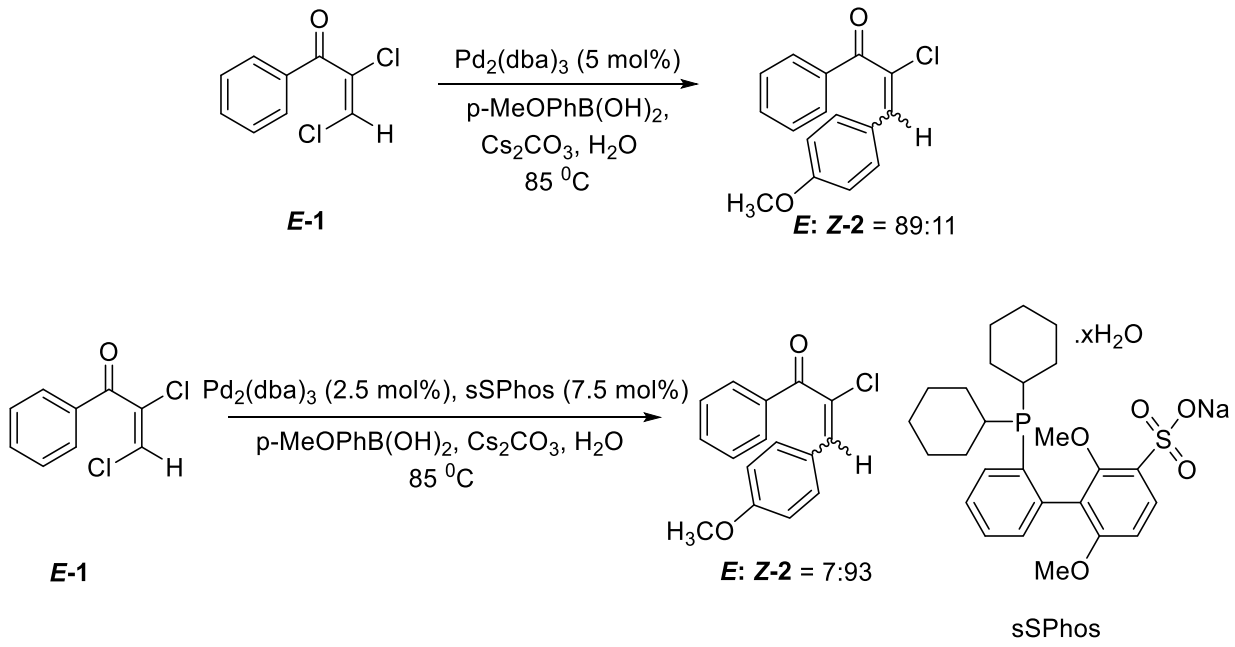

*Scheme 119: Selective Suzuki cross coupling on **E-1** in the presence of water as a reaction solvent.*

The Suzuki cross coupling in water conditions was only performed with p-MeOPhB(OH)$_2$. Since the project concentrated on finding the reason of the loss of stereochemistry in the Suzuki cross coupling of ***E*-1**, the further studies on reactions in presence of water as a reaction solvent were not carried.

Other cross couplings

This project can also be extended to other cross couplings like Sonogashira (Scheme 120) and Negishi reactions. Although, one would expect the isomerization of the product whenever

palladium source and phosphine ligand would be present. Nevertheless, it would be interesting to verify isomerization under reaction conditions of different cross coupling reactions.

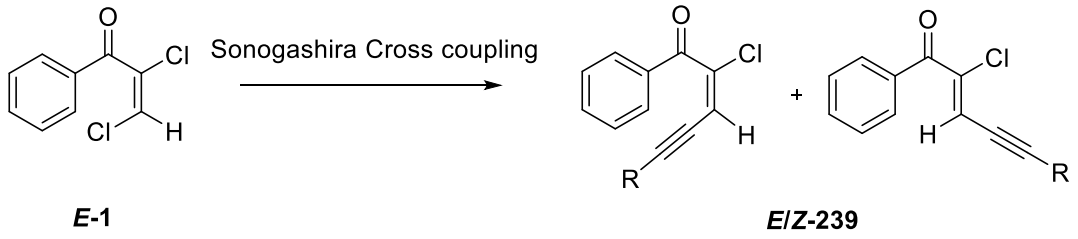

***E*-1** **E/Z-239**

Scheme 120: Extension of project with Sonogashira on (***E*-1**).

To avoid the isomerization, it is essential to find a coupling catalyst which would give a much faster cross coupling and very slow isomerization. One might also want to use an effective quenching method to stop isomerization. This should be kept in mind while trying cross coupling reactions with the isomerization-prone substrates like enones and probably also acrylates.

Role of aryl boronic acid

While performing "standalone individual reagent and their combination" studies (discussed in section 4.7.4.) it was observed that presence of p-methoxyphenylboronic acid along with $Pd_2(dba)_3$ and DPEphos facilitates the isomerization of ***E*-2** to ***Z*-2**.

This thesis focussed on major contributor of the isomerization i.e. $Pd_2(dba)_3$ and DPEphos. As an extension of this project, it would be interesting to study whether arylboronic acid accelerates the rate of the isomerization. Some efforts were made to study the effect of the aryl boronic acid. An experiment was designed that could be monitored by NMR spectroscopy (Scheme 121). In this experiment, the reaction was supposed to be run with **Z-2** along with p-methoxyphenyl boronic acid, $Pd_2(dba)_3$ and DPEphos at 40 °C in d_8-toluene. This was supposed

to be monitored by NMR for about 1.5-2 hr and then compare the profile achieved with the profile of the reaction without p-methoxy phenylboronic acid.

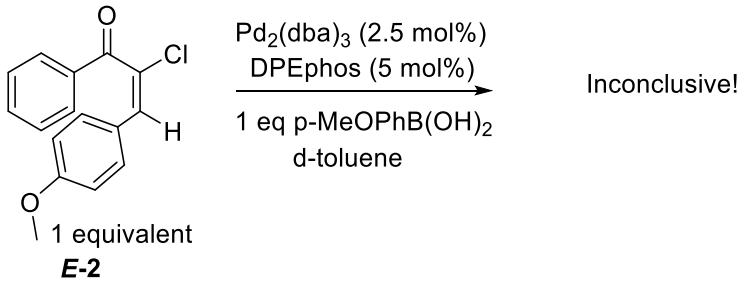

Scheme 121: Isomerization study of (***E*-2**) *in presence of [Pd] and aryl boronic acid.*

This reaction could not be performed because of the insolubility of p-methoxy phenylboronic acid in the d_8-toluene. Because of the lack of the time, further attempts were not made to find out whether the presence of aryl boronic acid along with palladium accelerates the isomerization or not.

Effect of substitution in ***E*-2** on isomerization

This thesis has focussed on isomerization studies of a specific substrate ***E*-2**. Concentrating on one substrate was crucial for the *simplification* purposes and to find an answer to the main question, i.e., whether the isomerization takes place inside or outside the catalytic cycle and eventually to find the conditions responsible for the isomerization. This project has successfully answered the above-mentioned question. At this point, the project can be extended further to study the effect of substituted aryl ring in ***E*-2** with electron rich and electron withdrawing groups on isomerization (***E*-240**). It should be noted that substituted substrate (***E*-240**) may or may not show isomerization with Pd/DPEphos conditions and hence demands the extensive screening of the ligands.

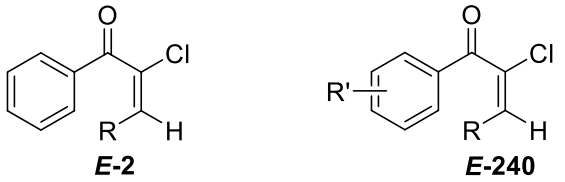

***E*-2** ***E*-240**

R=aryl groups and heteroaryl groups
R'=electron withdrawing or electron rich groups

It would be interesting to study the effect of some other group instead of the H atom in ***E*-2** and ***E*-240** on isomerization (**241** and **242**). Once again, ligand screening is expected in both cases.

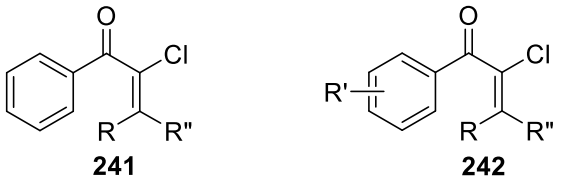

241 **242**

R = aryl groups and heteroaryl groups
R' = electron withdrawing or electron rich groups
R" ǂ H

Exploration of other functional groups that could lead to isomerization in the substrate

Isomerization in reactions is usually unwanted. Therefore, the prior knowledge of the behaviour of the substrate can be very useful. While coming up with a synthetic plan for a complex substrate, this kind of information is very important. This Ph.D. thesis has demonstrated that the presence of enone functionality in the substrate can potentially lead to *E*-*Z* isomerization of the substrate in the presence of the palladium catalyst. The studies can be further extended to find out what other functional groups can display isomerization when exposed to the palladium catalyst. It should be noted that Pd/DPEphos is the right combination for ***E*-2** substrate and it may or may not be the right combination for other substrates. Therefore,

these studies would demand exploration of the right conditions to control selectivities in different substrates.

Other classes of compounds that can be envisioned to isomerize in the presence of palladium catalyst are **243** and **244**. For this, reactions can be done using **243** and **244** with palladium catalyst respectively. The $^{3}J_{H,H}$ or $^{3}J_{C,H}$ can easily distinguish between *E* and *Z* isomers.

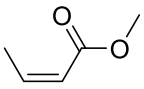

(Z)-Methylbut-2-enoate

243

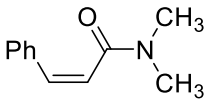

(Z)-N,N-dimethyl-3-phenylprop-2-enamide

244

Another class of compounds that can potentially lead to the isomerization are the ones possessing an unsaturated sulfonyl functionality. Visentin et. al explored isomerization of the disulfonic derivative (**245**) in the presence of the palladium catalyst **246**[60] He observed isomerization of ***Z*-245** to ***E*-245** in the presence of **246**.

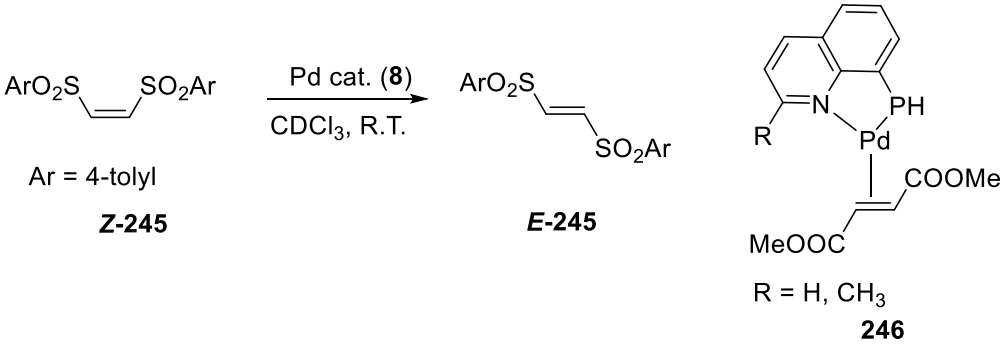

Ar = 4-tolyl

***Z*-245**

***E*-245**

R = H, CH_3

246

Scheme 122: E-Z isomerization of disulfonic derivative.

The compound ***Z*-245** would be worth exploring for isomerization in the presence of Pd/phosphine system. The exploration of the right combination of palladium and phosphine ligand would have to be done. The distinction between *E* and *Z* isomers of **245** can be made by studying $^{3}J_{H,H}$ coupling constants.

On the same lines, substrates like vinyl phosphonate diesters (**247**) can be studied for isomerization in the presence of the palladium catalyst. For this **247** can be exposed to the right combination of palladium and phosphine ligand and $^{3}J_{H,H}$ can again be used to distinguish between *E* and *Z* isomers.

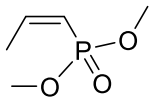

247

Conjugated dienes can be other class of compounds that can be tested for isomerization. This can be done by doing Suzuki cross coupling of commercially available 2-bromofuran (**248**) and cis-propenylboronic acid (**249**).

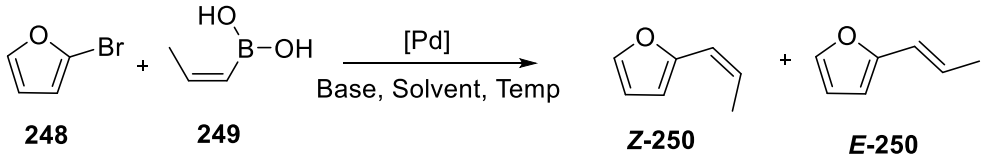

248 **249** ***Z*-250** ***E*-250**

Scheme 123: Plausible way of testing E-Z isomerization in conjugated dienes.

The expected product would be the formation of ***Z*-250**. The formation of ***E*-250** would imply isomerization arising in the product because of the conjugated diene. The both isomers can be distinguished using $^{3}J_{H,H}$, $^{3}J_{C,H}$ and NOE. This being said, the absence of ***E*-250** with one combination of Pd/P would not disprove the concept. In such a case, there would be a need of screening of various ligands.

Computational studies

All the computation studies were performed by Dr. Peter Budzelaar. The ligand employed was dmpe for the isomerization studies and $P(Me)_3$ for the zwitterionic mechanism. Further studies can be performed with ligands used in the project i.e. *t*-Bu-Xantphos and DPEphos. This

might further shine the light upon the reason for the fast isomerization when DPEphos is used and the slow isomerization when *t*-Bu-Xantphos is used as a ligand. Due to the lack of the time, no attempts were made to do computational studies with *t*-Bu-Xantphos and DPEphos.

Chapter 4: Experimental Procedures

4.1 General consideration

For analytical purposes, thin layer chromatography (TLC) was performed on pre-coated (175-225 µm layer thickness) silica gel on aluminium base (TLC Silica gel 60 F254, EMD Millipore Corporation). The eluent system used was n-hexanes: ethyl acetate = 9:1, unless otherwise mentioned. The plates were visualized under UV light. For purification purposes, manual flash chromatography was performed using Silicycle Silica-P flash silica gel (230-400 mesh). Melting points were measure using a DigiMelt (Stanford Research systems) apparatus with parameters: ramp rate of 1 °C and starting temperature set at 26 °C, unless otherwise mentioned. Melting points obtained were uncorrected. ^{1}H NMR (300 MHz) and ^{13}C NMR (75MHz) were recorded at 298 K on a Bruker Avance 300 spectrometer whereas ^{1}H NMR (500 MHz) and ^{13}C NMR (125 MHz) were recorded at 298 K on a Bruker AvanceIII 500 spectrometer for compound characterization. Chloroform-d1 ($CDCl_3$) containing 99.8 atom % D was used as a NMR solvent unless otherwise noted. The chemical shifts were calibrated with reference to the residual peak of $CDCl_3$ (7.26 ppm for ^{1}H and 77 ppm for ^{13}C). The abbreviations s, t, m signify singlet, triplet, multiplet and AA′BB′, AA′BB′C signify second order splitting patterns where C symbolizes the para proton present in a monosubstituted aromatic ring. All chemicals were purchased from Sigma-Aldrich and were used without purification, unless otherwise mentioned.

4.2 Compounds from section 2.2

(*E*)-3,4-Dichloro-2-(dimethylamino)-2-phenylbut-3-enenitrile (***E*-167**)

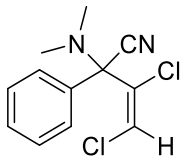

Compound (***E*-167**) was synthesized using a literature method.[65] The ^{1}H chemical shifts were consistent with those reported. Compound **166** (3.2 gm, 20 mmol) and tetrabutylammonium hydrogen sulphate (1 g, 3 mmol) and NaOH (3 g dissolved in 6 mL water) were placed in the round bottomed flask. When the temperature of the reaction mixture was between 5-10 ℃, trichloroethylene (2.20 mL, 24 mmol) was carefully to flask. The reaction was let run for 4-5 hr. The reaction was quenched with cold water. The mixture was extracted with ethyl acetate (ca. 15 mL × 3). The combined organic extract was washed with brine (ca. 30 mL) and dried over anhydrous sodium sulphate. The compound ***E*-167** (2.04 g) was isolated in 40 % yield. The *E* configuration of the compound was validated by the crystal structure.

White solid (mp 113.8-114.2 ℃);

^{1}H NMR (300 MHz, $CDCl_3$) δ 2.32 (s, 6H), 6.35 (s, 1H), 7.39-7.43 (AA′BB′C, 3H), 7.76-7.79 (AA′BB′, 2H) ppm;

^{13}C NMR (75 MHz, $CDCl_3$) δ 40.92, 74.42, 113.23, 117.45, 126.74, 128.85, 129.58, 132.75, 135 ppm;

HRMS: Calculated for $C_{12}H_{12}N_2Cl_2$: 254.0378, Found: 254.0366.

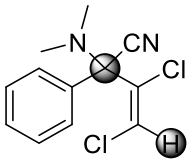

$^{3}J_{C,H}$ = 6.7 Hz

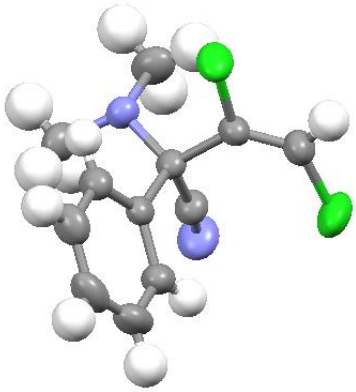

(2*E*)-2,3-Dichloro-1-phenylprop-2-en-1-one (***E*-1**)

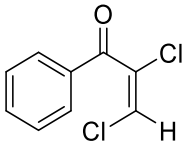

The synthetic procedure described by Jonczyk et al. for ***E*-2** did not give complete conversion. However, another procedure from the same laboratory for methyl 2-formylphenylacetate gave full conversion and was used for the synthesis of ***E*-2**.[66]

Compound ***E*-167** (1.18 g, 4.61 mmol) was dissolved in THF (13.82 mL, 3 mL/mmol) and added to the round bottom flask. To this vigorously stirred solution, $CuSO_4$ (2.30 g, 9.22 mmol) dissolved in water (13.82 mL, 1.5 mL/mmol) was added in one portion. The reaction was refluxed and monitored by tlc until complete consumption of ***E*-167** was observed. After that, the reaction mixture was cooled to the room temperature and then quenched with the cold water. The mixture was extracted with ethyl acetate (ca. 20 mL × 3). The combined organic extract was washed with brine (ca. 30 mL) and dried over anhydrous sodium sulphate. The compound ***E*-1** (787.47 mg) was isolated in 85% yield.

The ^{1}H chemical shifts we observed for ***E*-1** were not consistent with those reported by Jonczyk et al. The *E*-stereochemistry of compound ***E*-1** was validated by synthesizing its *Z* isomer and comparing their $^{3}J_{C,H}$ values.

Yellow oil;

^{1}H NMR (500 MHz, $CDCl_3$) δ 6.69 (s, 1H), 7.51-7.54 (AA′BB′, 2H), 7.64-7.67 (AA′BB′**C**, 1H), 7.96-7.97 (AA′BB′, 2H) ppm;

^{13}C NMR (125 MHz, $CDCl_3$) δ 118.89, 127.73, 129.03, 129.83, 133.50, 134.66, 188.25 ppm;

HRMS: Calculated for $C_9H_6OCl_2$: 199.9796, Found: 199.9798

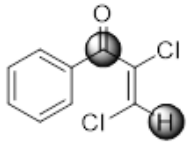

$^{3}J_{C,H}$ = 7.0 Hz

4.3 Compounds from section 2.3 and 2.4

Initial Suzuki reaction and Ozonolysis procedure

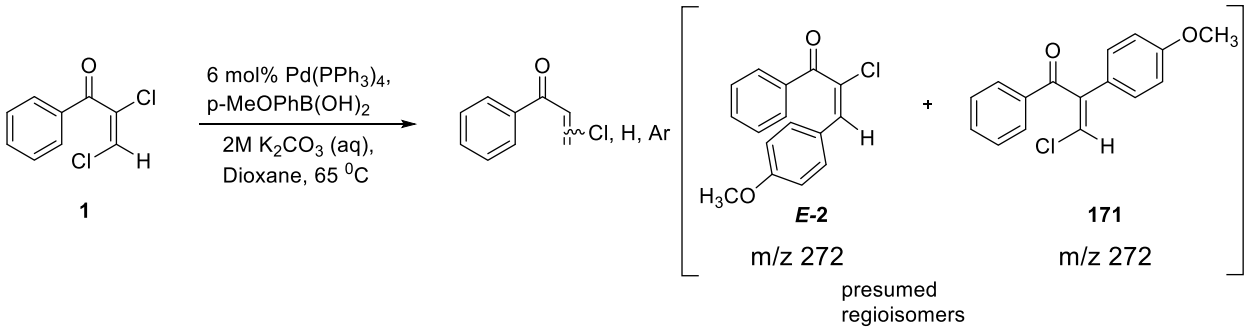

Compound ***E*-1** (100.5 mg, 0.5 mmol), $Pd(PPh_3)_4$ (17.33 mg, 0.015 mmol), p-$MeOPhB(OH)_2$ (76.0 mg, 0.5 mmol), and aqueous 2M K_2CO_3 (276.4 mg, 2 mmol) were placed in a glass tube with a septum fitted screw cap. Dioxane (5 mL) was added to the glass tube. The stirred solution

was heated at 65 °C until tlc analysis indicated full conversion (~ 40 min). GC-MS analysis of the reaction mixture revealed two products, both of m/z 272, in the ratio of 26:74.

Ozonolysis

The isolated isomer i.e. mixture (***E*-2** and ***Z*-2**) (50 mg, 0.184 mmol) was dissolved in dichloromethane (0.5 mL). The solution was cooled to -78 °C. Ozone gas was bubbled through the solution. The reaction was monitored till the complete conversion of the starting material. The solution was then warmed to the room temperature. Dimethyl sulfide (27 µL, 0.368 mmol) was added to quench the reaction. The crude product mixtures were analyzed by GC-MS. Formation of p-methoxybenzaldehyde was observed from both the isomers.

(2*E*/*Z*)-3-(4-Methoxyphenyl)-2-methyl-1-phenylprop-2-en-1-one (**179**)

Mixture of isomers ***E*/*Z*-1** (50 mg, 0.18 mmol), methylboronic acid (16.46 mg, 0.28 mmol,), palladium acetate (1.12 mg, 0.005 mmol), S-Phos (3.69 mg, 0.009 mmol) and K_3PO_4 (77.69 mg, 0.37 mmol) were added to the test tube with a septum fitted screw cap. Anhydrous toluene (2.6 mL, 0.07M with respect to ***E*/*Z*-1**) was added to the test tube. The stirred mixture was refluxed.

The reaction mixture was cooled to the room temperature and ice-cold water was added. The reaction mixture was washed with ethyl acetate (ca. 6 mL×3). The combined organic extract was washed with brine (ca. 20 ml) and dried over anhydrous sodium sulphate. After filtration, the filtrate was concentrated, and the residue was purified by silica-gel chromatography. The mixture of isomers (***E*/*Z*-179**) was formed in the ratio 89:11 was isolated in 74% yield (33.60 mg).

Major isomer characterization:

^{1}H NMR (500 MHz, $CDCl_3$) δ 2.28 (d, *J* =1.2 Hz, 3H), 3.85 (s, 3H), 6.93-6.96 (AA'BB', 2H), 7.16 (s, 1H), 7.40 - 7.47 (AA'BB', 4H), 7.52-7.55 (AA'BB'**C**, 1H), 7.71-7.72 (AA'BB', 2H) ppm;

^{13}C NMR (75 MHz, $CDCl_3$) δ 14.38, 55.36, 113.99, 128.15, 128.42, 129.41, 131.36, 131.59, 134.90, 138.97, 142.64, 160.00, 199.58 ppm;

HRMS: No HRMS was obtained for this compound.

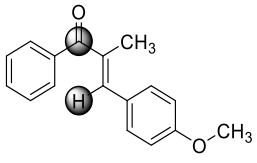

$^{3}J_{C,H}$ = 7.1 Hz

(2*Z*)-2,3-Dichloro-1-phenylprop-2-en-1-one (***Z*-1**)

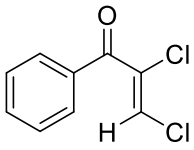

The compound ***E*-1** (100 mg, 1 mmol) and DPEphos (13.46 mg, 0.025 mmol) was added to the 25 mL round bottom flask fitted with a condenser. Anhydrous dioxane (3 mL, 0.166 M with respect to ***E*-1**) was added to the flask. The stirred mixture was refluxed until complete conversion (~24 hr).

The reaction mixture was the cooled to the room temperature and ice-cold water was added. The reaction mixture was washed with ethyl acetate (ca. 6 mL×3). The combined organic extract was washed with brine (ca. 20 mL) and dried over anhydrous sodium sulphate. After filtration, the filtrate was concentrated, and the residue was purified by silica-gel chromatography. The compound ***Z*-1** was obtained in 78% yield (78 mg).

Yellow oil;

^{1}H NMR (500 MHz, $CDCl_3$) δ 7.29 (s, 1H), 7.48-7.51 (AA′BB′, 2H), 7.60-7.63 (AA′BB′**C**, 1H), 7.74-7.75 (AA′BB′, 2H) ppm;

^{13}C NMR (125 MHz, $CDCl_3$) δ 128.68, 129.45, 133.27, 133.60, 135.45, 135.90, 187.64 ppm;

HRMS: Calculated for $C_9H_6OCl_2$: 199.9789, Found: 199.9796.

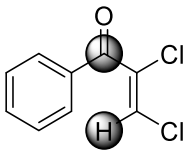

$^{3}J_{C,H}$ = 2.9 Hz

4.4. Optimization studies from section 2.5

Palladium catalysts

The compound ***E*-1** (50 mg, 0.25 mmol), p-MeOPhB(OH)$_2$ (49.25 mg, 0.32 mmol), palladium catalyst (0.012 mmol) and Cs_2CO_3 (243.39 mg, 0.75 mmol) were placed in a glass tube with a screw cap. Anhydrous dioxane (1.5 mL, 0.166 M with respect to ***E*-1**) was added to the glass tube. The stirred solution was heated at 65 °C for one hour. The aliquot taken was quenched with cold water and extracted with dichloromethane. The sample was analyzed by GC-MS.

Base and solvent

The compound ***E*-1** (50 mg, 0.25 mmol), p-MeOPhB(OH)$_2$ (49.25 mg, 0.32 mmol), $Pd_2(dba)_3$ (10.99 mg, 0.012 mmol) and base (0.75 mmol) were placed in a glass tube with a screw cap. Anhydrous dioxane/toluene (1.5 mL, 0.166 M with respect to ***E*-1**) was added to the

glass tube. The stirred solution was heated at 65 ℃ for one hour. The aliquot taken was quenched with cold water and extracted with dichloromethane. The sample was analyzed by GC-MS.

Ligand studies

The compound ***E*-1** (50 mg, 0.25 mmol), p-MeOPhB$(OH)_2$ (37.84 mg, 0.25 mmol), $Pd_2(dba)_3$ (5.49 mg, 0.006 mmol), phosphine ligand (5 mol% bidentate and 7.5 mol% monodentate ligand) and Cs_2CO_3 (243.39 mg, 0.75, 3 eq) were placed in a glass tube with a screw cap. Anhydrous dioxane (1.5 mL, 0.166 M with respect to ***E*-1**) was added to the glass tube. The stirred solution was heated at 85 ℃ for one hour. The aliquot taken after 1 hr and 24 hr were quenched with cold water and extracted with dichloromethane. The sample was analyzed by GC-MS.

4.5. Compounds from Section 2.6

General procedure for Suzuki cross-coupling on (***E*-1**)

Conditions A: The compound ***E*-1** (1 eq), p-MeOPhB$(OH)_2$ (1 eq), **$Pd_2(dba)_3$** (5 mol%) and Cs_2CO_3 (3 eq) were placed in a glass tube with a screw cap. Anhydrous dioxane (0.166 M with respect to ***E*-1**) was added to the glass tube. The stirred solution was heated at 85 ℃ until complete consumption of ***E*-1**. The reaction mixture was the cooled to the room temperature and ice-cold water was added. The reaction mixture was washed with ethyl acetate (ca. 5 mL×3). The combined organic extract was washed with brine (ca. 15 mL) and dried over anhydrous sodium sulphate. After filtration, the filtrate was concentrated, and the residue was purified by silica-gel chromatography.

Conditions B: The compound ***E*-1** (1 eq), p-MeOPhB(OH)$_2$ (1 eq), **Pd$_2$(dba)$_3$** (2.5 mol%), **t-BuXantphos** (5 mol%) and Cs_2CO_3 (3 eq) were placed in a glass tube with a screw cap. Anhydrous dioxane (0.166 M with respect to ***E*-1**) was added to the glass tube. The stirred solution was heated at 85 ℃ until complete consumption of ***E*-1**. The reaction mixture was the cooled to the room temperature and ice-cold water was added. The reaction mixture was washed with ethyl acetate (ca. 5 mL×3). The combined organic extract was washed with brine (ca. 15 mL) and dried over anhydrous sodium sulphate. After filtration, the filtrate was concentrated, and the residue was purified by silica-gel chromatography.

Conditions C: The compound ***E*-1** (1 eq), p-MeOPhB(OH)$_2$ (1 eq), **Pd$_2$(dba)$_3$** (2.5 mol%), **DPEphos** (5 mol%) and Cs_2CO_3 (3 eq) were placed in a glass tube with a screw cap. Anhydrous dioxane (0.166 M with respect to ***E*-1**) was added to the glass tube. The stirred solution was heated at 85 ℃ till complete consumption of ***E*-1**. The reaction mixture was the cooled to the room temperature and ice-cold water was added. The reaction mixture was washed with ethyl acetate (ca. 5 mL×3). The combined organic extract was washed with brine (ca. 15 mL) and dried over anhydrous sodium sulphate. After filtration, the filtrate was concentrated, and the residue was purified by silica-gel chromatography.

(*E*)-2-Chloro-3-(4-methoxyphenyl)-1-phenylprop-2-en-1-one (***E*-2**)

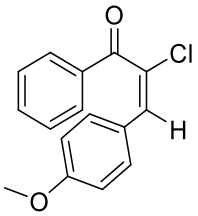

Yield: 78% (Conditions A), 73% (Conditions B)

Yellow solid (mp 91.7-93.1 ℃)[86];

^{1}H NMR (500 MHz, $CDCl_3$) δ 3.72 (s, 3H), 6.69-6.72 (AA′BB′, 2H), 7.09-7.12 (AA′BB′, 2H), 7.14 (s, 1H), 7.40-7.44 (AA′BB′, 2H), 7.53-7.57 (AA′BB′**C**, 1H), 7.96-7.98 (AA′BB′, 2H) ppm;

^{13}C NMR (125 MHz, $CDCl_3$) δ 55.19, 114.03, 124.76, 125.95, 128.81, 129.90, 129.95, 132.52, 134.12, 134.15, 159.84, 191.79 ppm;

HRMS: Calculated for $C_{16}H_{13}O_2Cl$: 272.0604, Found: 272.0605

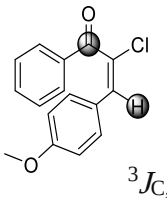

$^{3}J_{C,H}$ = 8.6 Hz

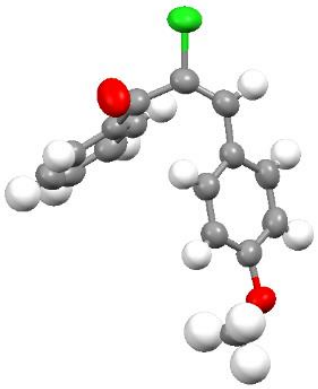

(*E*)-2-Chloro-3-(phenyl)-1-phenylprop-2-en-1-one (***E*-199**)

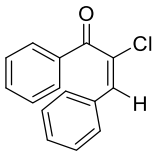

Yield: 69% (Conditions A)

Yellow oil;

^{1}H NMR (300 MHz, $CDCl_3$) δ 7.17-7.20 (m, 6H), 7.39-7.45 (AA'BB', 2H), 7.52-7.58 (AA'BB'**C**, 1H), 7.95-7.98 (AA'BB', 2H) ppm;

^{13}C NMR (75 MHz, $CDCl_3$) δ 127.06, 128.37, 128.63, 128.67, 128.85, 129.98, 132.77, 133.33, 133.98, 134.25, 191.43 ppm;

HRMS: Calculated for $C_{15}H_{11}OCl$: 242.0498, Found: 242.0492;

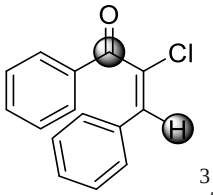

$^3J_{C,H}$ = 8.6 Hz

(*E*)-2-chloro-3-(4-methylphenyl)-1-phenylprop-2-en-1-one (***E*-198**)

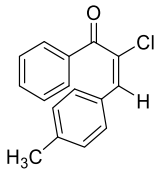

Yield: 75% (Conditions A)

Yellow oil;

^{1}H NMR (300 MHz, $CDCl_3$) δ 2.24 (s, 3H), 6.97-7.07 (AA'BB', 4H), 7.15 (s, 1H), 7.39-7.45 (AA'BB', 2H), 7.52-7.58 (1H, AA'BB'**C**), 7.95-7.98 (AA'BB', 2H) ppm;

^{13}C NMR (75 MHz, $CDCl_3$) δ 21.23, 125.96, 128.33, 128.84, 129.35, 129.99, 130.50, 132.73, 134.04, 134.19, 138.80, 191.66 ppm;

HRMS: Calculated for $C_{16}H_{13}OCl$: 256.0655, Found: 256.0653;

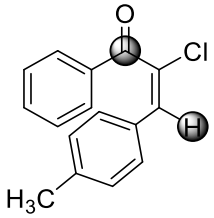

$^3J_{C,H}$ = 8.8 Hz

(2*E*)-2-chloro-1-phenyl-3-(thiophen-2-yl)prop-2-en-1-one (***E*-203**)

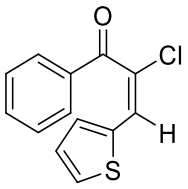

Yield: 77% (Conditions A)

Yellow oil;

^{1}H NMR (300 MHz, $CDCl_3$) δ 6.90-6.93 (m, 1H), 7.03-7.05 (m, 1H), 7.22-7.28 (m, 2H), 7.47-7.52 (m, 2H), 7.59-7.65 (m, 1H), 8.01-8.05 (m, 2H) ppm;

^{13}C NMR (75 MHz, $CDCl_3$) δ 124.81, 126.07, 127.34, 128.00, 128.87, 129.99, 130.02, 134.09, 134.29, 135.66, 191.19 ppm;

HRMS: Calculated for $C_{13}H_9OSCl$: 248.0063, Found: 248.0057;

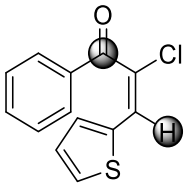

$^{3}J_{C,H}$ = 8.1 Hz

(2*E*)-3-(Benzofuran-2-yl)-2-chloro-1-phenylprop-2-en-1-one (***E*-202**)

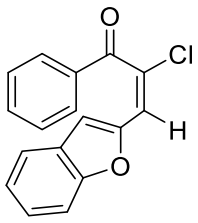

Yield: 76% (Conditions A)

Yellow solid (mp 104-105.5°C);

^{1}H NMR (300 MHz, $CDCl_3$) δ 6.70 (s, 1H), 7.02 (s, 1H), 7.10-7.22 (m, 3H), 7.45-7.50 (m, 3H), 7.56-7.61 (m, 1H), 8.03-8.06 (m, 2H) ppm;

^{13}C NMR (75 MHz, $CDCl_3$) δ 108.16, 111.17, 120.08, 121.35, 123.23, 125.53, 127.92, 127.96, 128.86, 129.73, 134.15, 134.33, 149.86, 155.10, 190.57 ppm;

HRMS: Calculated for $C_{17}H_{11}O_2Cl$: 282.0448, Found: 282.0445;

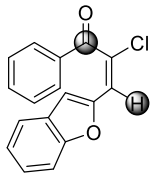

$^{3}J_{C,H}$ = 8.1 Hz

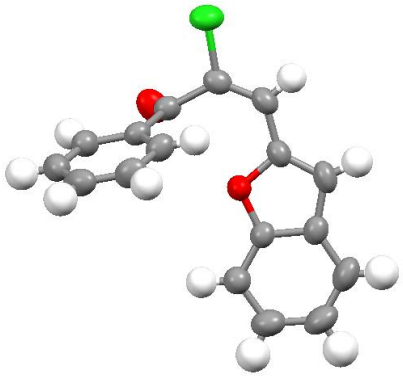

(*E*)-2-chloro-3-(4-fluorophenyl)-1-phenylprop-2-en-1-one (***E*-200**)

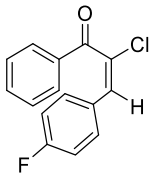

Yield: 72% (Conditions A)

Yellow oil;

^{1}H NMR (300 MHz, $CDCl_3$) δ 6.84-6.91 (AA'BB', 2H), 7.13-7.18 (m, 3H), 7.40-7.46 (AA'BB', 2H), 7.54-7.59 (AA'BB'**C**, 1H), 7.93-7.97 (AA'BB', 2H) ppm;

^{13}C NMR (75 MHz, $CDCl_3$) δ 115.60, 115.89, 127.01, 127.04, 128.91, 129.50, 129.56, 129.94, 130.17, 130.28, 131.63, 133.89, 134.39, 161.00, 164.32, 191.35 ppm;

HRMS: Calculated for $C_{15}H_{10}OClF$: 260.0404, Found: 260.0402;

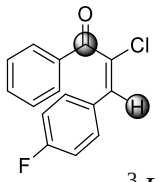

$^3J_{C,H}$ = 8.3 Hz

(*Z*)-2-chloro-3-(4-methoxyphenyl)-1-phenylprop-2-en-1-one (***Z*-2**)

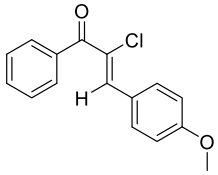

Yield: 80% (Conditions C)

White solid (mp 58.2-60 °C)

^{1}H NMR (500 MHz, CD_3OD) δ 3.84 (s, 3H), 6.99-7.01 (AA′BB′, 2H), 7.49 (s, 1H), 7.50-7.54 (AA′BB′, 2H), 7.60-7.64 (AA′BB′**C**, 1H), 7.72-7.73 (AA′BB′, 2H), 7.87-7.89 (AA′BB′, 2H) ppm;

^{13}C NMR (125 MHz, CD_3OD) δ 54.51, 113.79, 125.25, 127.55, 128.22, 128.94, 132.07, 132.71, 137.27, 140.59, 161.84, 191.75 ppm;

HRMS: Calculated for $C_{16}H_{13}O_2Cl$: 272.0604, Found: 272.0604

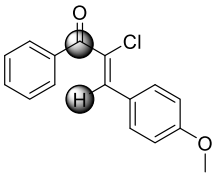

$^{3}J_{C,H}$ = 4.6 Hz

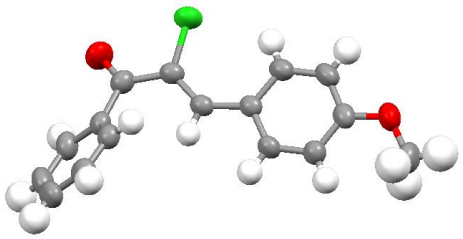

(2*Z*)-2-chloro-1-phenyl-3-(thiophen-2-yl)prop-2-en-1-one (***Z*-203**)

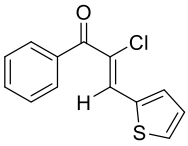

Yield: 62% (Conditions C)

Yellow oil

^{1}H NMR (500 MHz, $CDCl_3$) δ 7.15-7.17 (AA'BB', 1H), 7.46-7.52 (AA'BB', 3H), 7.58-7.61 (AA'BB'C, 1H), 7.67-7.68 (AA'BB', 1H), 7.74-7.78 (m, 3H) ppm;

^{13}C NMR (125 MHz, $CDCl_3$) δ 127.24, 127.98, 128.48, 129.24, 132.22, 132.33, 134.19, 134.83, 136.70, 137.22, 190.48 ppm;

HRMS: Calculated for $C_{13}H_9OClS$: 248.0063, Found: 248.0054;

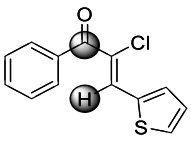

$^{3}J_{C,H}$ = 4.5 Hz

(*Z*)-2-chloro-3-(phenyl)-1-phenylprop-2-en-1-one (***Z*-199**)

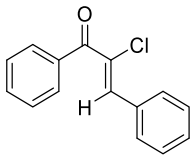

Yield: 70% (Conditions C)

Yellow oil

^{1}H NMR (300 MHz, $CDCl_3$) δ 7.42-7.53 (m, 6H), 7.57-7.63 (1H, AA'BB'**C**), 7.79-7.87 (AA'BB', 4H) ppm;

^{13}C NMR (125 MHz, $CDCl_3$) δ 128.47, 128.62, 129.54, 130.42, 130.44, 130.67, 132.53, 132.91, 136.86, 139.69, 191.28 ppm;

HRMS: Calculated for $C_{15}H_{11}OCl$: 242.0498, Found: 242.0493;

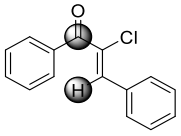

$^{3}J_{C,H}$ = 4.7 Hz

(*Z*)-2-chloro-3-(4-methylphenyl)-1-phenylprop-2-en-1-one (***Z*-198**)

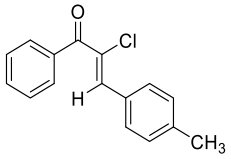

Yield: 76% (Conditions C)

Yellow solid (mp 58.2-58.4°C);

^{1}H NMR (300 MHz, $CDCl_3$) δ 2.42 (s, 3H), 7.28-7.29 (AA'BB', 2H), 7.48-7.53 (m, 3H), 7.58-7.64 (AA'BB'**C**, 1H), 7.77-7.82 (AA'BB', 4H) ppm;

^{13}C NMR (75 MHz, $CDCl_3$) δ 21.59, 128.45, 129.40, 129.50, 129.67, 130.17, 130.84, 132.38, 137.14, 140.12, 141.17, 191.40 ppm;

HRMS: Calculated for $C_{16}H_{13}OCl$: 256.0655, Found: 256.0655;

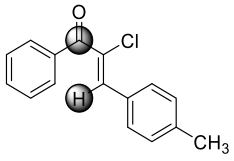

$^3J_{C,H}$ = 4.7 Hz

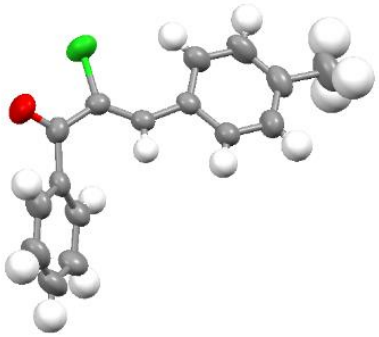

(2*Z*)-2-chloro-3-(2-fluoropyridin-4-yl)-1-phenylprop-2-en-1-one (***Z*-204**)

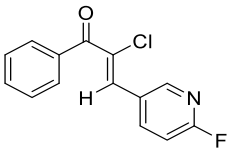

Yield: 69% (Conditions C)

Yellow oil;

^{1}H NMR (300 MHz, $CDCl_3$) δ 7.02-7.06 (AA'BB', 1H), 7.41 (s, 1H), 7.48-7.53 (AA'BB', 2H), 7.59-7.65 (AA'BB'**C**, 1H), 7.78-7.82 (AA'BB', 2H), 8.46-8.52 (AA'BB', 2H) ppm;

^{13}C NMR (75 MHz, $CDCl_3$) δ 109.52, 110.02, 127.25, 127.31, 128.67, 129.60, 132.25, 132.28, 133.04, 133.94, 136.13, 141.89, 142.00, 150.32, 150.53, 162.18, 165.42, 190.46 ppm;

HRMS: Calculated for $C_{14}H_9NOFCl$: 261.0357, Found: 261.0362;

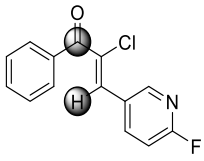

$^{3}J_{C,H}$ = 4.4 Hz

(2*Z*)-3-(Benzofuran-2-yl)-2-chloro-1-phenylprop-2-en-1-one (***Z*-202**)

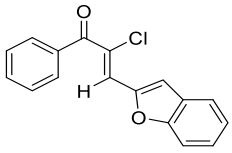

Yield: 74% (Conditions C)

Yellow solid (mp 62.5-65 °C);

^{1}H NMR (300 MHz, $CDCl_3$) δ 7.27-7.32 (m, 1H), 7.37-7.42 (m, 1H), 7.47-7.54 (m, 3H), 7.58-7.65 (m, 2H), 7.67-7.71 (m, 1H), 7.77-7.80 (m, 3H) ppm;

^{13}C NMR (75 MHz, $CDCl_3$) δ 111.48, 113.33, 122.38, 123.68, 127.0, 128.34, 128.60, 128.88, 129.42, 130.93, 132.58, 136.64, 150.26, 155.14, 190.11 ppm;

HRMS: Calculated for $C_{17}H_{11}O_2Cl$: 282.0448, Found: 282.0454;

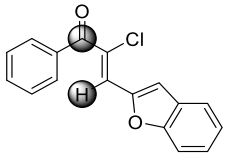

$^{3}J_{C,H}$ = 4.5 Hz

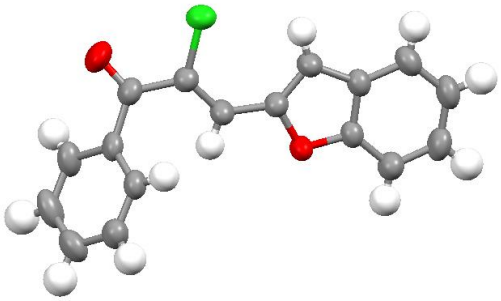

(2*Z*)-2-chloro-3-(4-fluorophenyl)-1-phenylprop-2-en-1-one (***Z*-200**)

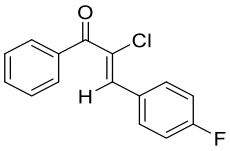

Yield: 78% (Conditions C)

Yellow oil;

^{1}H NMR (300 MHz, $CDCl_3$) δ 7.09-7.17 (AA'BB', 2H), 7.44-7.52 (m, 3H), 7.57-7.63 (AA'BB'**C**, 1H), 7.77-7.81 (AA'BB', 2H), 7.83-7.90 (AA'BB', 2H) ppm;

^{13}C NMR (75 MHz, $CDCl_3$) δ 115.73, 116.01, 128.53, 129.11, 129.16, 129.53, 130.13, 130.16, 132.61, 132.82, 132.93, 136.80, 138.39, 161.94, 165.30, 191.13 ppm;

HRMS: Calculated for $C_{15}H_{10}OClF$: 260.0404, Found: 260.0401;

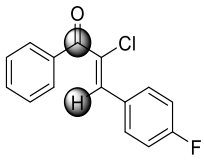

$^{3}J_{C,H}$ = 4.6 Hz

4.6. Compounds from Section 2.7.6.

General procedure for (***E*-220**)

Compound ***E*-2** (100 mg, 0.37 mmol) was dissolved in 0.4 M methanol (~ 1 mL) in a test tube. $CeCl_3.7H_2O$ (136.74 mg, 0.37 mmol) was added to the tube. After that $NaBH_4$ (13.88 mg, 0.37 mmol) was carefully added. The test tube was agitated from time to time to ensure complete mixing. Reaction was let go until tlc indicated complete conversion of ***E*-2**. Once completed, aqueous 0.5 M HCl was added to the test tube while shaking the tube.

The reaction mixture was then washed with ethyl acetate (ca. 5 mL×3). The combined organic extract was washed with brine (ca. 20 mL) and dried over anhydrous magnesium sulphate. After filtration, the filtrate was concentrated, and the residue was purified by silica-gel chromatography. The compound **220** was obtained in 82% yield (83.36 mg).

Colorless viscous oil;

^{1}H NMR (500 MHz, $CDCl_3$) δ 2.53 (1H, s), 3.81 (3H, s), 5.95 (1H, s), 6.88 – 6.90 (2H, m), 7.01 (1H, s), 7.21 – 7.23 (2H, m), 7.32 – 7.35 (1H, m), 7.38 – 7.41 (2H, m), 7.47 – 7.48 (2H, m) ppm;

^{13}C NMR (125 MHz, $CDCl_3$) δ 55.31, 70.90, 114.16, 126.13, 127.02, 127.94, 128.51, 129.67, 130.87, 136.07, 140.22, 159.42 ppm;

HRMS: Calculated for $C_{16}H_{15}O_2Cl$: 274.0773, Found: 274.074;

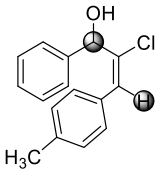

$^{3}J_{C,H}$ = 7.6 Hz

4.7. General Procedures from 2.7

Dimethyl maleate (***Z*-148**) in Suzuki cross coupling reaction conditions

The compound dimethyl maleate (31 µL, 0.25 mmol), p-MeOPhB$(OH)_2$ (37.84 mg, 0.25 mmol), $Pd_2(dba)_3$ (5.49 mg, 0.006 mmol), DPEphos (6.73 mg, 0.0125 mmol) and Cs_2CO_3 (243.39 mg, 0.75 mmol) were placed in a glass tube with a screw cap. Anhydrous dioxane (1.5 mL) was added to the glass tube. The stirred solution was heated at 85 °C for one hour. The aliquot taken was quenched with cold water and extracted with dichloromethane. The crude

sample was analyzed by NMR. The mixture of dimethyl maleate (**Z-148**): dimethyl fumarate (***E*-148**) = 20: 80 was observed.

Different dimethyl maleate (***Z*-148**) concentration in the reaction

The compound ***E*-1** (50 mg, 0.25 mmol), p-MeOPhB(OH)$_2$ (37.84 mg, 0.25 mmol), dimethyl maleate (different concentration), $Pd_2(dba)_3$ (5.49 mg, 0.006 mmol), DPEphos (6.73 mg, 0.0125 mmol) and Cs_2CO_3 (243.39 mg, 0.75) were placed in a glass tube with a screw cap. Anhydrous dioxane (1.5 mL, 0.166 M with respect to ***E*-1**) was added to the glass tube. The stirred solution was heated at 85 ℃ for one hour. The aliquot taken was quenched with cold water and extracted with dichloromethane. The sample was analyzed by GC-MS.

TEMPO (**209**) and quinone studies

The compound ***E*-1** (100 mg, 0.5 mmol), p-MeOPhB(OH)$_2$ (75.54 mg, 0.5 mmol), $Pd_2(dba)_3$ (10.99 mg, 0.012 mmol), DPEphos (13.46 mg, 0.025 mmol), TEMPO (1.88 mg, 0.012 mmol) / quinone (1.30 mg, 0.012 mmol) and Cs_2CO_3 (485.50 mg, 1.49 mmol) were placed in a glass tube with a screw cap. Anhydrous dioxane (3 mL, 0.166 M with respect to ***E*-1**) was added to the glass tube. The stirred solution was heated at 85 ℃ until complete consumption of ***E*-1**. The aliquot taken was quenched with cold water and extracted with dichloromethane. The reaction was analyzed by GC-MS. The isomerization of 4: 96 (***Z*-2**: ***E*-2**) was observed.

The compound ***E*-2** (27.16 mg, 0.09 mmol), $Pd_2(dba)_3$ (2.29 mg, 0.025 mmol), DPEphos (2.69 mg, 0.005 mmol), TEMPO (0.78 mg, 0.005 mmol) in d_8-toluene (0.6 mL) were placed in a NMR tube. The tube was placed in NMR instrument (at 313 K) and automated script was acquired every 3 minutes. The reaction was let go for 3.5 hr. At the end of 3.5 hr, 55% ***E*-2** and 45% ***Z*-2** was observed.

Base study

The compound ***E*-2** (50 mg, 0.18 mmol), p-MeOPhB(OH)$_2$ (27.81 mg, 0.18 mmol), $Pd_2(dba)_3$ (4.58 mg, 0.005 mmol), DPEphos (4.85 mg, 0.009 mmol,) and triethyl amine (77 µL, 0.55 mmol) were placed in a glass tube with a screw cap. Anhydrous dioxane (1.1 mL, 0.166 M with respect to ***E*-2**) was added to the glass tube. The stirred solution was heated at 85 °C for one hour. The aliquot taken was quenched with cold water and extracted with dichloromethane. The sample was analyzed by GC-MS. The formation of ***E*-2**: ***Z*-2** = 4: 96 was observed.

Suzuki cross coupling with an organic base

The compound ***E*-1 (**50 mg, 0.25 mmol), p-MeOPhB(OH)$_2$ (37.85 mg, 0.25 mmol), $Pd_2(dba)_3$ (5.68 mg, 0.006 mmol), DPEphos (6.73 mg, 0.0125 mmol) and triethyl amine (104 µL, 0.75 mmol) were placed in a glass tube with a screw cap. Anhydrous dioxane (1.5 mL, 0.166 M with respect to ***E*-1**) was added to the glass tube. The stirred solution was heated at 85 °C. The aliquot taken was quenched with cold water and extracted with dichloromethane. The sample was analyzed by GC-MS. No Suzuki cross coupled product formation was observed.

(***E*-2**) with 2.5 mol% $Pd_2(dba)_3$ at 350 K

The compound ***E*-2** (27.16 mg, 0.09 mmol) was dissolved in 0.5 mL of d_8-toluene and placed in a NMR tube. Then a 0.1 mL of premixed mixture of 5 mg $Pd_2(dba)_3$ in deuterated toluene (0.2 mL) was added to the NMR tube. The experiment was set up for 5 hours at 350 K, such that each scan was acquired after 3 minutes. No isomerization was observed after 5 hours.

(***E*-2**) with 5 mol% DPEphos at 350 K

The compound ***E*-2** (27.16 mg, 0.09 mmol) was dissolved in 0.5 mL of d_8-toluene and placed in a NMR tube. Then a 0.1 mL of premixed mixture of 5.4 mg DPEphos were dissolved in deuterated toluene (0.2 mL) was added to the NMR tube. The experiment was set up for about 3.5 hours at 350 K, such that each scan was acquired after 3 minutes. No isomerization was observed after ~ 3.5 hour.

(***E*-2**) with 5 mol% Pd/DPEphos at 350 K

The compound ***E*-2** (27.16 mg, 0.09 mmol) was dissolved in 0.5 mL of d_8-toluene and placed in a NMR tube. Then a 0.1 mL of premixed mixture of 5 mg $Pd_2(dba)_3$and 5.4 mg DPEphos were dissolved in deuterated toluene (0.2 mL) was added to the NMR tube. The experiment was set up for about five hours at 350 K, such that each scan was acquired after 3 minutes. The ratio of ***E***: ***Z*- 2** = 4: 96 was observed in 30 min.

(***E*-2**) with 5 mol% Pd/DPEphos at 313 K

The compound ***E*-2** (27.16 mg, 0.09 mmol) was dissolved in 0.5 mL of d_8-toluene and placed in a NMR tube. Then a 0.1 mL of premixed mixture of 5 mg $Pd_2(dba)_3$and 5.4 mg DPEphos were dissolved in deuterated toluene (0.2 mL) was added to the NMR tube. The experiment was set up for about 3.5 hour at 313 K, such that each scan was acquired after 3 minutes. The ratio of ***E***:***Z*-2** = 46: 54 was observed after 3.5 hour.

Dimethyl maleate (***Z*-148**) with 5mol% Pd/DPEphos at 350 K

The compound dimethyl maleate (12.46 µL, 0.09 mmol) was dissolved in 0.5 mL d_8-toluene and placed in NMR tube. Then a 0.1 mL of premixed mixture of 5 mg $Pd_2(dba)_3$and 5.4 mg

DPEphos were dissolved in deuterated toluene (0.2 mL) was added to the NMR tube. The tube was placed in a NMR instrument at 350 K. The experiment was set up for about ~ 1.5 hour at 350K, such that each scan was acquired after 3 minutes. No isomerization was observed after 1.5 hr.

Compound (***E*-1**) and (***E*-2**) with 5mol% Pd/DPEphos at 350 K

The compound ***E*-2** (20.03 mg, 0.09 mmol) and compound ***E*-1** (27.16 mg, 0.09 mmol) was dissolved in 0.5 mL of d_8-toluene and placed in a NMR tube. Then a 0.1 mL of premixed mixture of 5 mg $Pd_2(dba)_3$and 5.4 mg DPEphos were dissolved in deuterated toluene (0.2 mL) was added to the NMR tube. The experiment was set up for about 3.5 at 350 K, such that each scan was acquired after 3 minutes. Neither the isomerization of ***E*-2** and ***E*-1** was observed after 3.5 hour.

Cis stilbene **(*Z*-161)** with 5mol% Pd/DPEphos at 350 K

The compound cis-stilbene (17.76 µL, 0.09 mmol) was dissolved in 0.5 mL d_8-toluene and placed in NMR tube. Then a 0.1 mL of premixed mixture of 5 mg $Pd_2(dba)_3$and 5.4 mg DPEphos were dissolved in deuterated toluene (0.2 mL) was added to the NMR tube. The tube was placed in a NMR instrument at 350 K. The experiment was set up for about 1.5 hour at 350 K, such that each scan was acquired after 3 minutes. No isomerization was observed after 1.5 hr.

(***E*-220**) with 5mol% Pd/DPEphos at 350 K

The compound ***E*-222** (27.16 mg, 0.0996 mmol) was dissolved in 0.5 mL d_8-toluene and placed in NMR tube. Then a 0.1 mL of premixed mixture of 5 mg $Pd_2(dba)_3$and 5.4 mg

DPEphos were dissolved in deuterated toluene (0.2 mL) was added to the NMR tube. The tube was placed in a NMR instrument at 350 K. The experiment was set up for about 3.5 hour such that each scan was acquired after 3 minutes. No isomerization was observed after 3.5 hr.

Dimethyl maleate **(*Z*-148)** and (***E*-2**) 1:1 ratio with 5mol% Pd/DPEphos at 313 K

The compound ***E*-2** (27.16 mg, 0.09 mmol) was dissolved in 0.5 mL d_8-toluene and placed in NMR tube. Then a 0.1 mL of premixed mixture of dimethyl maleate (12.46 μL, 0.09 mmol), 5 mg $Pd_2(dba)_3$and 5.4 mg DPEphos were dissolved in deuterated toluene (0.2 ml) was added to the NMR tube. The tube was placed in a NMR instrument at 313 K. The experiment was set up for about 3.5 hour such that each scan was acquired after 3 minutes. No isomerization of ***E*-2** to ***Z*-2** was observed after 3.5 hr.

Dimethyl maleate **(*Z*-148)** and (***E*-2**) in 0.5:1 ratio with 5mol% Pd/DPEphos at 313 K

The compound ***E*-2** (27.16 mg, 0.09 mmol) was dissolved in 0.5 mL d_8-toluene and placed in NMR tube. Then a 0.1 mL of premixed mixture of dimethyl maleate (6.23 μL, 0.05 mmol), 5 mg $Pd_2(dba)_3$and 5.4 mg DPEphos were dissolved in deuterated toluene (0.2 mL) was added to the NMR tube. The tube was placed in a NMR instrument at 313 K. The experiment was set up for about 3.5 hour such that each scan was acquired after 3 minutes. No isomerization of ***E*-2** to ***Z*-2** was observed after 3.5 hr.

Dimethyl maleate **(*Z*-148)** and (***E*-2**) in 0.01:1 ratio with 5mol% Pd/DPEphos at 313 K

The compound ***E*-2** (27.16 mg, 0.09 mmol) was dissolved in 0.5 mL d_8-toluene and placed in NMR tube. Then a 0.1 mL of premixed mixture of dimethyl maleate (0.13 μL, 0.00 mmol), 5 mg $Pd_2(dba)_3$and 5.4 mg DPEphos were dissolved in deuterated toluene (0.2 mL) was added to the NMR tube. The tube was placed in a NMR instrument at 313 K. The experiment was set up for about 5 hour such that each scan was acquired after 3 minutes. The ratio of ***E*-2**: ***Z*-2** = 69: 31 was observed after 3.5 hr.

(***E*-2**) with 5 mol% Pd/*t*-Bu-Xantphos at 350 K

The compound ***E*-2** (27.16 mg, 0.0996 mmol) was dissolved in 0.5 mL d_8-toluene and placed in NMR tube. Then a 0.1 mL of premixed mixture of 5 mg $Pd_2(dba)_3$and 5 mg *t*-Bu-Xantphos was dissolved in deuterated toluene (0.2 mL) was added to the NMR tube. The tube was placed in a NMR instrument at 350 K. The experiment was set up for about 4 hour such that each scan was acquired after 3 minutes. The ratio of ***E*-2**: ***Z*-2** = 94: 4 was observed after 4 hr.

Chapter 5: References

[1] C. C. C. Johansson Seechurn, M. O. Kitching, T. J. Colacot, V. Snieckus, *Angew. Chem., Int. Ed.* **2012**, *51*, 5062-5085.

[2] a) A. Suzuki, in *Handbook of Organopalladium Chemistry for Organic Chemistry, Vol. 1* (Ed.: E. Negishi), Wiley, New York, **2002**, pp. 249-262; b) K. Sonogashira, in *Handbook of Organopalladium Chemistry for Organic Synthesis, Vol. 1* (Ed.: E. Negishi), Wiley, New York, **2002**; c) E. Negishi, in *Handbook of Organopalladium Chemistry for Organic synthesis* (Ed.: E. Negishi), Wiley, New York, **2002**, pp. 229-247; d) M. Kosugi, K. Fugami, in *Handbook of Organopalladium Chemistry for Organic Synthesis, Vol. 1* (Ed.: E. Negishi), Wiley, New York, **2002**; e) T. Hiyama, E. Shirakawa, in *Handbook of Organopalladium Chemistry for Organic Syntheis, Vol. 1* (Ed.: E. Negishi), Wiley, New York, **2002**, pp. 285-310.

[3] The Nobel Prize in Chemistry 2010. Nobelprize.org. (accessed 11 Feb 2017).

[4] C. Amatore, A. Jutand, in *Handbook of Organopalladium Chemistry for Organic Synthesis, Vol. 1* (Ed.: E. Negishi), Wiley, New York, **2002**.

[5] a) D. Steinborn, *Funadamentals of Organometallic Catalysis*, First ed., Wiley, Germany, **2012**; b) A. M. Echavarren, D. J. Cardenas, in *Metal-Catalyzed Cross-Coupling Reactions, Vol. 1* (Eds.: A. d. Meijere, F. Diederich), Wiley, Weinheim, **2004**.

[6] R. H. Crabtree, *The organometallic chemistry of the transition metals*, 5 ed., Wiley, **2009**.

[7] C. A. Tolman, *Chem. Rev.* **1977**, *77*, 313-348.

[8] Z. Freixa, P. W. N. M. Van Leeuwen, *Dalton Trans.* **2003**, 1890-1901.

[9] a) M. S. Kharasch, E. K. Fields, *J. Am. Chem. Soc.* **1941**, *63*, 2316-2320; b) M. S. Kharasch, C. F. Fuchs, *J. Am. Chem. Soc.* **1943**, *65*, 504-507.

[10] R. J. P. Corriu, J. P. Masse, *J. Chem. Soc., Chem. Commun.* **1972**, 144.

[11] K. Tamao, K. Sumitani, M. Kumada, *J. Amer. Chem. Soc.* **1972**, *94*, 4374-4376.

[12] a) S. Murahashi, M. Yamamura, K. Yanagisawa, N. Mita, K. Kondo, *J. Org. Chem.* **1979**, *44*, 2408-2417; b) M. Yamamura, I. Moritani, S.-I. Murahashi, *J. Organomet. Chem.* **1975**, *91*, C39-C42.

[13] R. D. Stephens, C. E. Castro, *J. Org. Chem.* **1963**, *28*, 3313-3315.

[14] L. Cassar, *J. Organomet. Chem.* **1975**, *93*, 253-257.

[15] H. A. Dieck, F. R. Heck, *J. Organomet. Chem.* **1975**, *93*, 259-263.

[16] K. Sonogashira, Y. Tohda, N. Hagihara, *Tetrahedron Lett.* **1975**, 4467-4470.

[17] E. Negishi, S. Baba, *J. Chem. Soc., Chem. Commun.* **1976**, 596-597.

[18] a) E. Negishi, A. O. King, N. Okukado, *J. Org. Chem.* **1977**, *42*, 1821-1823; b) A. O. King, N. Okukado, E. Negishi, *J. Chem. Soc., Chem. Commun.* **1977**, 683-684.

[19] N. Miyaura, K. Yamada, A. Suzuki, *Tetrahedron Lett.* **1979**, 3437-3440.

[20] N. Miyaura, T. Yanagi, A. Suzuki, *Synth. Commun.* **1981**, *11*, 513-519.

[21] a) C. Amatore, G. Le Duc, A. Jutand, *Chem. - Eur. J.* **2013**, *19*, 10082-10093; b) A. J. J. Lennox, G. C. Lloyd-Jones, *Angew. Chem., Int. Ed.* **2013**, *52*, 7362-7370; c) C. Amatore, A. Jutand, G. Le Duc, *Angew. Chem., Int. Ed.* **2012**, *51*, 1379-1382, S1379/1371-S1379/1374.

[22] N. Miyaura, A. Suzuki, *J. Chem. Soc., Chem. Commun.* **1979**, 866-867.

[23] A. J. J. Lennox, G. C. Lloyd-Jones, *Chem. Soc. Rev.* **2014**, *43*, 412-443.

[24] G. Berionni, B. Maji, P. Knochel, H. Mayr, *Chem. Sci.* **2012**, *3*, 878-882.

[25] M. Kosugi, K. Sasazawa, Y. Shimizu, T. Migita, *Chem. Lett.* **1977**, 301-302.

[26] a) D. Milstein, J. K. Stille, *J. Am. Chem. Soc.* **1978**, *100*, 3636-3638; b) D. Milstein, J. K. Stille, *J. Org. Chem.* **1979**, *44*, 1613-1618.

[27] a) D. Milstein, J. K. Stille, *J. Am. Chem. Soc.* **1979**, *101*, 4981-4991; b) D. Milstein, J. K. Stille, *J. Am. Chem. Soc.* **1979**, *101*, 4992-4998.

[28] T. N. Mitchell, *J. Organomet. Chem.* **1986**, *304*, 1-16.

[29] J. Yoshida, K. Tamao, H. Yamamoto, T. Kakui, T. Uchida, M. Kumada, *Organometallics (Washington, D. C.)* **1982**, *1*, 542-549.

[30] Y. Hatanaka, T. Hiyama, *J. Org. Chem.* **1988**, *53*, 918-920.

[31] a) R. F. Heck, *J. Amer. Chem. Soc.* **1968**, *90*, 5518-5526; b) R. F. Heck, *J. Amer. Chem. Soc.* **1968**, *90*, 5535-5538; c) R. F. Heck, *J. Amer. Chem. Soc.* **1968**, *90*, 5546-5548.

[32] a) T. Mizoroki, K. Mori, A. Ozaki, *Bull. Chem. Soc. Jap.* **1971**, *44*, 581; b) K. Mori, T. Mizoroki, A. Ozaki, *Bull. Chem. Soc. Jap.* **1973**, *46*, 1505-1508.

[33] R. F. Heck, J. P. Nolley, Jr., *J. Org. Chem.* **1972**, *37*, 2320-2322.

[34] a) J. Uenishi, J. M. Beau, R. W. Armstrong, Y. Kishi, *J. Am. Chem. Soc.* **1987**, *109*, 4756-4758; b) D. A. Evans, J. T. Starr, *Angew. Chem., Int. Ed.* **2002**, *41*, 1787-1790; c) N. C. Kallan, R. L. Halcomb, *Org. Lett.* **2000**, *2*, 2687-2690; d) P. J. Mohr, R. L. Halcomb, *J Am Chem Soc* **2003**, *125*, 1712-1713; e) D.-S. Su, D. Meng, P. Bertinato, A. Balog, E. J. Sorensen, S. J. Danishefsky, Y.-H. Zheng, T.-C. Chou, L. He, S. B. Horwitz, *Angew. Chem., Int. Ed. Engl.* **1997**, *36*, 757-759; f) V. Domingo, L. Lorenzo, J. F. Quilez del Moral, A. F. Barrero, *Org. Biomol. Chem.* **2013**, *11*, 559-562; g) S. Ducki, G. MacKenzie, B. Greedy, S. Armitage, J. Fournier Dit Chabert, E. Bennett, J. Nettles, J. P. Snyder, N. J. Lawrence, *Bioorg. Med. Chem.* **2009**, *17*, 7711-7722; h) D. J. Kerr, E. Hamel, M. K. Jung, B. L. Flynn, *Bioorg. Med. Chem.* **2007**, *15*, 3290-3298; i) V. Domingo, L. Silva, H. R. Dieguez, J. F. Arteaga, J. F. Quilez del Moral, A. F. Barrero, *J. Org. Chem.* **2009**, *74*, 6151-6156; j) A. Francais, A. Leyva, G. Etxebarria-Jardi, S. V. Ley, *Org. Lett.* **2010**, *12*, 340-343; k) R. Rossi, A. Carpita, M. G. Quirici, *Tetrahedron* **1981**, *37*, 2617-2623; l) A. Torrado, B. Iglesias, S. Lopez, A. R. de Lera, *Tetrahedron* **1995**, *51*, 2435-2454.

[35] M. Al-Masum, E. Ng, M. C. Wai, *Tetrahedron Lett.* **2011**, *52*, 1008-1010.

[36] V. P. Baillargeon, J. K. Stille, *J. Am. Chem. Soc.* **1986**, *108*, 452-461.

[37] G. P. Roth, C. E. Fuller, *J. Org. Chem.* **1991**, *56*, 3493-3496.

[38] K.-i. Gouda, E. Hagiwara, Y. Hatanaka, T. Hiyama, *J. Org. Chem.* **1996**, *61*, 7232-7233.

[39] L. Labaudiniere, J. F. Normant, *Tetrahedron Lett.* **1992**, *33*, 6139-6142.

[40] J. W. Labadie, J. K. Stille, *J. Am. Chem. Soc.* **1983**, *105*, 6129-6137.

[41] V. Farina, B. Krishnan, *J. Am. Chem. Soc.* **1991**, *113*, 9585-9595.

[42] J. W. Labadie, D. Tueting, J. K. Stille, *J. Org. Chem.* **1983**, *48*, 4634-4642.

[43] W. F. Goure, M. E. Wright, P. D. Davis, S. S. Labadie, J. K. Stille, *J. Am. Chem. Soc.* **1984**, *106*, 6417-6422.

[44] C. J. O'Brien, Z. S. Nixon, A. J. Holohan, S. R. Kunkel, J. L. Tellez, B. J. Doonan, E. E. Coyle, F. Lavigne, L. J. Kang, K. C. Przeworski, *Chem. - Eur. J.* **2013**, *19*, 15281-15289.

[45] S. Kamijo, Y. Sasaki, C. Kanazawa, T. Schusseler, Y. Yamamoto, *Angew. Chem., Int. Ed.* **2005**, *44*, 7718-7721.

[46] a) D. Gauthier, A. T. Lindhardt, E. P. K. Olsen, J. Overgaard, T. Skrydstrup, *J. Am. Chem. Soc.* **2010**, *132*, 7998-8009; b) I. S. Kim, G. R. Dong, Y. H. Jung, *J. Org. Chem.* **2007**, *72*, 5424-5426; c) J. Yu, M. J. Gaunt, J. B. Spencer, *J. Org. Chem.* **2002**, *67*, 4627-4629.

[47] a) M. J. Hilton, L.-P. Xu, P.-O. Norrby, Y.-D. Wu, O. Wiest, M. S. Sigman, *J. Org. Chem.* **2014**, *79*, 11841-11850; b) E. Larionov, L. Lin, L. Guenee, C. Mazet, *J. Am. Chem. Soc.* **2014**, *136*, 16882-16894; c) E. W. Werner, T.-S. Mei, A. J. Burckle, M. S. Sigman, *Science (Washington, DC, U. S.)* **2012**, *338*, 1455-1458; d) T.-S. Mei, E. W. Werner, A. J. Burckle, M. S. Sigman, *J. Am. Chem. Soc.* **2013**, *135*, 6830-6833; e) L. Xu, M. J. Hilton, X. Zhang, P.-O. Norrby, Y.-D. Wu, M. S. Sigman, O. Wiest, *J. Am. Chem. Soc.* **2014**, *136*, 1960-1967; f) H. H. Patel, M. S. Sigman, *J. Am. Chem. Soc.* **2015**, *137*, 3462-3465.

[48] a) A. L. Hansen, J.-P. Ebran, M. Ahlquist, P.-O. Norrby, T. Skrydstrup, *Angew. Chem., Int. Ed.* **2006**, *45*, 3349-3353; b) J.-P. Ebran, A. L. Hansen, T. M. Gogsig, T. Skrydstrup, *J. Am. Chem. Soc.* **2007**, *129*, 6931-6942.

[49] a) A. T. Lindhardt, T. M. Goegsig, T. Skrydstrup, *J. Org. Chem.* **2009**, *74*, 135-143; b) A. L. Hansen, J.-P. Ebran, T. M. Gogsig, T. Skrydstrup, *J. Org. Chem.* **2007**, *72*, 6464-6472.

[50] J. Yu, J. B. Spencer, *J. Am. Chem. Soc.* **1997**, *119*, 5257-5258.

[51] a) G.-p. Lu, K. R. Voigtritter, C. Cai, B. H. Lipshutz, *Chem. Commun. (Cambridge, U. K.)* **2012**, *48*, 8661-8663; b) A. Krasovskiy, B. H. Lipshutz, *Org. Lett.* **2011**, *13*, 3818-3821; c) G.-P. Lu, K. R. Voigtritter, C. Cai, B. H. Lipshutz, *J. Org. Chem.* **2012**, *77*, 3700-3703.

[52] V. Farina, G. P. Roth, *Tetrahedron Lett.* **1991**, *32*, 4243-4246.

[53] a) C. Amatore, S. Bensalem, S. Ghalem, A. Jutand, *J. Organomet. Chem.* **2004**, *689*, 4642-4646; b) K. A. Brady, T. A. Nile, *J. Organomet. Chem.* **1981**, *206*, 299-304; c) D.

Zargarian, H. Alper, *Organometallics* **1991**, *10*, 2914-2921; d) D. Zargarian, H. Alper, *Organometallics* **1993**, *12*, 712-724.

[54] a) D. W. Hart, J. Schwartz, *J. Organomet. Chem.* **1975**, *87*, C11-C14; b) L. W. Chung, Y.-D. Wu, B. M. Trost, Z. T. Ball, *J. Am. Chem. Soc.* **2003**, *125*, 11578-11582.

[55] S. Park, K. J. Shin, J. H. Seo, *Synlett* **2015**, *26*, 2296-2300.

[56] G. R. Dong, S. Park, D. Lee, K. J. Shin, J. H. Seo, *Synlett* **2013**, *24*, 1993-1997.

[57] J.-M. Weibel, A. Blanc, P. Pale, *Chem. Rev. (Washington, DC, U. S.)* **2008**, *108*, 3149-3173.

[58] W. Cabri, I. Candiani, A. Bedeschi, S. Penco, R. Santi, *J. Org. Chem.* **1992**, *57*, 1481-1486.

[59] J. M. Huggins, R. G. Bergman, *J. Am. Chem. Soc.* **1981**, *103*, 3002-3011.

[60] L. Canovese, C. Santo, F. Visentin, *Organometallics* **2008**, *27*, 3577-3581.

[61] Y. Yu, K. J. Shin, J. H. Seo, *J. Org. Chem.* **2017**, *82*, 1864-1871.

[62] Q. Zhao, V. Tognetti, L. Joubert, T. Besset, X. Pannecoucke, J.-P. Bouillon, T. Poisson, *Org. Lett.* **2017**, *19*, 2106-2109.

[63] E. Richmond, J. Moran, *J. Org. Chem.* **2015**, *80*, 6922-6929.

[64] a) L. M. Geary, P. G. Hultin, *Eur. J. Org. Chem.* **2010**, 5563-5573, S5563/5561-S5563/5185; b) L. M. Geary, P. G. Hultin, *J. Org. Chem.* **2010**, *75*, 6354-6371.

[65] A. Jonczyk, A. H. Gierczak, *Synthesis* **1998**, 962-964.

[66] A. Kowalkowska, A. Jonczyk, *Synth. Commun.* **2011**, *41*, 3308-3317.

[67] a) D. Seebach, *Angew. Chem.* **1979**, *91*, 259-278; b) D. Seebach, E. J. Corey, *J. Org. Chem.* **1975**, *40*, 231-237.

[68] a) T. Opatz, *Synthesis* **2009**, 1941-1959; b) D. Enders, J. P. Shilvock, *Chem. Soc. Rev.* **2000**, *29*, 359-373.

[69] a) C. R. Hauser, H. M. Taylor, T. G. Ledford, *J. Am. Chem. Soc.* **1960**, *82*, 1786-1789; b) C. R. Hause, G. F. Morri, *J. Org. Chem.* **1961**, *26*, 4740-4741.

[70] a) J. Taillades, A. Commeyras, *Tetrahedron* **1974**, *30*, 127-132; b) G. Stork, A. A. Ozorio, A. Y. W. Leong, *Tetrahedron Lett.* **1978**, 5175-5178; c) V. Reutrakul, S. Nimgirawath, S. Panichanun, P. Ratananukul, *Chem. Lett.* **1979**, 399-400; d) G. Buechi, P. H. Liang, H. Wuest, *Tetrahedron Lett.* **1978**, 2763-2764; e) D. Enders, A. S. Amaya, F. Pierre, *New J. Chem.* **1999**, *23*, 261-262; f) A. Jonczyk, *ARKIVOC (Gainesville, FL, U. S.)* **2004**, 176-184; g) A. Jonczyk, A. H. Gierczak, *Synthesis* **2001**, 93-96.

[71] J. Pielichowski, R. Popielarz, *Synthesis* **1984**, 433-434.

[72] a) A. Jonczyk, Z. Pakulski, *Tetrahedron Lett.* **1996**, *37*, 8909-8912; b) A. S. Kende, P. Fludzinski, J. H. Hill, *J. Am. Chem. Soc.* **1984**, *106*, 3551-3562; c) S. I. Miller, J. I. Dickstein, *Acc. Chem. Res.* **1976**, *9*, 358-363.

[73] A. Suzuki, *Angew. Chem., Int. Ed.* **2011**, *50*, 6722-6737.

[74] S. T. Handy, Y. Zhang, *Chem. Commun. (Cambridge, U. K.)* **2006**, 299-301.

[75] M. Hussain, N.-T. Hung, R. A. Khera, A. Villinger, P. Langer, *Tetrahedron Lett.* **2011**, *52*, 184-187.

[76] R. Rossi, F. Bellina, E. Raugei, *Synlett* **2000**, 1749-1752.

[77] T. Parella, J. F. Espinosa, *Prog. Nucl. Magn. Reson. Spectrosc.* **2013**, *73*, 17-55.

[78] a) C. A. Tolman, *J. Amer. Chem. Soc.* **1970**, *92*, 2956-2965; b) R. Martin, S. L. Buchwald, *Acc. Chem. Res.* **2008**, *41*, 1461-1473; c) M.-N. Birkholz, Z. Freixa, P. W. N. M. van Leeuwen, *Chem. Soc. Rev.* **2009**, *38*, 1099-1118.

[79] C. Dugave, L. Demange, *Chem. Rev. (Washington, DC, U. S.)* **2003**, *103*, 2475-2532.

[80] T. C. Malig, J. D. B. Koenig, H. Situ, N. K. Chehal, P. G. Hultin, J. E. Hein, *React. Chem. Eng.* **2017**, *2*, 309-314.

[81] P. d. Vaal, A. Dedieu, *J. Organomet. Chem.* **1994**, *478*, 121-129.

[82] E. H. P. Tan, G. C. Lloyd-Jones, J. N. Harvey, A. J. J. Lennox, B. M. Mills, *Angew. Chem., Int. Ed.* **2011**, *50*, 9602-9606, S9602/9601-S9602/9643.

[83] I. D. Hills, G. C. Fu, *J. Am. Chem. Soc.* **2004**, *126*, 13178-13179.

[84] J. M. Merritt, J. Y. Buser, A. N. Campbell, J. W. Fennell, N. J. Kallman, T. M. Koenig, H. Moursy, M. A. Pietz, N. Scully, U. K. Singh, *Org. Process Res. Dev.* **2014**, *18*, 246-256.

[85] J. Zhu, C. Zhong, H.-F. Lu, G.-Y. Li, X. Sun, *Synlett* **2008**, 458-462.

[86] K. Brosche, F. G. Weber, G. Westphal, E. Reimann, *Z. Chem.* **1979**, *19*, 96-97.

Chapter 6: NMR spectra

(*E*)-3,4-Dichloro-2-(dimethylamino)-2-phenylbut-3-enenitrile (***E*-167**) - ^{1}H NMR

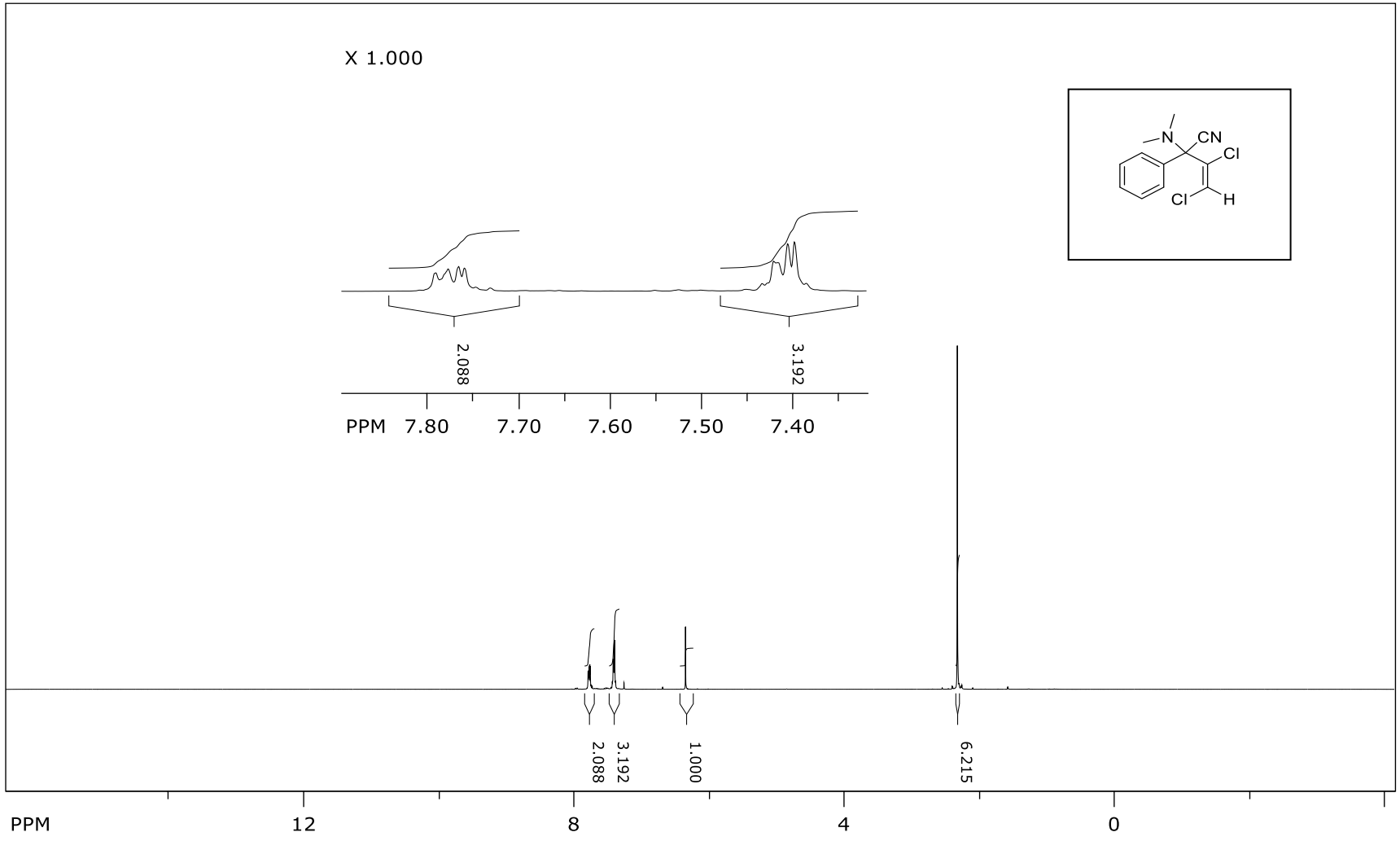

file: ...\NMR 300\NKC_7_startingmat_2\1\fid expt: <zg30>
transmitter freq.: 300.131853 MHz
time domain size: 65536 points
width: 6172.84 Hz = 20.5671 ppm = 0.094190 Hz/pt
number of scans: 16

freq. of 0 ppm: 300.130012 MHz
processed size: 32768 complex points
LB: 0.300 GF: 0.0000

(*E*)-3,4-Dichloro-2-(dimethylamino)-2-phenylbut-3-enenitrile (***E*-167**) - ^{13}C NMR

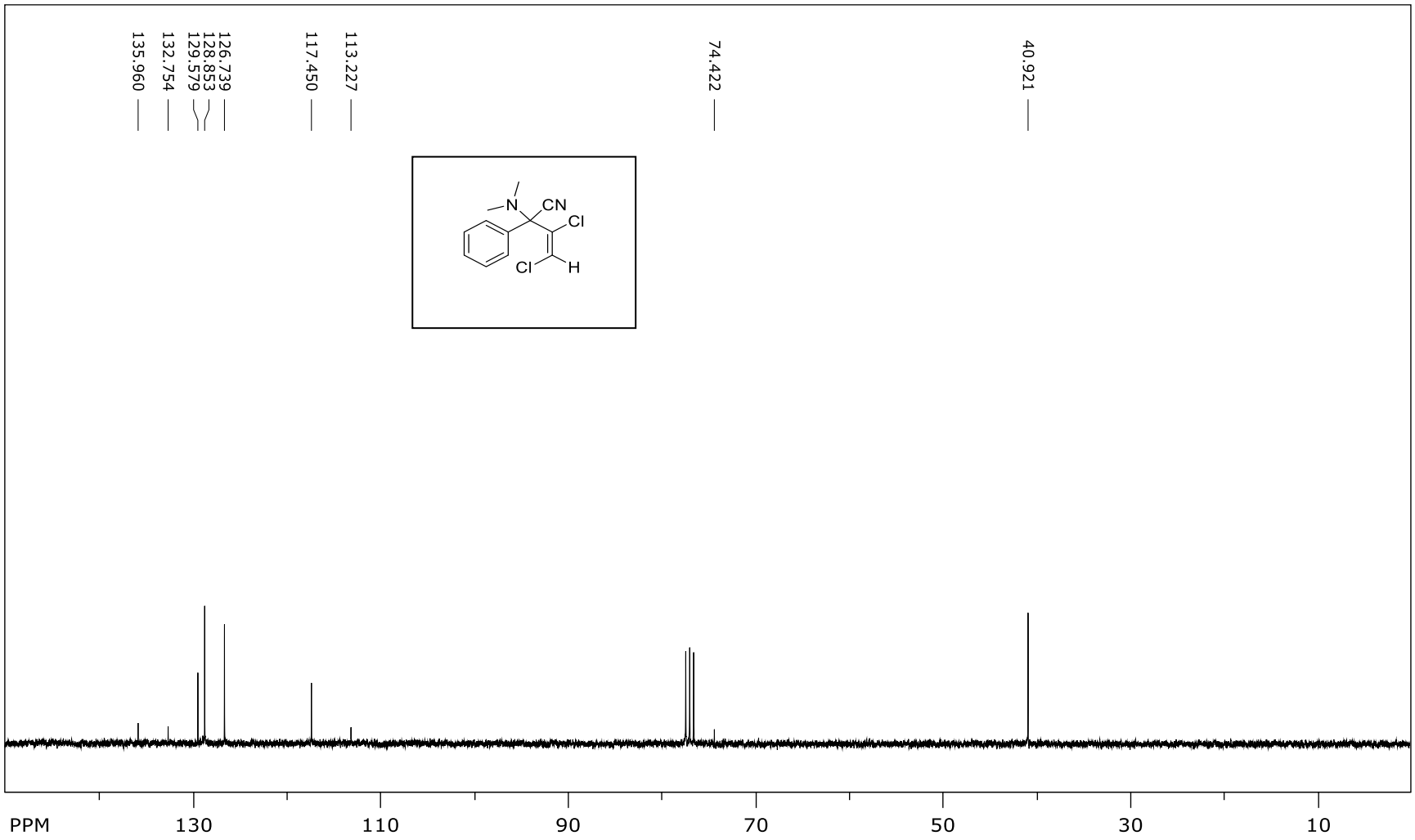

file: ...\NMR 300\NKC_7_startingmat_2\2\fid expt: <zgpg30>
transmitter freq.: 75.475295 MHz
time domain size: 65536 points
width: 17985.61 Hz = 238.2980 ppm = 0.274439 Hz/pt
number of scans: 32

freq. of 0 ppm: 75.467749 MHz
processed size: 32768 complex points
LB: 1.000 GF: 0.0000

(*E*)-3,4-Dichloro-2-(dimethylamino)-2-phenylbut-3-enenitrile (***E*-167**) - $^{3}J_{C,H}$

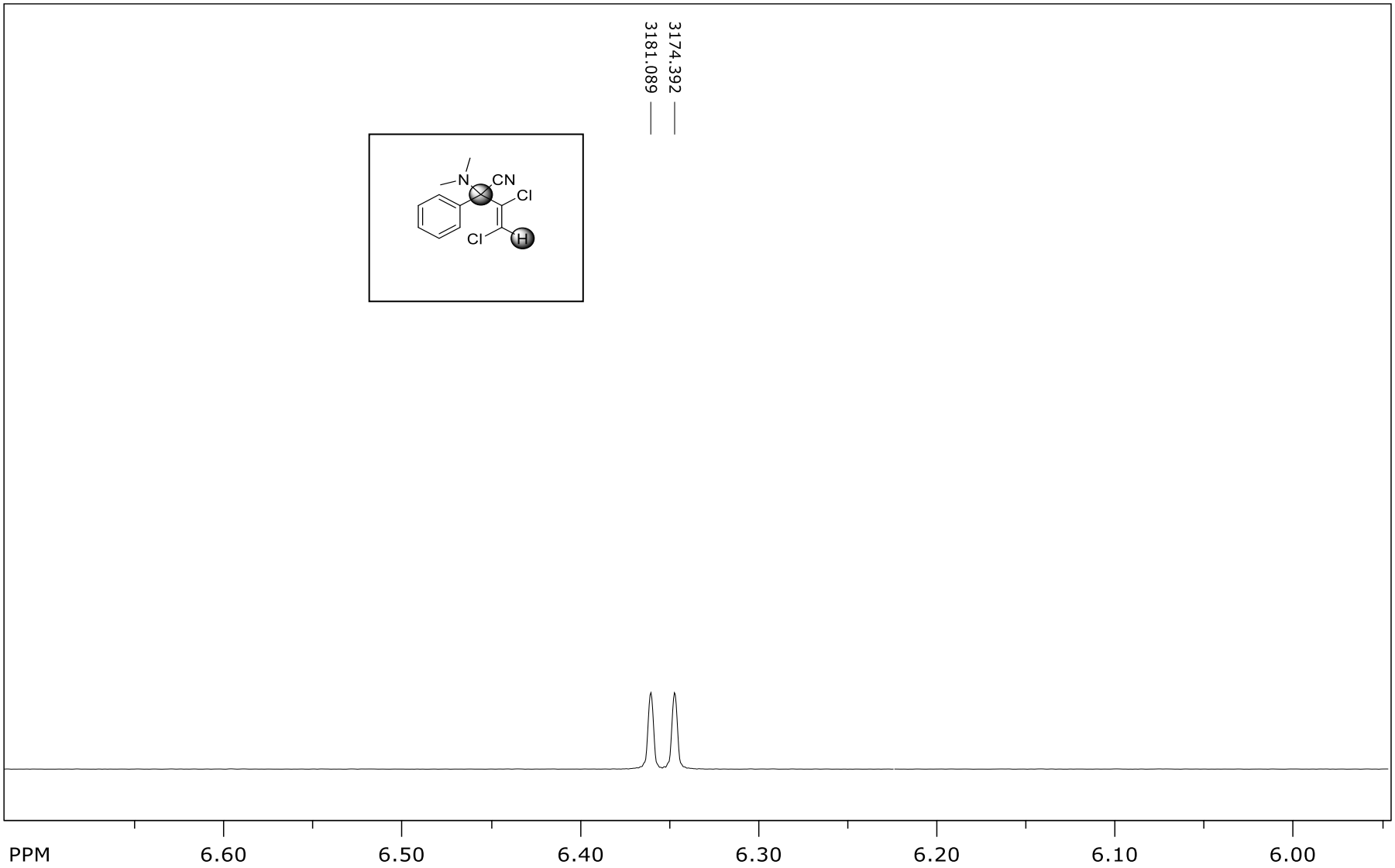

file: D:\nmr 500\NKC_7_78\2\ser expt: <hmbcgplpndqf>
transmitter freq.: 500.132201 MHz
time domain size: 8192 points
width: 4000.00 Hz = 7.9979 ppm = 0.488281 Hz/pt
number of scans: 16

freq. of 0 ppm: 500.130000 MHz
processed size: 16384 complex points
LB: 0.000 GF: 0.0000

(2*E*)-2,3-Dichloro-1-phenylprop-2-en-1-one (***E*-1**) - ^{1}H NMR

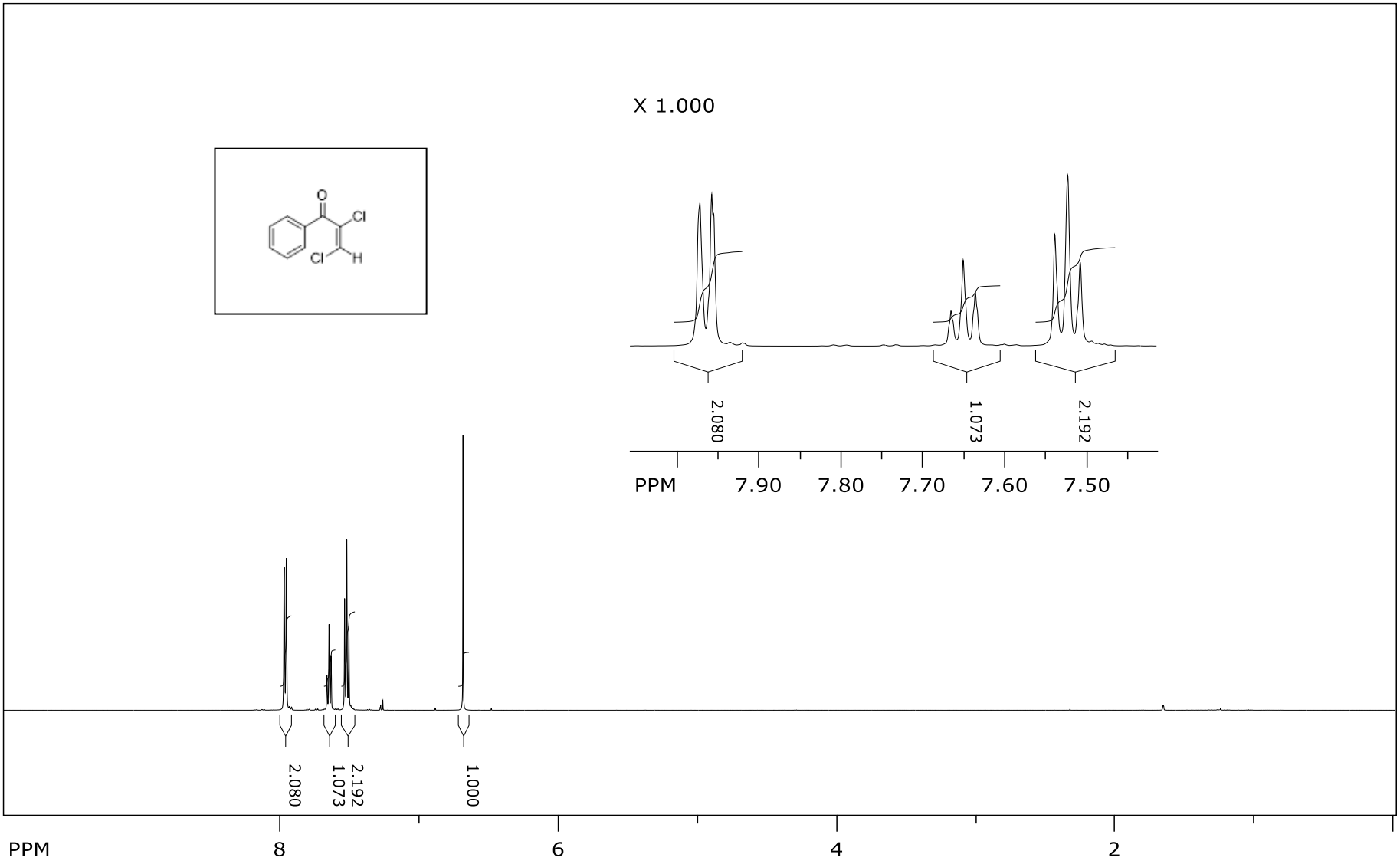

file: D:\nmr 500\NKC_8_65_trans\1\fid expt: <zg30>
transmitter freq.: 500.133089 MHz
time domain size: 65536 points
width: 10000.00 Hz = 19.9947 ppm = 0.152588 Hz/pt
number of scans: 16

freq. of 0 ppm: 500.130000 MHz
processed size: 65536 complex points
LB: 0.300 GF: 0.0000

(2*E*)-2,3-Dichloro-1-phenylprop-2-en-1-one (***E*-1**) - ^{13}C NMR

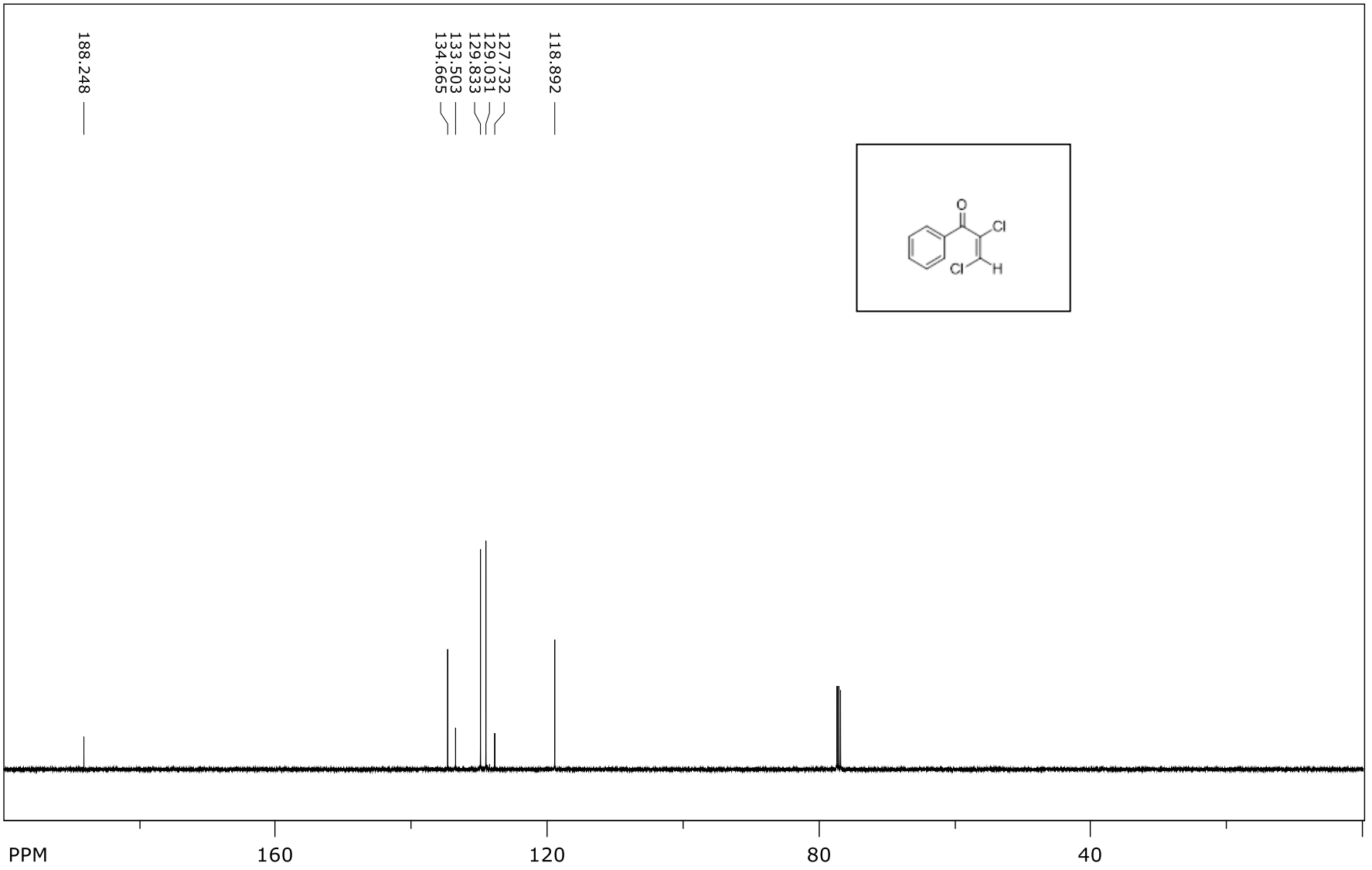

file: D:\nmr 500\NKC_8_65_trans\3\fid expt: <zgpg30>
transmitter freq.: 125.770364 MHz
time domain size: 65536 points
width: 29761.90 Hz = 236.6369 ppm = 0.454131 Hz/pt
number of scans: 28

freq. of 0 ppm: 125.757789 MHz
processed size: 32768 complex points
LB: 1.000 GF: 0.0000

(2*E*)-2,3-Dichloro-1-phenylprop-2-en-1-one (***E*-1**) - $^{3}J_{C,H}$

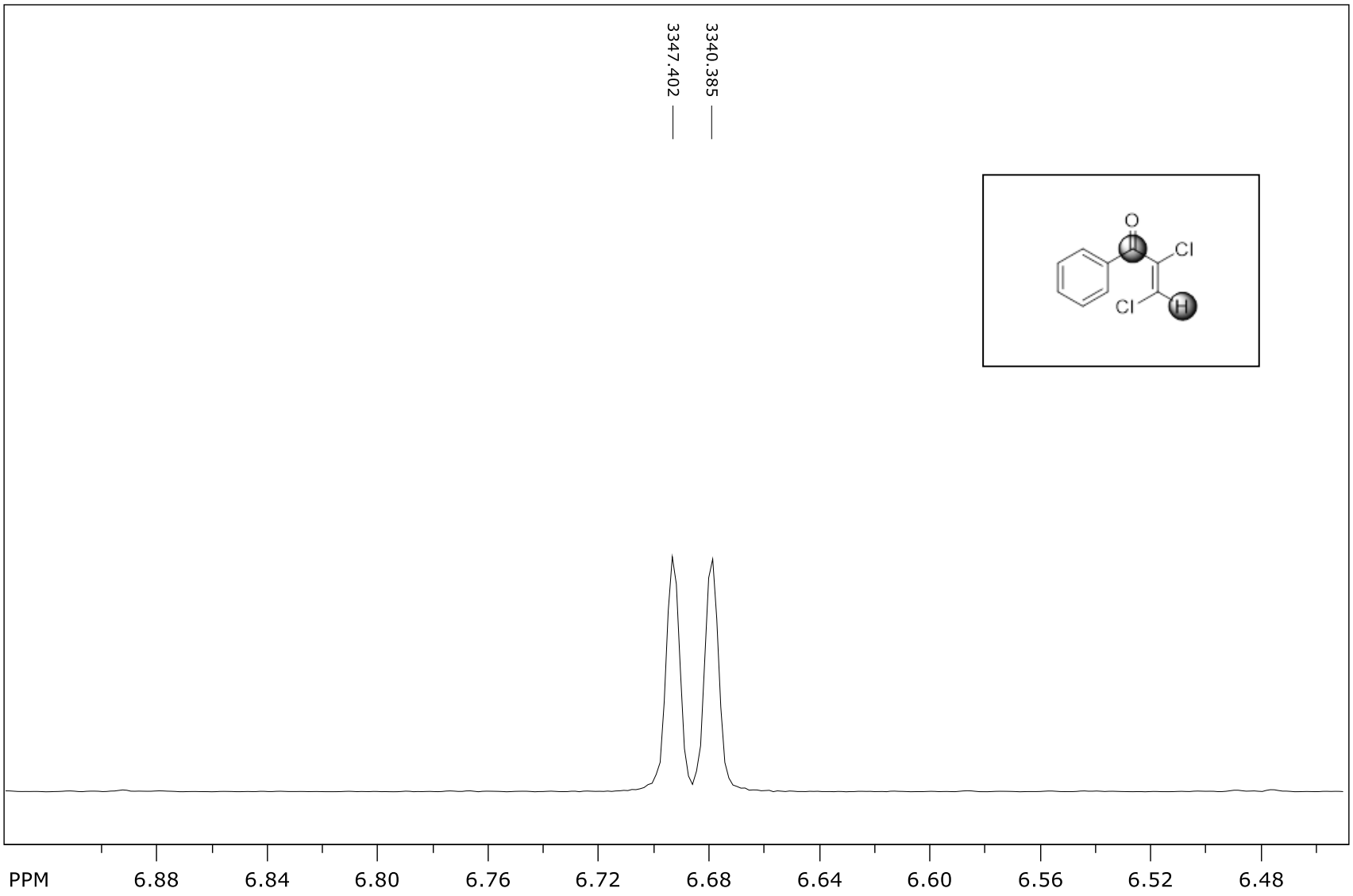

file: D:\nmr 500\NKC_8_65_trans\2\ser expt: <hmbcgplpndqf>
transmitter freq.: 500.132851 MHz
time domain size: 4096 points
width: 3001.20 Hz = 6.0008 ppm = 0.732715 Hz/pt
number of scans: 4

freq. of 0 ppm: 500.130000 MHz
processed size: 4096 complex points
LB: 0.000 GF: 0.0000

(2*E*/*Z*)-3-(4-Methoxyphenyl)-2-methyl-1-phenylprop-2-en-1-one (***E*/*Z*-179**) - ^{1}H NMR

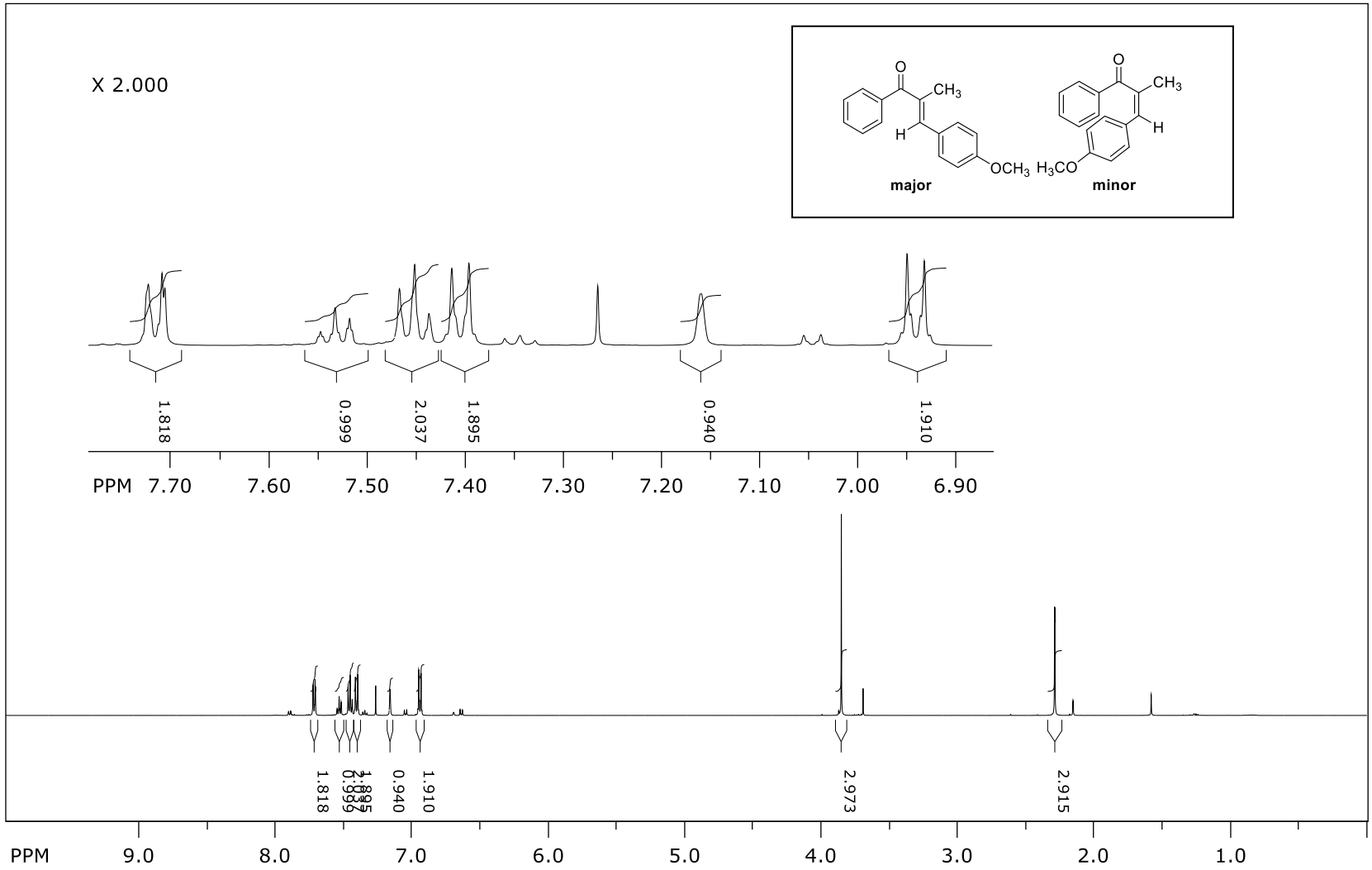

file: D:\nmr 500\NKC_7_74\1\fid expt: <zg30>
transmitter freq.: 500.133089 MHz
time domain size: 65536 points
width: 10000.00 Hz = 19.9947 ppm = 0.152588 Hz/pt
number of scans: 16

freq. of 0 ppm: 500.130000 MHz
processed size: 65536 complex points
LB: 0.300 GF: 0.0000

(2*E*/*Z*)-3-(4-Methoxyphenyl)-2-methyl-1-phenylprop-2-en-1-one (***E*/*Z*-179**) - ^{13}C NMR

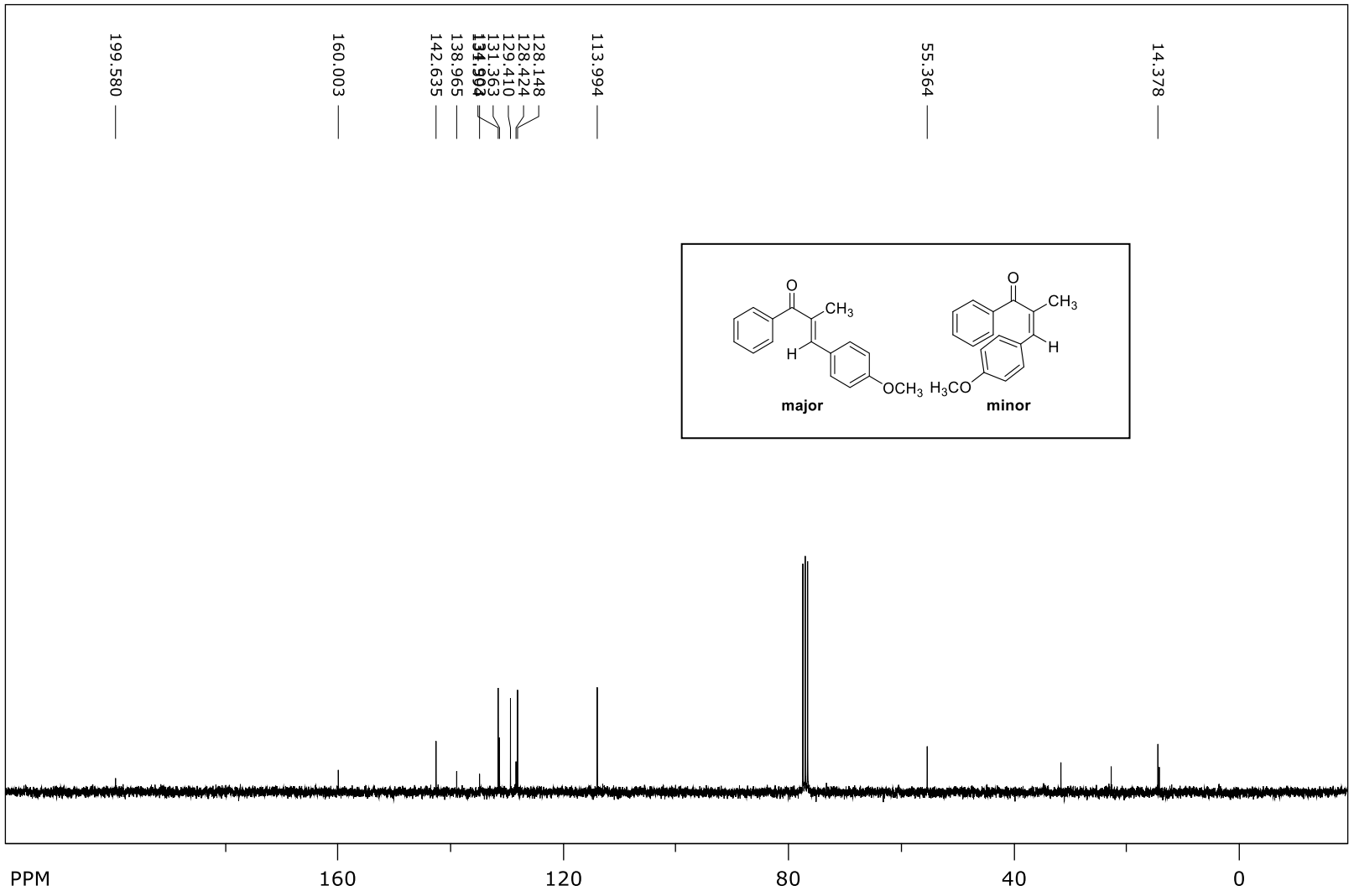

file: ...300\NKC_7_74_methyl_purified\2\fid expt: <zgpg30>
transmitter freq.: 75.475295 MHz
time domain size: 65536 points
width: 17985.61 Hz = 238.2980 ppm = 0.274439 Hz/pt
number of scans: 128

freq. of 0 ppm: 75.467749 MHz
processed size: 32768 complex points
LB: 1.000 GF: 0.0000

(2*E*)-3-(4-Methoxyphenyl)-2-methyl-1-phenylprop-2-en-1-one (***E*-179**) - $^{3}J_{C,H}$

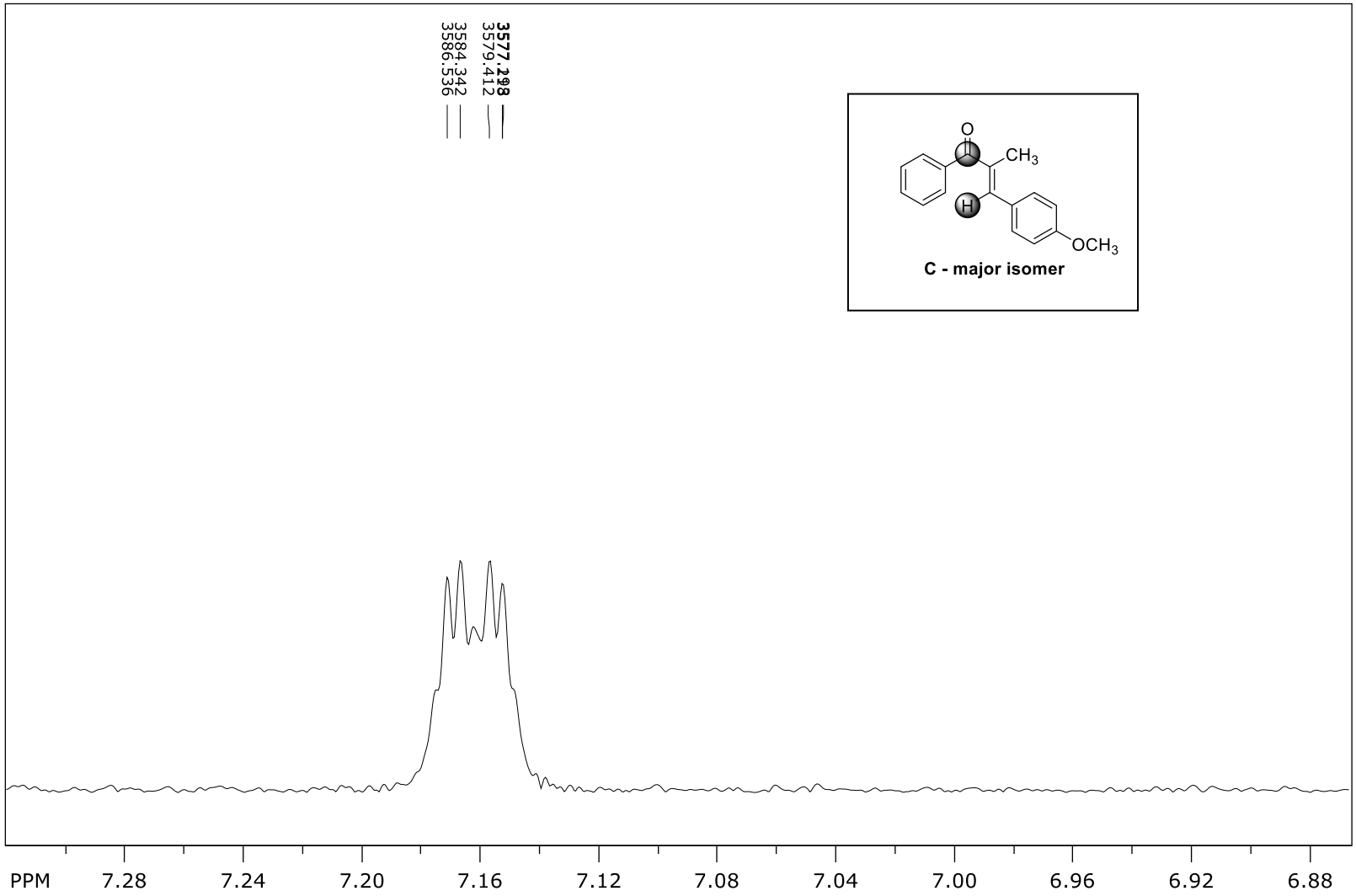

file: D:\nmr 500\NKC_7_81\101\ser expt: <hmbcgplpndqf>
transmitter freq.: 500.132201 MHz
time domain size: 8192 points
width: 4000.00 Hz = 7.9979 ppm = 0.488281 Hz/pt
number of scans: 16

freq. of 0 ppm: 500.130000 MHz
processed size: 16384 complex points
LB: 0.000 GF: 0.0000

(2*Z*)-3-(4-Methoxyphenyl)-2-methyl-1-phenylprop-2-en-1-one (***Z*-179**) - $^{3}J_{C,H}$

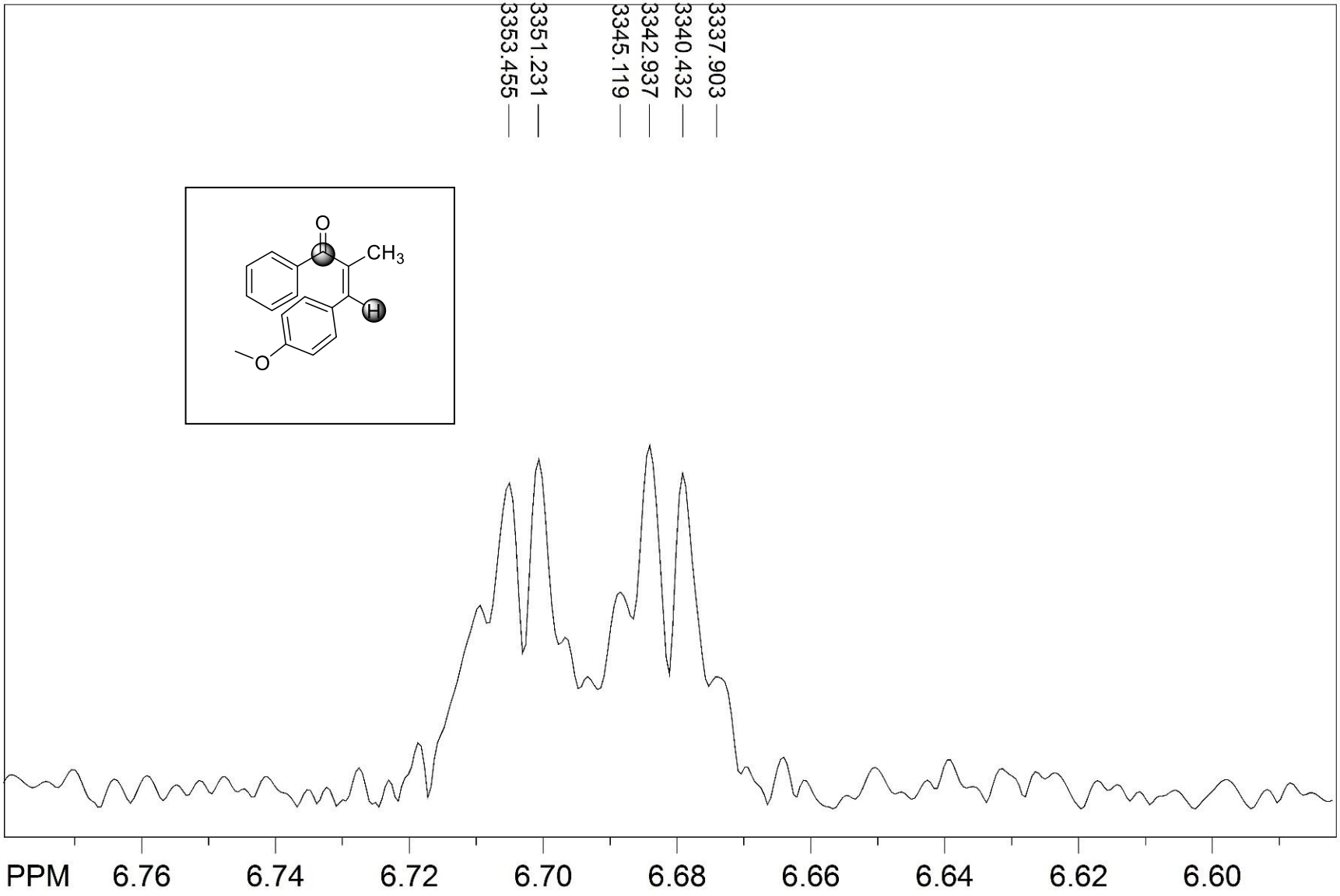

file: ...ers\chehal\Desktop\NKC 7 81\10/ser expt: <hmbcgplpndqfreq of 0 ppm: 500.130000 MHz
transmitter freq.: 500.132201 MHz processed size: 16384 points
time domain size: 8192 points LB: 0.000 GF: 0.0000
width: 4000.00 Hz = 7.9979 ppm = 0.488281 Hz/pt Hz/cm: 4.147 ppm/cm: 0.00829
number of scans: 128

(2*E*)-3-(4-Methoxyphenyl)-2-methyl-1-phenylprop-2-en-1-one (***E*-179**) – NOE

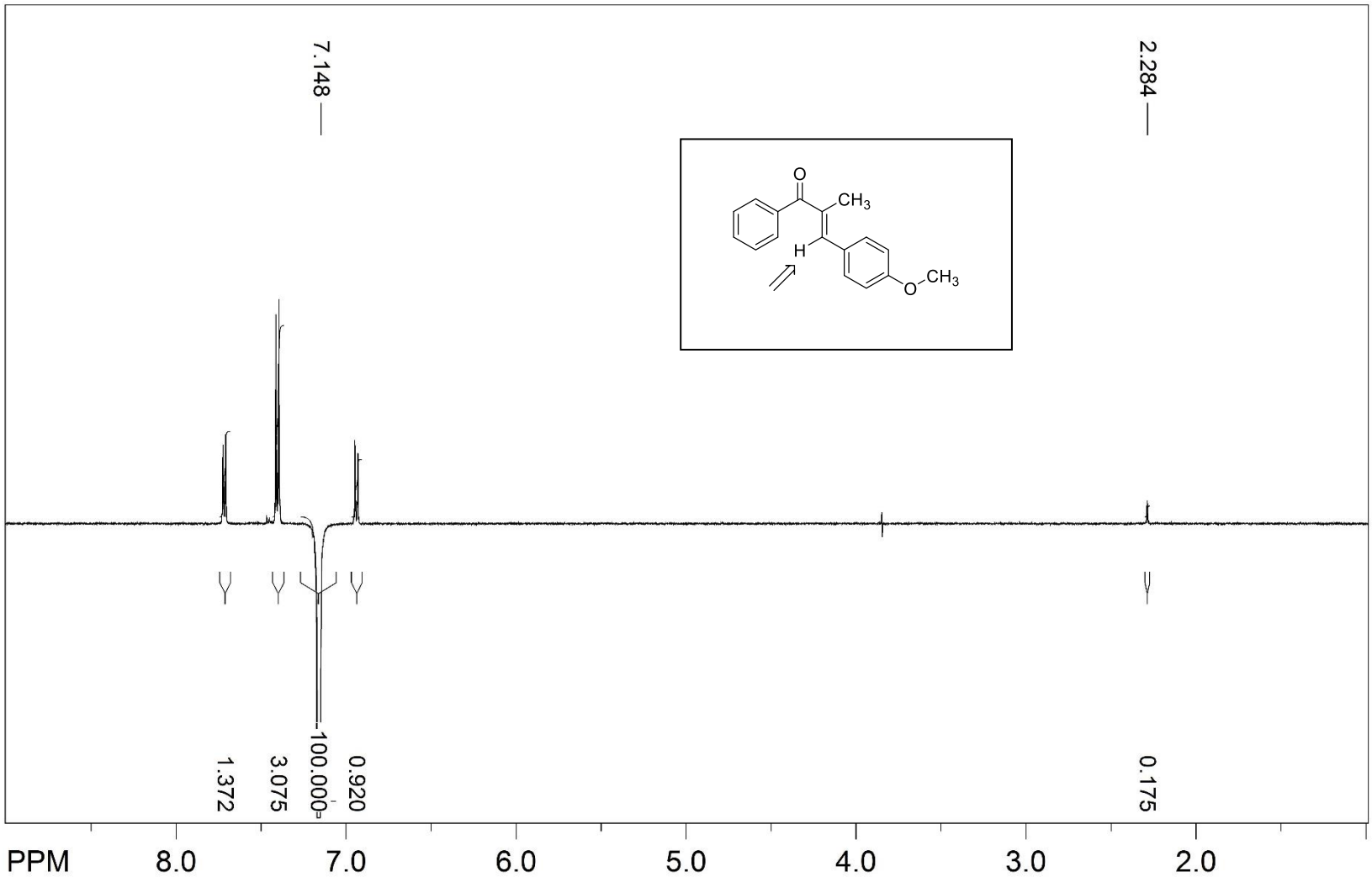

file: ...sers\chehal\Desktop\NKC 7_81\5/fid expt: <selnogp>
transmitter freq.: 500.133089 MHz
time domain size: 65536 points
width: 10000.00 Hz = 19.9947 ppm = 0.152588 Hz/pt
number of scans: 64

freq of 0 ppm: 500.130000 MHz
processed size: 65536 points
LB: 0.300 GF: 0.0000
Hz/cm: 160.466 ppm/cm: 0.32085

(2*Z*)-3-(4-Methoxyphenyl)-2-methyl-1-phenylprop-2-en-1-one (***Z*-179**) - NOE

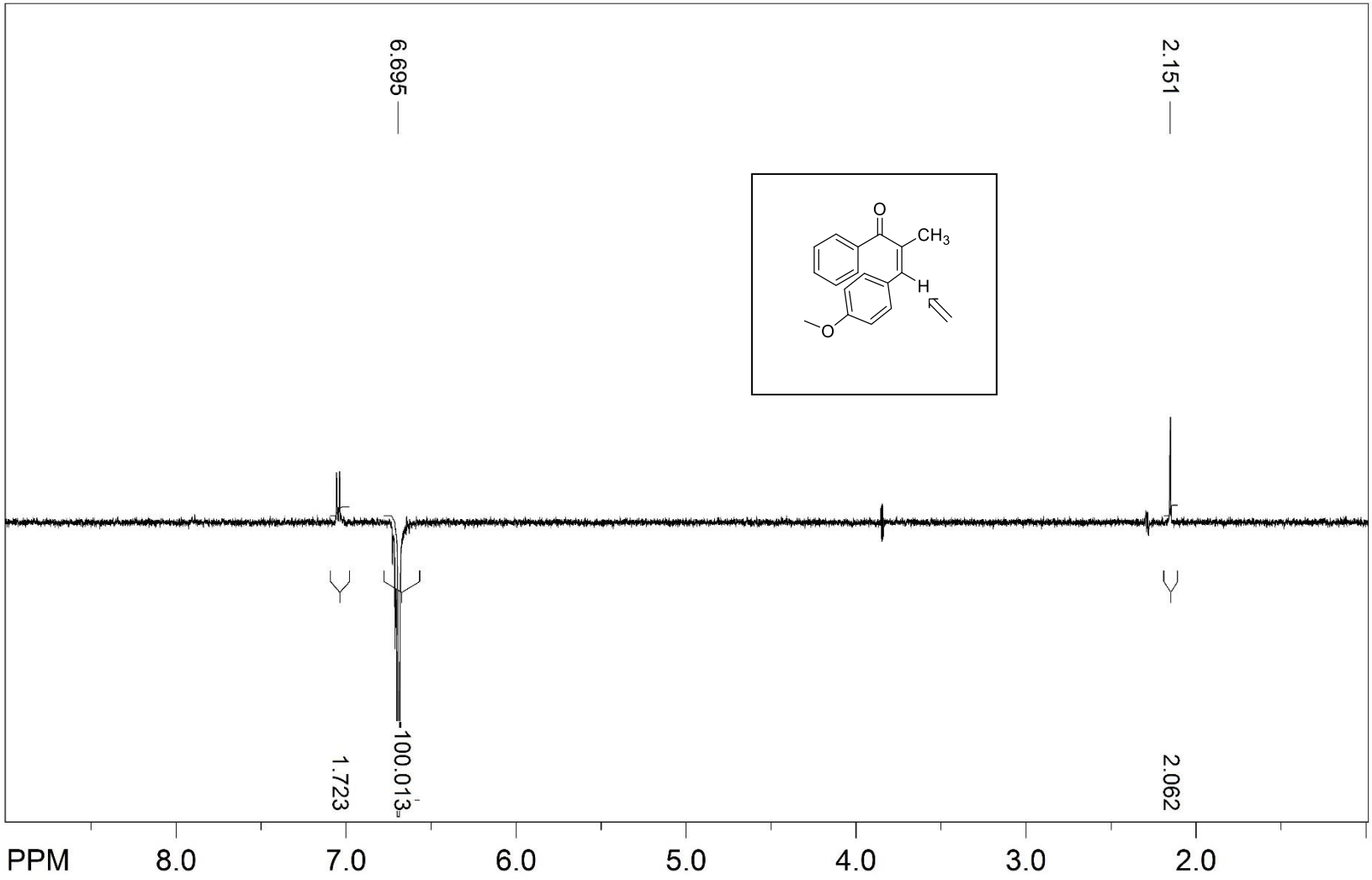

file: ...sers\chehal\Desktop\NKC 7 81\6/fid expt: <selnogp>
transmitter freq.: 500.133089 MHz
time domain size: 65536 points
width: 10000.00 Hz = 19.9947 ppm = 0.152588 Hz/pt
number of scans: 64

freq of 0 ppm: 500.130000 MHz
processed size: 65536 points
LB: 0.300 GF: 0.0000
Hz/cm: 160.466 ppm/cm: 0.32085

(2*E*)-3-(4-Methoxyphenyl)-2-methyl-1-phenylprop-2-en-1-one (***E*-179**) - NOE

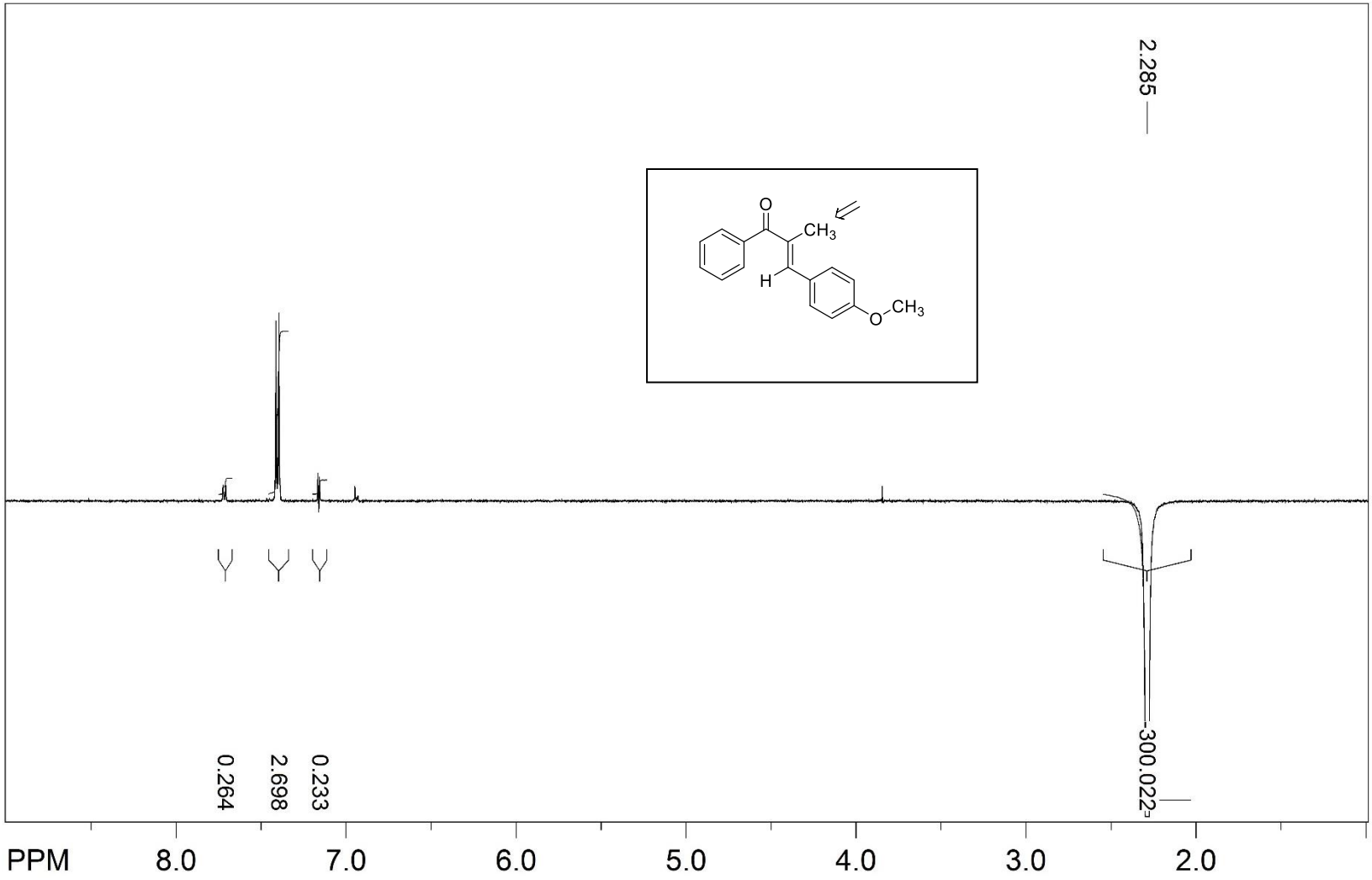

file: ...sers\chehal\Desktop\NKC 7 81\7/fid expt: <selnogp>
transmitter freq.: 500.133089 MHz
time domain size: 65536 points
width: 10000.00 Hz = 19.9947 ppm = 0.152588 Hz/pt
number of scans: 64

freq of 0 ppm: 500.130000 MHz
processed size: 65536 points
LB: 0.300 GF: 0.0000
Hz/cm: 160.466 ppm/cm: 0.32085

(2*Z*)-3-(4-Methoxyphenyl)-2-methyl-1-phenylprop-2-en-1-one (***Z*-179**) - NOE

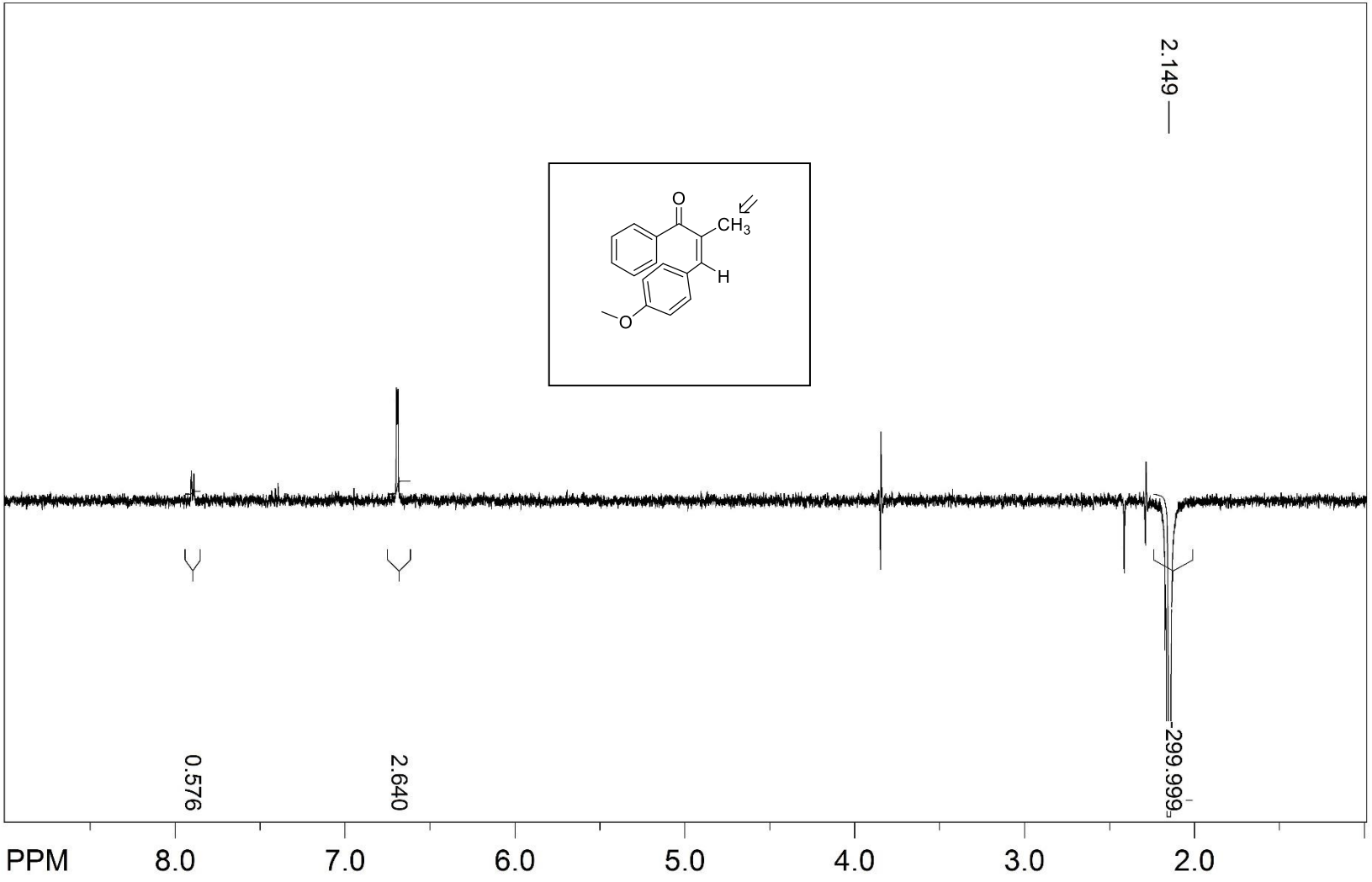

file: ...sers\chehal\Desktop\NKC 7 81\8/fid expt: <selnogp>
transmitter freq.: 500.133089 MHz
time domain size: 65536 points
width: 10000.00 Hz = 19.9947 ppm = 0.152588 Hz/pt
number of scans: 64

freq of 0 ppm: 500.130000 MHz
processed size: 65536 points
LB: 0.300 GF: 0.0000
Hz/cm: 160.466 ppm/cm: 0.32085

(2*Z*)-2,3-Dichloro-1-phenylprop-2-en-1-one (***Z*-1**) - ^{1}H NMR

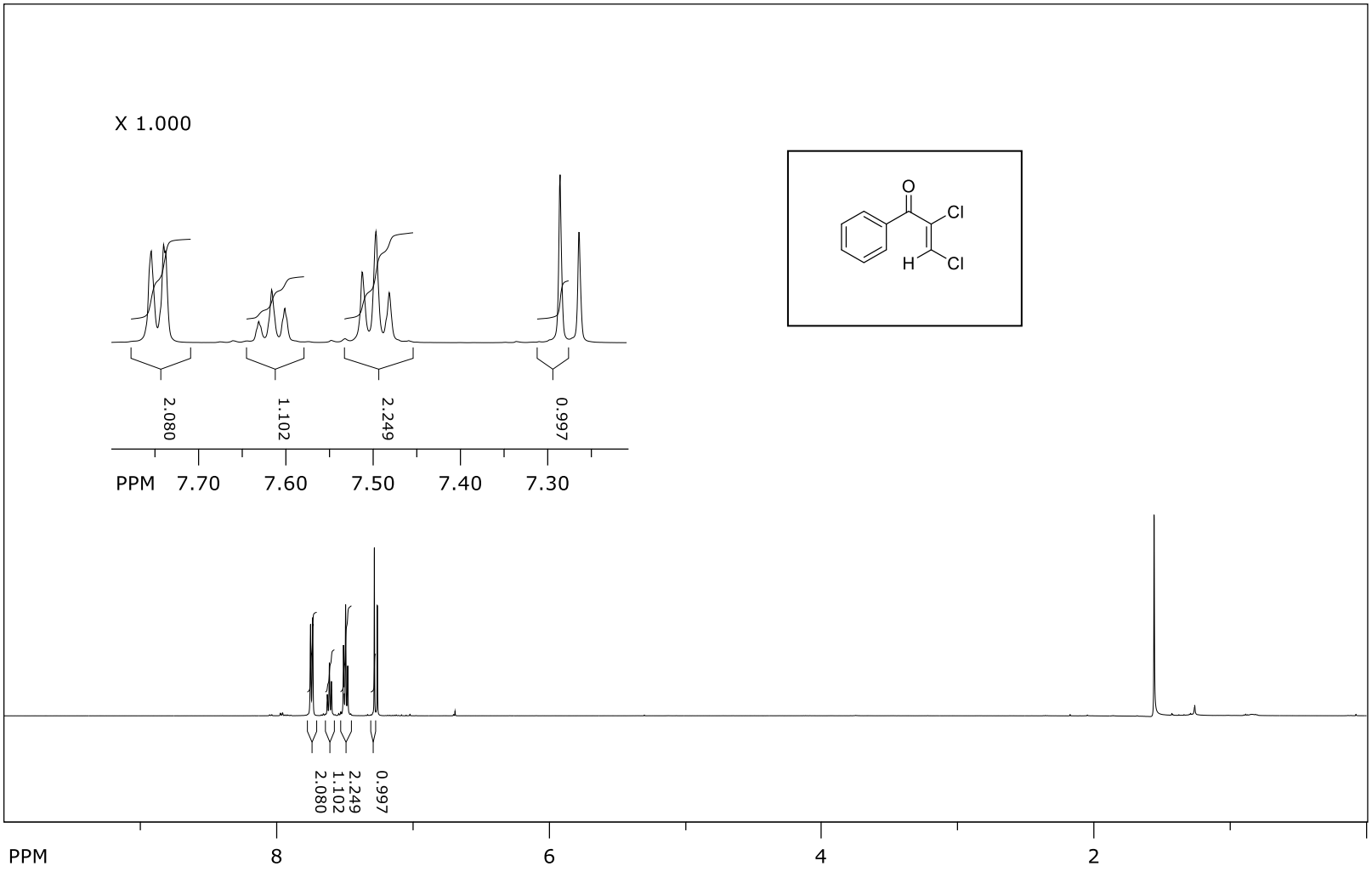

file: D:\nmr 500\NKC_10_cisisomer\1\fid expt: <zg30>
transmitter freq.: 500.133088 MHz
time domain size: 65536 points
width: 10000.00 Hz = 19.9947 ppm = 0.152588 Hz/pt
number of scans: 128

freq. of 0 ppm: 500.130000 MHz
processed size: 32768 complex points
LB: 0.300 GF: 0.0000

(2*Z*) -2,3-Dichloro-1-phenylprop-2-en-1-one (***Z*-1**) - ^{13}C NMR

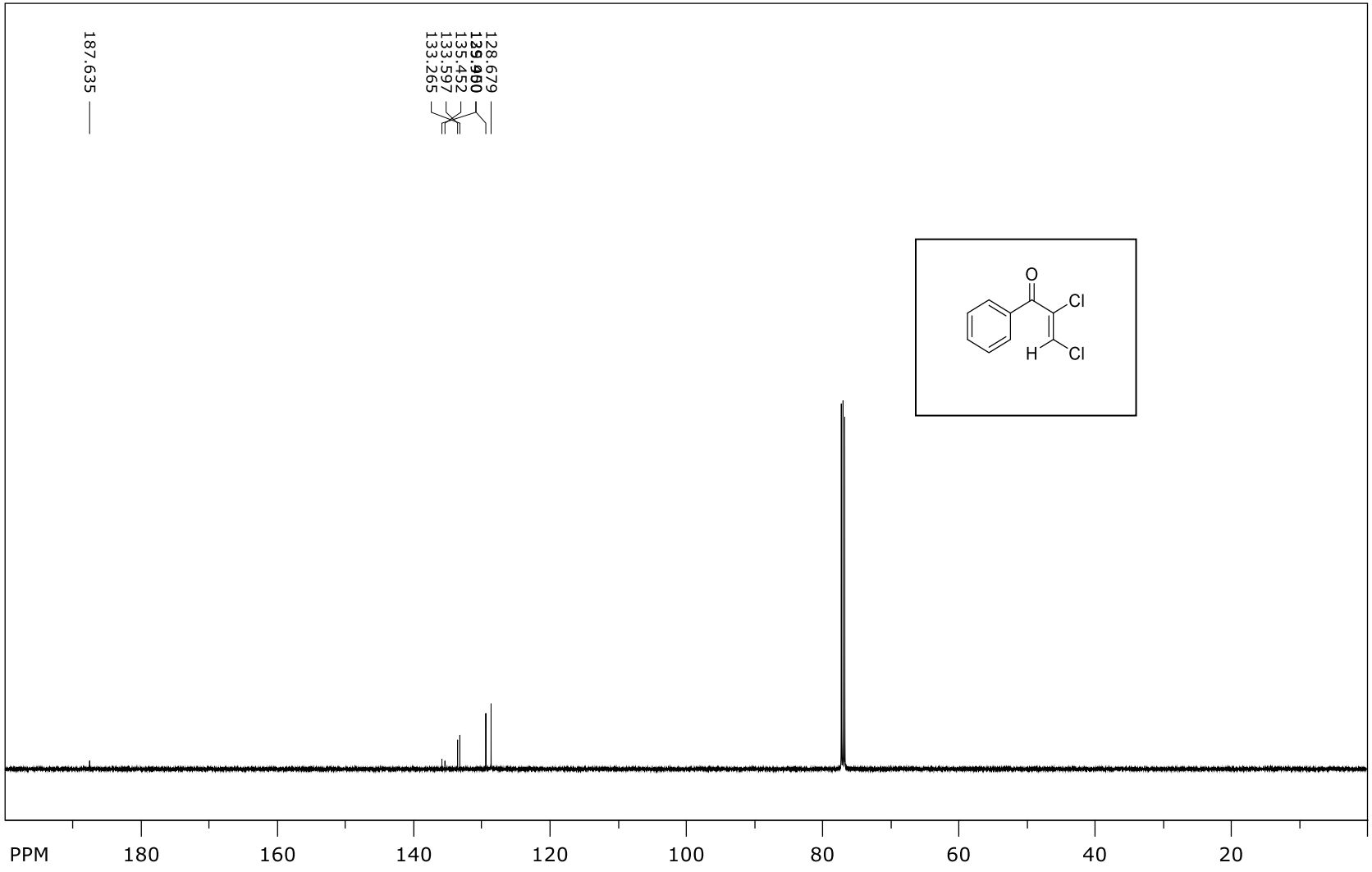

file: D:\nmr 500\NKC_10_cisisomer\2\fid expt: <zgpg30>
transmitter freq.: 125.770364 MHz
time domain size: 65536 points
width: 29761.90 Hz = 236.6369 ppm = 0.454131 Hz/pt
number of scans: 1024

freq. of 0 ppm: 125.757789 MHz
processed size: 32768 complex points
LB: 1.000 GF: 0.0000

(2*Z*)-2,3-Dichloro-1-phenylprop-2-en-1-one (***Z*-1**) - ^{13}C NMR

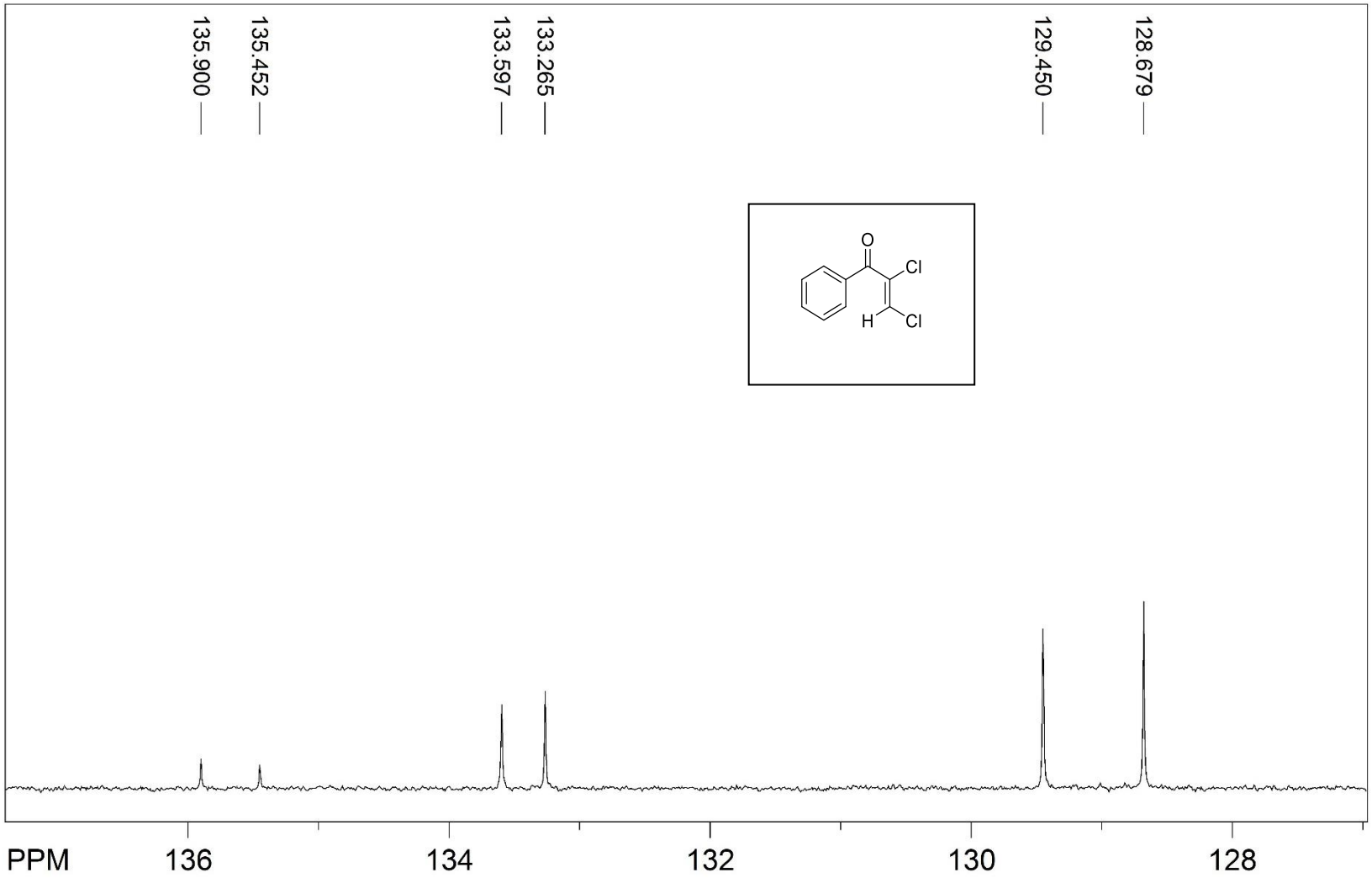

file: ...hal\Desktop\NKC 10 cisisomer\2\fid expt: <zgpg30>
transmitter freq.: 125.770364 MHz
time domain size: 65536 points
width: 29761.91 Hz = 236.6369 ppm = 0.454131 Hz/pt
number of scans: 1024

freq of 0 ppm: 125.757789 MHz
processed size: 32768 points
LB: 1.000 GF: 0.0000
Hz/cm: 52.509 ppm/cm: 0.41750

(2*Z*)-2,3-Dichloro-1-phenylprop-2-en-1-one (***Z*-1**) - $^{3}J_{C,H}$

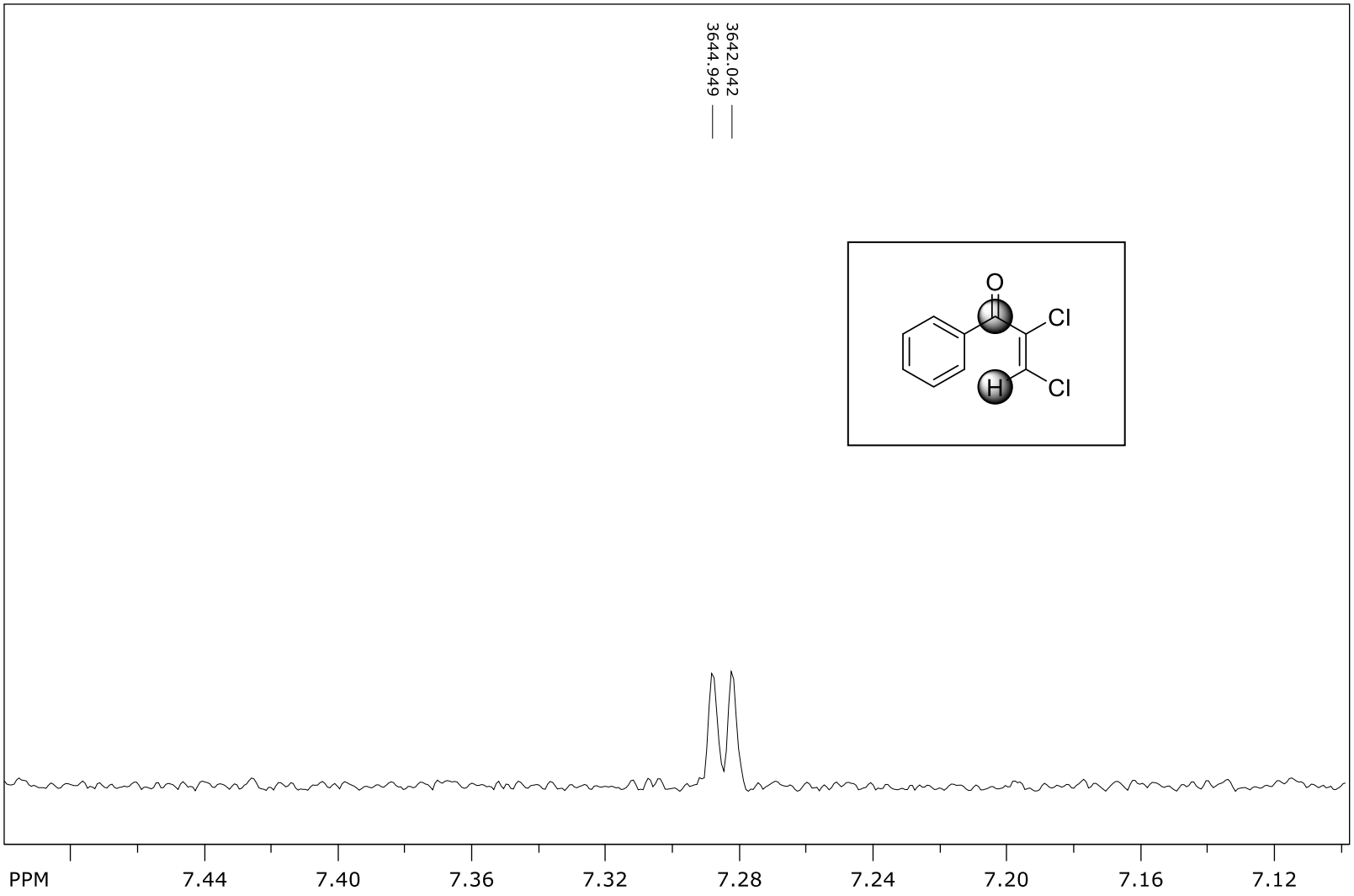

file: D:\nmr 500\NKC_10_cisisomer\6\ser expt: <hmbcgplpndqf>
transmitter freq.: 500.133651 MHz
time domain size: 4096 points
width: 1500.60 Hz = 3.0004 ppm = 0.366357 Hz/pt
number of scans: 4

freq. of 0 ppm: 500.130000 MHz
processed size: 4096 complex points
LB: 0.000 GF: 0.0000

(*E*)-2-Chloro-3-(4-methoxyphenyl)-1-phenylprop-2-en-1-one (***E*-2**) – ^{1}H NMR

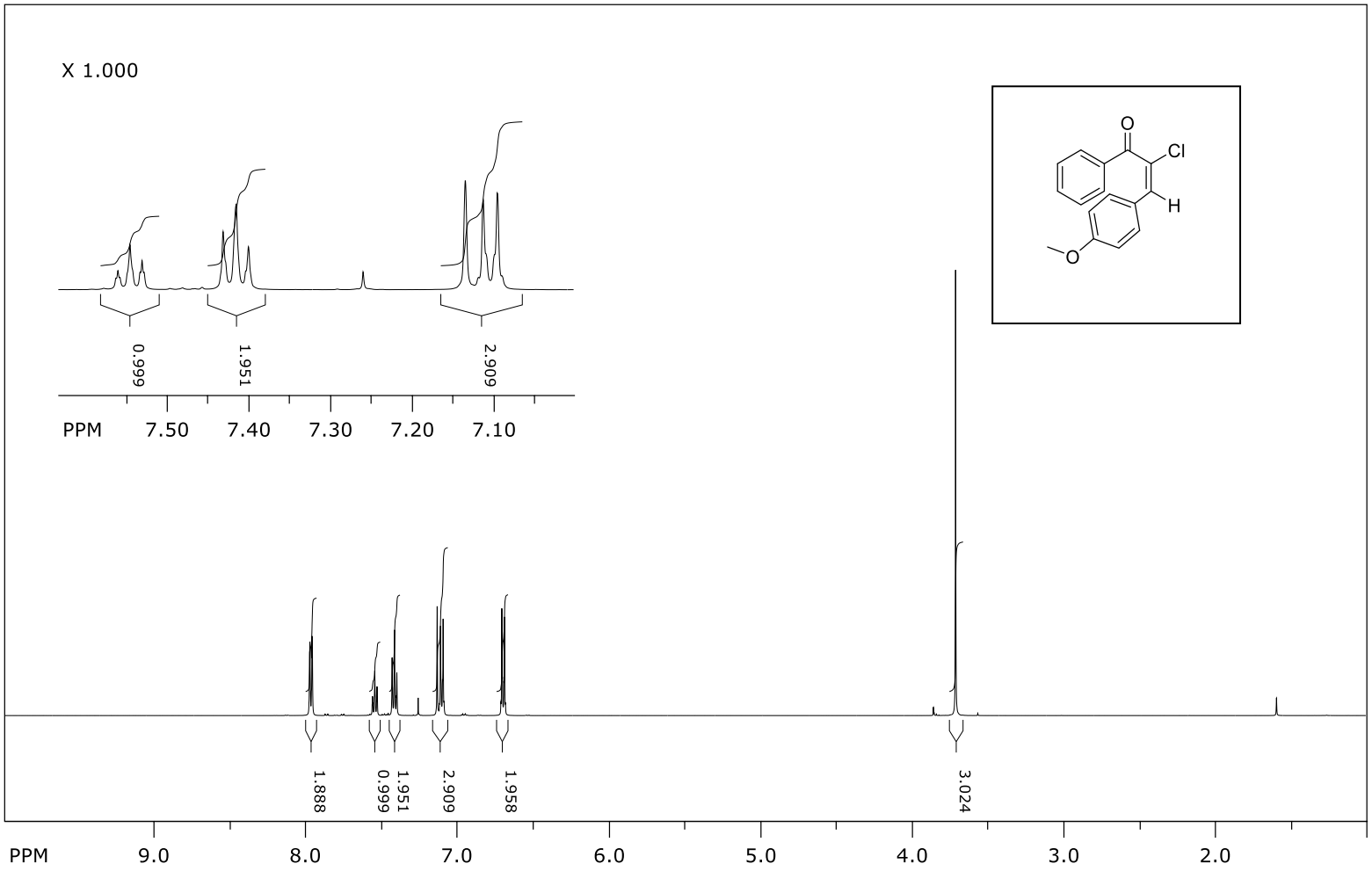

file: D:\nmr 500\NKC_8_44_F6-14\1\fid expt: <zg30>
transmitter freq.: 500.133089 MHz
time domain size: 65536 points
width: 10000.00 Hz = 19.9947 ppm = 0.152588 Hz/pt
number of scans: 16

freq. of 0 ppm: 500.130002 MHz
processed size: 65536 complex points
LB: 0.300 GF: 0.0000

(*E*)-2-Chloro-3-(4-methoxyphenyl)-1-phenylprop-2-en-1-one (***E*-2**) – ^{13}C NMR

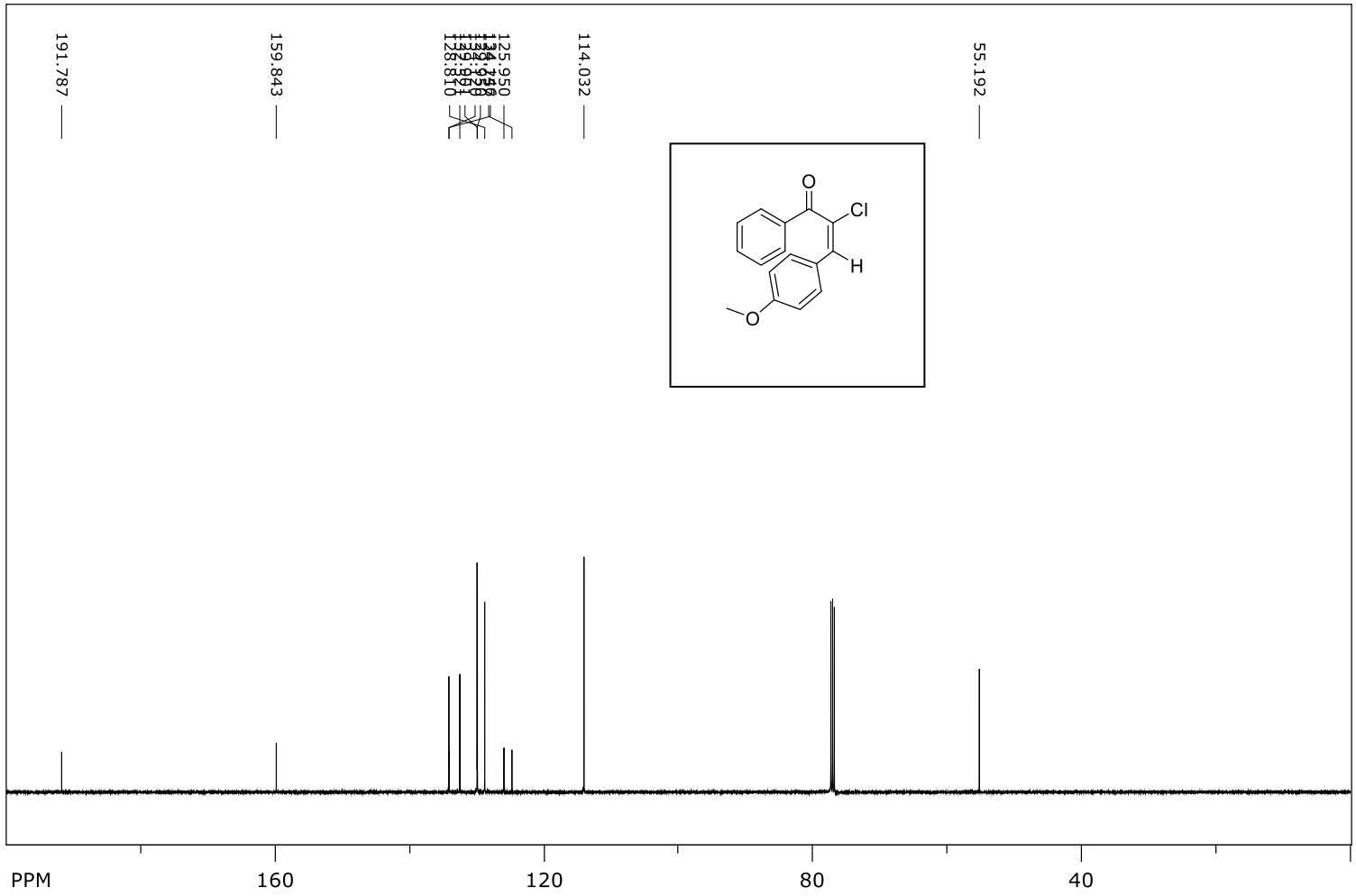

file: D:\nmr 500\NKC_8_44_F6-14\3\fid expt: <zgpg30>
transmitter freq.: 125.770364 MHz
time domain size: 65536 points
width: 29761.90 Hz = 236.6369 ppm = 0.454131 Hz/pt
number of scans: 1024

freq. of 0 ppm: 125.757789 MHz
processed size: 32768 complex points
LB: 1.000 GF: 0.0000

(*E*)-2-Chloro-3-(4-methoxyphenyl)-1-phenylprop-2-en-1-one (***E*-2**) – ^{13}C NMR (zoomed)

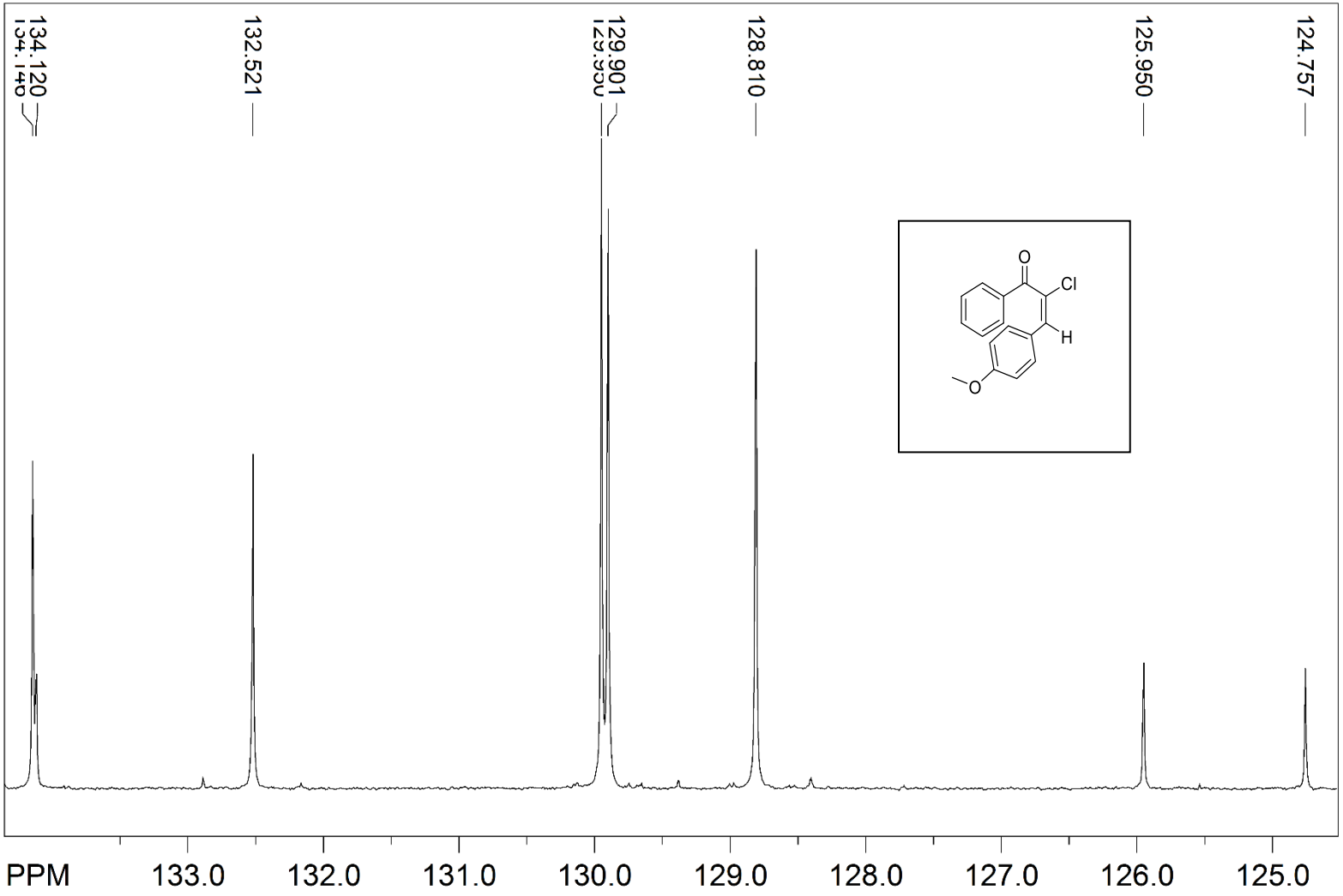

file: ...ktop\NMR data\NKC 8 44 F6-14\3\fid expt: <zgpg30>
transmitter freq.: 125.770364 MHz
time domain size: 65536 points
width: 29761.90 Hz = 236.6369 ppm = 0.454131 Hz/pt
number of scans: 1024

freq of 0 ppm: 125.757789 MHz
processed size: 32768 points
LB: 1.000 GF: 0.0000
Hz/cm: 51.547 ppm/cm: 0.40985

(*E*)-2-Chloro-3-(4-methoxyphenyl)-1-phenylprop-2-en-1-one (***E*-2**) - $^{3}J_{C,H}$

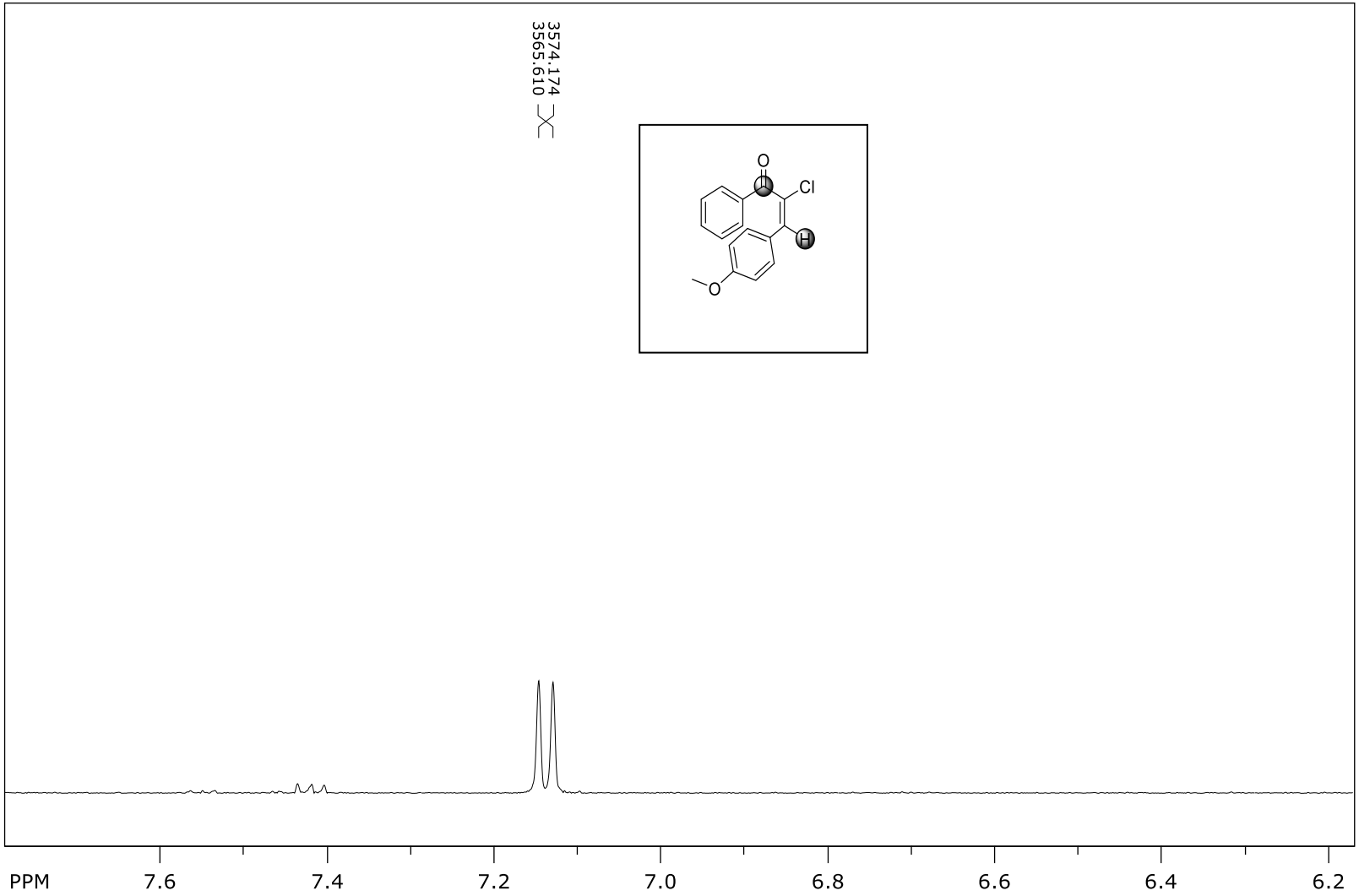

file: D:\nmr 500\NKC_8_44_F6-14\2\ser expt: <hmbcgplpndqf>
transmitter freq.: 500.132201 MHz
time domain size: 8192 points
width: 4000.00 Hz = 7.9979 ppm = 0.488281 Hz/pt
number of scans: 8

freq. of 0 ppm: 500.130000 MHz
processed size: 16384 complex points
LB: 0.000 GF: 0.0000

(*E*)-2-Chloro-3-(phenyl)-1-phenylprop-2-en-1-one (***E*-199**) – ^{1}H NMR

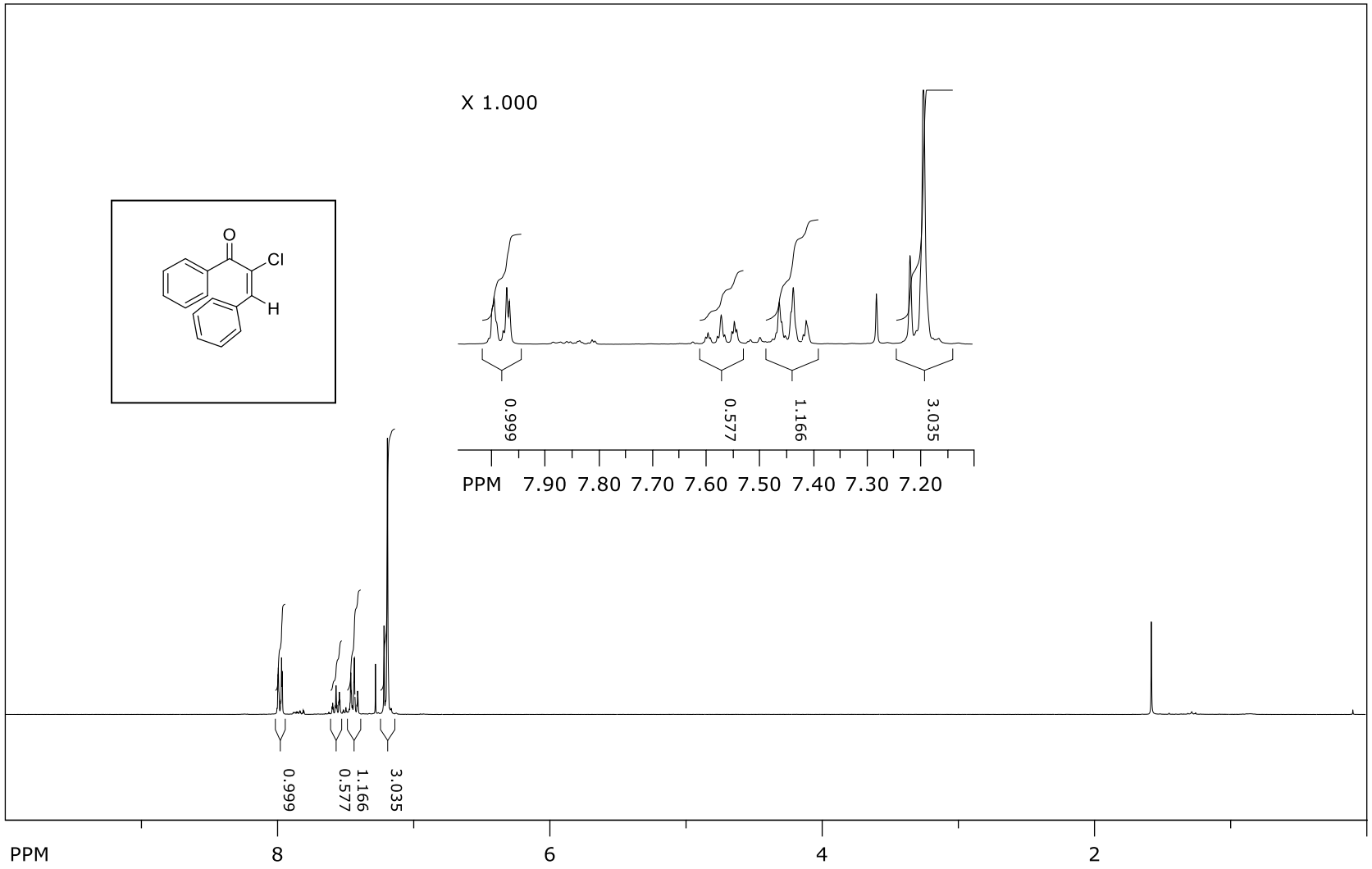

file: D:\NKC_10_phenyltrans\1\fid expt: <zg30>
transmitter freq.: 300.131853 MHz
time domain size: 65536 points

freq. of 0 ppm: 300.130006 MHz
processed size: 32768 complex points
LB: 0.300 GF: 0.0000

(*E*)-2-Chloro-3-(phenyl)-1-phenylprop-2-en-1-one (***E*-199**) – ^{13}C NMR

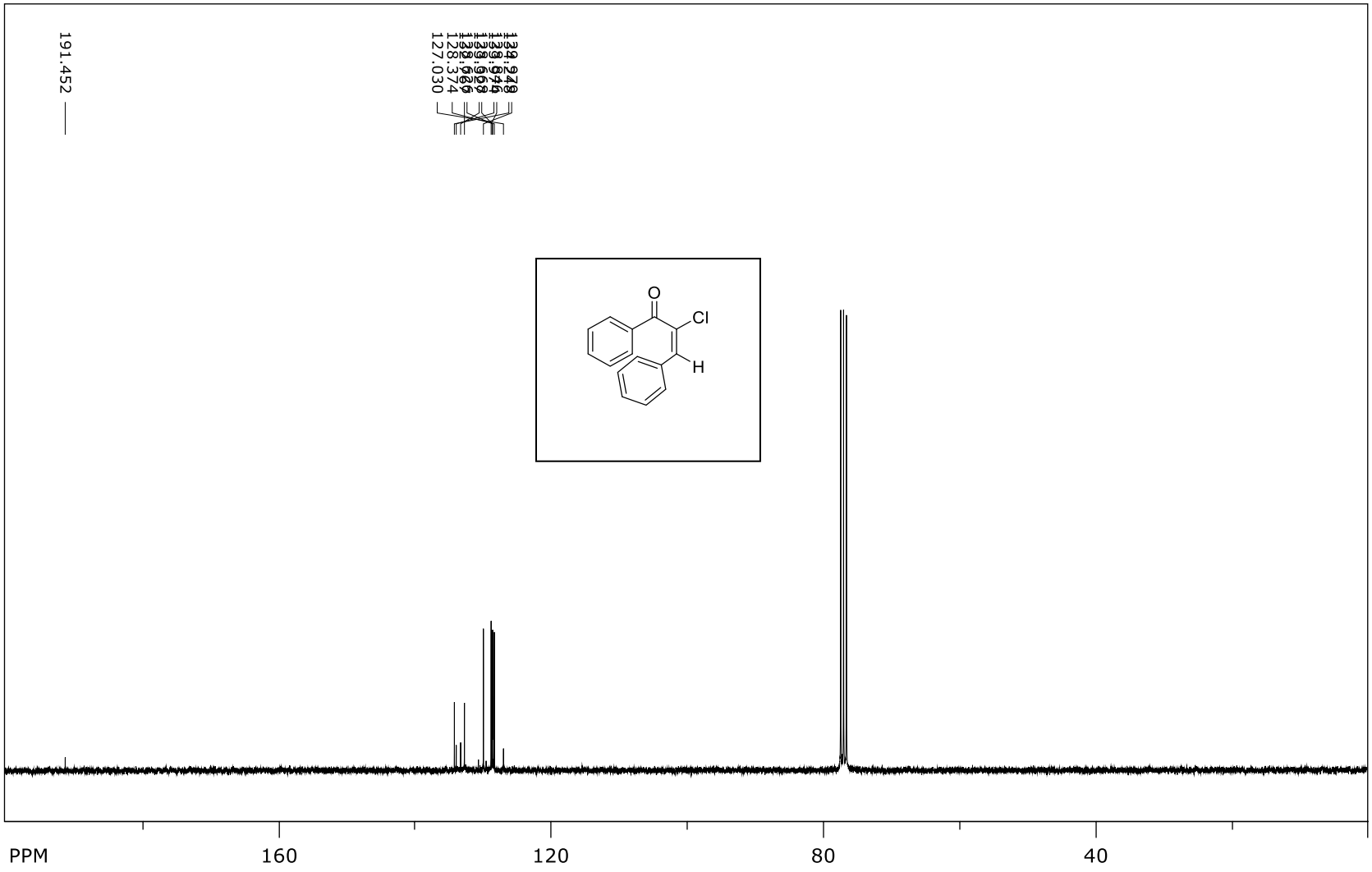

file: D:\NKC_10_phenyltrans\2\fid expt: <zgpg30>
transmitter freq.: 75.475295 MHz
time domain size: 65536 points
width: 17985.61 Hz = 238.2980 ppm = 0.274439 Hz/pt
number of scans: 1024

freq. of 0 ppm: 75.467749 MHz
processed size: 32768 complex points
LB: 1.000 GF: 0.0000

(*E*)-2-Chloro-3-(phenyl)-1-phenylprop-2-en-1-one (***E*-199**) – $^{3}J_{C,H}$

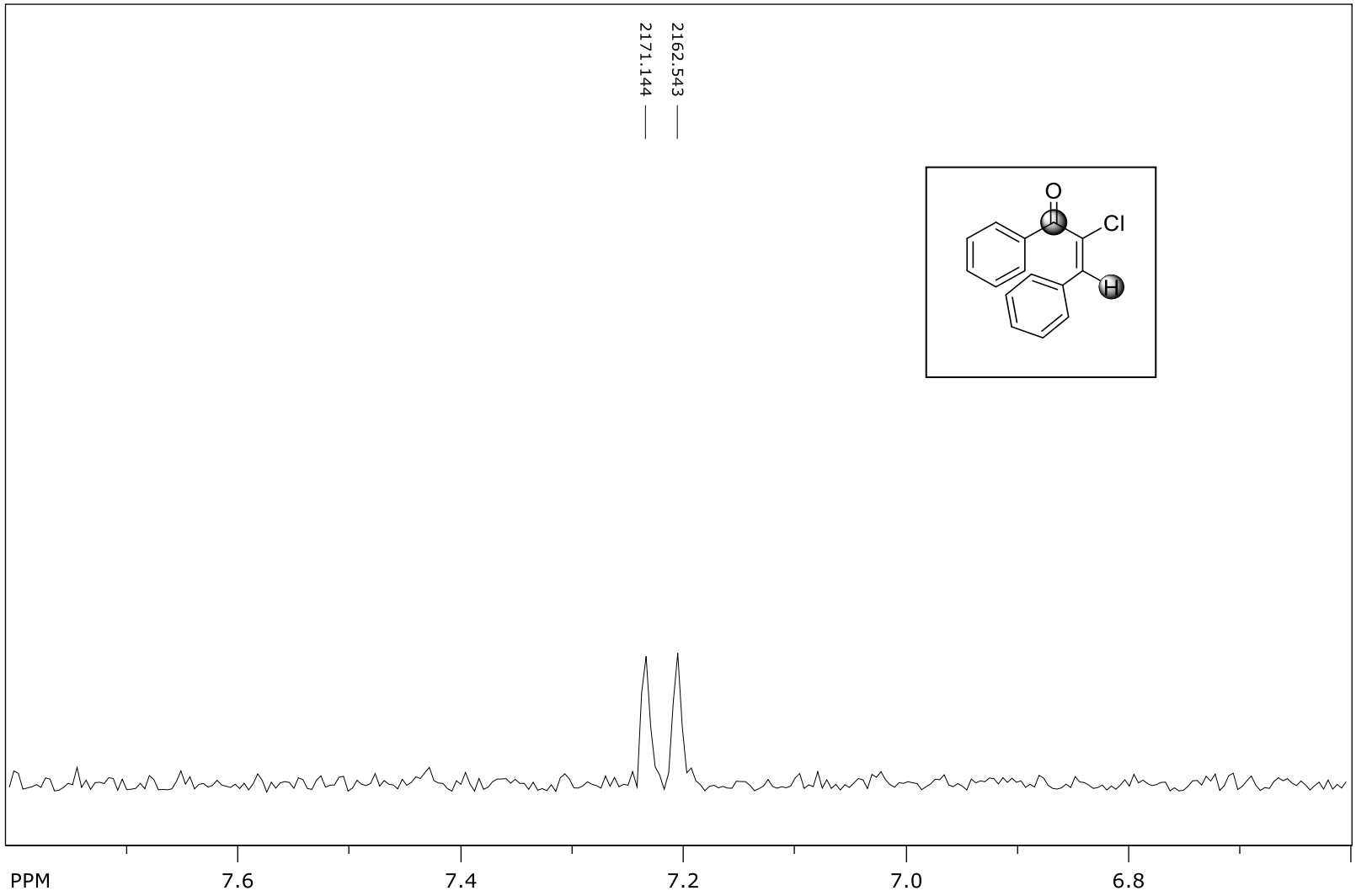

file: D:\NKC_10_phenyltrans\7\ser expt: <hmbcgplpndqf>
transmitter freq.: 300.131346 MHz
time domain size: 4096 points
width: 2495.01 Hz = 8.3131 ppm = 0.609133 Hz/pt
number of scans: 8

freq. of 0 ppm: 300.130006 MHz
processed size: 2048 complex points
LB: 0.000 GF: 0.0000

(*E*)-2-Chloro-3-(4-methylphenyl)-1-phenylprop-2-en-1-one (***E*-198**) - ^{1}H NMR

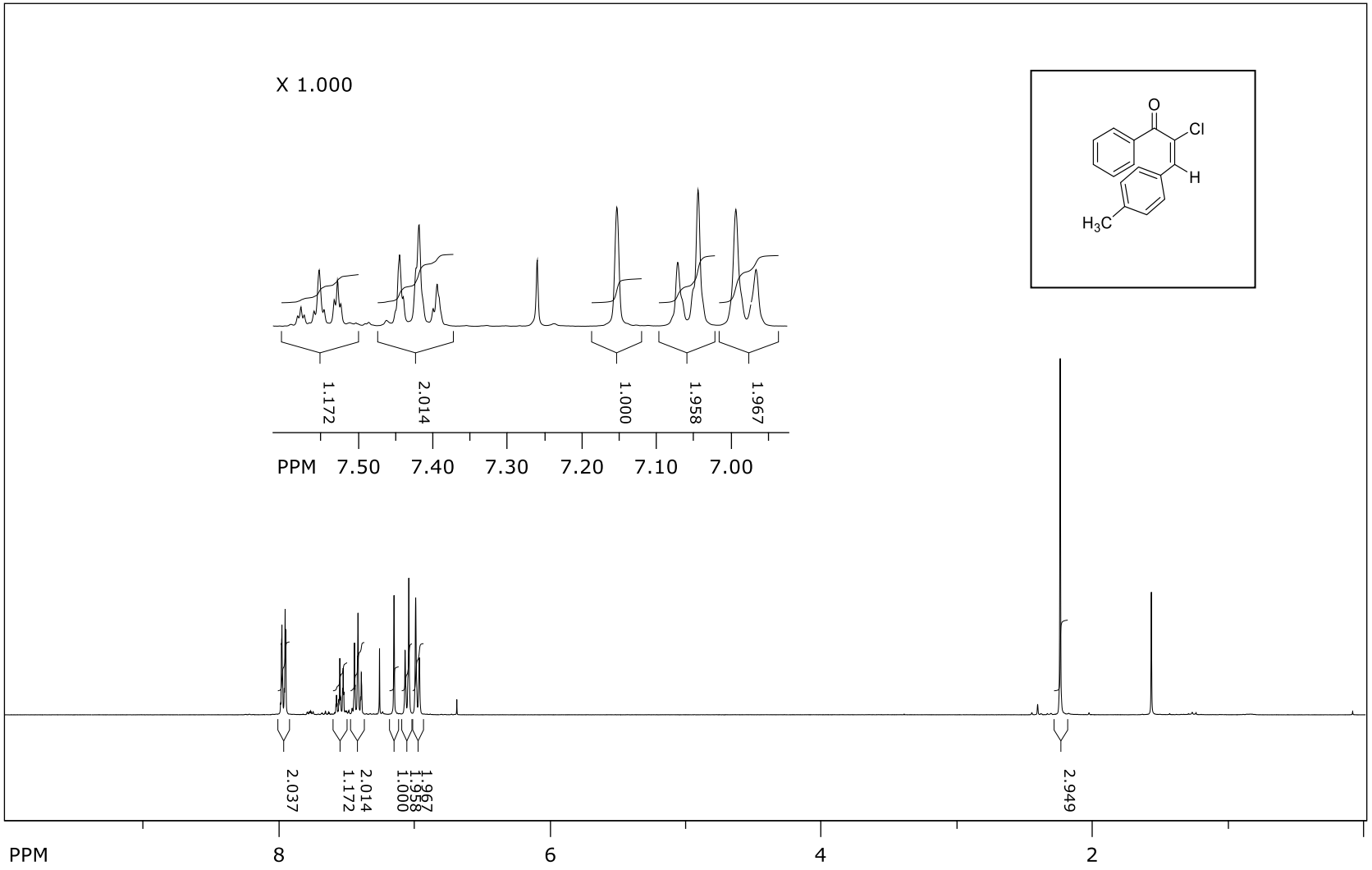

file: D:\NKC_10_methylphenyltrans\1\fid expt: <zg30>
transmitter freq.: 300.131853 MHz
time domain size: 65536 points
width: 6172.84 Hz = 20.5671 ppm = 0.094190 Hz/pt
number of scans: 16

freq. of 0 ppm: 300.130012 MHz
processed size: 32768 complex points
LB: 0.300 GF: 0.0000

(*E*)-2-Chloro-3-(4-methylphenyl)-1-phenylprop-2-en-1-one (***E*-198**)- ^{13}C NMR

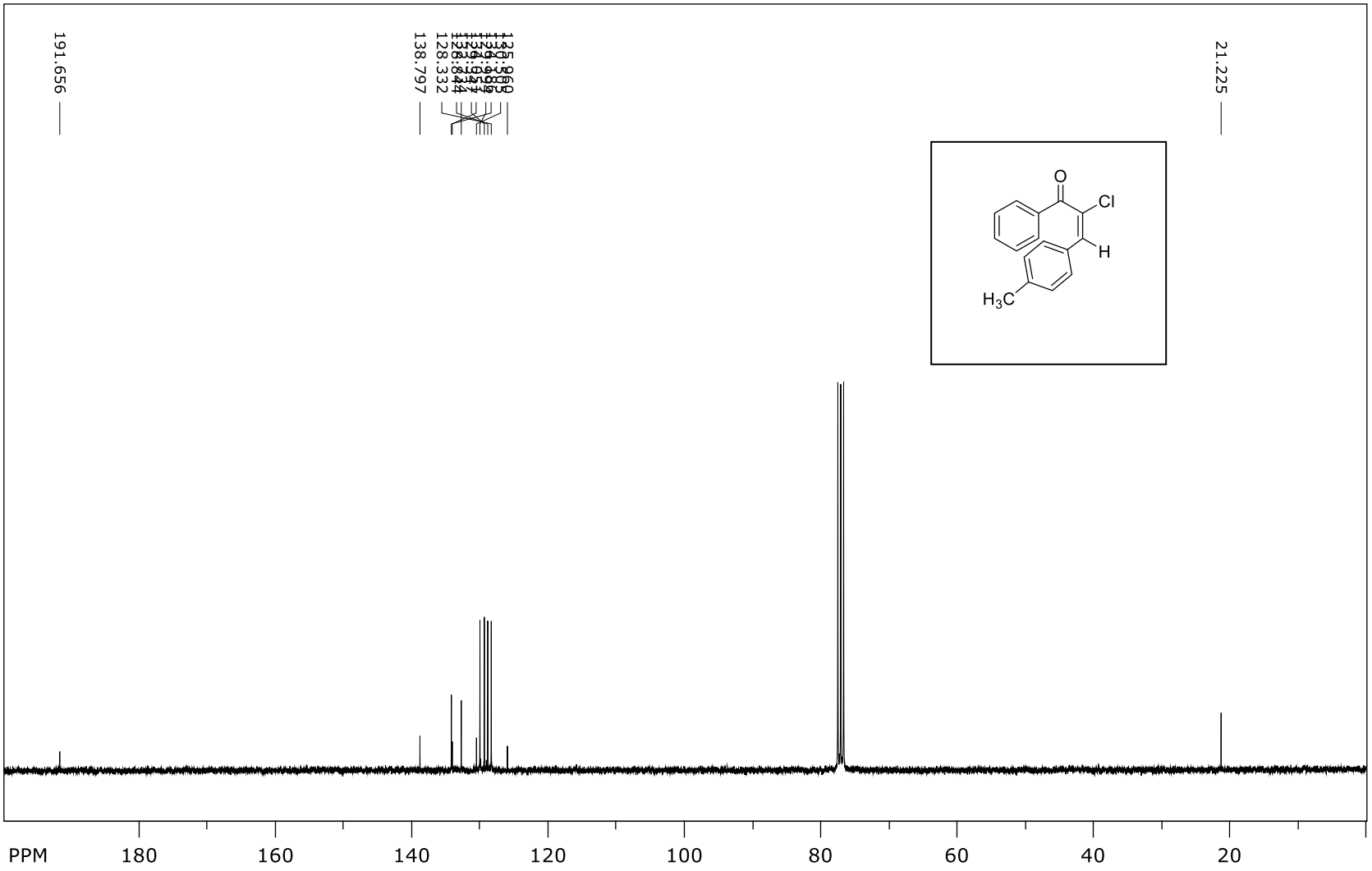

file: D:\NKC_10_methylphenyltrans\2\fid expt: <zgpg30>
transmitter freq.: 75.475295 MHz
time domain size: 65536 points
width: 17985.61 Hz = 238.2980 ppm = 0.274439 Hz/pt
number of scans: 1024

freq. of 0 ppm: 75.467749 MHz
processed size: 32768 complex points
LB: 1.000 GF: 0.0000

(*E*)-2-Chloro-3-(4-methylphenyl)-1-phenylprop-2-en-1-one (***E*-198**) - $^{3}J_{C,H}$

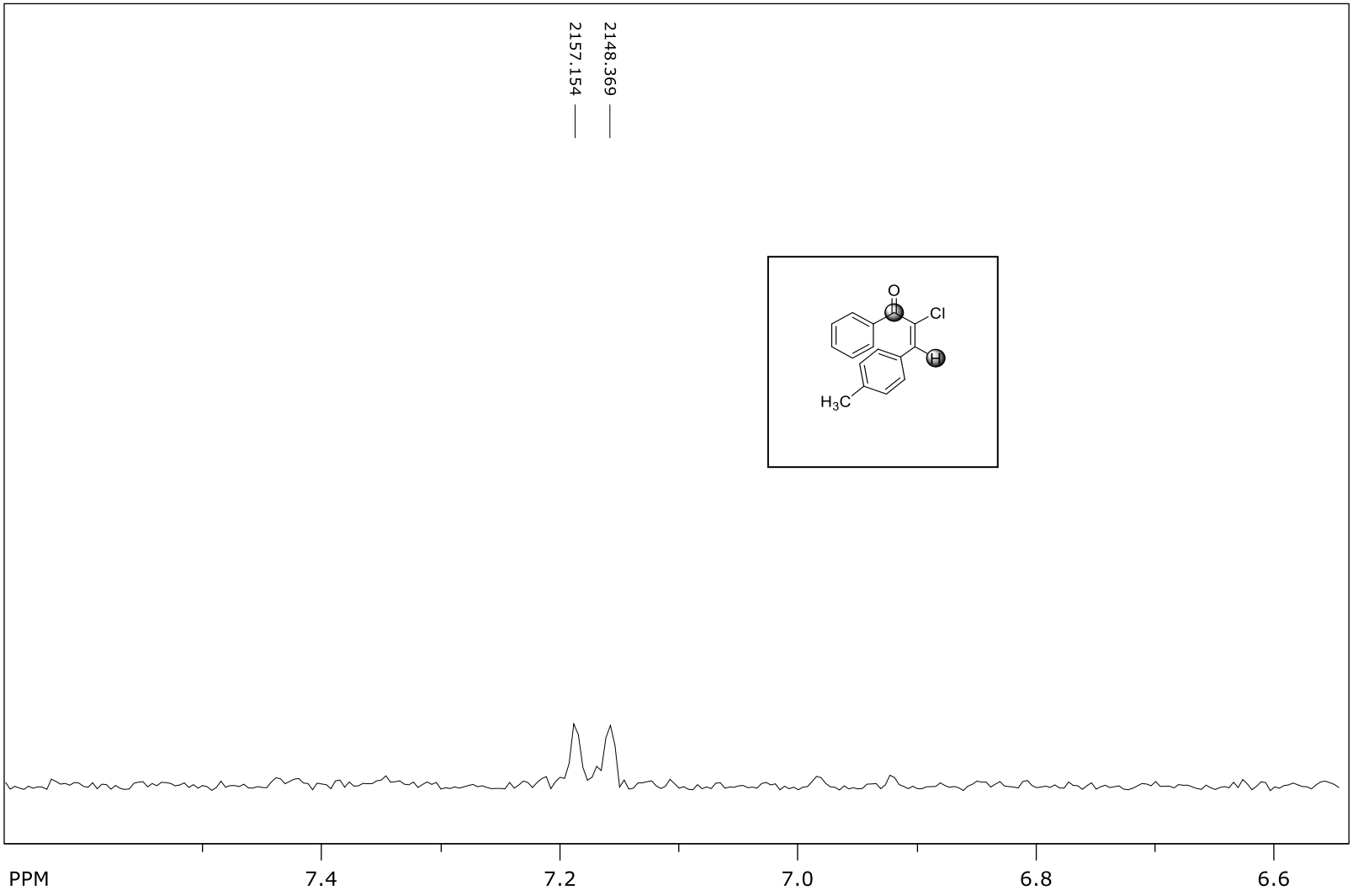

file: D:\NKC_10_methylphenyltrans\8\ser expt: <hmbcgplpndqf>
transmitter freq.: 300.131409 MHz
time domain size: 4096 points
width: 2367.42 Hz = 7.8880 ppm = 0.577984 Hz/pt
number of scans: 8

freq. of 0 ppm: 300.130006 MHz
processed size: 2048 complex points
LB: 0.000 GF: 0.0000

(2*E*)-2-Chloro-1-phenyl-3-(thiophen-2-yl)prop-2-en-1-one (***E*-203**) - ^{1}H NMR

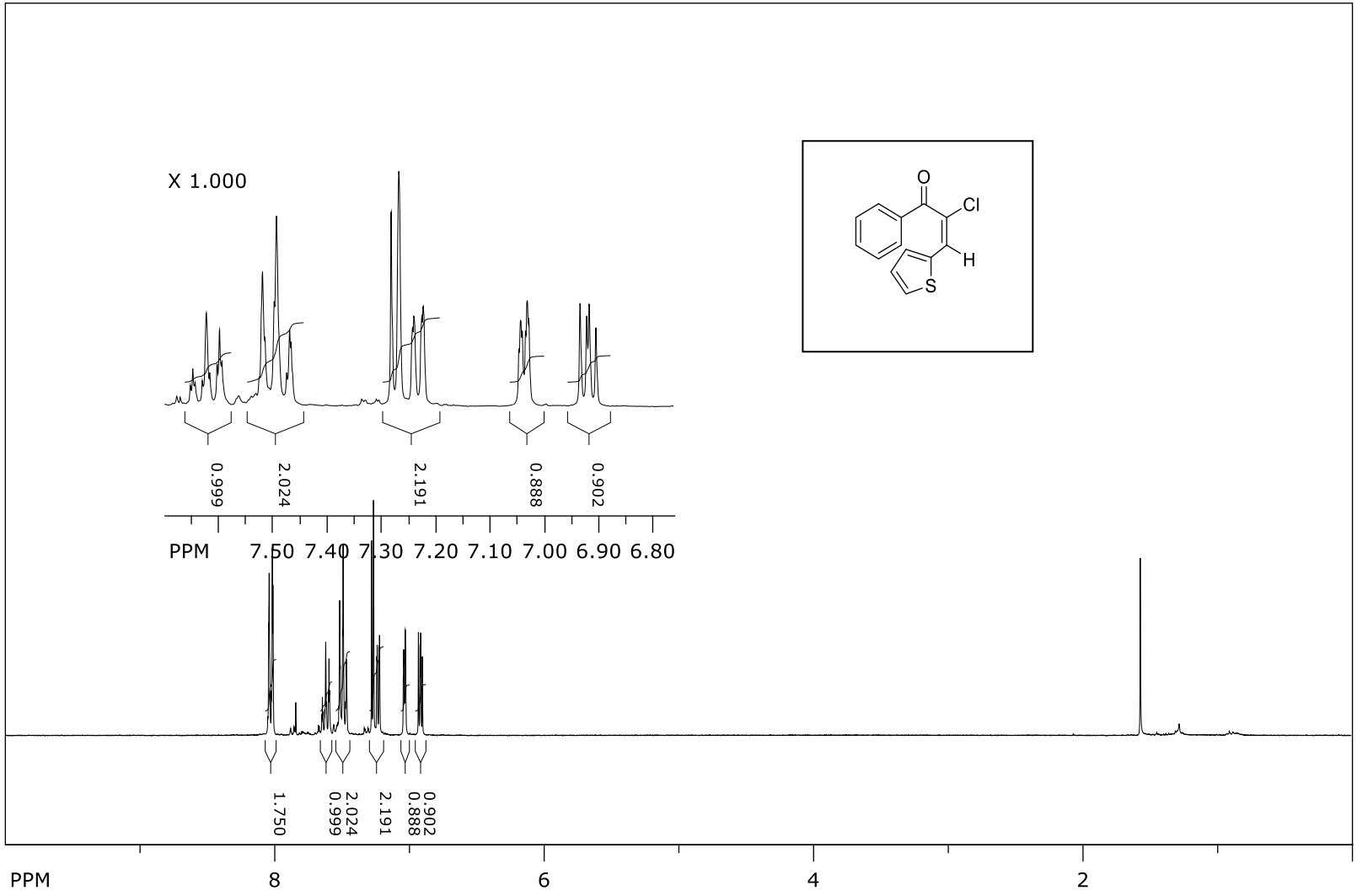

file: D:\NKC_10_48_thienyl_trans\1\fid expt: <zg30>
transmitter freq.: 300.131853 MHz
time domain size: 65536 points
width: 6172.84 Hz = 20.5671 ppm = 0.094190 Hz/pt
number of scans: 16

freq. of 0 ppm: 300.130006 MHz
processed size: 32768 complex points
LB: 0.300 GF: 0.0000

(2*E*)-2-Chloro-1-phenyl-3-(thiophen-2-yl)prop-2-en-1-one (***E*-203**) – ^{13}C NMR

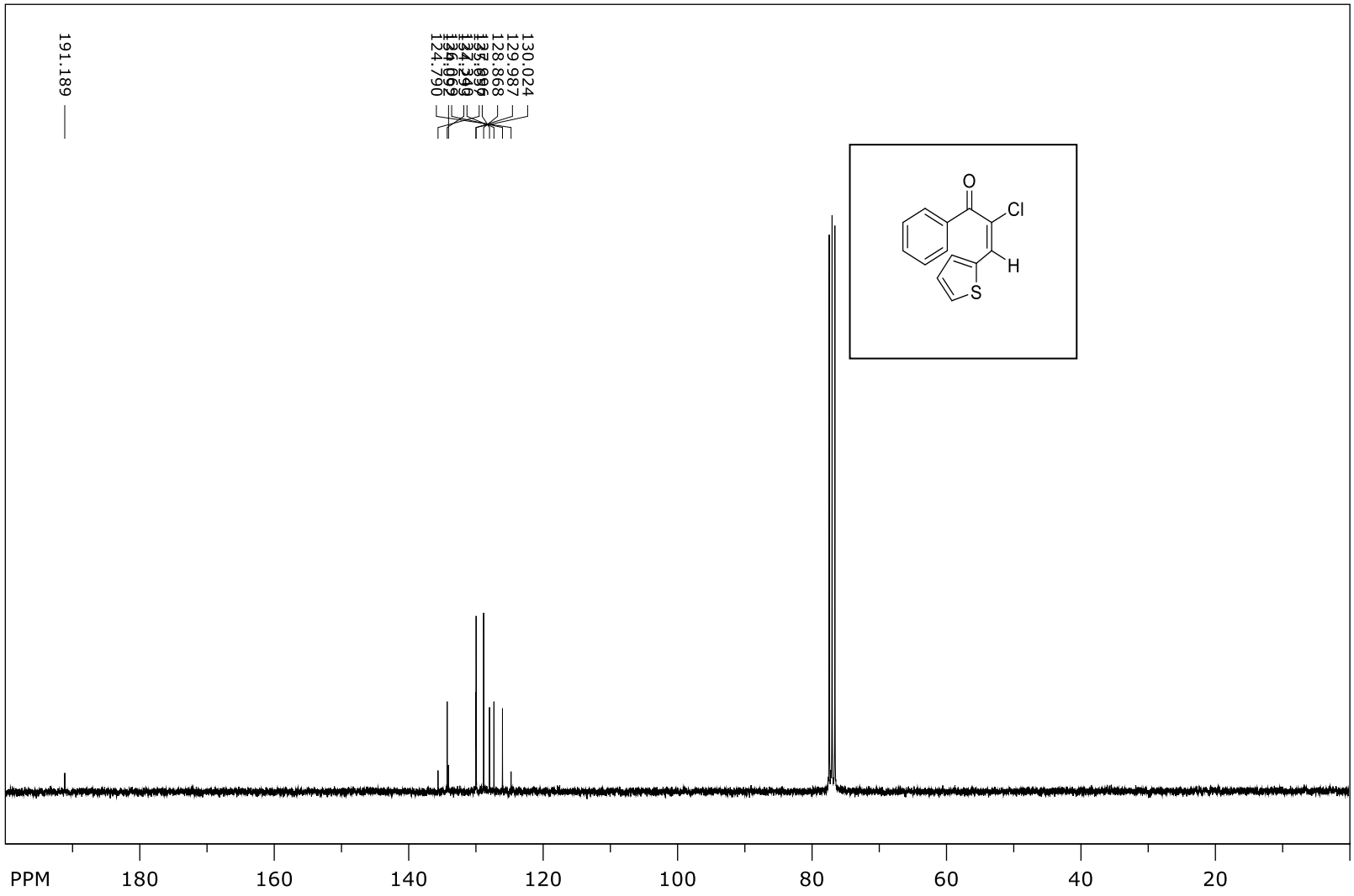

file: D:\NKC_10_48_thienyl_trans\3\fid expt: <zgpg30>
transmitter freq.: 75.475295 MHz
time domain size: 65536 points
width: 17985.61 Hz = 238.2980 ppm = 0.274439 Hz/pt

freq. of 0 ppm: 75.467749 MHz
processed size: 32768 complex points
LB: 1.000 GF: 0.0000

(2*E*)-2-Chloro-1-phenyl-3-(thiophen-2-yl)prop-2-en-1-one (***E*-203**) - $^{3}J_{C,H}$

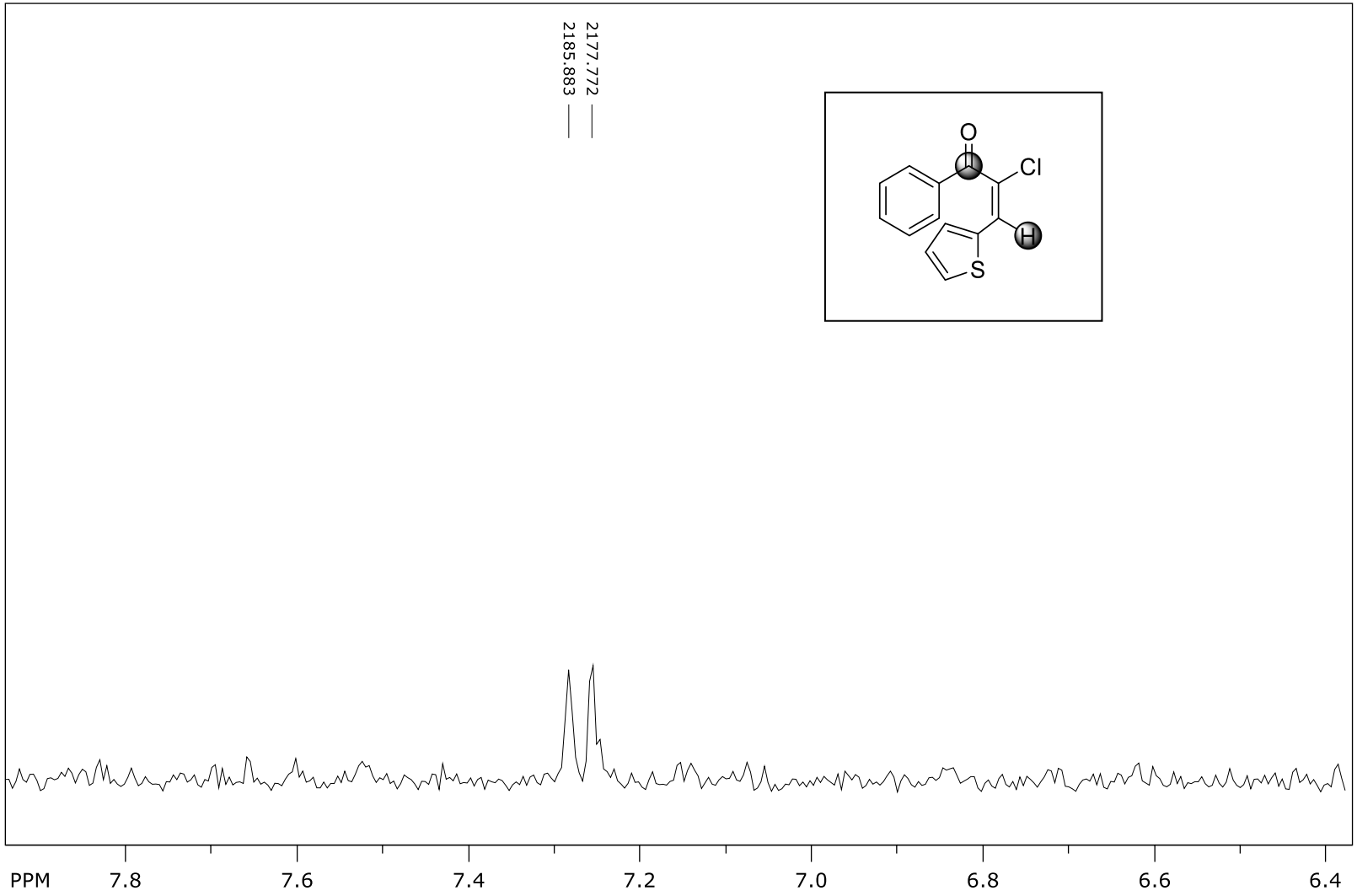

file: ... 300\NKC_10_48_thienyl_trans\8\ser expt: <hmbcgplpndqf>
transmitter freq.: 300.131355 MHz
time domain size: 4096 points
width: 2510.04 Hz = 8.3631 ppm = 0.612803 Hz/pt
number of scans: 8

freq. of 0 ppm: 300.130006 MHz
processed size: 2048 complex points
LB: 0.000 GF: 0.0000

(2*E*)-3-(Benzofuran-2-yl)-2-chloro-1-phenylprop-2-en-1-one (***E*-202)** - ^{1}H NMR

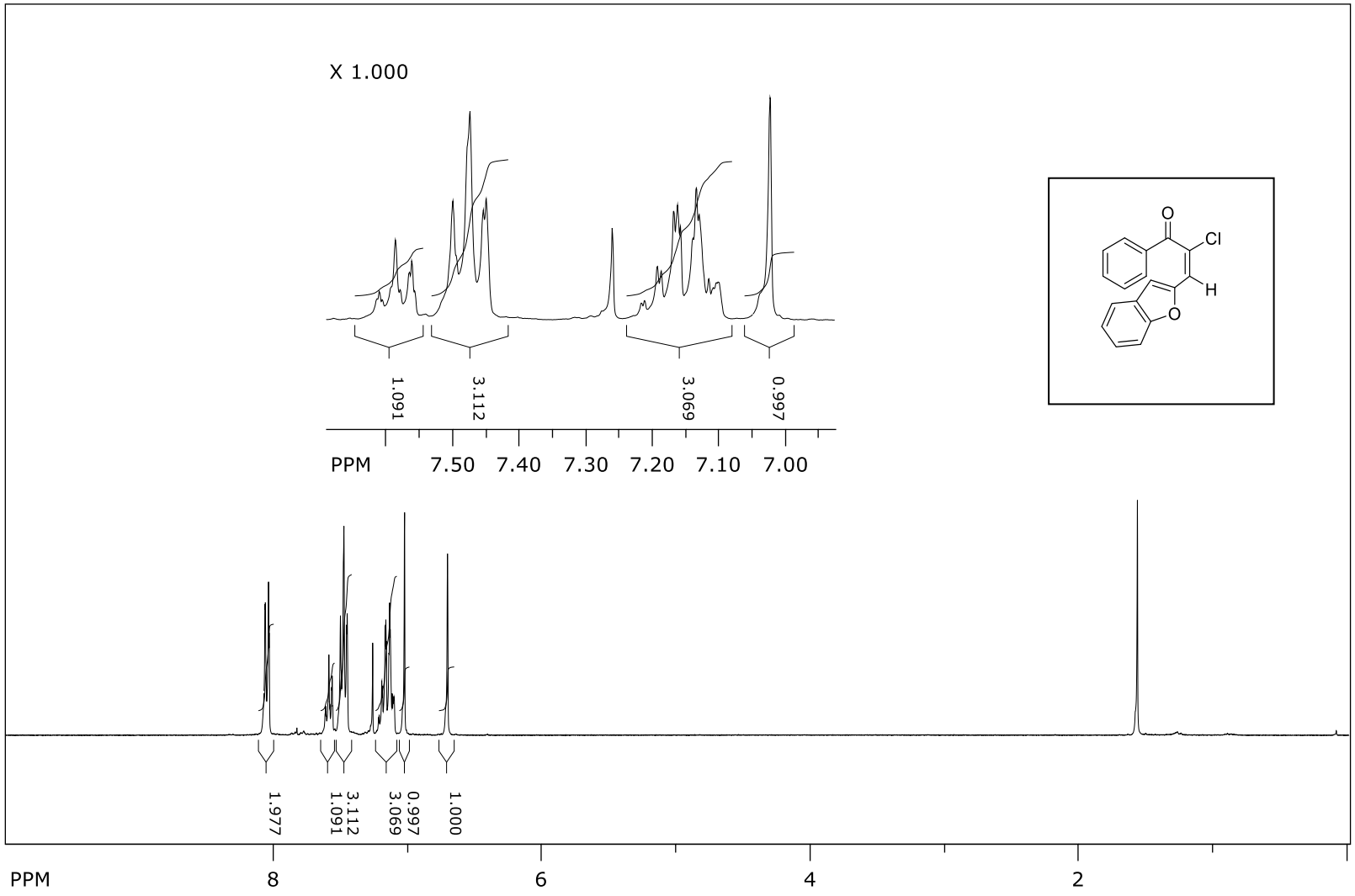

file: ...:\NMR 300\NKC_10_45_bdftrans\1\fid expt: <zg30>
transmitter freq.: 300.131853 MHz
time domain size: 65536 points
width: 6172.84 Hz = 20.5671 ppm = 0.094190 Hz/pt
number of scans: 16

freq. of 0 ppm: 300.130012 MHz
processed size: 32768 complex points
LB: 0.300 GF: 0.0000

(2*E*)-3-(Benzofuran-2-yl)-2-chloro-1-phenylprop-2-en-1-one (***E*-202**) – ^{13}C NMR

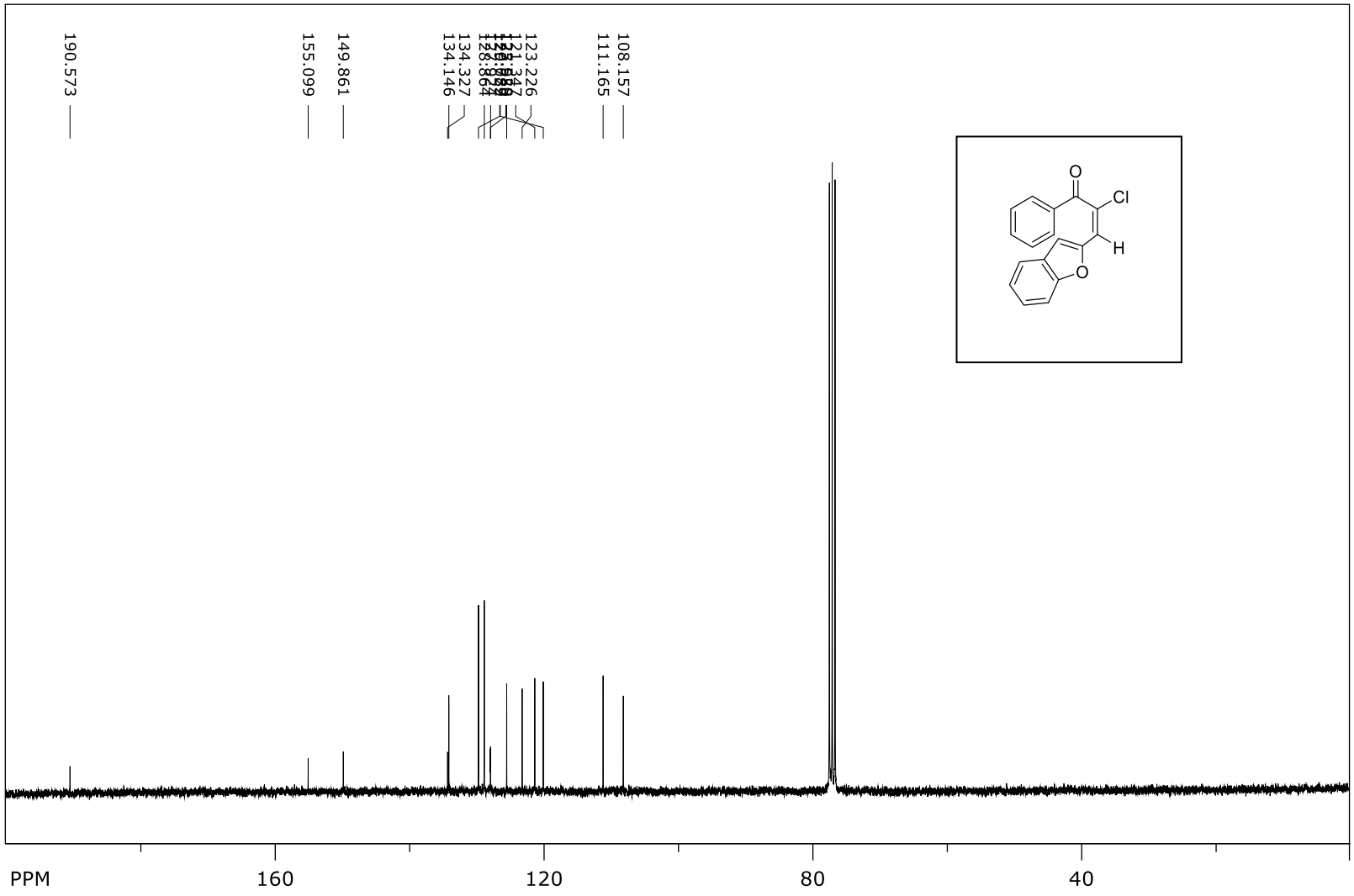

file: ...:\NMR 300\NKC_10_45_bdftrans\2\fid expt: <zgpg30>
transmitter freq.: 75.475295 MHz
time domain size: 65536 points
width: 17985.61 Hz = 238.2980 ppm = 0.274439 Hz/pt
number of scans: 1024

freq. of 0 ppm: 75.467749 MHz
processed size: 32768 complex points
LB: 1.000 GF: 0.0000

(2*E*)-3-(Benzofuran-2-yl)-2-chloro-1-phenylprop-2-en-1-one (***E*-202**) - $^{3}J_{C,H}$

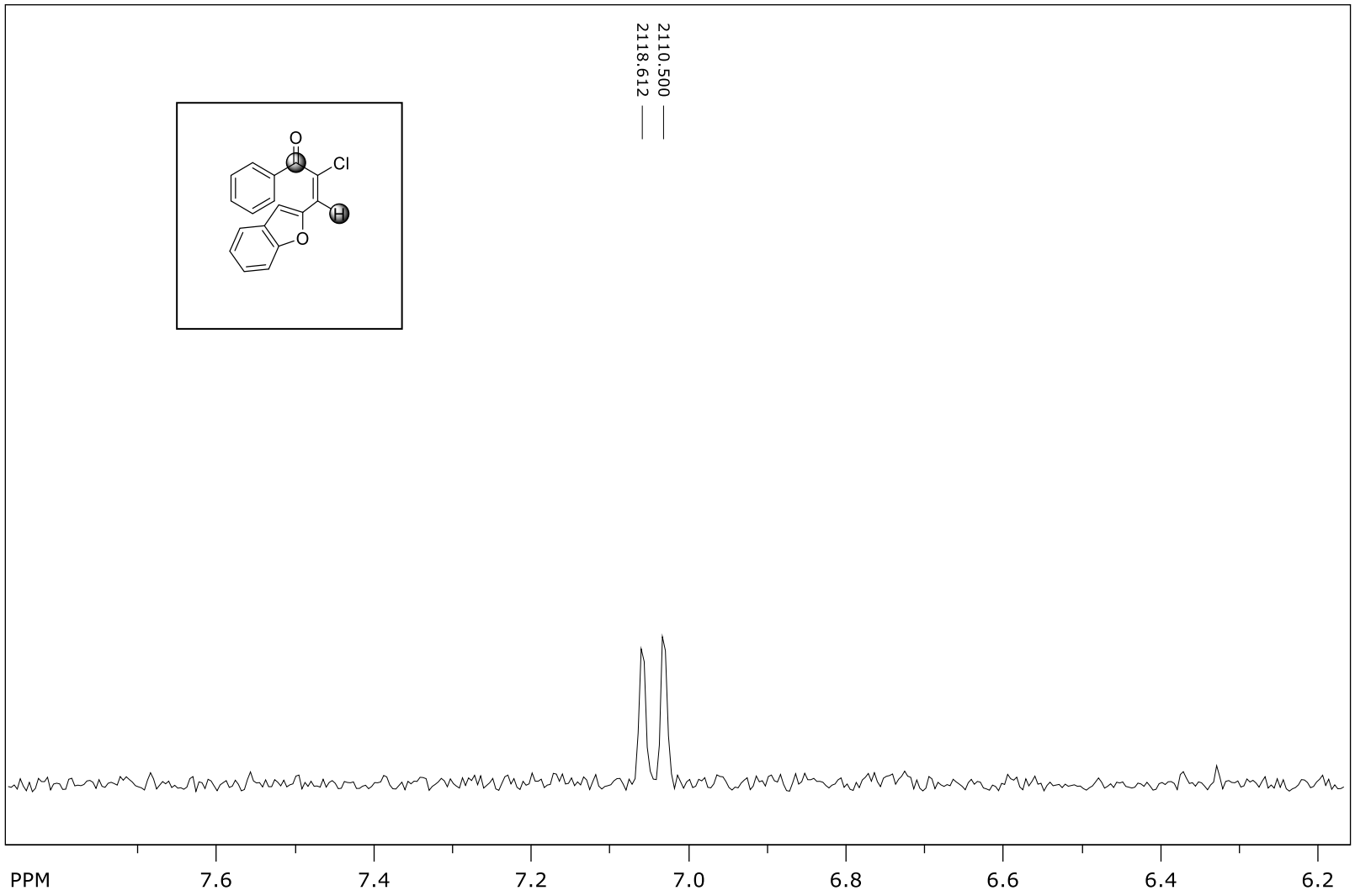

file: ...:\NMR 300\NKC_10_45_bdftrans\7\ser expt: <hmbcgplpndqf>
transmitter freq.: 300.131418 MHz
time domain size: 4096 points
width: 2367.42 Hz = 7.8880 ppm = 0.577984 Hz/pt
number of scans: 8

freq. of 0 ppm: 300.130006 MHz
processed size: 2048 complex points
LB: 0.000 GF: 0.0000

(*E*)-2-Chloro-3-(4-fluorophenyl)-1-phenylprop-2-en-1-one (***E*-200**) - ^{1}H NMR

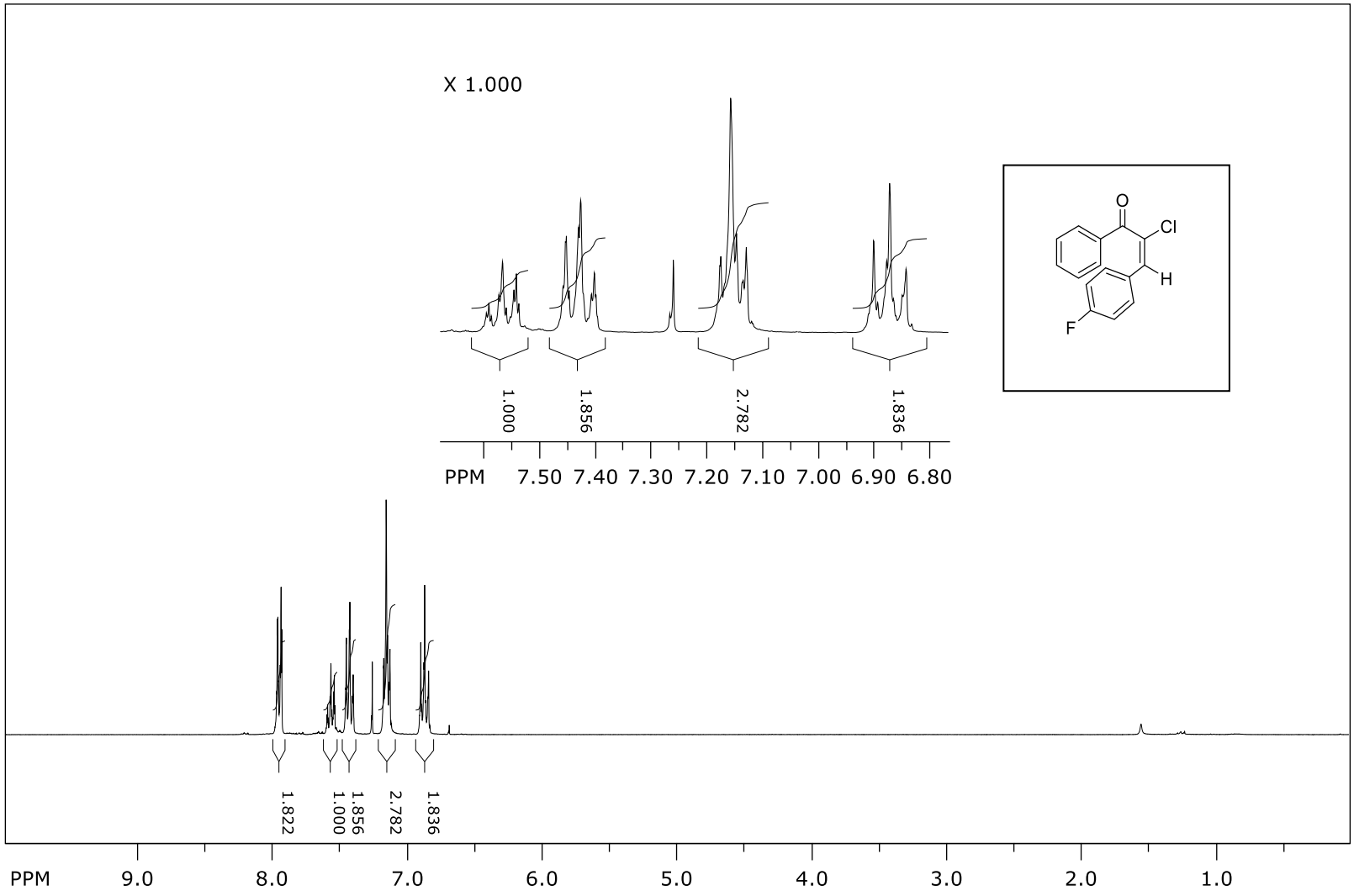

file: ...:\NMR 300\NKC_9_28_f1_pure_2\1\fid expt: <zg30>
transmitter freq.: 300.131853 MHz
time domain size: 65536 points
width: 6172.84 Hz = 20.5671 ppm = 0.094190 Hz/pt
number of scans: 16

freq. of 0 ppm: 300.130012 MHz
processed size: 32768 complex points
LB: 0.300 GF: 0.0000

(*E*)-2-Chloro-3-(4-fluorophenyl)-1-phenylprop-2-en-1-one (***E*-200**)– ^{13}C NMR

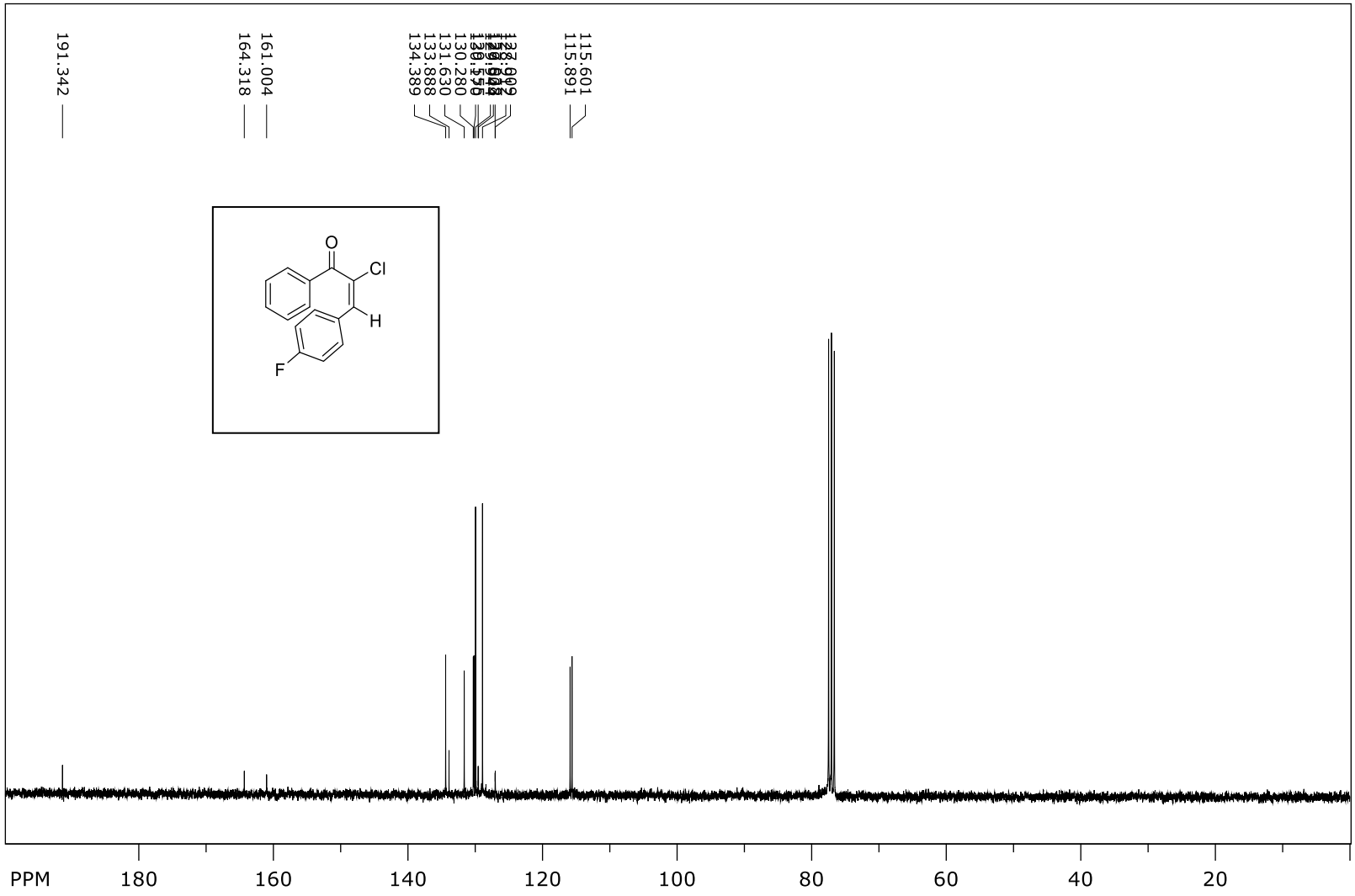

file: ...:\NMR 300\NKC_9_28_f1_pure_2\9\fid expt: <zgpg30>
transmitter freq.: 75.475295 MHz
time domain size: 65536 points
width: 17985.61 Hz = 238.2980 ppm = 0.274439 Hz/pt
number of scans: 512

freq. of 0 ppm: 75.467749 MHz
processed size: 32768 complex points
LB: 1.000 GF: 0.0000

(*E*)-2-Chloro-3-(4-fluorophenyl)-1-phenylprop-2-en-1-one (***E*-200**) - $^{3}J_{C,H}$

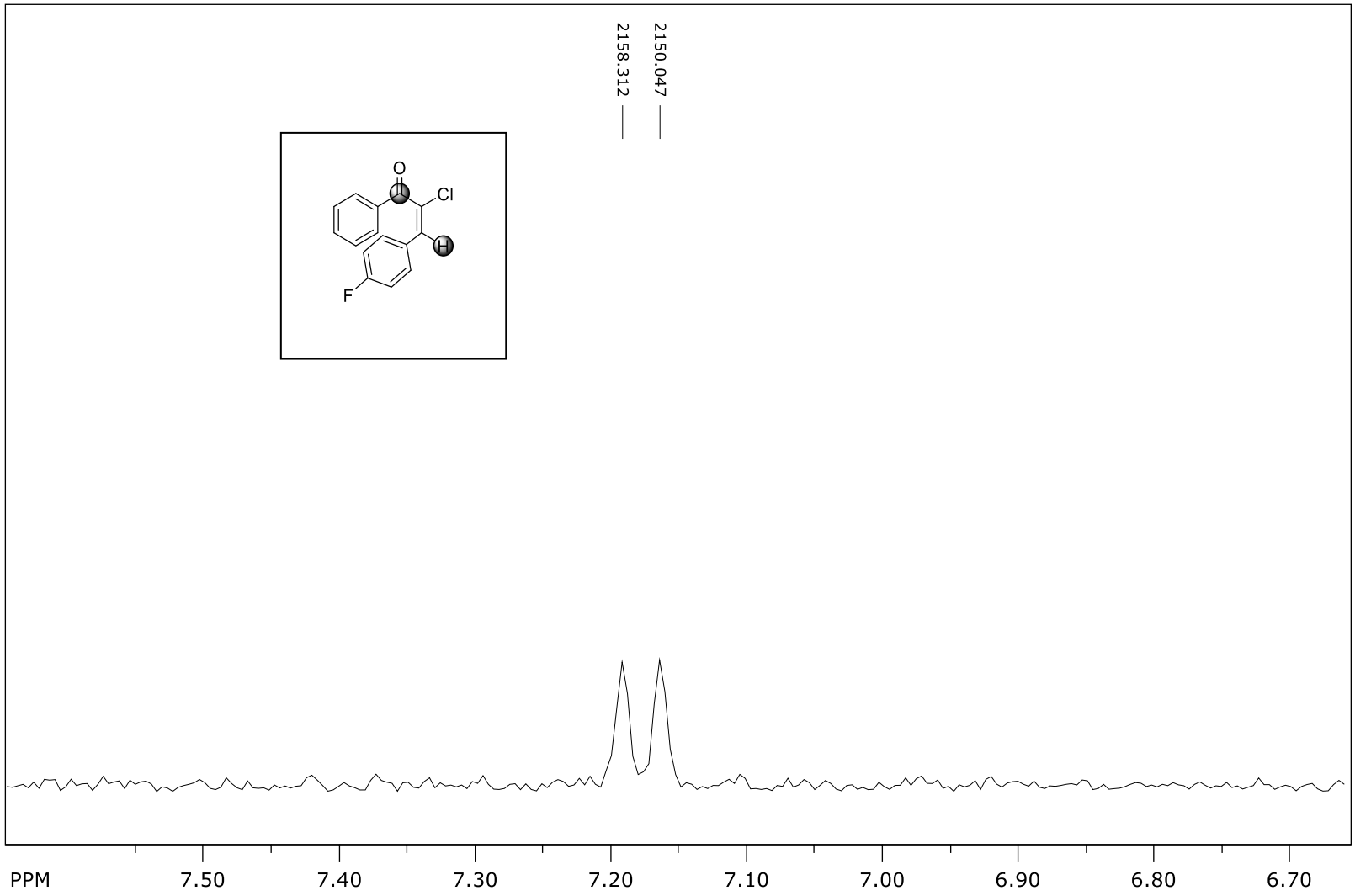

file: ...:\NMR 300\NKC_9_28_f1_pure_2\4\ser expt: <hmbcgplpndqf>
transmitter freq.: 300.131380 MHz
time domain size: 4096 points
width: 2422.48 Hz = 8.0714 ppm = 0.591426 Hz/pt
number of scans: 8

freq. of 0 ppm: 300.130006 MHz
processed size: 2048 complex points
LB: 0.000 GF: 0.0000

(*Z*)-2-Chloro-3-(4-methoxyphenyl)-1-phenylprop-2-en-1-one (***Z*-2**) - ^{1}H NMR

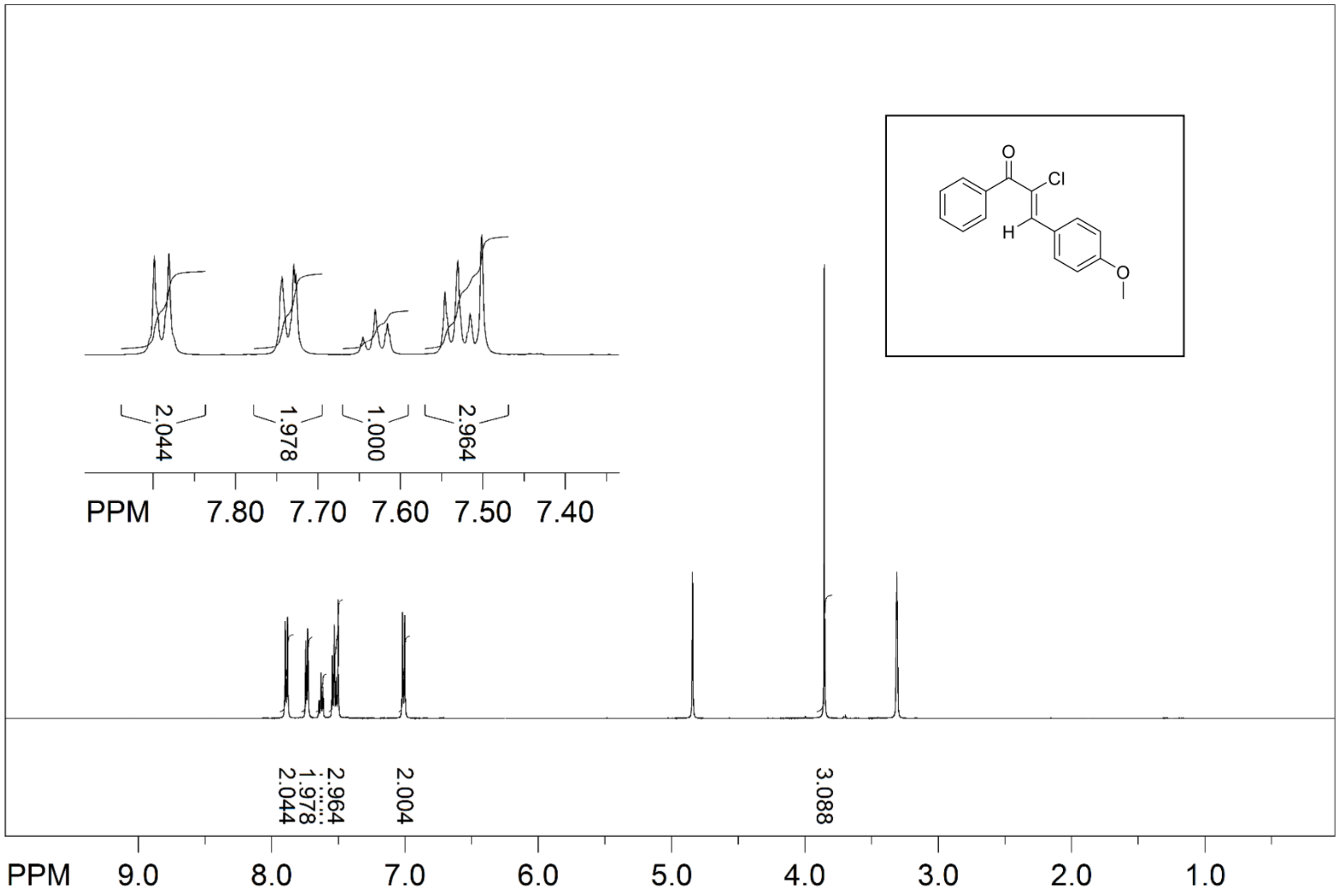

file: ...ers\chehal\Desktop\NKC_12_49\2\fid expt: <zg30>
transmitter freq.: 500.133089 MHz
time domain size: 65536 points
width: 10000.00 Hz = 19.9947 ppm = 0.152588 Hz/pt
number of scans: 32

freq of 0 ppm: 500.129994 MHz
processed size: 65536 points
LB: 0.300 GF: 0.0000
Hz/cm: 207.827 ppm/cm: 0.41554

(*Z*)-2-Chloro-3-(4-methoxyphenyl)-1-phenylprop-2-en-1-one (***Z*-2**) – ^{13}C NMR

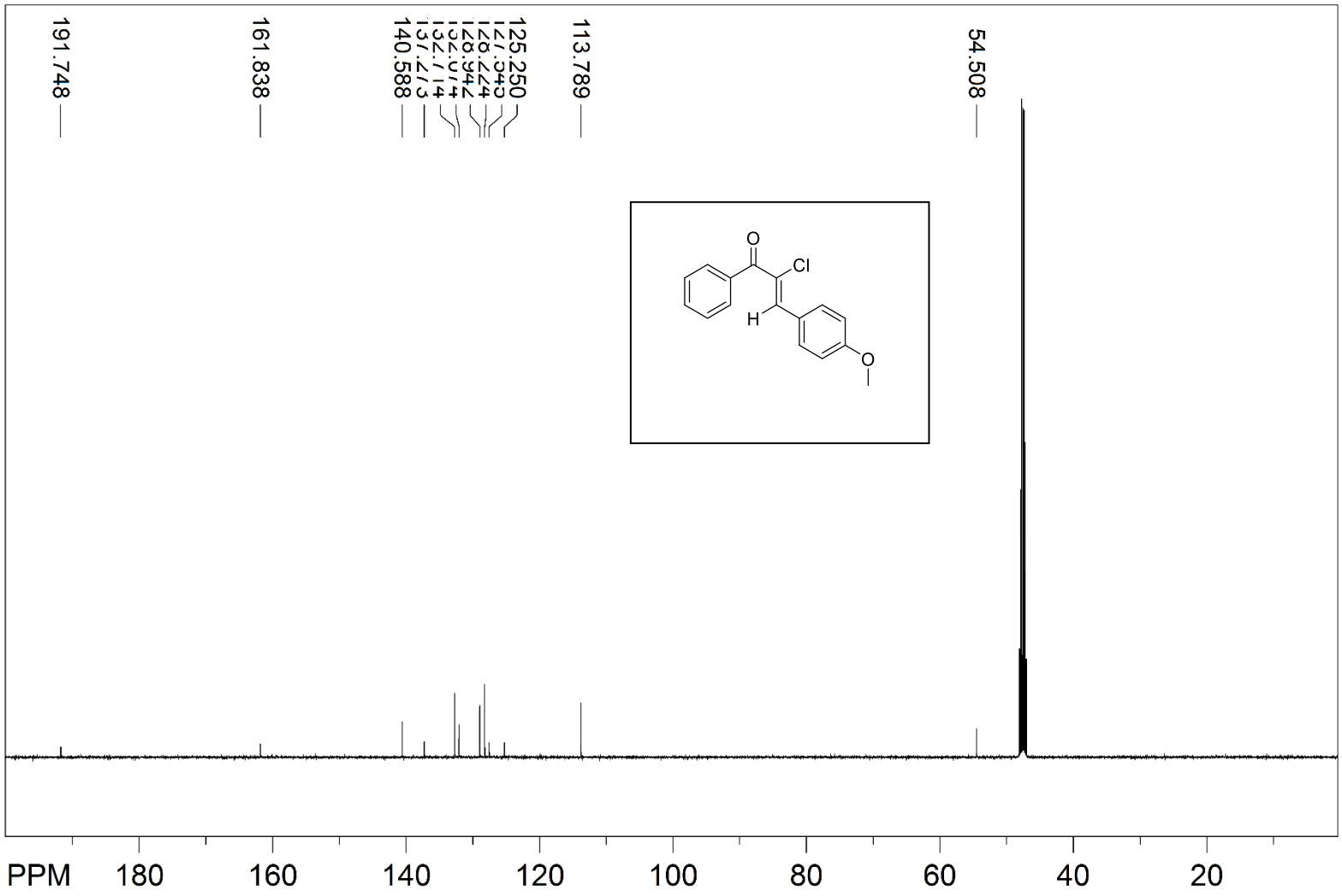

file: ...ers\chehal\Desktop\NKC 12 49\1\fid expt: <zgpg30>
transmitter freq.: 125.770364 MHz
time domain size: 65536 points
width: 29761.90 Hz = 236.6369 ppm = 0.454131 Hz/pt
number of scans: 1024

freq of 0 ppm: 125.757789 MHz
processed size: 32768 points
LB: 1.000 GF: 0.0000
Hz/cm: 1046.148 ppm/cm: 8.31792

(*Z*)-2-Chloro-3-(4-methoxyphenyl)-1-phenylprop-2-en-1-one (***Z*-2**) – ^{13}C NMR (zoomed)

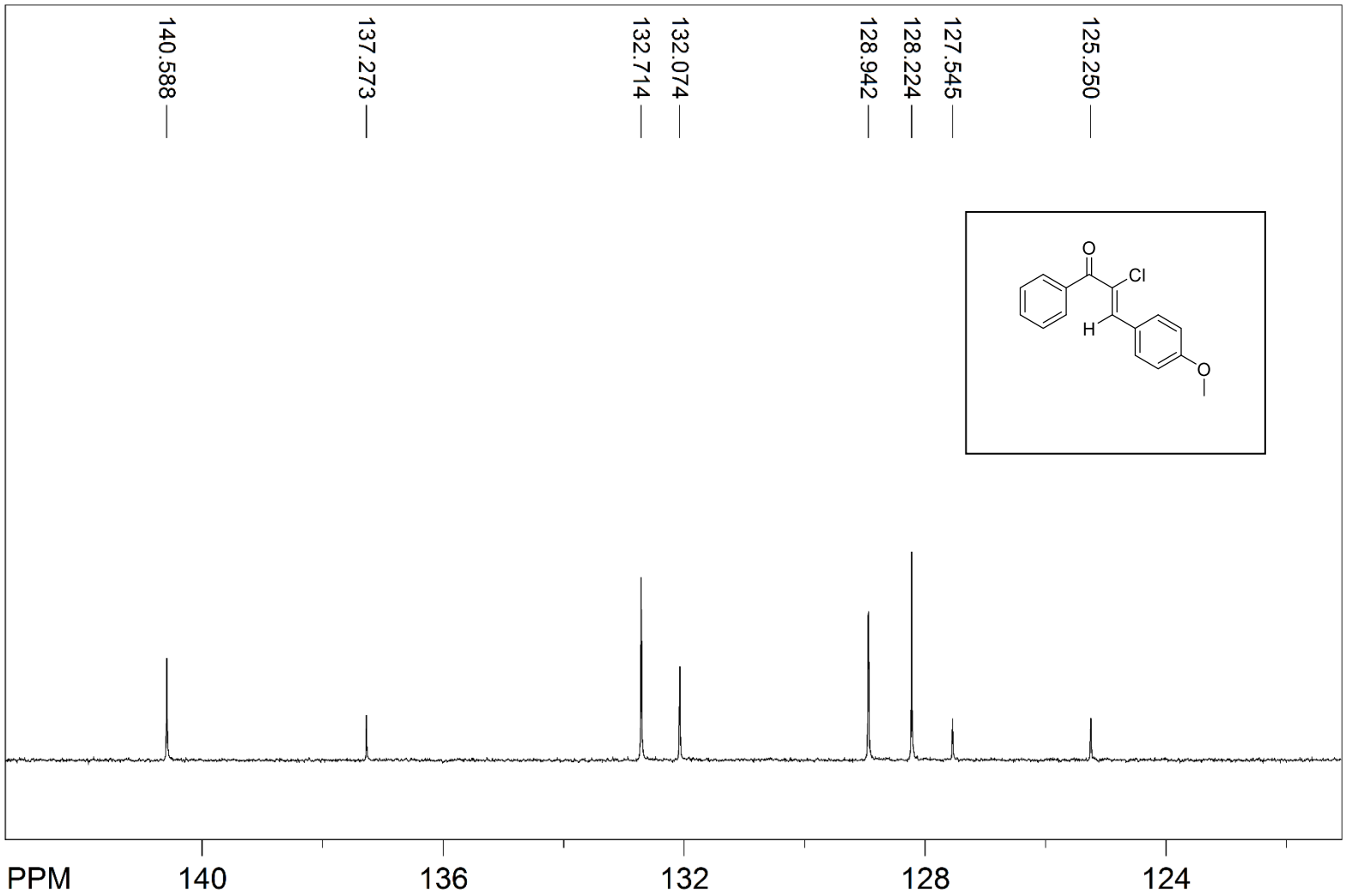

file: ...ers\chehal\Desktop\NKC 12 49\1\fid expt: <zgpg30>
transmitter freq.: 125.770364 MHz
time domain size: 65536 points
width: 29761.90 Hz = 236.6369 ppm = 0.454131 Hz/pt
number of scans: 1024

freq of 0 ppm: 125.757789 MHz
processed size: 32768 points
LB: 1.000 GF: 0.0000
Hz/cm: 116.239 ppm/cm: 0.92421

(*Z*)-2-Chloro-3-(4-methoxyphenyl)-1-phenylprop-2-en-1-one (***Z*-2**) - $^{3}J_{C,H}$

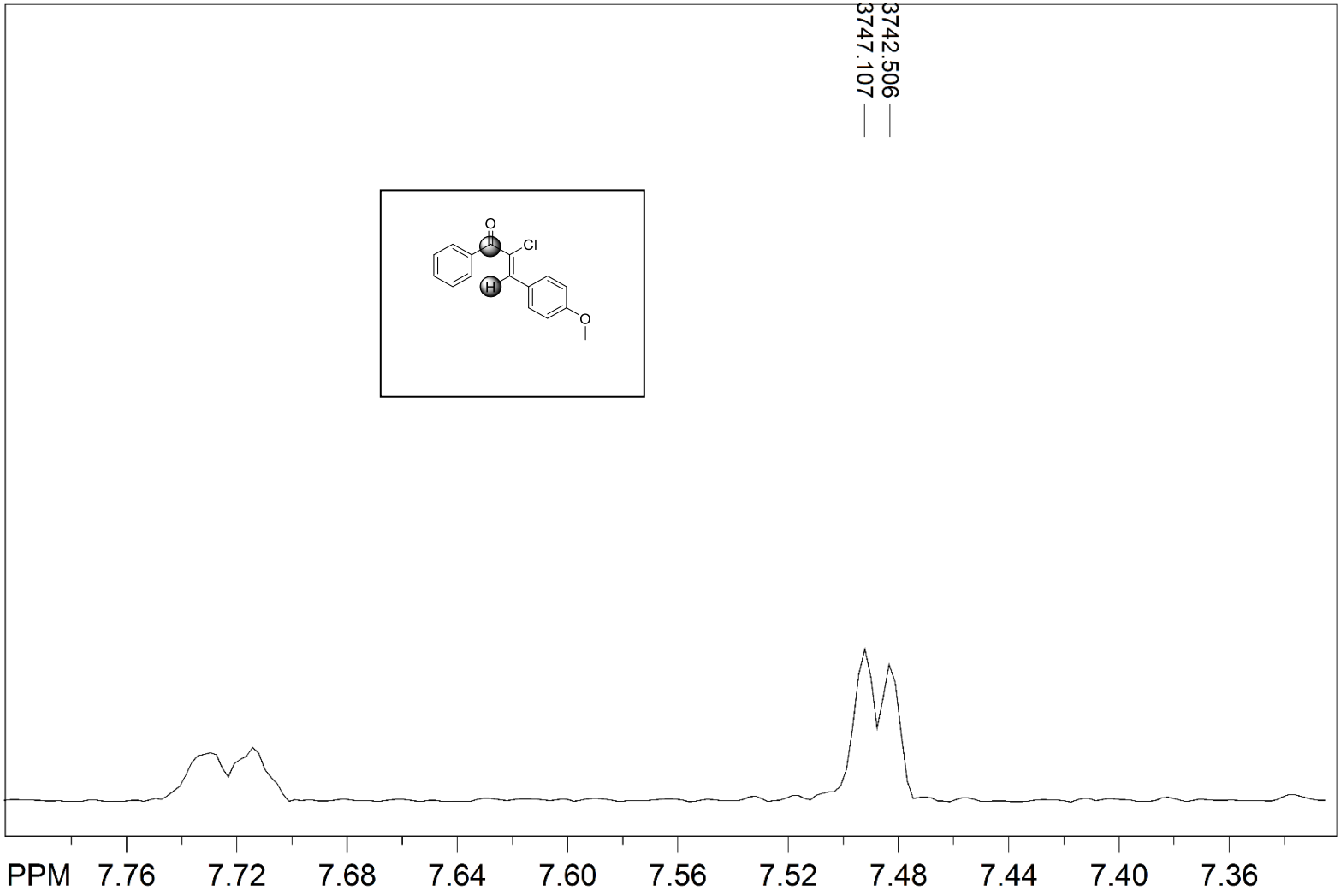

file: ...ers\chehal\Desktop\NKC 12 49\3\ser expt: <hmbcgplpndqfreq of 0 ppm: 500.130000 MHz
transmitter freq.: 500.132751 MHz processed size: 4096 points
time domain size: 4096 points LB: 0.000 GF: 0.0000
width: 4504.51 Hz = 9.0066 ppm = 1.099733 Hz/pt Hz/cm: 10.065 ppm/cm: 0.02012
number of scans: 8

(2*Z*)-2-Chloro-1-(phenyl)-3-(thiophen-2-yl)prop-2-en-1-one (***Z*-203**) - ^{1}H NMR

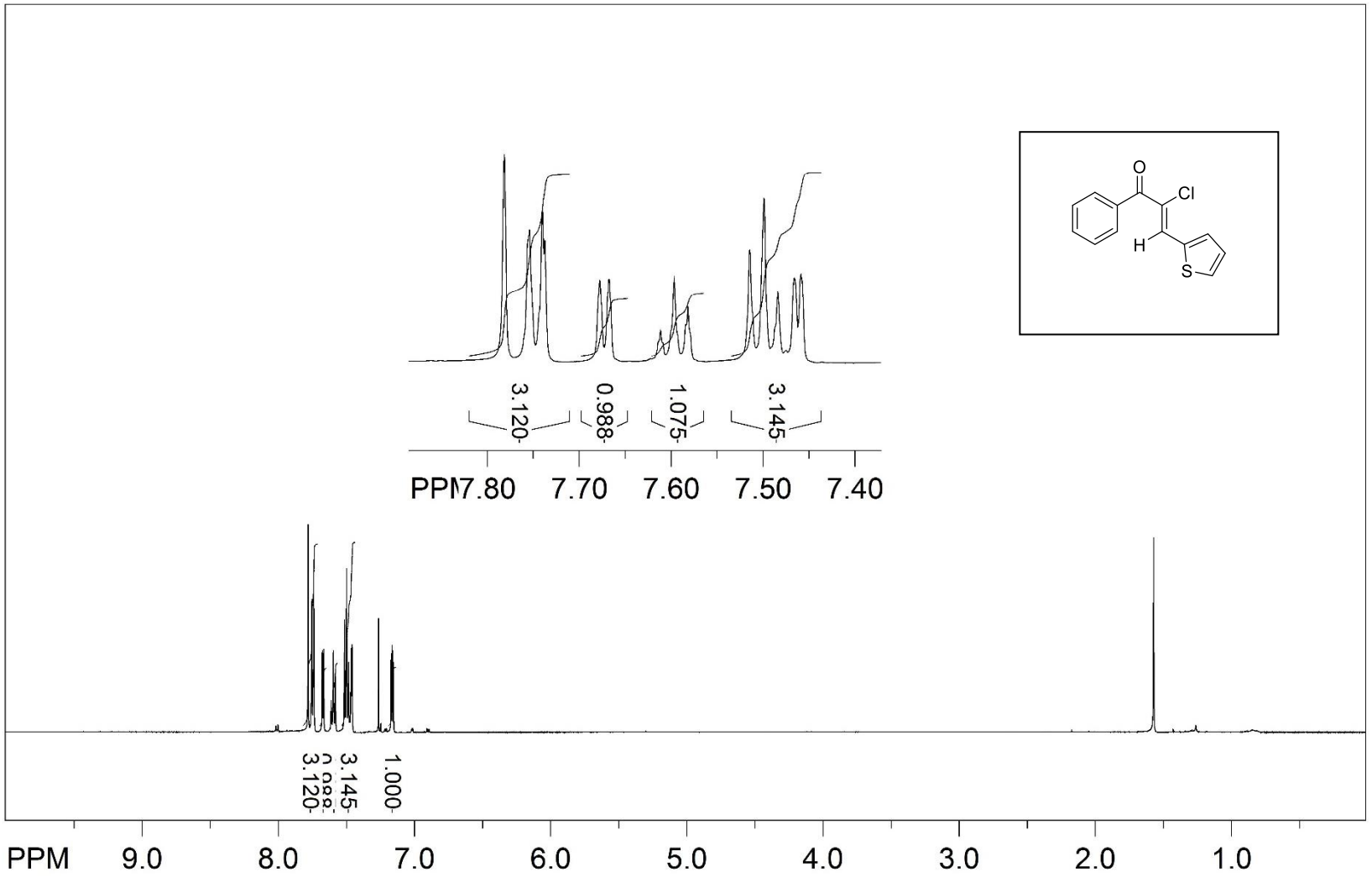

file: ...hal\Desktop\NKC 10 thiophene\1\fid expt: <zg30>
transmitter freq.: 500.133089 MHz
time domain size: 65536 points
width: 10000.00 Hz = 19.9947 ppm = 0.152588 Hz/pt

freq of 0 ppm: 500.130000 MHz
processed size: 65536 points
LB: 0.300 GF: 0.0000
Hz/cm: 199.903 ppm/cm: 0.39970

(2*Z*)-2-Chloro-1-(phenyl)-3-(thiophen-2-yl)prop-2-en-1-one (***Z*-203**) – ^{13}C NMR

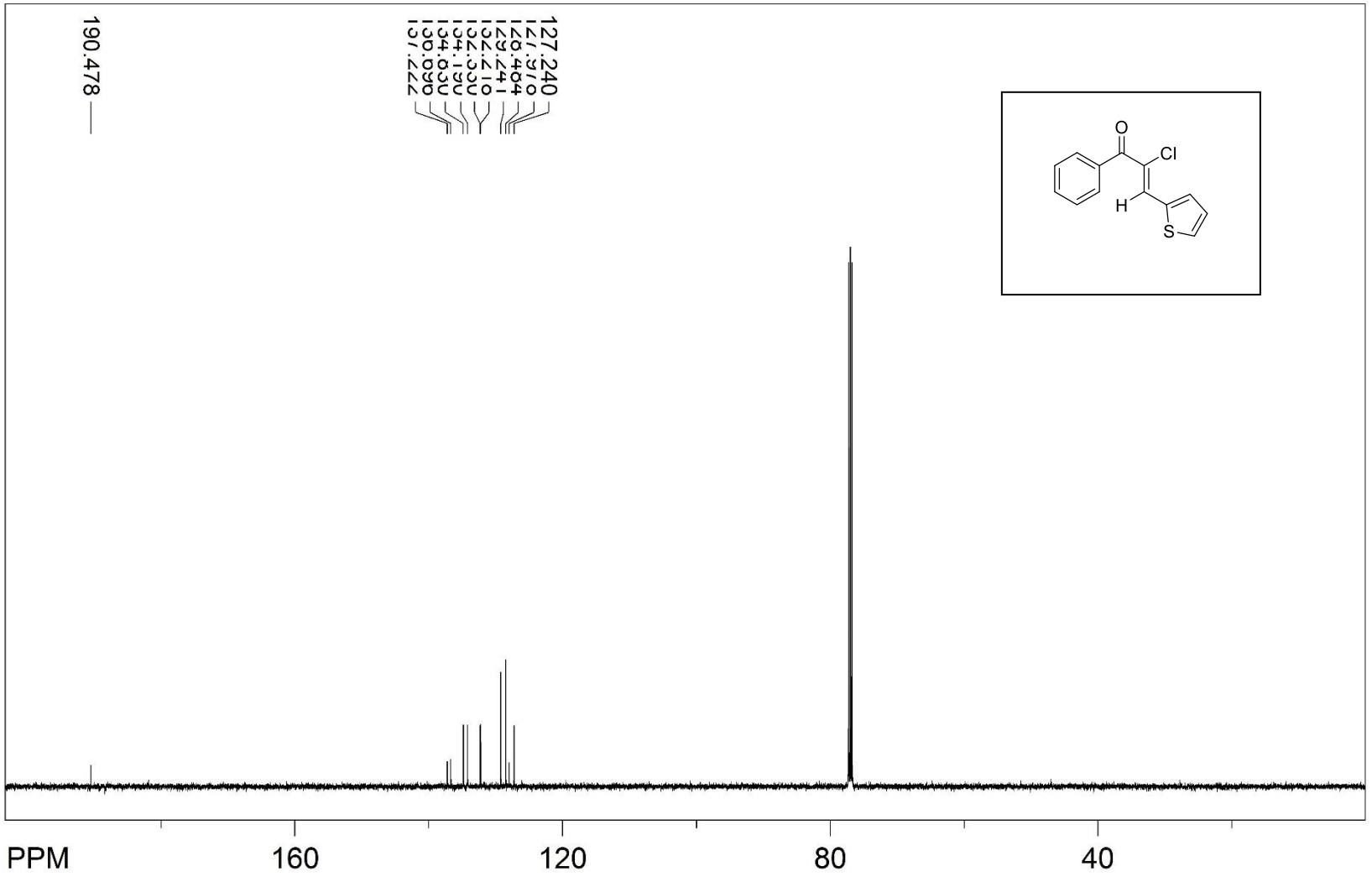

file: ...sktop\NKC 10 thiophenecarbon\2\fid expt: <zgpg30>
transmitter freq.: 125.770364 MHz
time domain size: 65536 points
width: 29761.90 Hz = 236.6369 ppm = 0.454131 Hz/pt
number of scans: 141

freq of 0 ppm: 125.757789 MHz
processed size: 65536 points
LB: 1.000 GF: 0.0000
Hz/cm: 1022.225 ppm/cm: 8.12771

(2*Z*)-2-Chloro-1-(phenyl)-3-(thiophen-2-yl)prop-2-en-1-one (***Z*-203**) - $^{3}J_{C,H}$

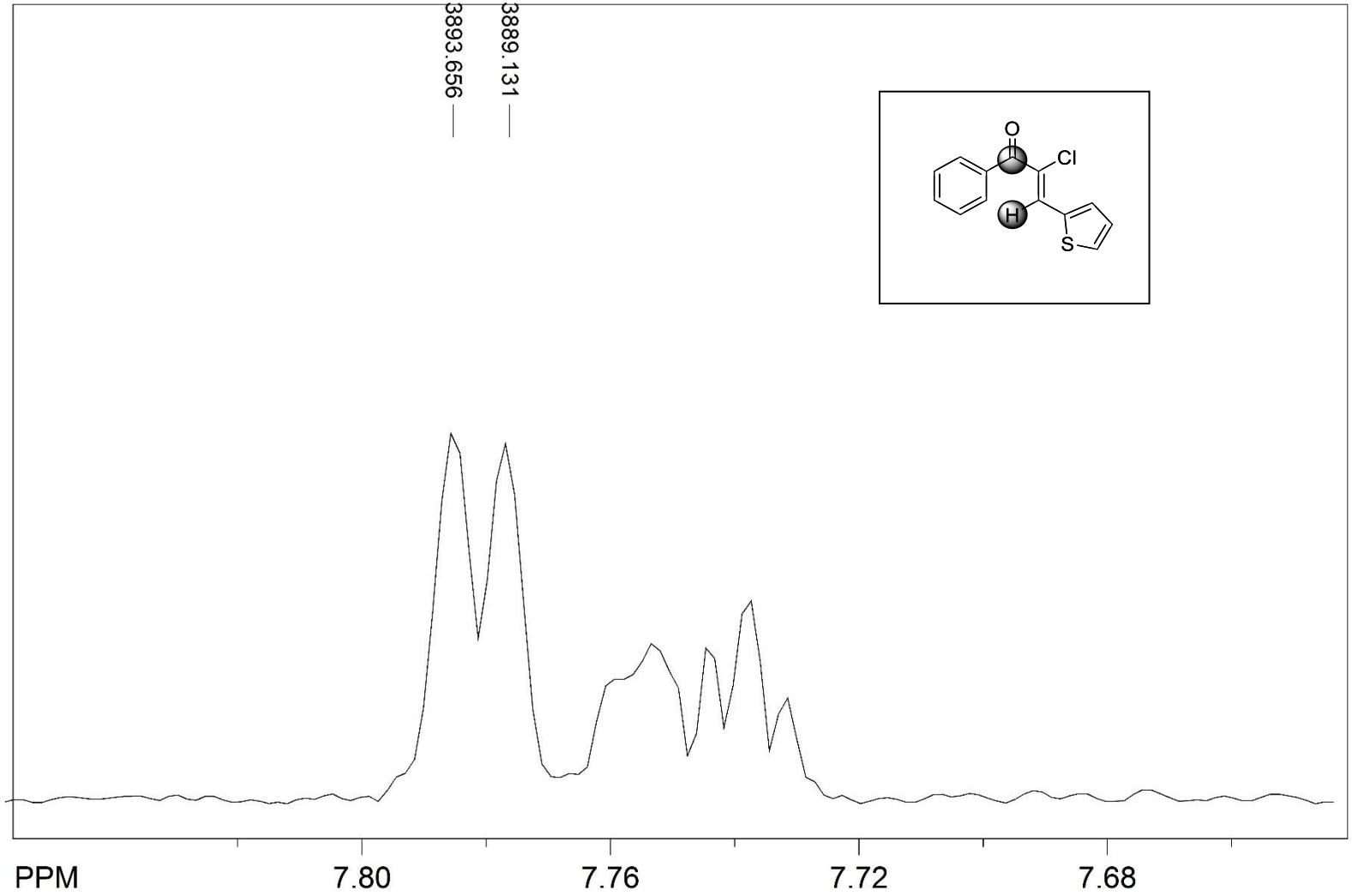

file: ...esktop\NKC 10 thiophene hmbc\3\ser expt: <hmbcgplpndfreq of 0 ppm: 500.130000 MHz
transmitter freq.: 500.133751 MHz processed size: 2048 points
time domain size: 2048 points LB: 0.000 GF: 0.0000
width: 1500.60 Hz = 3.0004 ppm = 0.732715 Hz/pt Hz/cm: 4.477 ppm/cm: 0.00895
number of scans: 8

(*Z*)-2-Chloro-3-(phenyl)-1-phenylprop-2-en-1-one (***Z*-199**) – ^{1}H NMR

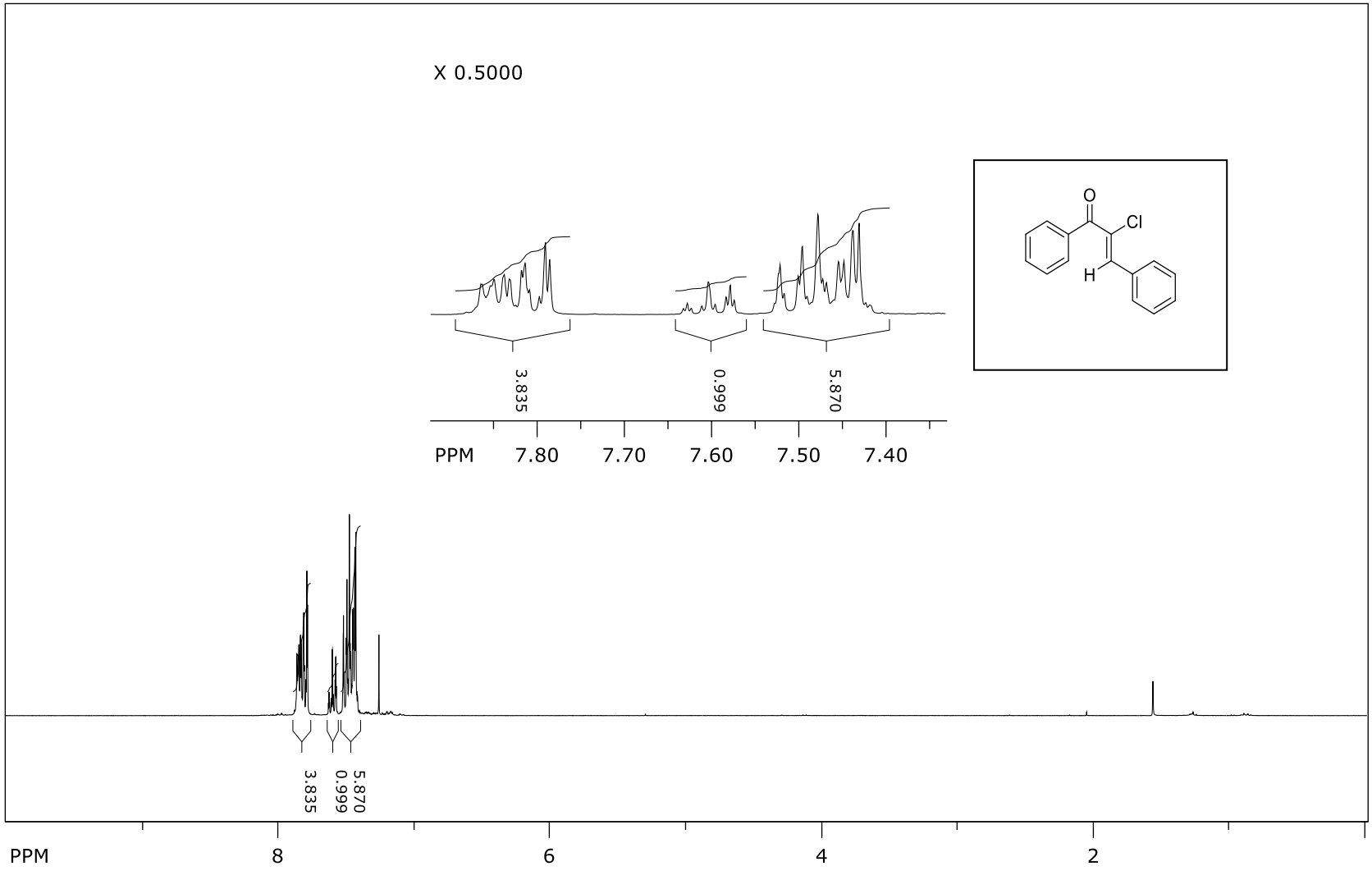

file: D:\NMR 300\NKC_10_22_phenyl\1\fid expt: <zg30>
transmitter freq.: 300.131853 MHz
time domain size: 65536 points
width: 6172.84 Hz = 20.5671 ppm = 0.094190 Hz/pt
number of scans: 16

freq. of 0 ppm: 300.130012 MHz
processed size: 32768 complex points
LB: 0.300 GF: 0.0000

(*Z*)-2-Chloro-3-(phenyl)-1-phenylprop-2-en-1-one (***Z*-199**) – ^{13}C NMR

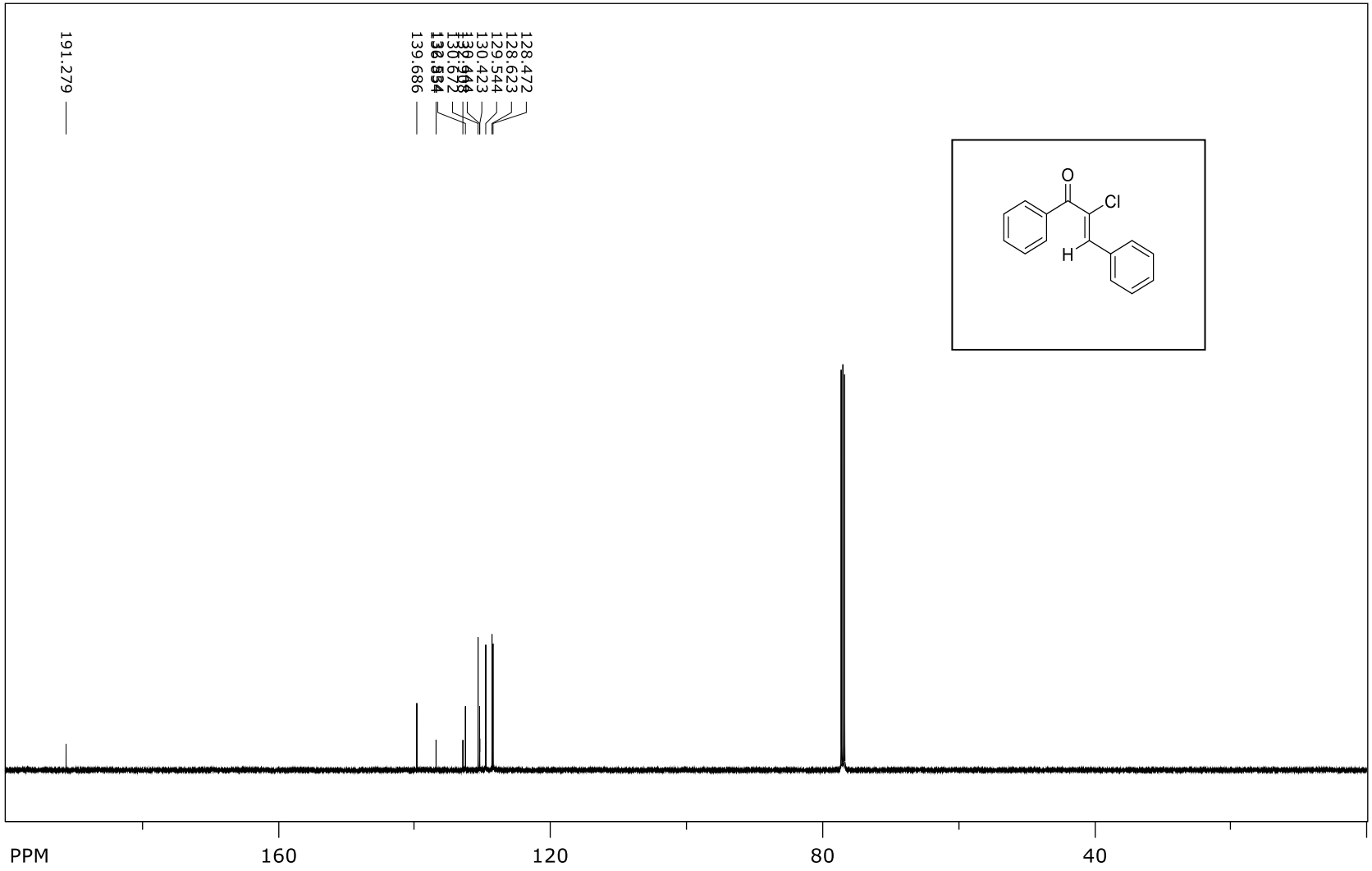

file: ...C_10_phenyl_longerrelaxdelay\2\fid expt: <zgpg30>
transmitter freq.: 125.770364 MHz
time domain size: 65536 points
width: 29761.90 Hz = 236.6369 ppm = 0.454131 Hz/pt
number of scans: 323

freq. of 0 ppm: 125.757789 MHz
processed size: 65536 complex points
LB: 1.000 GF: 0.0000

(*Z*)-2-Chloro-3-(phenyl)-1-phenylprop-2-en-1-one (***Z*-199**) - $^{3}J_{C,H}$

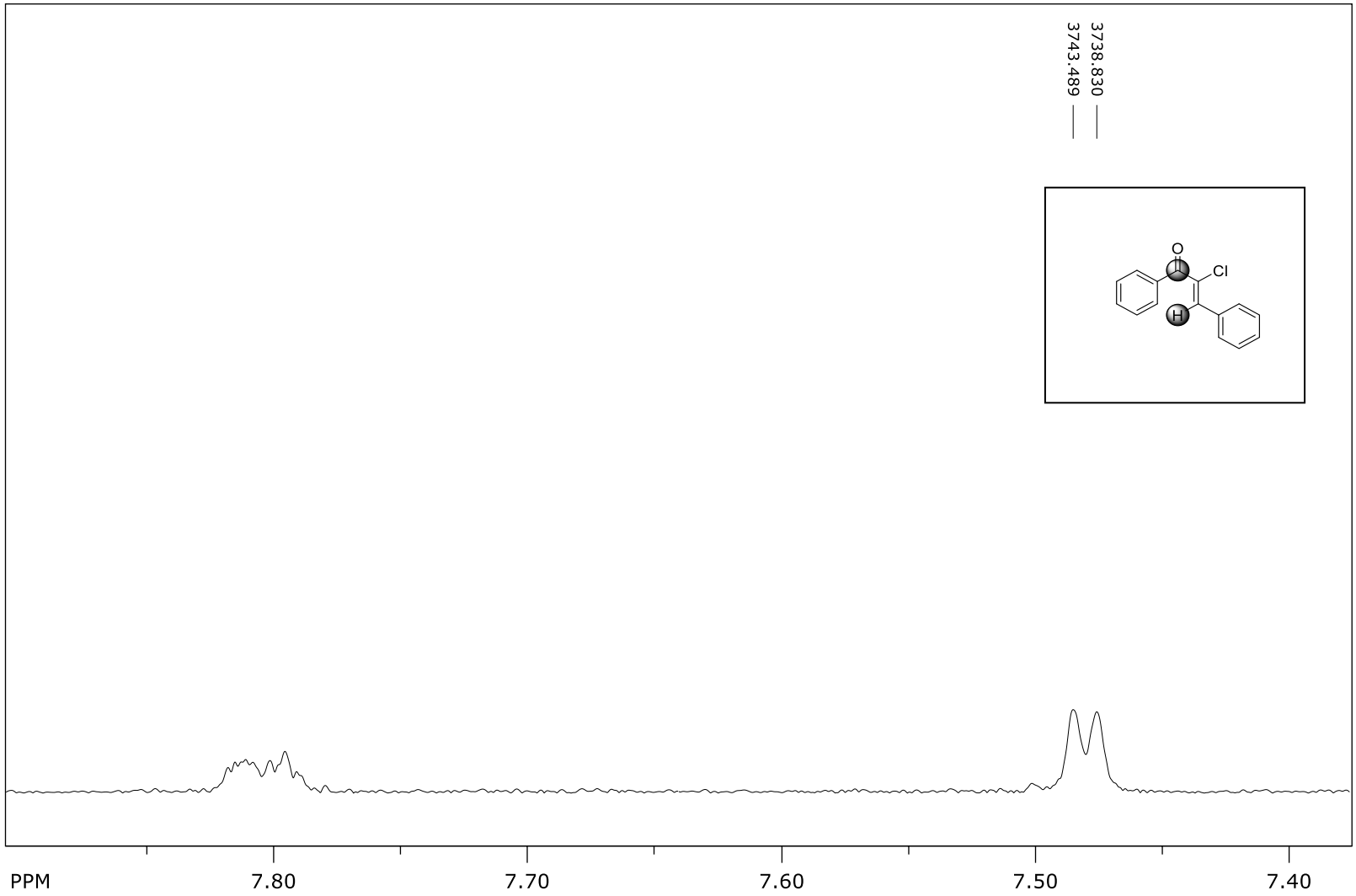

file: ...C_10_phenyl_longerrelaxdelay\3\ser expt: <hmbcgplpndqf>
transmitter freq.: 500.133821 MHz
time domain size: 824 points
width: 265.11 Hz = 0.5301 ppm = 0.321737 Hz/pt
number of scans: 4

freq. of 0 ppm: 500.130000 MHz
processed size: 2048 complex points
LB: 0.000 GF: 0.0000

(*Z*)-2-Chloro-3-(4-methyphenyl)-1-phenylprop-2-en-1-one (***Z*-198**) – ^{1}H NMR

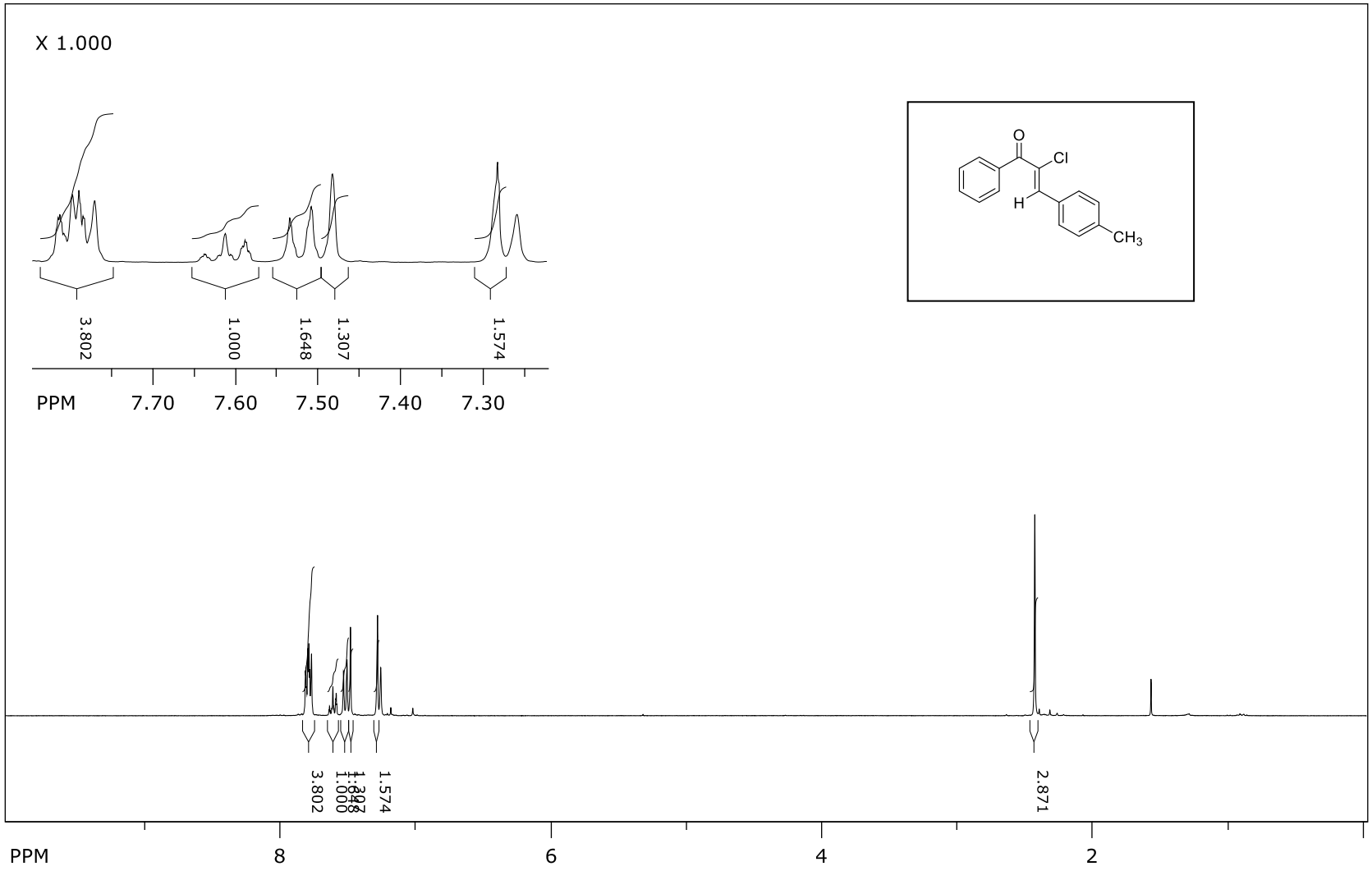

file: D:\NKC_10_21_methyl_3\1\fid expt: <zg30>
transmitter freq.: 300.131853 MHz
time domain size: 65536 points
width: 6172.84 Hz = 20.5671 ppm = 0.094190 Hz/pt
number of scans: 16

freq. of 0 ppm: 300.130006 MHz
processed size: 32768 complex points
LB: 0.300 GF: 0.0000

(*Z*)-2-Chloro-3-(4-methyphenyl)-1-phenylprop-2-en-1-one (***Z*-198**) – ^{13}C NMR

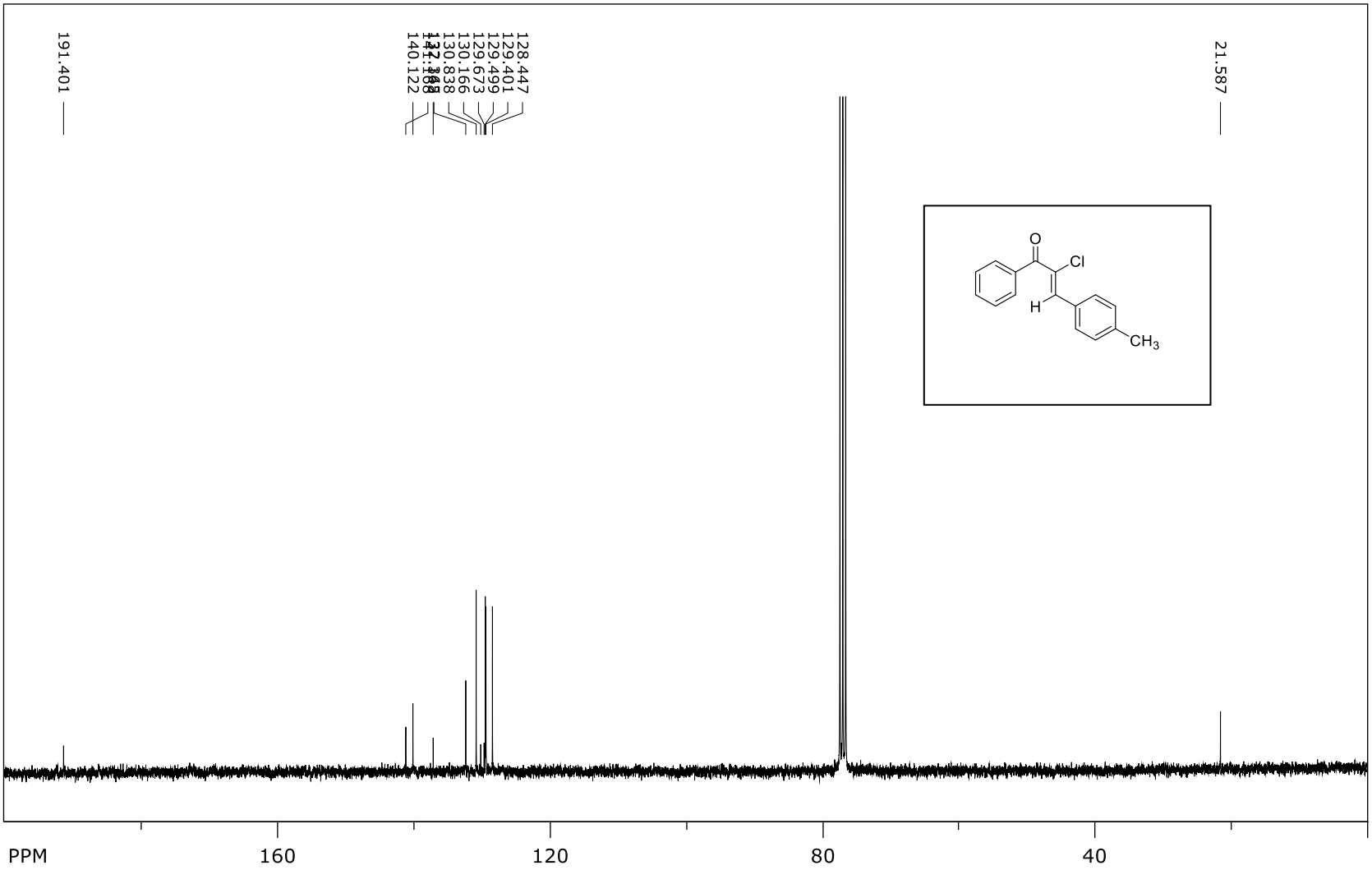

file: D:\NKC_10_21_methyl_3\2\fid expt: <zgpg30>
transmitter freq.: 75.475295 MHz
time domain size: 65536 points
width: 17985.61 Hz = 238.2980 ppm = 0.274439 Hz/pt
number of scans: 1024

freq. of 0 ppm: 75.467749 MHz
processed size: 32768 complex points
LB: 1.000 GF: 0.0000

(*Z*)-2-Chloro-3-(4-methyphenyl)-1-phenylprop-2-en-1-one (***Z*-198**) - $^{3}J_{C,H}$

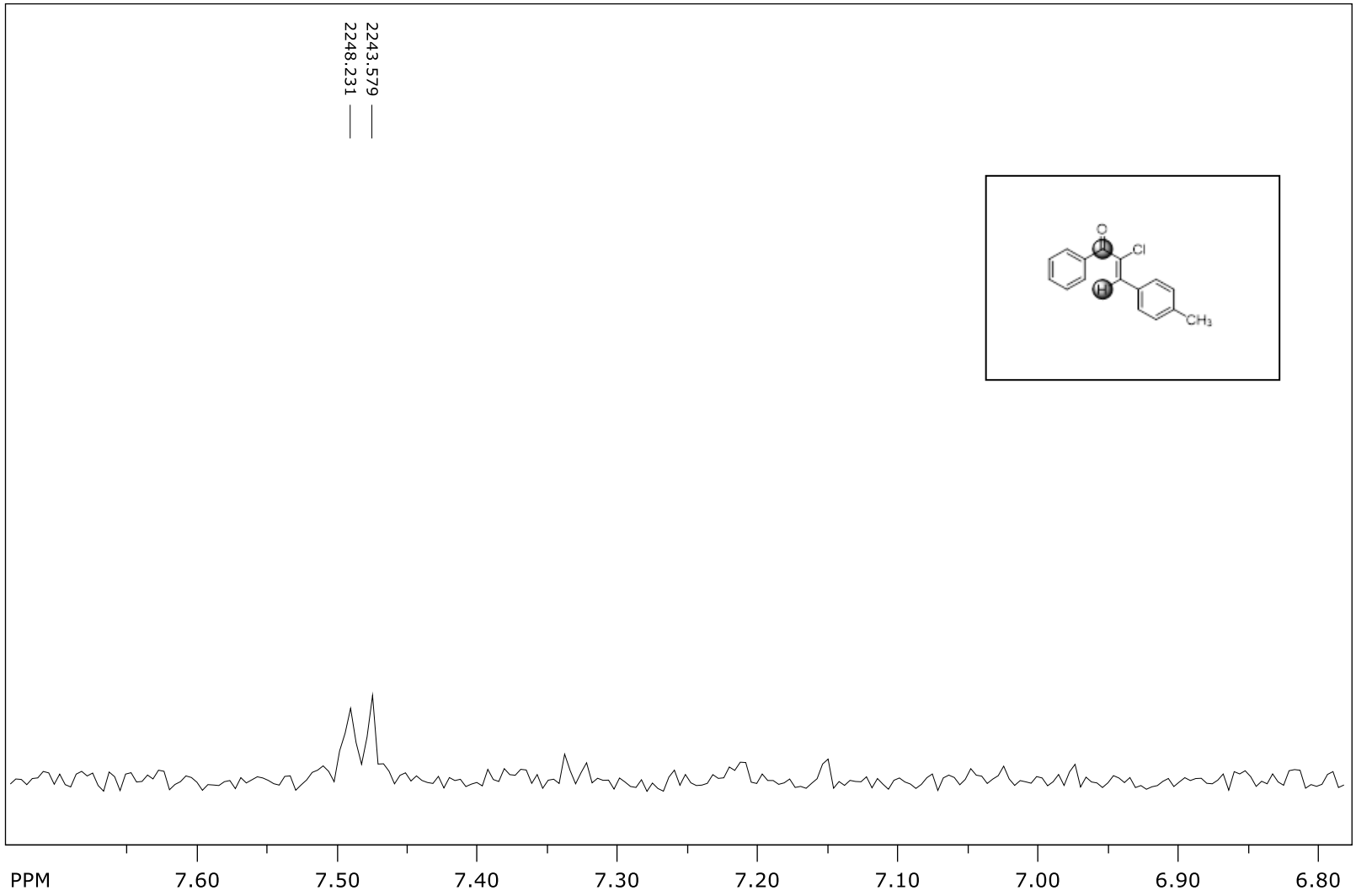

file: D:\NKC_10_21_methyl_3\3\ser expt: <hmbcgplpndqf>
transmitter freq.: 300.131323 MHz
time domain size: 4096 points
width: 2408.48 Hz = 8.0247 ppm = 0.588007 Hz/pt
number of scans: 8

freq. of 0 ppm: 300.130006 MHz
processed size: 2048 complex points
LB: 0.000 GF: 0.0000

(2*Z*)-2-Chloro-3-(2-fluoropyridin-4-yl)-1-phenylprop-2-en-1-one (***Z*-204**) – ^{1}H NMR

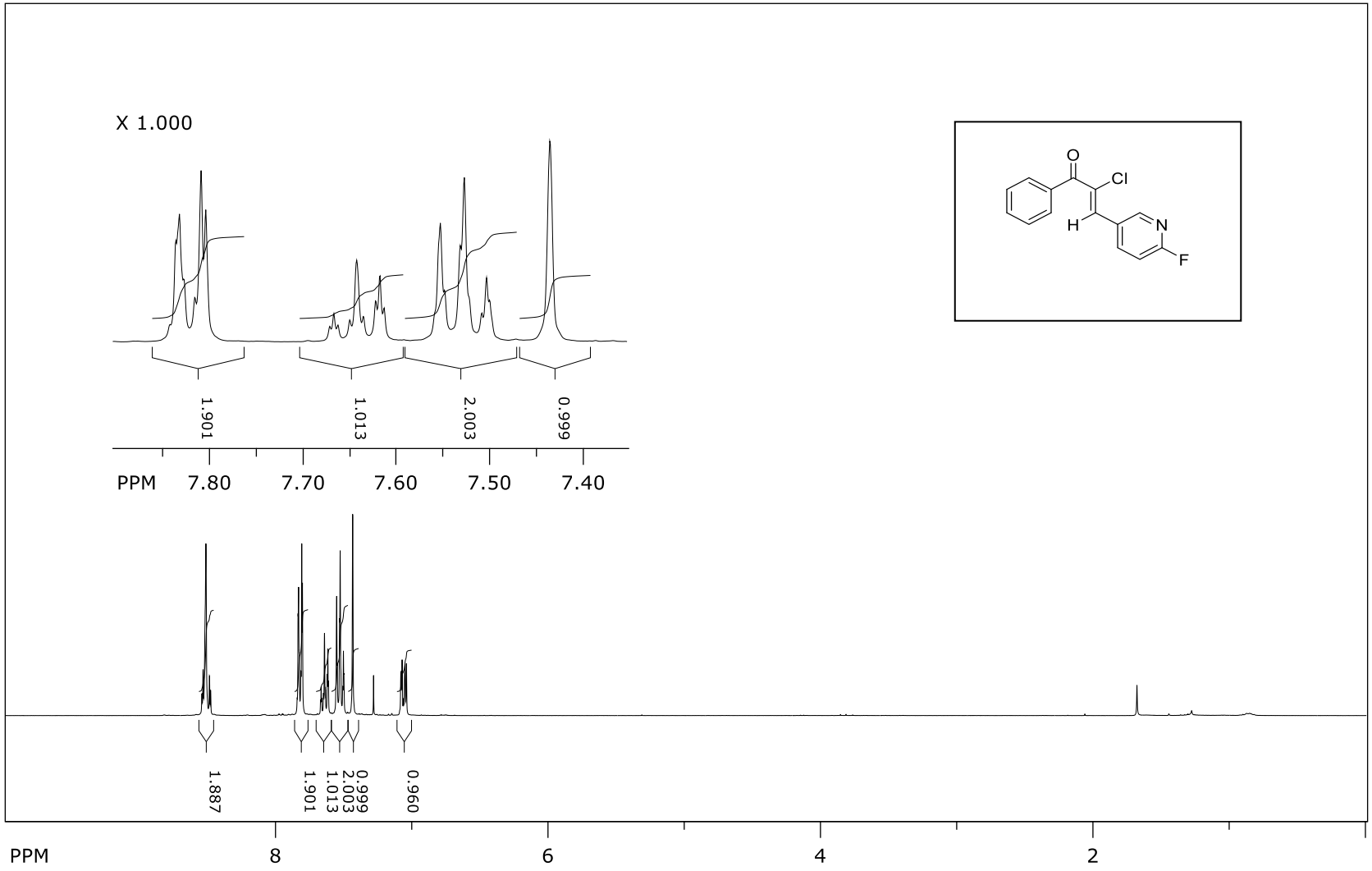

file: ...:\NKC_10_fluoropyridinecis_2\1\fid expt: <zg30>
transmitter freq.: 300.131853 MHz
time domain size: 65536 points
width: 6172.84 Hz = 20.5671 ppm = 0.094190 Hz/pt
number of scans: 16

freq. of 0 ppm: 300.130006 MHz
processed size: 32768 complex points
LB: 0.300 GF: 0.0000

(2*Z*)-2-Chloro-3-(2-fluoropyridin-4-yl)-1-phenylprop-2-en-1-one (***Z*-204**) – ^{13}C NMR

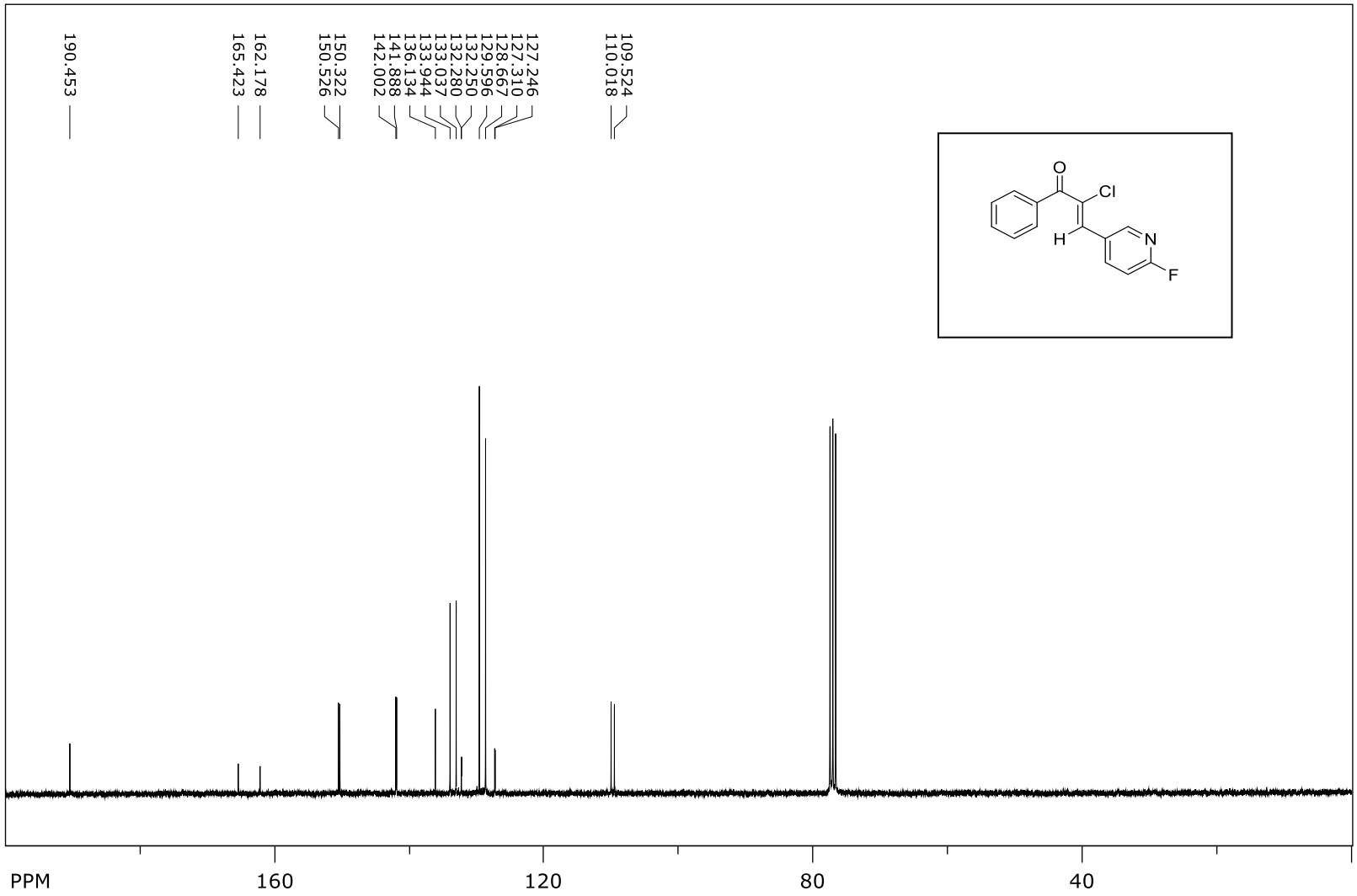

file: ...:\NKC_10_fluoropyridinecis_2\3\fid expt: <zgpg30>
transmitter freq.: 75.475295 MHz
time domain size: 65536 points
width: 17985.61 Hz = 238.2980 ppm = 0.274439 Hz/pt
number of scans: 1024

freq. of 0 ppm: 75.467749 MHz
processed size: 32768 complex points
LB: 1.000 GF: 0.0000

(2*Z*)-2-Chloro-3-(2-fluoropyridin-4-yl)-1-phenylprop-2-en-1-one (***Z*-204**) - $^{3}J_{C,H}$

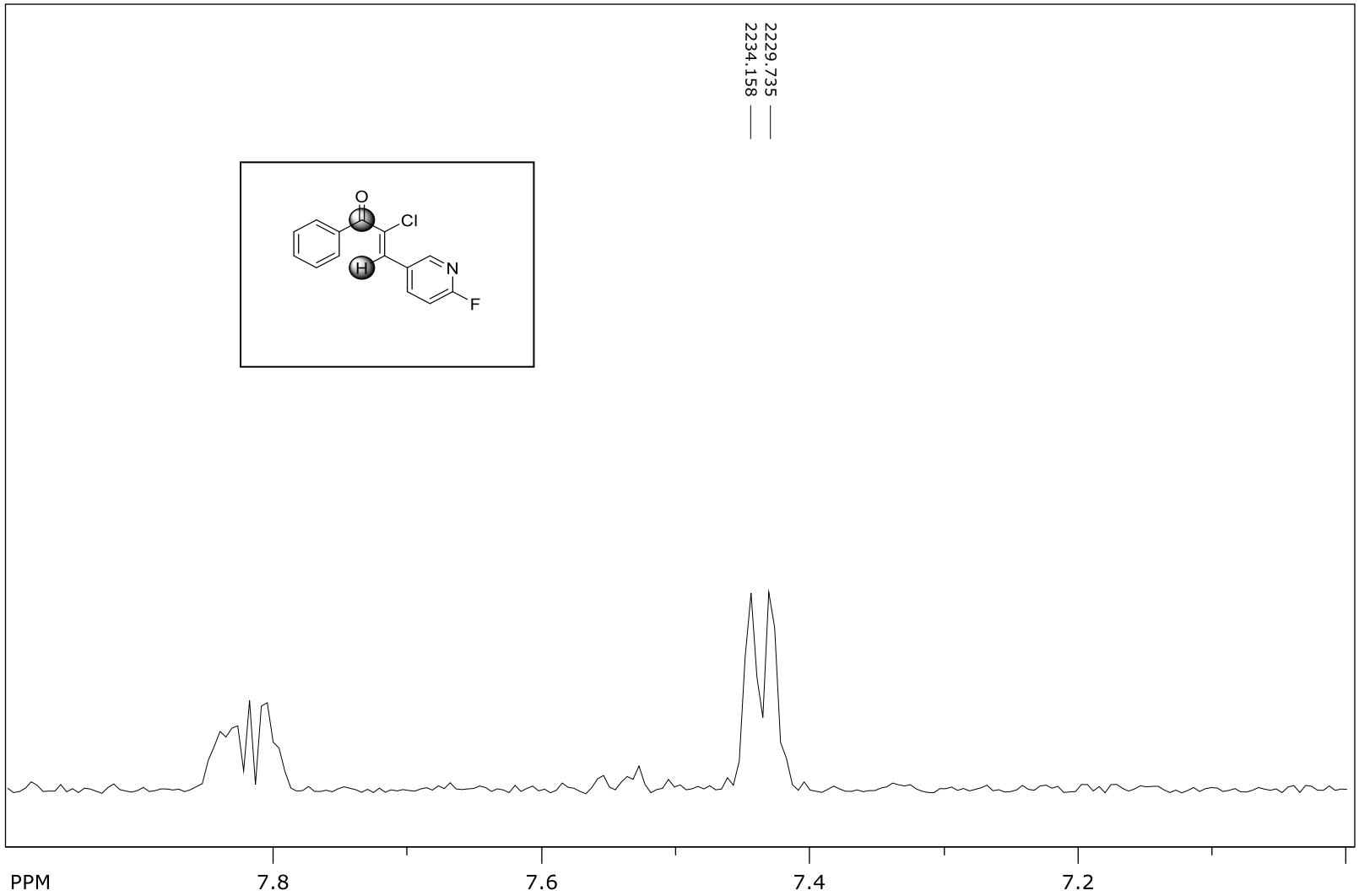

file: ...:\NKC_10_fluoropyridinecis_2\2\ser expt: <hmbcgplpndqf>
transmitter freq.: 300.131421 MHz
time domain size: 4096 points
width: 2705.63 Hz = 9.0148 ppm = 0.660554 Hz/pt
number of scans: 8

freq. of 0 ppm: 300.130006 MHz
processed size: 2048 complex points
LB: 0.000 GF: 0.0000

(2*Z*)-3-(Benzofuran-2-yl)-2-chloro-1-phenylprop-2-en-1-one (***Z*-202**) – ^{1}H NMR

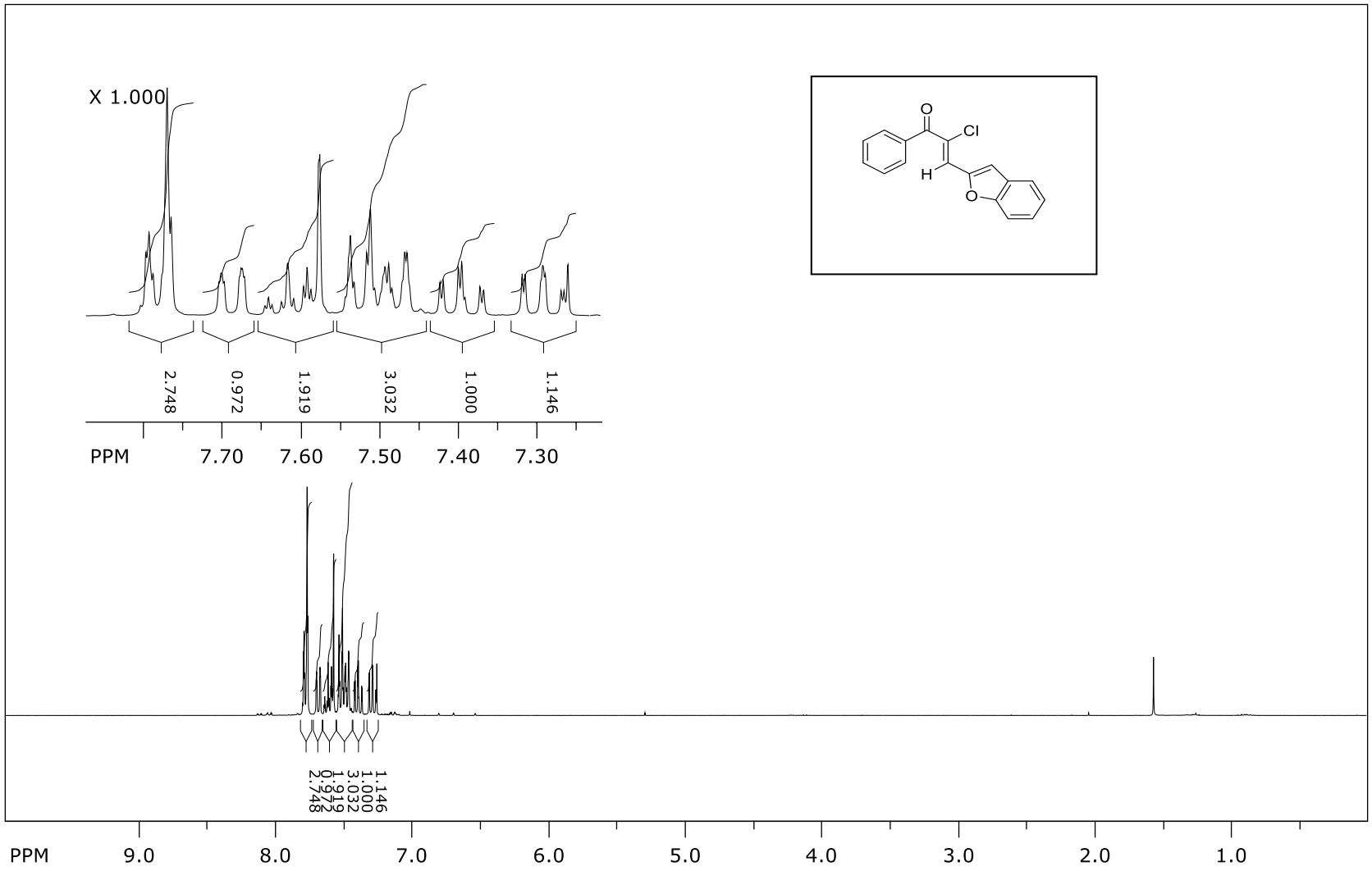

file: D:\NKC_10_benzofurancis\1\fid expt: <zg30>
transmitter freq.: 300.131853 MHz
time domain size: 65536 points
width: 6172.84 Hz = 20.5671 ppm = 0.094190 Hz/pt
number of scans: 16

freq. of 0 ppm: 300.130012 MHz
processed size: 32768 complex points
LB: 0.300 GF: 0.0000

(2*Z*)-3-(Benzofuran-2-yl)-2-chloro-1-phenylprop-2-en-1-one (***Z*-202**) – ^{13}C NMR

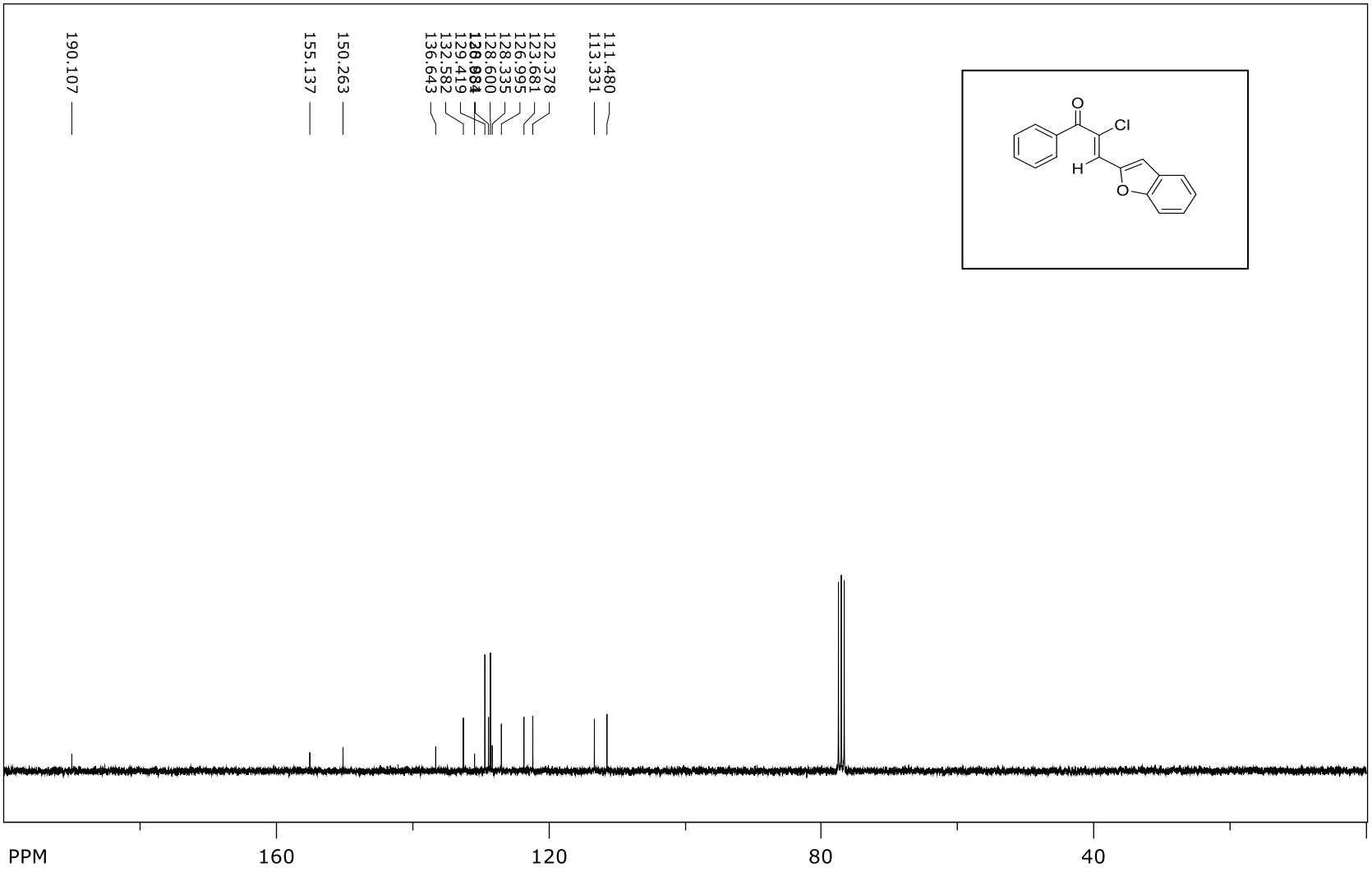

file: D:\NKC_10_benzofurancis\2\fid expt: <zgpg30>
transmitter freq.: 75.475295 MHz
time domain size: 65536 points
width: 17985.61 Hz = 238.2980 ppm = 0.274439 Hz/pt
number of scans: 128

freq. of 0 ppm: 75.467749 MHz
processed size: 32768 complex points
LB: 1.000 GF: 0.0000

(2*Z*)-3-(Benzofuran-2-yl)-2-chloro-1-phenylprop-2-en-1-one (***Z*-202**) - $^{3}J_{C,H}$

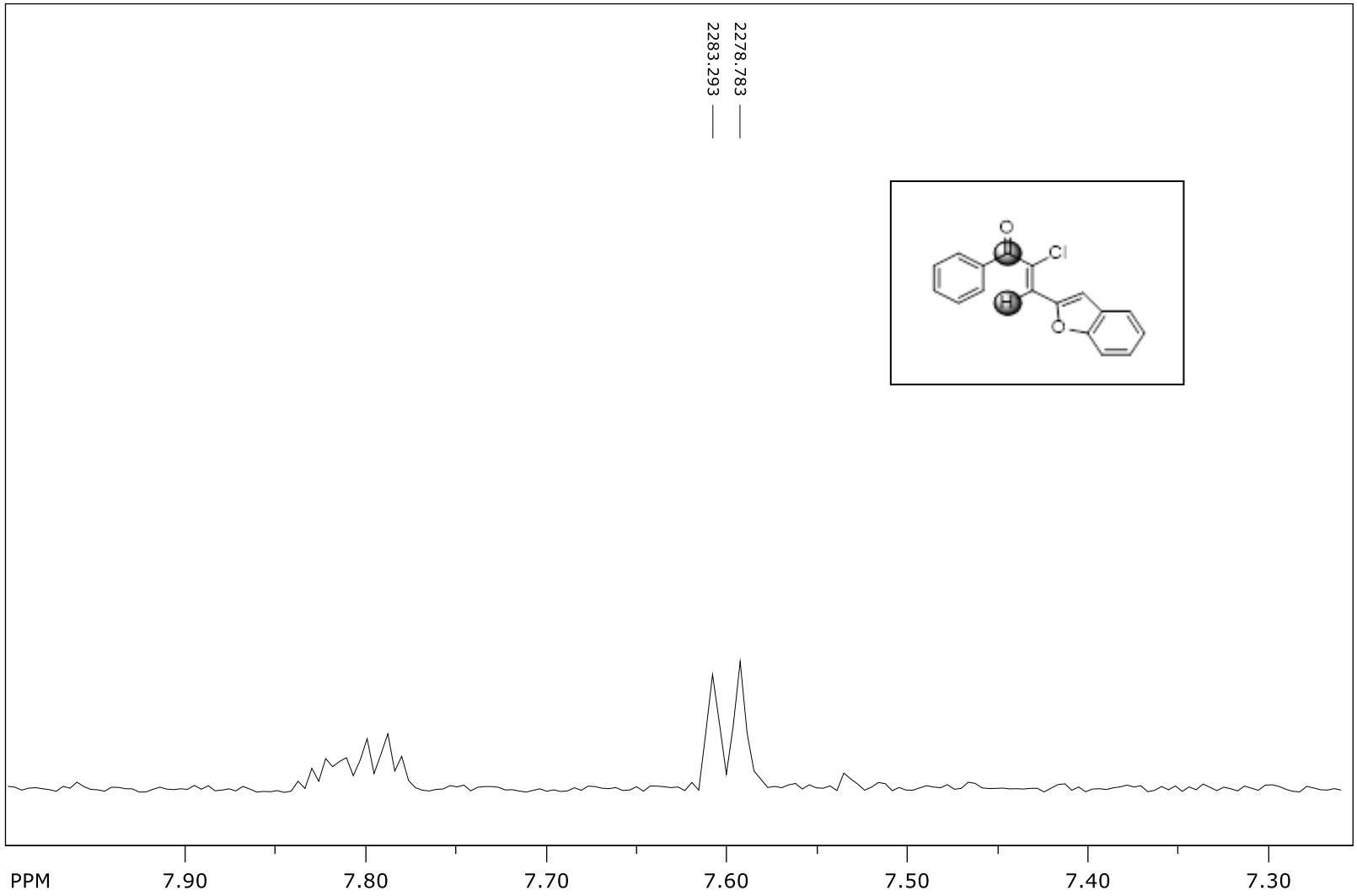

file: D:\NKC_10_benzofurancis\3\ser expt: <hmbcgplpndqf>
transmitter freq.: 300.131417 MHz
time domain size: 4096 points
width: 2354.05 Hz = 7.8434 ppm = 0.574719 Hz/pt
number of scans: 8

freq. of 0 ppm: 300.130006 MHz
processed size: 2048 complex points
LB: 0.000 GF: 0.0000

(2*Z*)-2-Chloro-3-(4-fluorophenyl)-1-phenylprop-2-en-1-one (***Z*-200**) – ^{1}H NMR

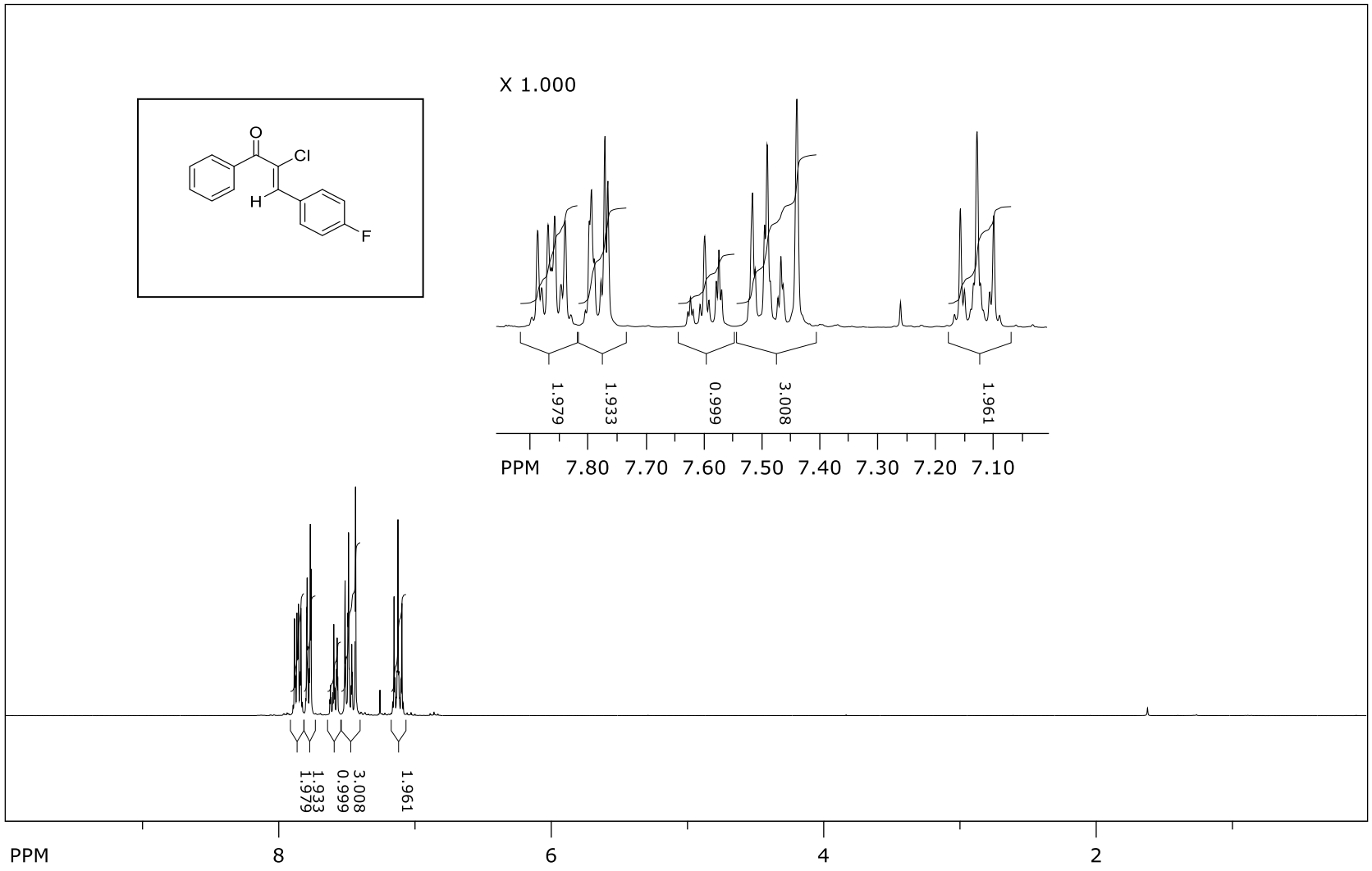

file: D:\NKC_10_23_pfluoro2\1\fid expt: <zg30>
transmitter freq.: 300.131853 MHz
time domain size: 65536 points
width: 6172.84 Hz = 20.5671 ppm = 0.094190 Hz/pt
number of scans: 16

freq. of 0 ppm: 300.130012 MHz
processed size: 32768 complex points
LB: 0.300 GF: 0.0000

(2*Z*)-2-Chloro-3-(4-fluorophenyl)-1-phenylprop-2-en-1-one (***Z*-200**) – ^{13}C NMR

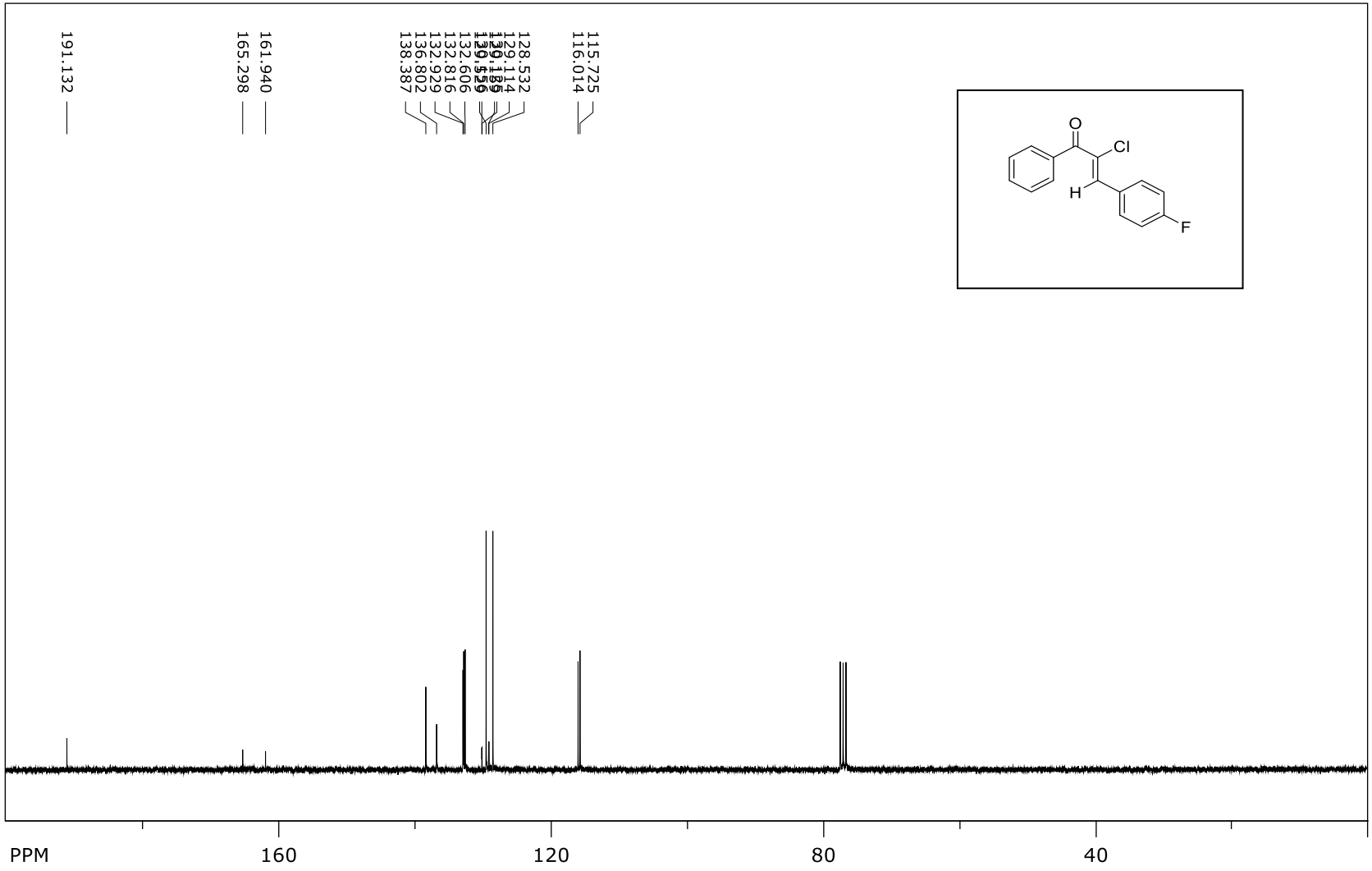

file: D:\NKC_10_23_pfluoro2\2\fid expt: <zgpg30>
transmitter freq.: 75.475295 MHz
time domain size: 65536 points
width: 17985.61 Hz = 238.2980 ppm = 0.274439 Hz/pt
number of scans: 128

freq. of 0 ppm: 75.467749 MHz
processed size: 32768 complex points
LB: 1.000 GF: 0.0000

(2*Z*)-2-Chloro-3-(4-fluorophenyl)-1-phenylprop-2-en-1-one (***Z*-200**) - $^{3}J_{C,H}$

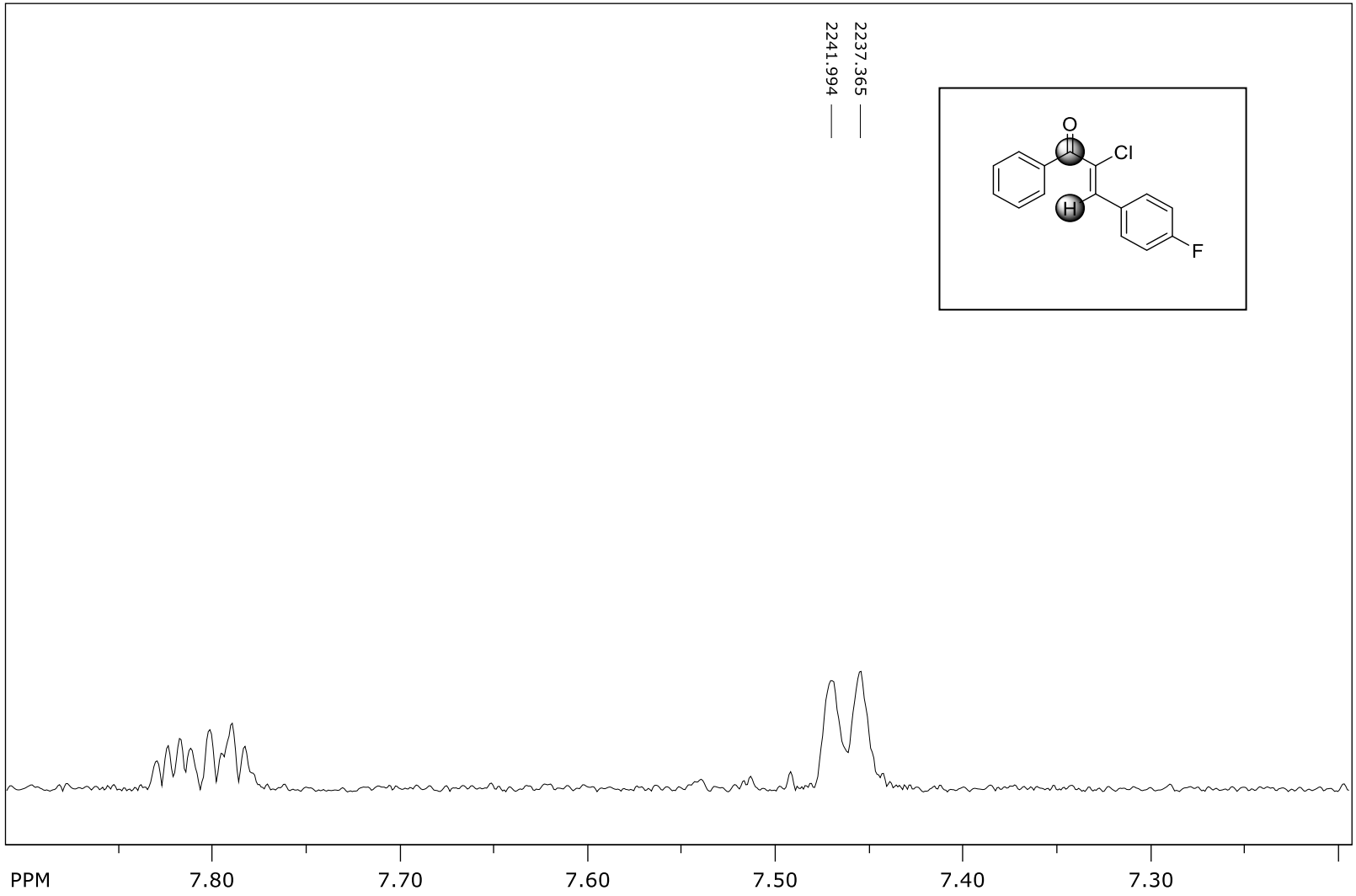

file: D:\NKC_10_23_pfluoro2\4\ser expt: <hmbcgplpndqf>
transmitter freq.: 300.132259 MHz
time domain size: 2008 points
width: 524.33 Hz = 1.7470 ppm = 0.261120 Hz/pt
number of scans: 8

freq. of 0 ppm: 300.130006 MHz
processed size: 2048 complex points
LB: 0.000 GF: 0.0000

(2*E*)-2-Chloro-3-(4-methoxyphenyl)-1-phenylprop-2-en-1-ol (***Z*-220**) – ^{1}H NMR

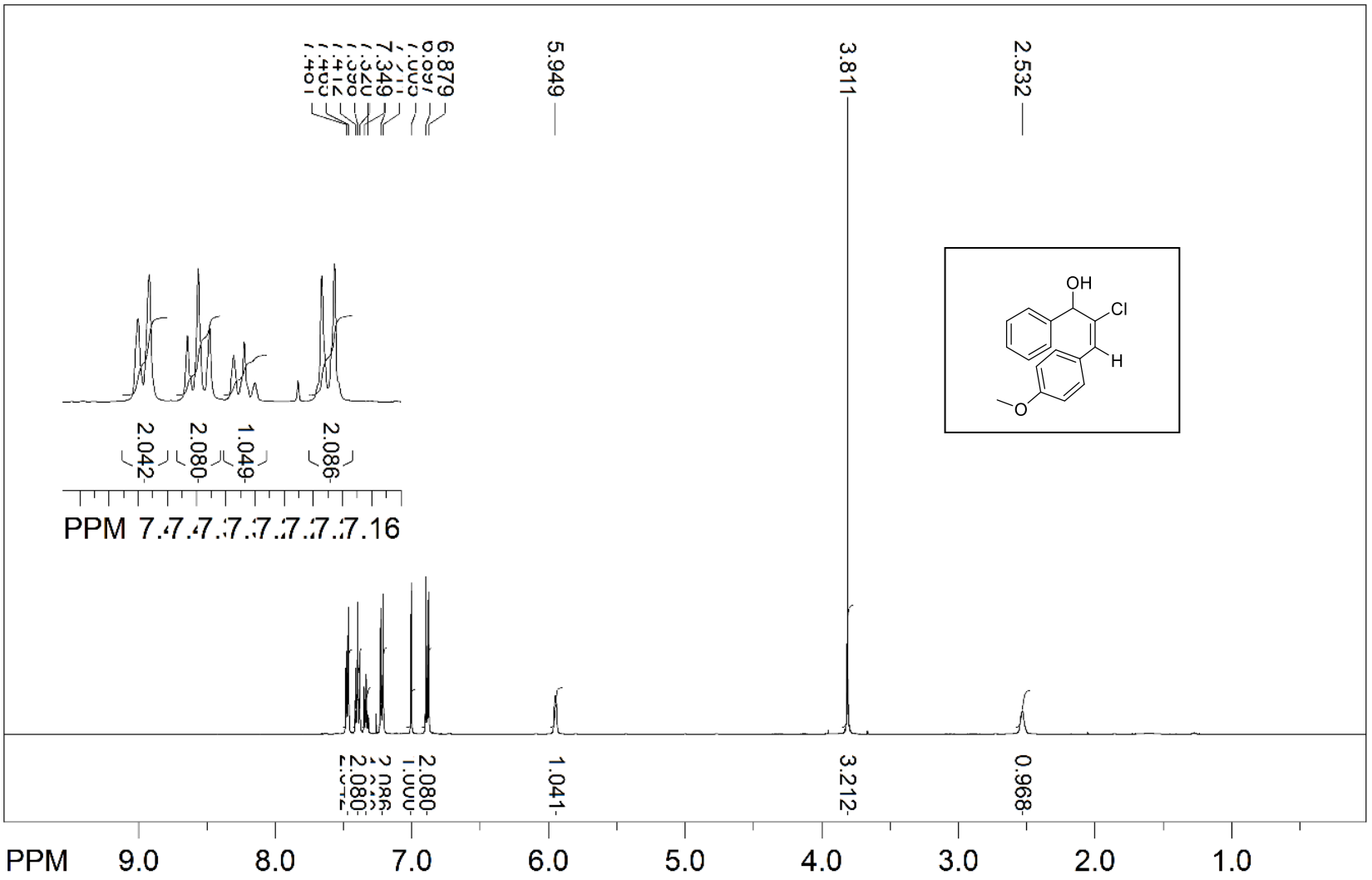

file: ...ehal\Desktop\NKC 12 46 luche\1\fid expt: <zg30>
transmitter freq.: 500.133089 MHz
time domain size: 65536 points
width: 10000.00 Hz = 19.9947 ppm = 0.152588 Hz/pt
number of scans: 16

freq of 0 ppm: 500.130000 MHz
processed size: 65536 points
LB: 0.300 GF: 0.0000
Hz/cm: 199.514 ppm/cm: 0.39892

(2*E*)-2-Chloro-3-(4-methoxyphenyl)-1-phenylprop-2-en-1-ol (***Z*-220**) - ^{13}C NMR

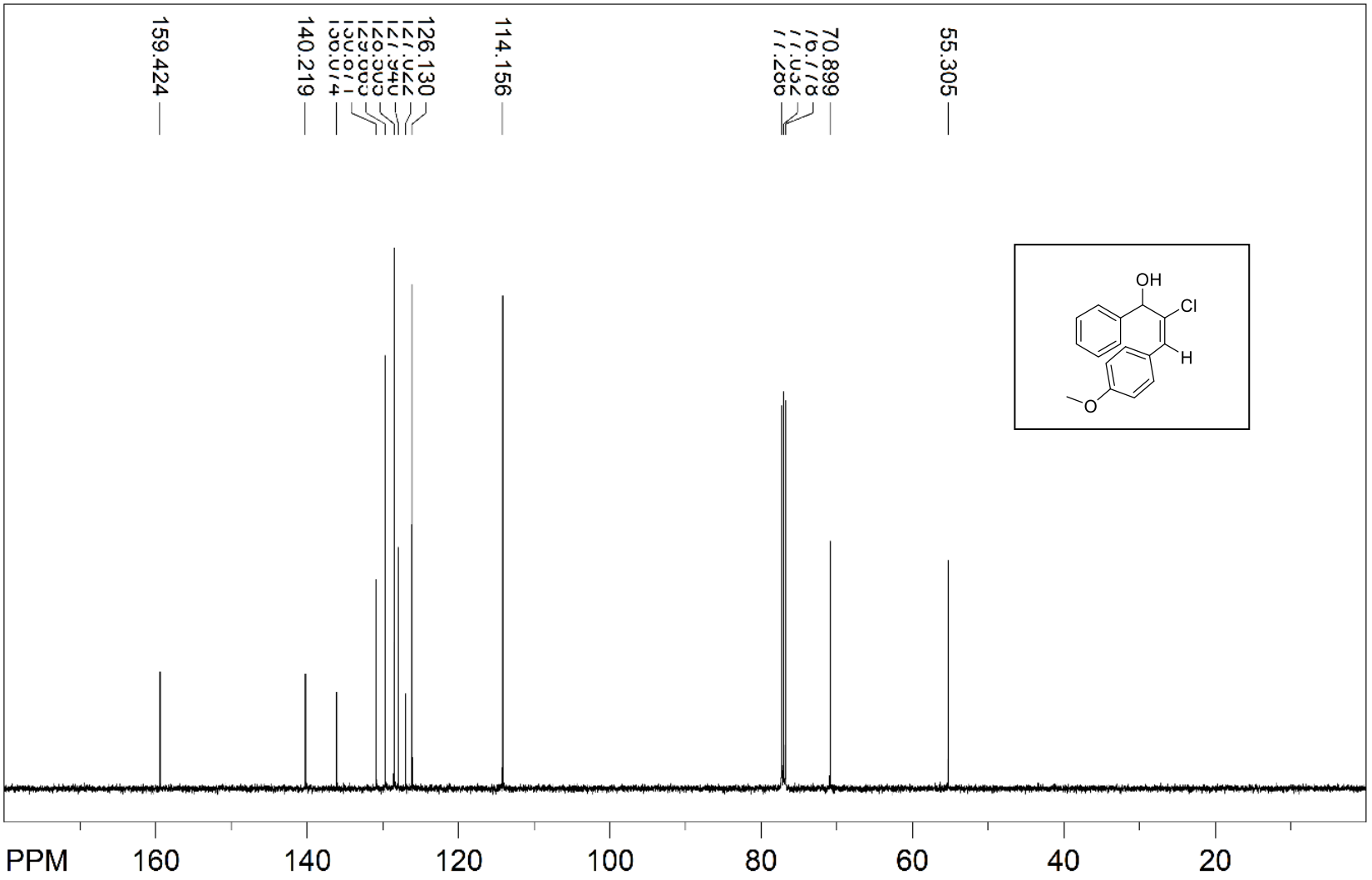

file: ...ehal\Desktop\NKC 12 46 luche\2\fid expt: <zgpg30>
transmitter freq.: 125.770364 MHz
time domain size: 65536 points
width: 29761.91 Hz = 236.6369 ppm = 0.454131 Hz/pt
number of scans: 183

freq of 0 ppm: 125.757789 MHz
processed size: 32768 points
LB: 1.000 GF: 0.0000
Hz/cm: 905.433 ppm/cm: 7.19909

(2*E*)-2-Chloro-3-(4-methoxyphenyl)-1-phenylprop-2-en-1-ol (***Z*-220**) - $^{3}J_{C,H}$

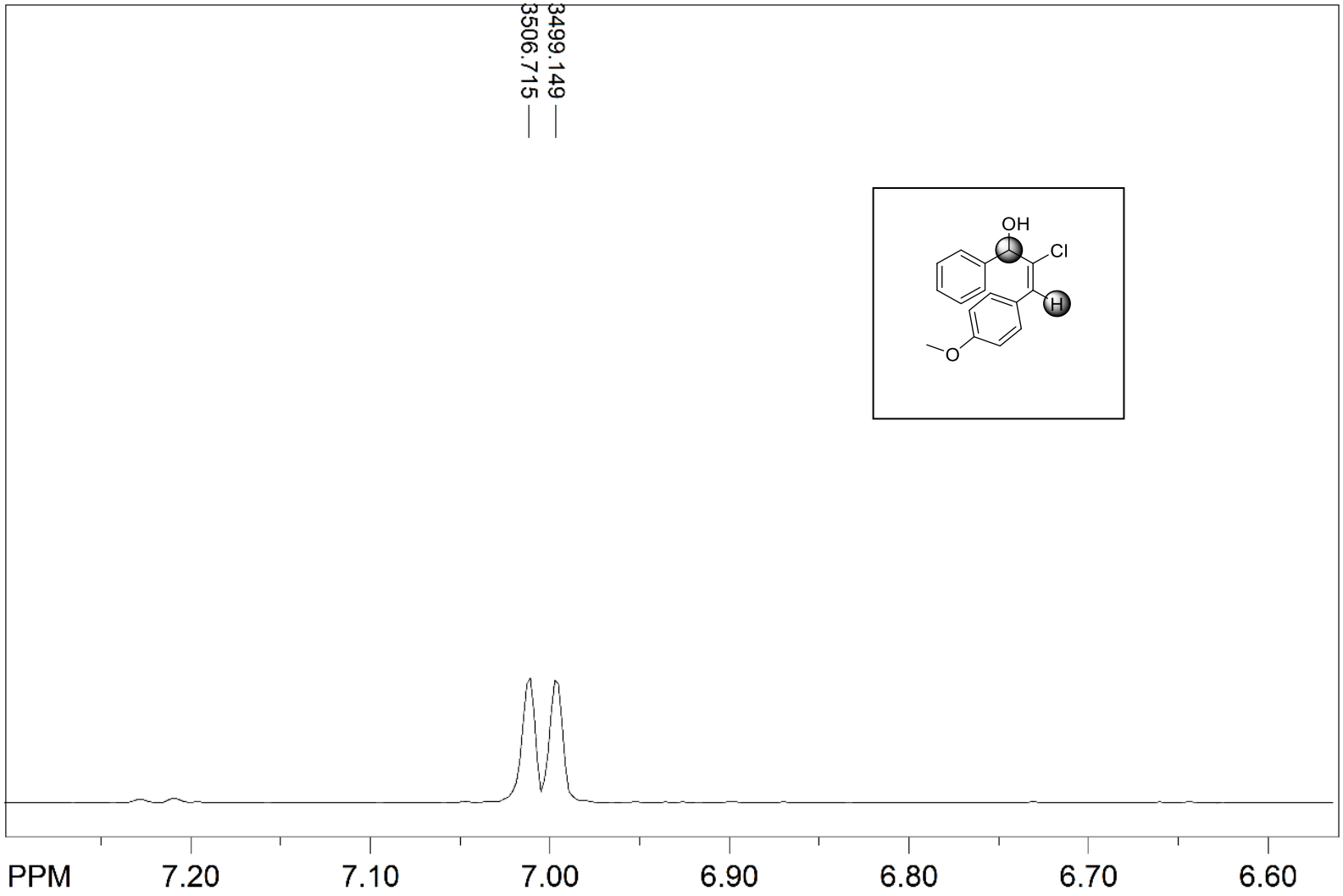

file: ...ehal\Desktop\NKC 12 46 luche\3\ser expt: <hmbcgplpnd freq of 0 ppm: 500.130000 MHz
transmitter freq.: 500.132001 MHz processed size: 4096 points
time domain size: 4096 points LB: 0.000 GF: 0.0000
width: 4000.00 Hz = 7.9979 ppm = 0.976563 Hz/pt Hz/cm: 15.468 ppm/cm: 0.03093
number of scans: 8

(***E*-2**) with 2.5 mol% $Pd_2(dba)_3$ in d_8-toluene at 350K (first scan and last scan after~5 hr)

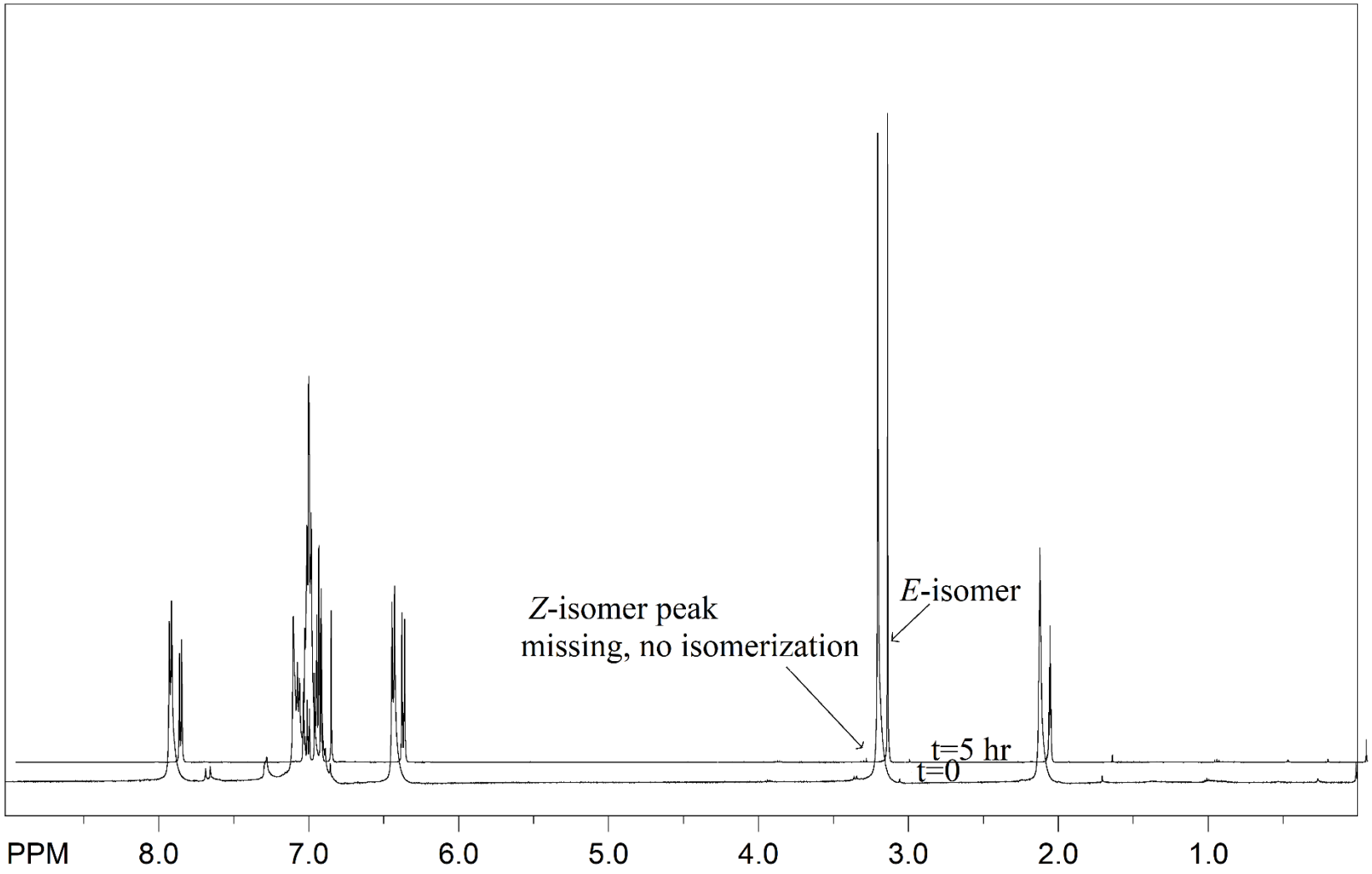

file: ...s\chehal\Desktop\NKC 12 60\101\fid expt: <zg30>
transmitter freq.: 500.133001 MHz
time domain size: 65536 points
width: 10000.00 Hz = 19.9947 ppm = 0.152588 Hz/pt
number of scans: 4

freq of 0 ppm: 500.130000 MHz
processed size: 65536 points
LB: 0.300 GF: 0.0000
Hz/cm: 180.476 ppm/cm: 0.36086

(***E*-2**) with 5 mol% DPEphos in d_8-toluene at 350 K (first scan and last scan after ~ 3.5 hr)

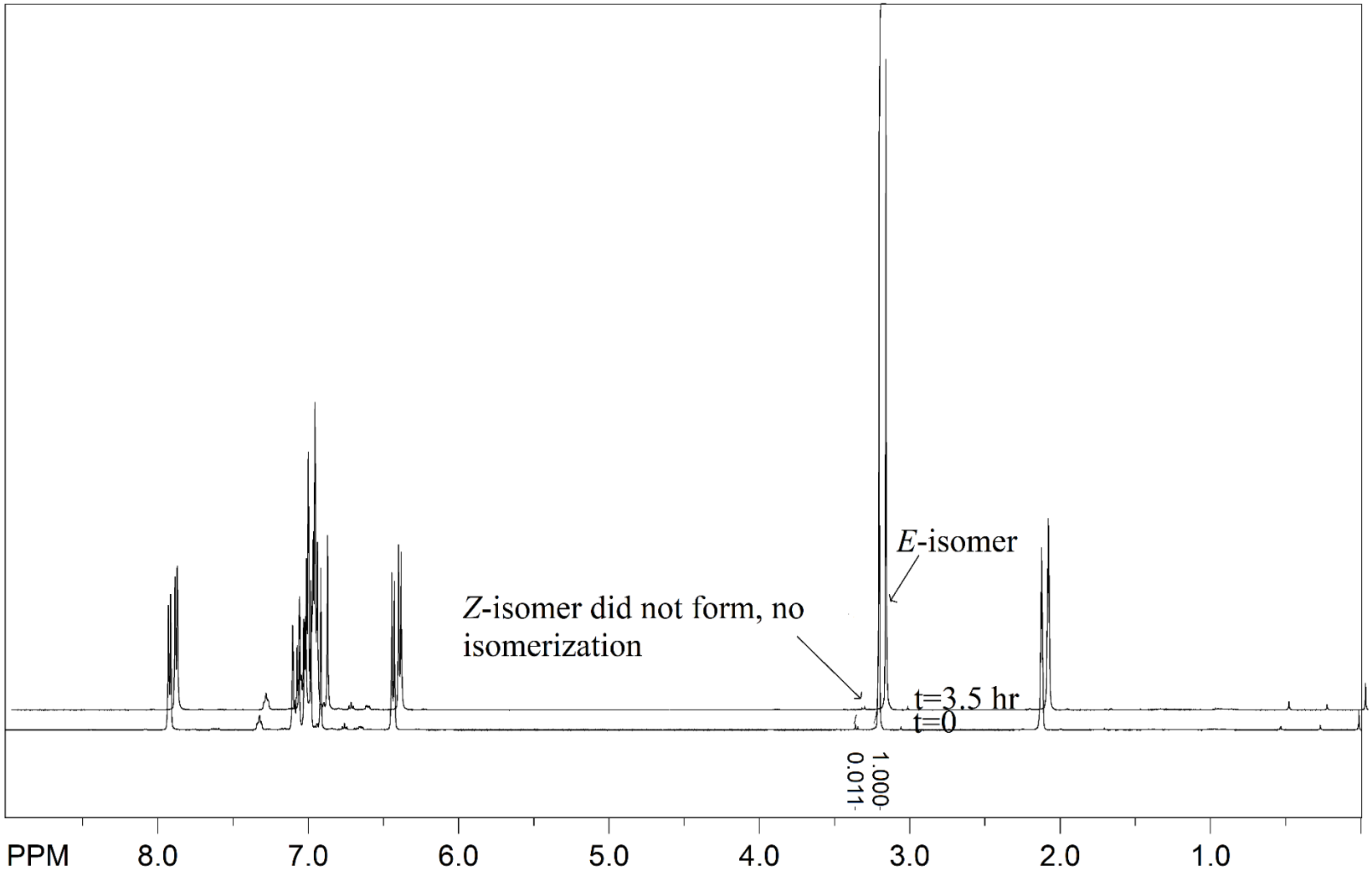

file: ...rs\chehal\Desktop\NKC 12 61\67\fid expt: <zg30>
transmitter freq.: 500.133001 MHz
time domain size: 65536 points
width: 10000.00 Hz = 19.9947 ppm = 0.152588 Hz/pt
number of scans: 4

freq of 0 ppm: 500.130000 MHz
processed size: 65536 points
LB: 0.300 GF: 0.0000
Hz/cm: 180.476 ppm/cm: 0.36086

(***E*-2**) with 5 mol% TEMPO and 5mol% Pd/DPEphos in d_8-toluene at 313 K (t=0 and t=3.5 hr)

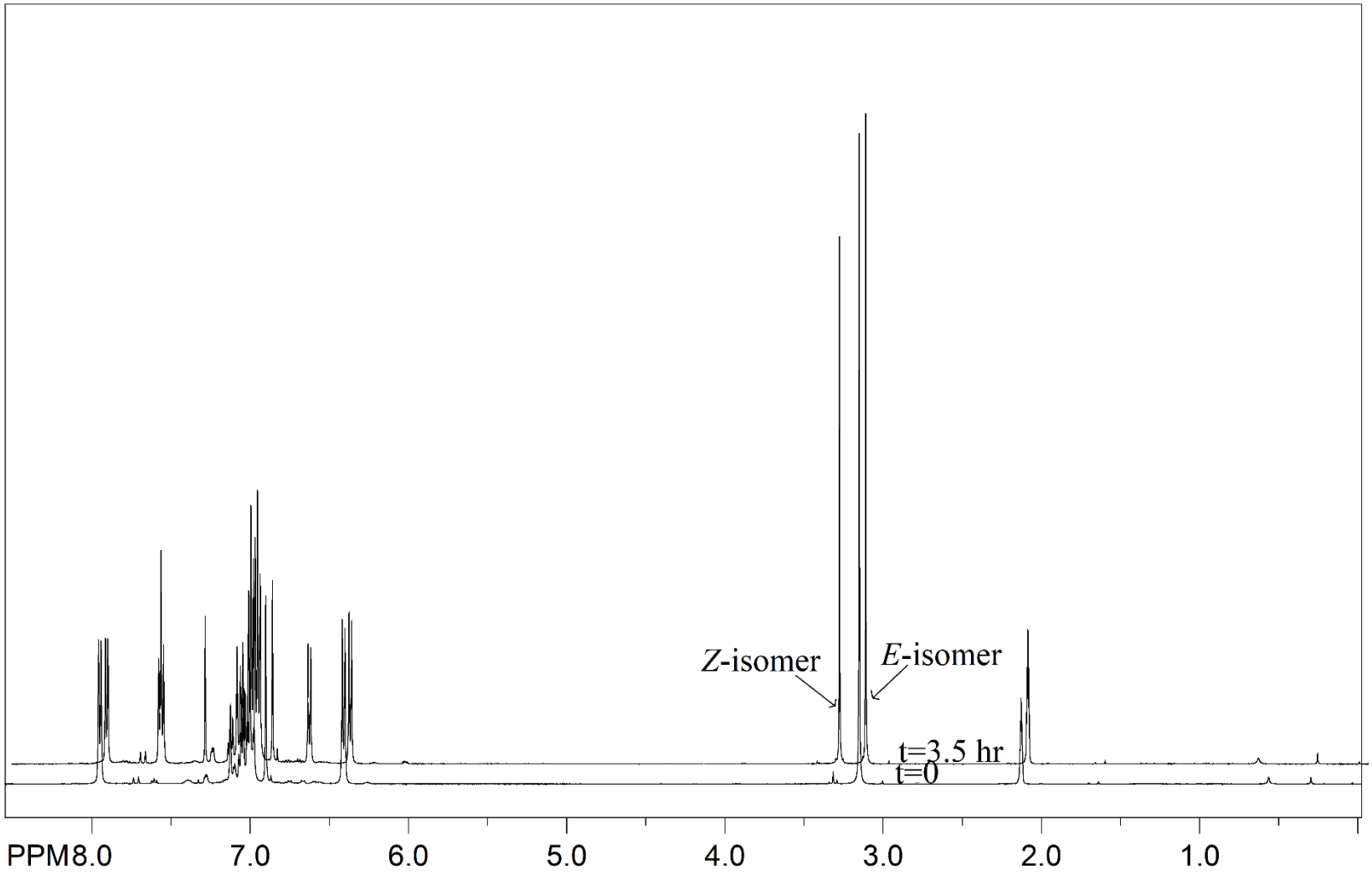

file: ...hehal\Desktop\NKC 12 42 rxn\70\fid expt: <zg30>
transmitter freq.: 500.133001 MHz
time domain size: 65536 points
width: 10000.00 Hz = 19.9947 ppm = 0.152588 Hz/pt
number of scans: 4

freq of 0 ppm: 500.130000 MHz
processed size: 65536 points
LB: 0.300 GF: 0.0000
Hz/cm: 171.540 ppm/cm: 0.34299

(***E*-2**) with 5mol% Pd/DPEphos in d_8-toluene at 313 K (at t=0 and t=3.5 hr)

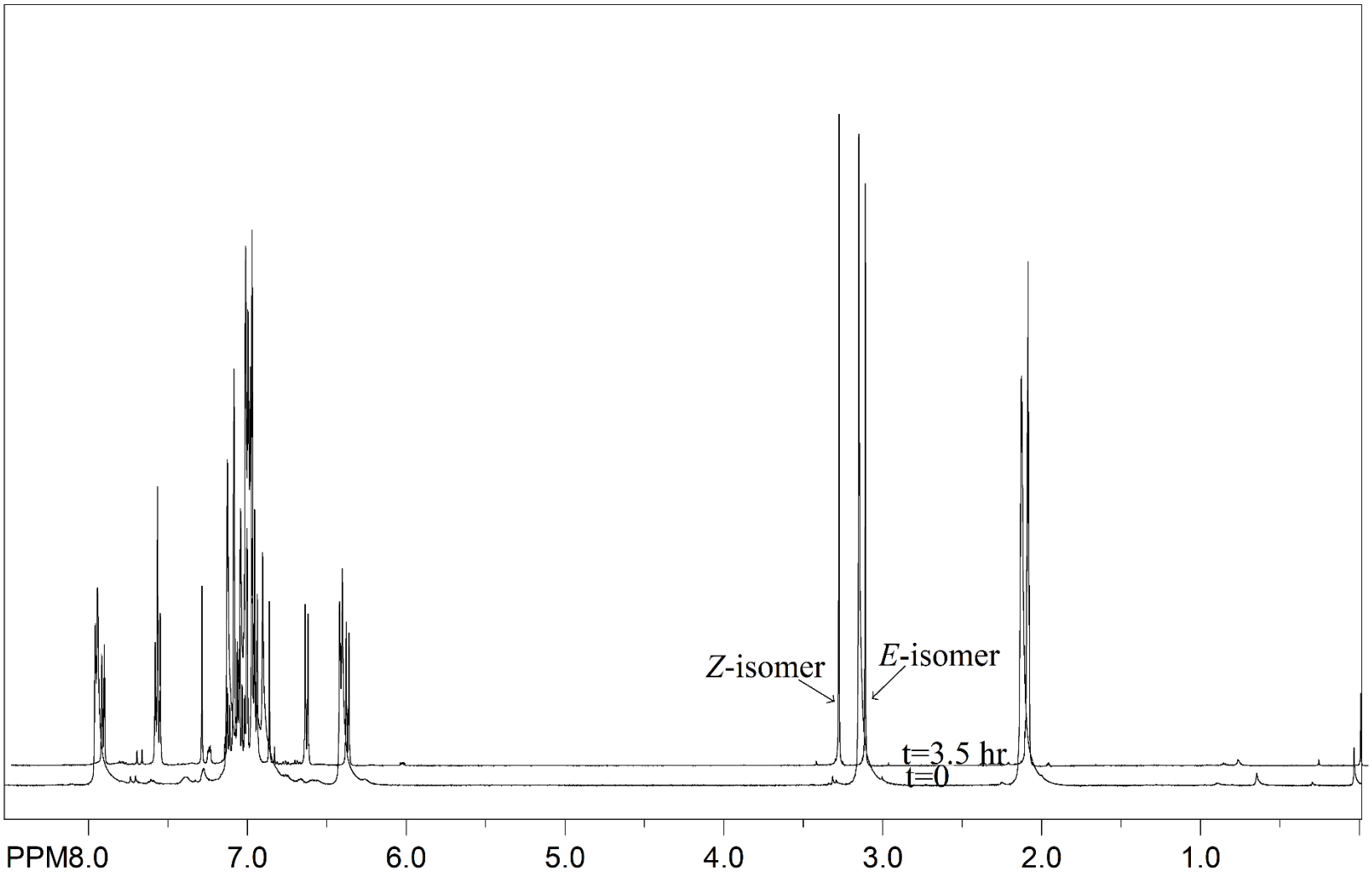

file: ...rs\chehal\Desktop\NKC 12 25\71\fid expt: <zg30>
transmitter freq.: 500.133001 MHz
time domain size: 65536 points
width: 10000.00 Hz = 19.9947 ppm = 0.152588 Hz/pt
number of scans: 4

freq of 0 ppm: 500.130000 MHz
processed size: 65536 points
LB: 0.300 GF: 0.0000
Hz/cm: 170.957 ppm/cm: 0.34182

(***E*-1**) with 5 mol% DPEphos at 350 K (after 5 hr)

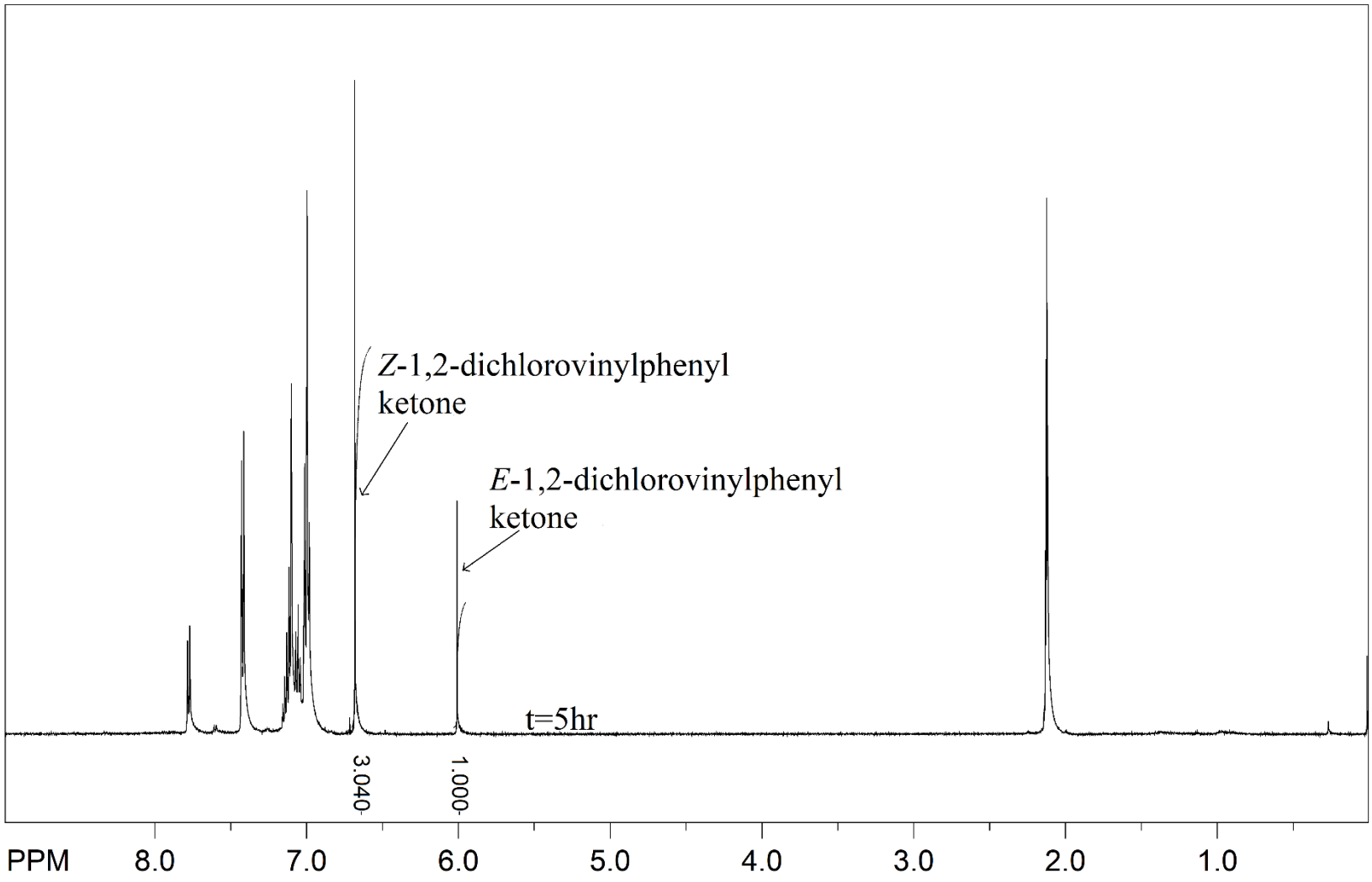

file: ...s\chehal\Desktop\NKC 12 62\101\fid expt: <zg30>
transmitter freq.: 500.133001 MHz
time domain size: 65536 points
width: 10000.00 Hz = 19.9947 ppm = 0.152588 Hz/pt
number of scans: 4

freq of 0 ppm: 500.130000 MHz
processed size: 65536 points
LB: 0.000 GF: 0.0000
Hz/cm: 179.699 ppm/cm: 0.35930

Reduced ketone functionality (**220**) with 5 mol% Pd/DPEphos at 350 K (after 3.5 hr)

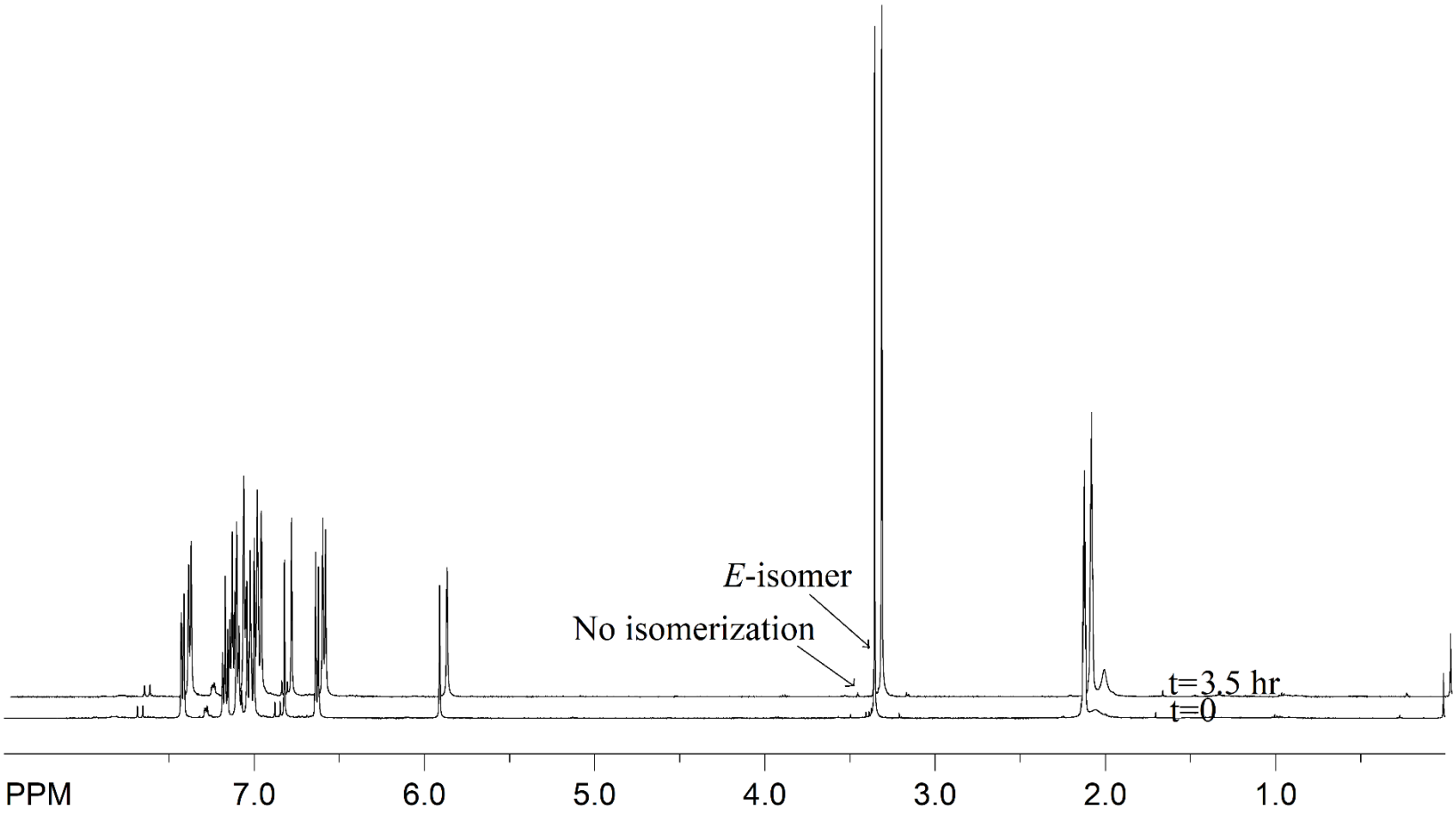

file: ...rs\chehal\Desktop\NKC 12 53\71\fid expt: <zg30>
transmitter freq.: 500.133001 MHz
time domain size: 65536 points
width: 10000.00 Hz = 19.9947 ppm = 0.152588 Hz/pt
number of scans: 4

freq of 0 ppm: 500.130000 MHz
processed size: 65536 points
LB: 0.300 GF: 0.0000
Hz/cm: 169.403 ppm/cm: 0.33872

(***E*-2**) with 5 mol% Pd/DPEphos and 1 mol% dimethyl maleate at 313 K (at t=0 and t=5 hr)

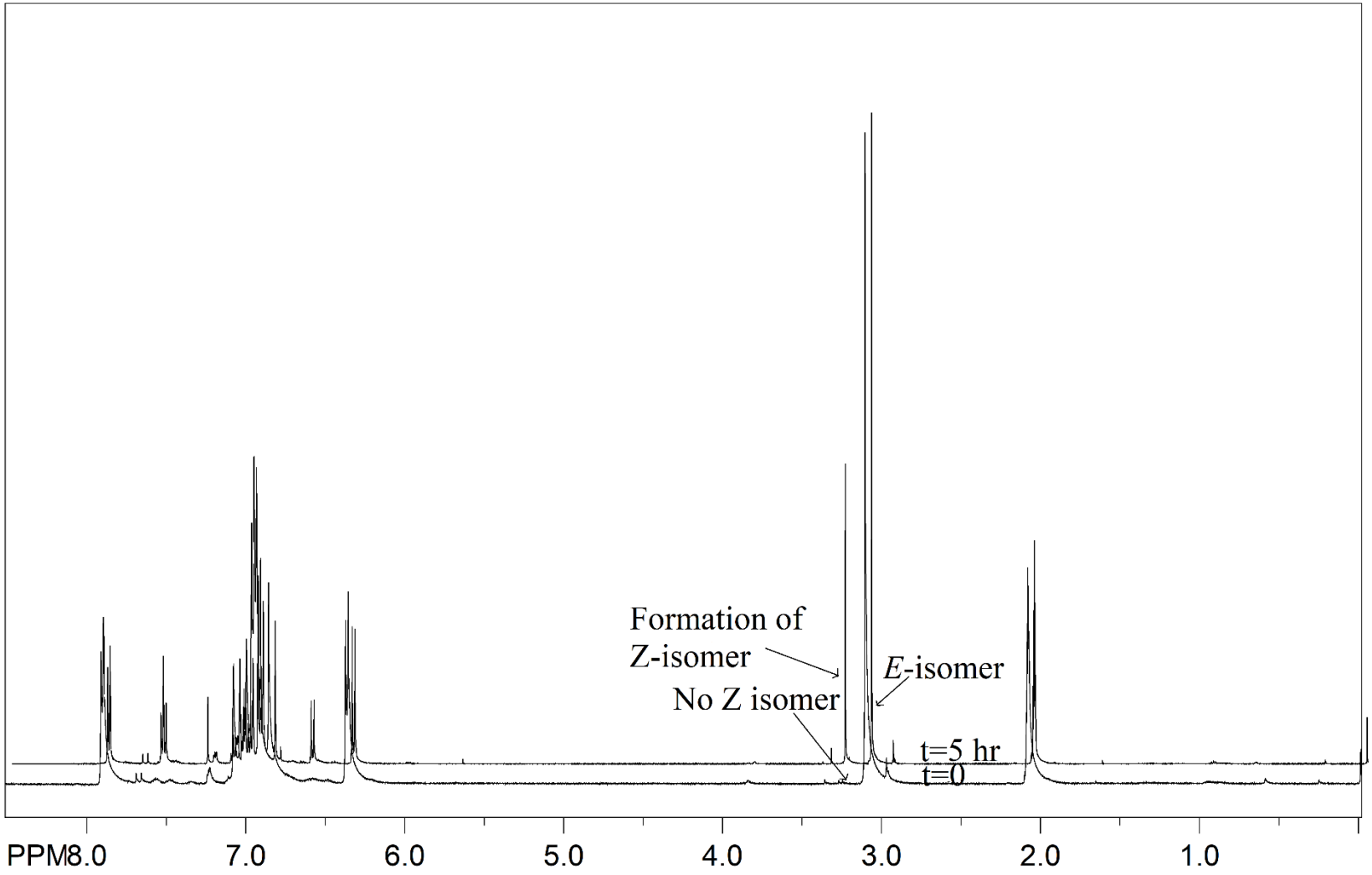

file: ...s\chehal\Desktop\NKC 12 59\101\fid expt: <zg30>
transmitter freq.: 500.133001 MHz
time domain size: 65536 points
width: 10000.00 Hz = 19.9947 ppm = 0.152588 Hz/pt
number of scans: 4

freq of 0 ppm: 500.130022 MHz
processed size: 65536 points
LB: 0.000 GF: 0.0000
Hz/cm: 170.763 ppm/cm: 0.34143

(***E*-2**) with 5 mol% Pd/DPEphos and 1 eq dimethyl maleate (***E*-148**) at 313 K (at t=0 and t=3.5 hr)

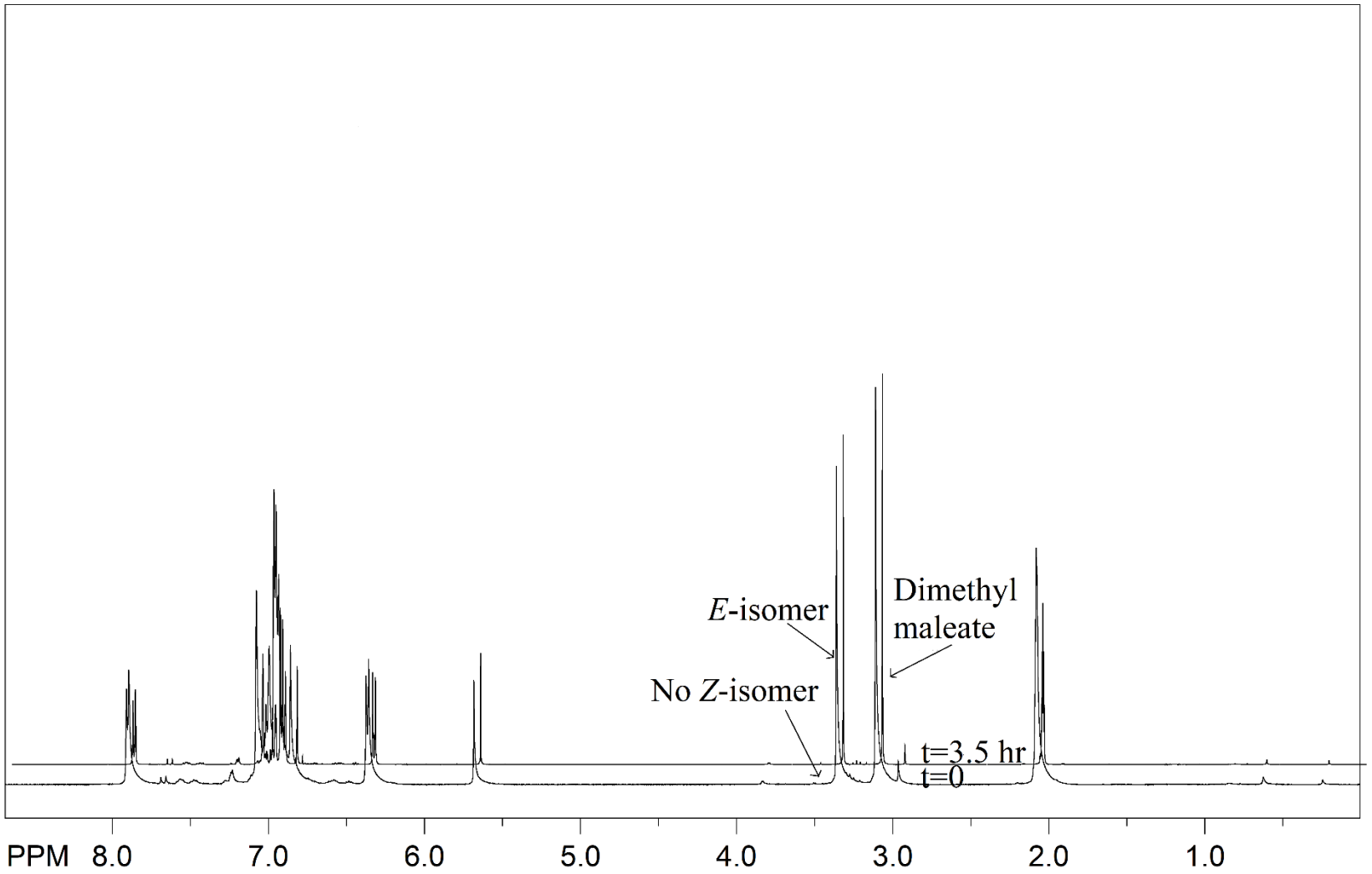

file: ...ers\chehal\Desktop\NKC_12_34\2\fid expt: <zg30>
transmitter freq.: 500.133001 MHz
time domain size: 65536 points
width: 10000.00 Hz = 19.9947 ppm = 0.152588 Hz/pt
number of scans: 4

freq of 0 ppm: 500.130024 MHz
processed size: 65536 points
LB: 0.000 GF: 0.0000
Hz/cm: 173.677 ppm/cm: 0.34726

(***E*-2**) with 5 mol% Pd/DPEphos and 0.5 eq dimethyl maleate (***E*-148**) at 313 K (at t=0 and t=3.5 hr)

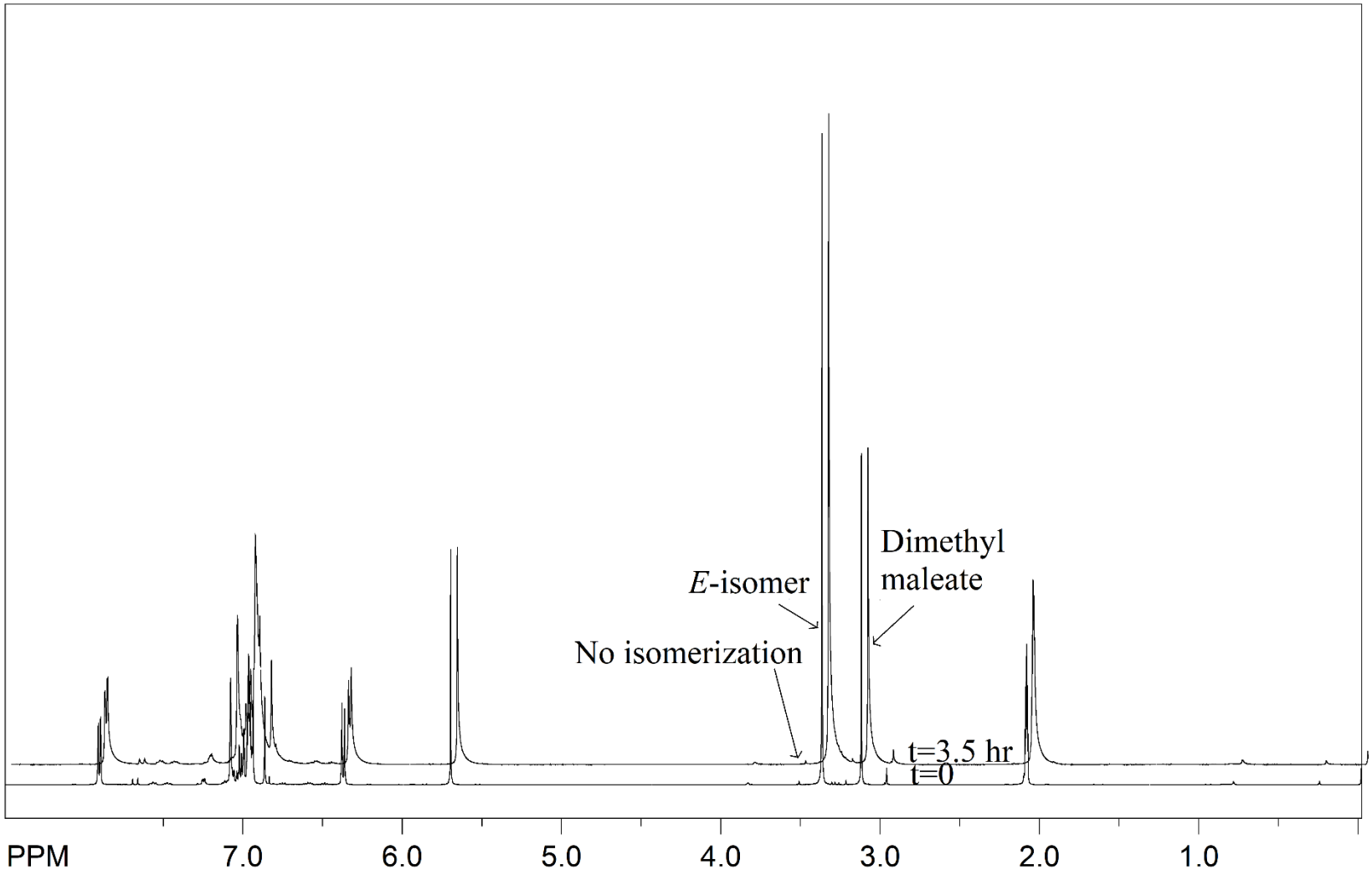

file: ...rs\chehal\Desktop\NKC 12 35\71\fid expt: <zg30>
transmitter freq.: 500.133001 MHz
time domain size: 65536 points
width: 10000.00 Hz = 19.9947 ppm = 0.152588 Hz/pt
number of scans: 4

freq of 0 ppm: 500.130023 MHz
processed size: 65536 points
LB: 0.000 GF: 0.0000
Hz/cm: 170.374 ppm/cm: 0.34066

Cis-stilbene (***Z*-161**) with 5 mol% Pd/DPEphos at 313 K (at t=0 and t=3.5 hr)

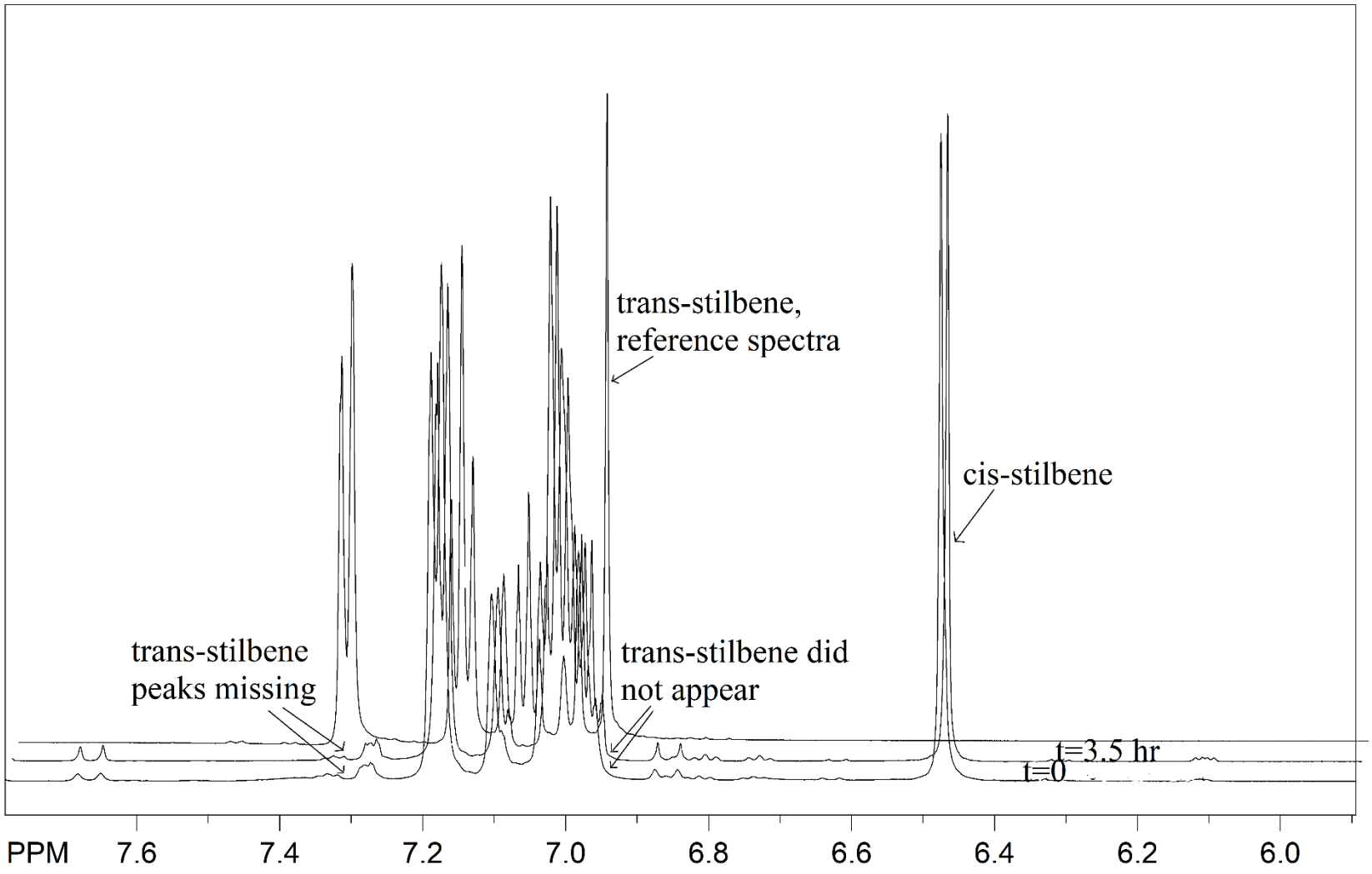

file: ...ers\chehal\Desktop\NKC 12 54\1\fid expt: <zg30>
transmitter freq.: 500.133001 MHz
time domain size: 65536 points
width: 10000.00 Hz = 19.9947 ppm = 0.152588 Hz/pt
number of scans: 4

freq of 0 ppm: 500.130000 MHz
processed size: 65536 points
LB: 0.300 GF: 0.0000
Hz/cm: 37.809 ppm/cm: 0.07560

(***E*-2**) with 5 mol% Pd/DPEphos and 1 eq cis-stilbene (***Z*-161**) at at 313 K (at t=0 and t=3.5 hr)

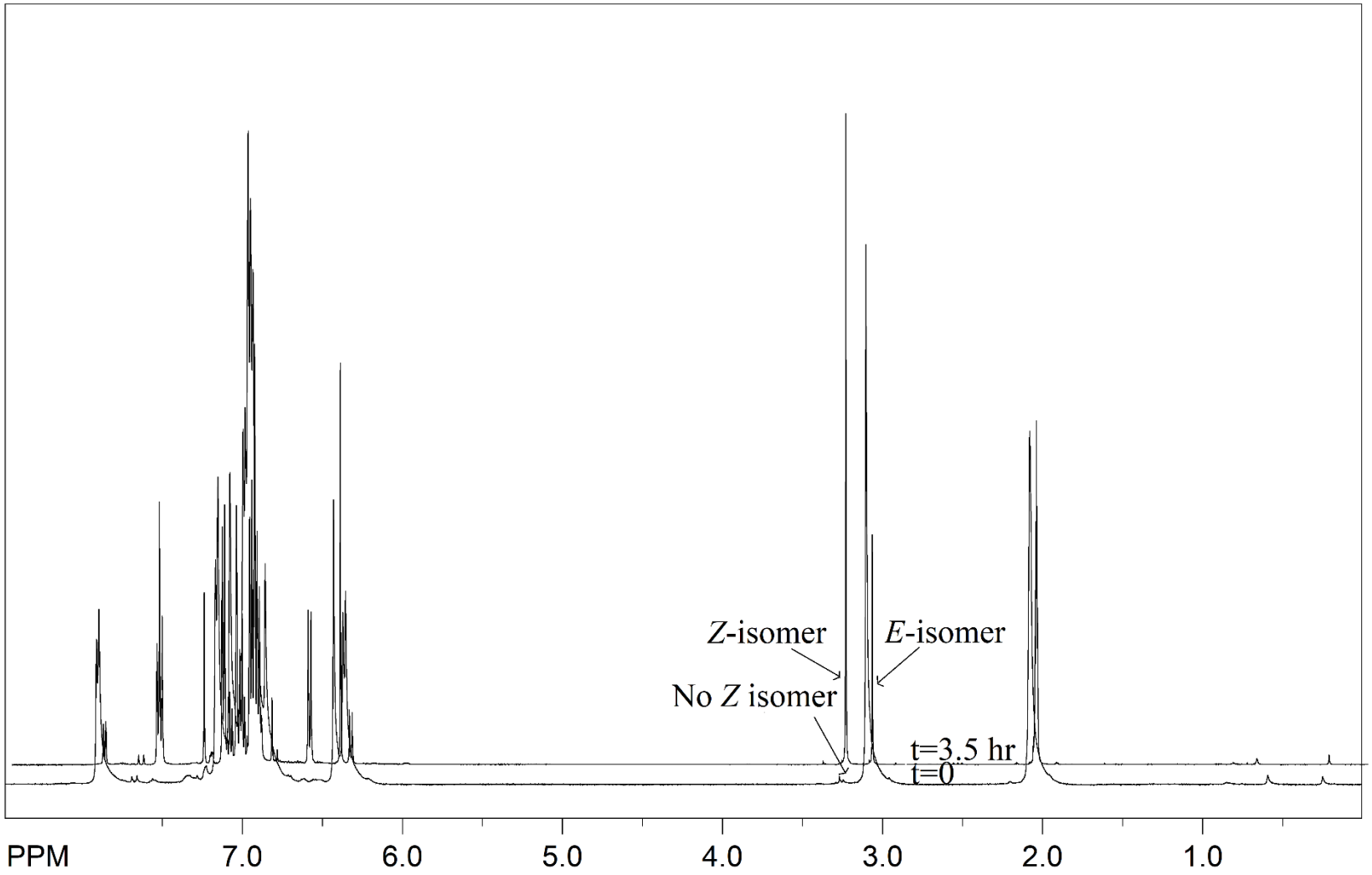

file: ...rs\chehal\Desktop\NKC 12 36\71\fid expt: <zg30>
transmitter freq.: 500.133001 MHz
time domain size: 65536 points
width: 10000.00 Hz = 19.9947 ppm = 0.152588 Hz/pt
number of scans: 4

freq of 0 ppm: 500.130024 MHz
processed size: 65536 points
LB: 0.000 GF: 0.0000
Hz/cm: 169.597 ppm/cm: 0.33910

(***E*-1**) and (***E*-2**) with 5 mol% Pd/DPEphos at 350 K (at t=0 and t=3.5 hr)

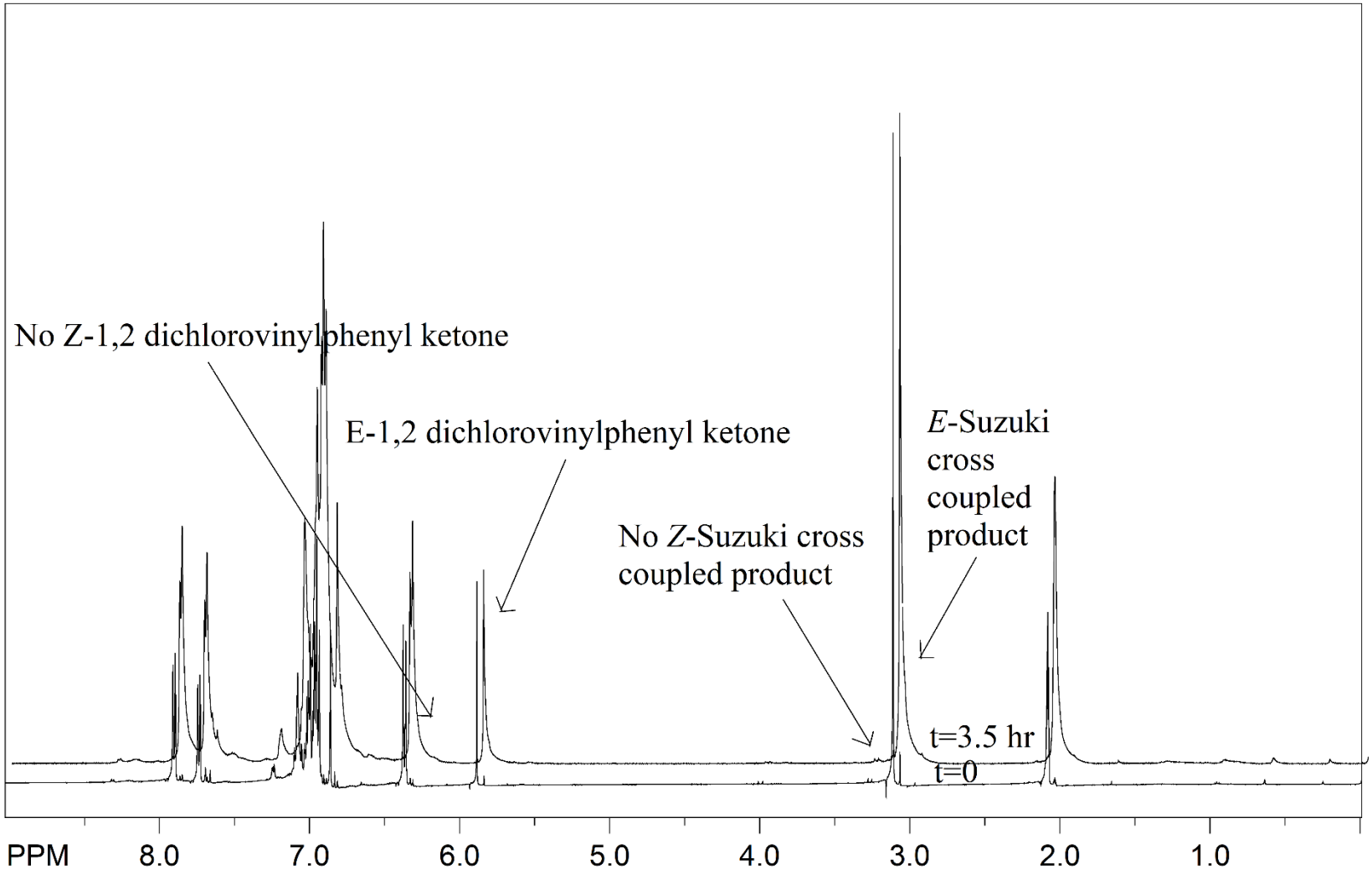

file: ...rs\chehal\Desktop\NKC 12 56\71\fid expt: <zg30>
transmitter freq.: 500.133001 MHz
time domain size: 65536 points
width: 10000.00 Hz = 19.9947 ppm = 0.152588 Hz/pt
number of scans: 4

freq of 0 ppm: 500.130023 MHz
processed size: 65536 points
LB: 0.300 GF: 0.0000
Hz/cm: 180.864 ppm/cm: 0.36163

(3*E*)-3,4-Dichloro-2-(dimethylamino)-2-phenylbut-3-enenitrile (***E*-167**).

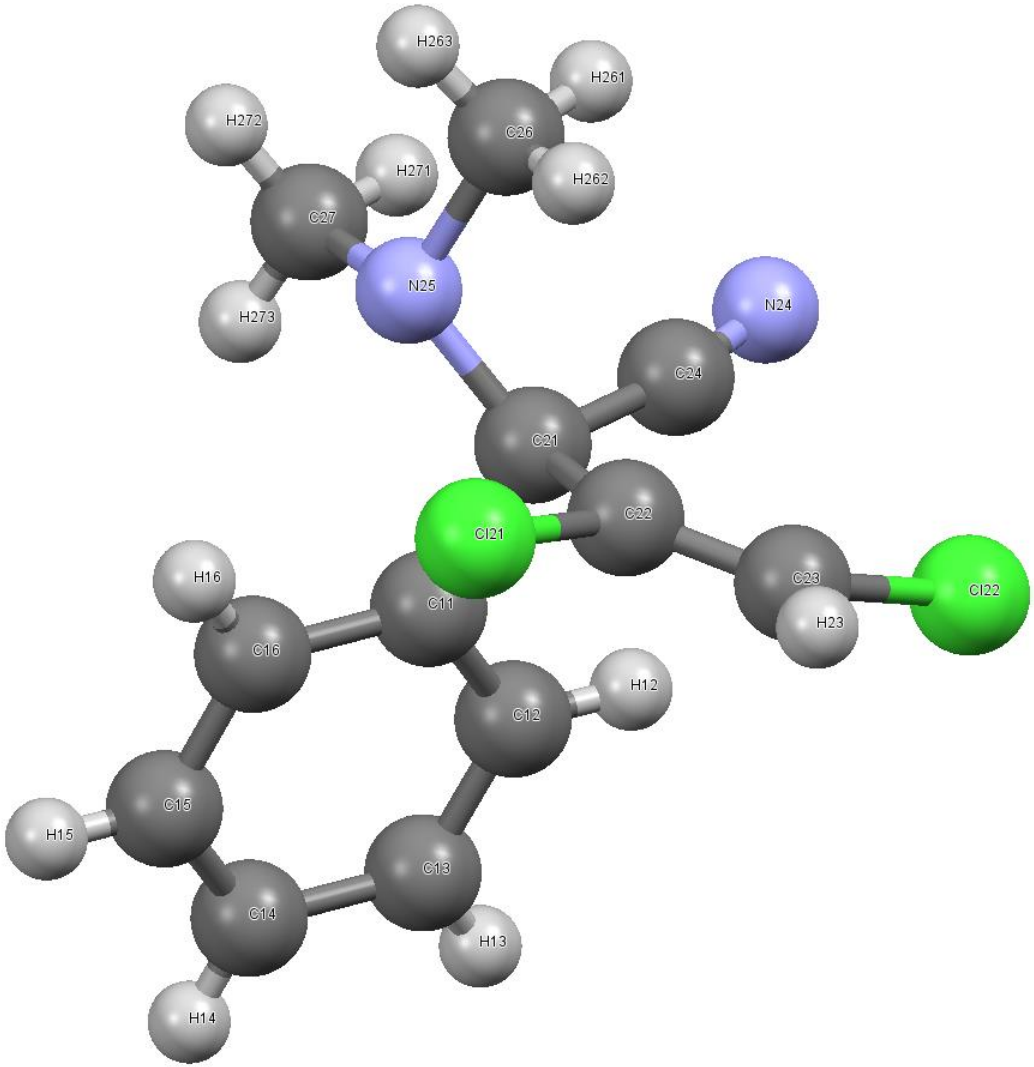

Molecular formula - $C_{12}H_{12}Cl_2N_2$

Molecular Mass - 255.14

Symmetry cell setting – monoclinic

Cell length - a = 13.368(5), b= 7.287(2), c = 14.142(5) Å

Cell angle - α= 90.0, β= 113.436(8), γ= 90.0,

Cell volume, U = 1264.0(7) $Å^3$

Cell measurement temperature - 293 K

Symmetry space group - P21/c

Cell formula units, (_cell_formula_units_Z) – 4

Total number of measured intensities (_diffrn_reflns_number) – 9000

Total number of reflections (_reflns_number_total) – 2353

Rint (_diffrn_reflns_av_R_equivalents) – 0.0128

wR(F2) (_refine_ls_wR_factor_ref) - 0.1369

Fractional coordinates

Number	Label	SybylType	Xfrac + ESD	Yfrac + ESD	Zfrac + ESD	Symm. op.
1	C11	C.2	0.30735(17)	-0.2431(3)	0.27882(16)	x,y,z
2	C12	C.2	0.3020(2)	-0.2876(3)	0.18154(19)	x,y,z
3	H12	H	0.2424	-0.2501	0.1233	x,y,z
4	C13	C.2	0.3847(3)	-0.3876(4)	0.1707(2)	x,y,z
5	H13	H	0.3804	-0.4172	0.1052	x,y,z
6	C14	C.2	0.4731(2)	-0.4433(4)	0.2560(3)	x,y,z
7	H14	H	0.5288	-0.51	0.2485	x,y,z
8	C15	C.2	0.4790(2)	-0.3999(4)	0.3529(2)	x,y,z
9	H15	H	0.5387	-0.4381	0.4108	x,y,z
10	C16	C.2	0.39683(19)	-0.3002(3)	0.36488(19)	x,y,z
11	H16	H	0.4015	-0.2715	0.4306	x,y,z
12	C21	C.3	0.21991(17)	-0.1212(3)	0.29138(16)	x,y,z
13	C22	C.3	0.26164(19)	0.0771(3)	0.30109(17)	x,y,z
14	C23	C.2	0.2449(2)	0.2071(4)	0.2318(2)	x,y,z
15	H23	H	0.2825	0.3167	0.2545	x,y,z
16	Cl21	Cl	0.35862(6)	0.13161(10)	0.42286(5)	x,y,z
17	Cl22	Cl	0.16042(9)	0.19345(13)	0.10359(6)	x,y,z

18	N25	N.3	0.19884(15)	-0.1728(3)	0.38210(15)	x,y,z
19	C24	C.1	0.11543(19)	-0.1420(3)	0.19792(18)	x,y,z
20	N24	N.1	0.03311(19)	-0.1759(4)	0.13458(19)	x,y,z
21	C26	C.3	0.1190(2)	-0.0508(5)	0.3974(2)	x,y,z
22	H261	H	0.0487	-0.0686	0.3425	x,y,z
23	H262	H	0.1412	0.0745	0.3976	x,y,z
24	H263	H	0.1148	-0.0786	0.4621	x,y,z
25	C27	C.3	0.1642(2)	-0.3646(4)	0.3790(2)	x,y,z
26	H271	H	0.0966	-0.3824	0.3207	x,y,z
27	H272	H	0.1547	-0.393	0.4411	x,y,z
28	H273	H	0.2189	-0.4437	0.373	x,y,z

(*Z*)-2-Chloro-3-(4-methylphenyl)-1-phenylprop-2-en-1-one (***Z*-198**)

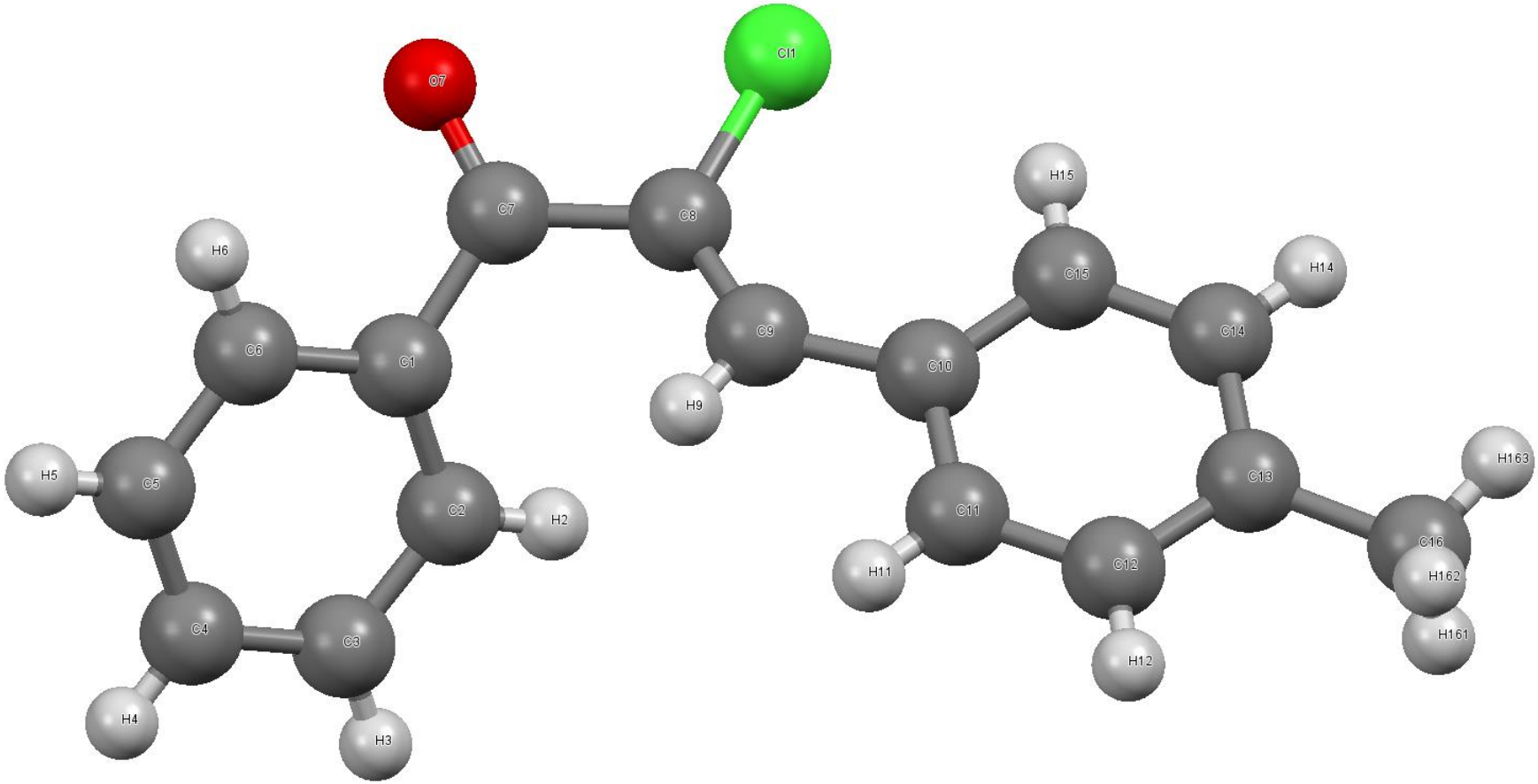

Molecular formula - $C_{16}H_{13}ClO$

Molecular Mass - 256.71

Symmetry cell setting - orthorhombic

Cell length - a = 8.8054(8), b= 11.6093(11), c = 26.7629(15) Å

Cell angle - α= 90.0, β= 90, γ= 90.0

Cell volume, U - 2735.8(4) $Å^3$

Cell measurement temperature - 293 K

Symmetry space group - Pbca

Cell formula units (_cell_formula_units_Z) - 8

Total number of measured intensities (_diffrn_reflns_number) - 18840 reflections measured

Total number of reflections (_reflns_number_total) - 2543 unique

Rint (_diffrn_reflns_av_R_equivalents) - 0.0144

wR(F2) (_refine_ls_wR_factor_ref) - 0.1132

Fractional cordinates

Number	Label	SybylType	Xfrac + ESD	Yfrac + ESD	Zfrac + ESD	Symm. op.
1	Cl1	Cl	0.15762(5)	0.42777(4)	0.43621(2)	x,y,z
2	C1	C.2	0.44300(17)	0.55611(13)	0.33059(5)	x,y,z
3	C2	C.2	0.41701(19)	0.67414(14)	0.33150(6)	x,y,z
4	H2	H	0.3504	0.7054	0.3548	x,y,z
5	C3	C.2	0.4900(2)	0.74502(17)	0.29778(6)	x,y,z
6	H3	H	0.4706	0.8238	0.298	x,y,z
7	C4	C.2	0.5916(2)	0.7000(2)	0.26371(6)	x,y,z
8	H4	H	0.641	0.7483	0.2413	x,y,z
9	C5	C.2	0.6196(3)	0.5835(2)	0.26303(7)	x,y,z
10	H5	H	0.6891	0.5532	0.2404	x,y,z
11	C6	C.2	0.5448(2)	0.51140(16)	0.29586(6)	x,y,z
12	H6	H	0.5626	0.4325	0.2948	x,y,z
13	C7	C.2	0.35310(17)	0.47362(13)	0.36142(6)	x,y,z
14	O7	O.2	0.31145(18)	0.38329(11)	0.34318(5)	x,y,z
15	C8	C.3	0.31254(16)	0.50338(12)	0.41382(5)	x,y,z
16	C9	C.2	0.39517(16)	0.57592(11)	0.44156(5)	x,y,z

17	H9	H	0.4782	0.6056	0.4244	x,y,z
18	C10	C.2	0.38489(15)	0.61904(12)	0.49249(5)	x,y,z
19	C11	C.2	0.49035(19)	0.70280(13)	0.50574(6)	x,y,z
20	H11	H	0.5655	0.7231	0.483	x,y,z
21	C12	C.2	0.4867(2)	0.75665(15)	0.55158(6)	x,y,z
22	H12	H	0.5588	0.8126	0.559	x,y,z
23	C13	C.2	0.3779(2)	0.72896(16)	0.58658(6)	x,y,z
24	C14	C.2	0.2767(2)	0.64268(18)	0.57466(6)	x,y,z
25	H14	H	0.2049	0.6207	0.5983	x,y,z
26	C15	C.2	0.27795(18)	0.58753(15)	0.52876(6)	x,y,z
27	H15	H	0.2079	0.5296	0.522	x,y,z
28	C16	C.3	0.3707(3)	0.7935(2)	0.63575(8)	x,y,z
29	H161	H	0.3342	0.8703	0.63	x,y,z
30	H162	H	0.4703	0.7968	0.6503	x,y,z
31	H163	H	0.303	0.7543	0.6581	x,y,z

(*E*)-2-Chloro-3-(4-methoxyphenyl)-1-phenylprop-2-en-1-one (***E*-2**)

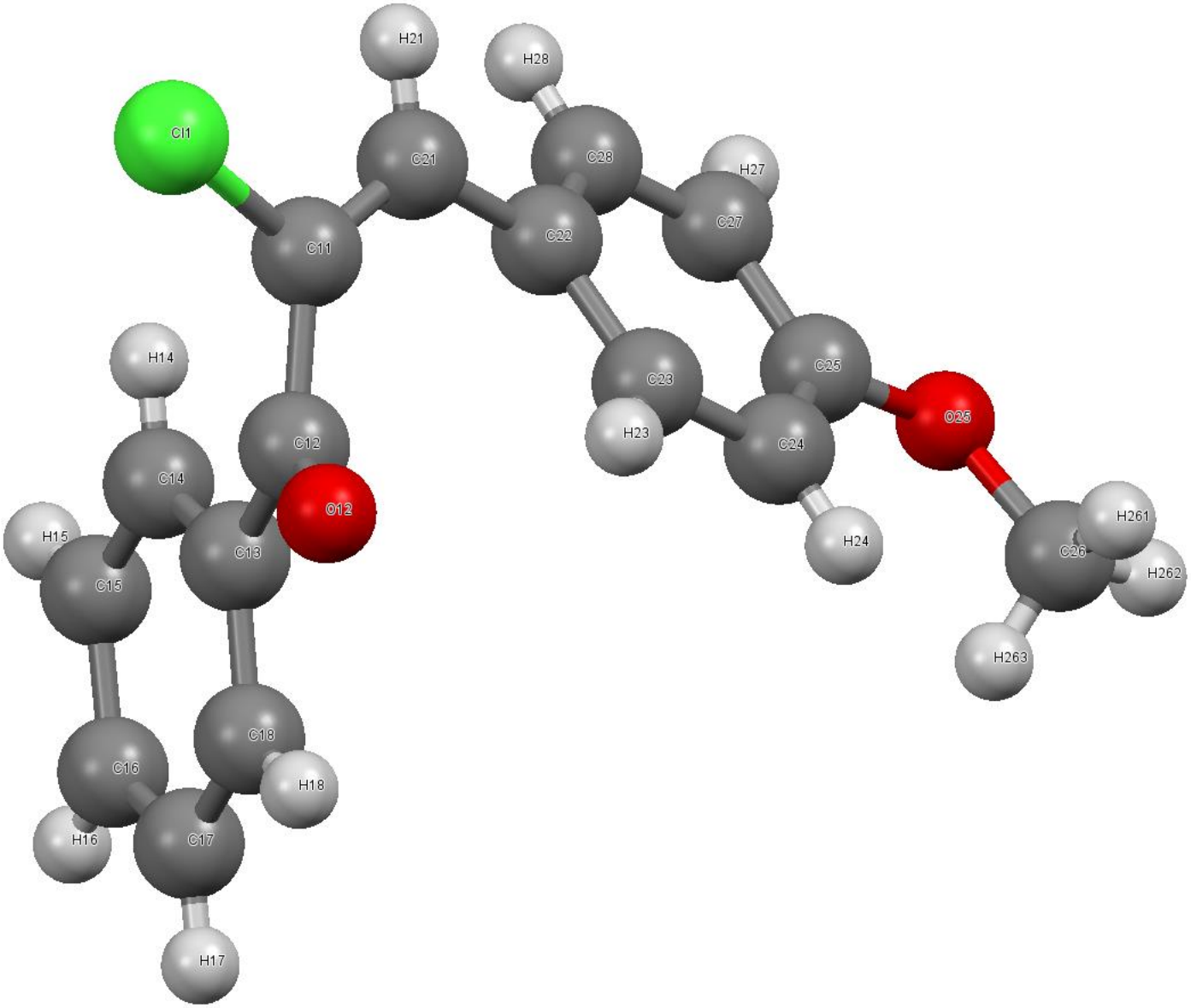

Molecular formula - $C_{16}H_{13}ClO_2$

Molecular Mass - 272.71

Symmetry cell setting - monoclinic

Cell length - a = 14.28(2), b= 9.823(14), c = 9.912(14) Å

Cell angle - α= 90.0, β= 98.27(2), γ= 90.0

Cell volume, U - 1376(3) $Å^3$

Cell measurement temperature - 293 K

Symmetry space group - P21/c

Cell formula units (_cell_formula_units_Z) - 4

Total number of measured intensities (_diffrn_reflns_number) - 9855

Total number of reflections (_reflns_number_total) - 2549

Rint (_diffrn_reflns_av_R_equivalents) - 0.0164

wR(F2) (_refine_ls_wR_factor_ref) - 0.1976

Fractional coordinates

Number	Label	SybylType	Xfrac + ESD	Yfrac + ESD	Zfrac + ESD	Symm. op.
1	Cl1	Cl	0.65034(5)	0.01525(7)	0.11730(6)	x,y,z
2	C11	C.3	0.71126(13)	-0.0405(2)	0.27127(19)	x,y,z
3	C12	C.2	0.70290(14)	0.0556(2)	0.3858(2)	x,y,z
4	O12	O.2	0.72850(15)	0.17158(15)	0.3806(2)	x,y,z
5	C13	C.2	0.65948(12)	0.00542(17)	0.50478(19)	x,y,z
6	C14	C.2	0.60997(13)	-0.11511(19)	0.5005(2)	x,y,z
7	H14	H	0.6062	-0.1707	0.424	x,y,z
8	C15	C.2	0.56578(16)	-0.1538(3)	0.6102(3)	x,y,z
9	H15	H	0.5315	-0.2345	0.607	x,y,z
10	C16	C.2	0.57308(17)	-0.0707(3)	0.7250(2)	x,y,z
11	H16	H	0.5441	-0.0966	0.7993	x,y,z
12	C17	C.2	0.62204(18)	0.0474(3)	0.7293(2)	x,y,z
13	H17	H	0.6268	0.1018	0.8068	x,y,z
14	C18	C.2	0.66499(14)	0.0880(2)	0.6202(2)	x,y,z
15	H18	H	0.6976	0.1701	0.6235	x,y,z
16	C21	C.2	0.76175(13)	-0.15452(19)	0.27499(19)	x,y,z

17	H21	H	0.7563	-0.2058	0.1954	x,y,z
18	C22	C.2	0.82474(12)	-0.20648(17)	0.39206(17)	x,y,z
19	C23	C.2	0.87957(12)	-0.12135(17)	0.4834(2)	x,y,z
20	H23	H	0.8736	-0.0276	0.4721	x,y,z
21	C24	C.2	0.94213(12)	-0.17112(18)	0.5895(2)	x,y,z
22	H24	H	0.9777	-0.1117	0.6494	x,y,z
23	C25	C.2	0.95217(12)	-0.31102(18)	0.60699(19)	x,y,z
24	C27	C.2	0.89832(14)	-0.39761(19)	0.5172(2)	x,y,z
25	H27	H	0.904	-0.4913	0.5294	x,y,z
26	C28	C.2	0.83668(13)	-0.34690(18)	0.4107(2)	x,y,z
27	H28	H	0.8022	-0.4066	0.3498	x,y,z
28	O25	O.3	1.01308(10)	-0.37164(14)	0.70671(15)	x,y,z
29	C26	C.3	1.07615(16)	-0.2866(3)	0.7926(3)	x,y,z
30	H261	H	1.114	-0.2352	0.7382	x,y,z
31	H262	H	1.1165	-0.3417	0.8565	x,y,z
32	H263	H	1.0406	-0.2254	0.8411	x,y,z

(*Z*)-2-Chloro-3-(4-methoxyphenyl)-1-phenylprop-2-en-1-one (***Z*-2**)

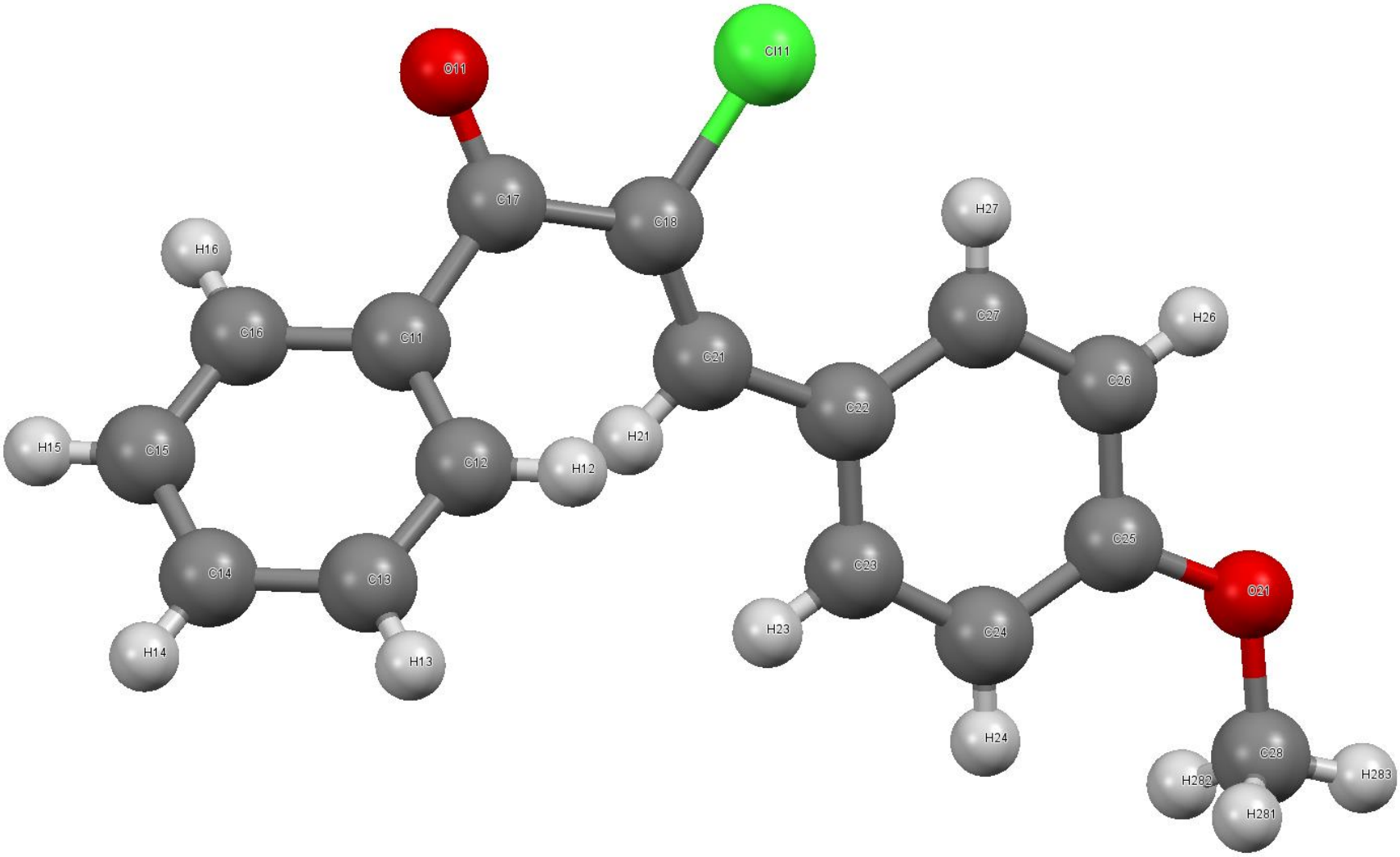

Molecular formula - $C_{16}H_{13}ClO_2$

Molecular Mass - 272.71

Symmetry cell setting - orthorhombic

Cell length - a = 8.858(3), b= 11.306(5), c = 27.121(11) Å

Cell angle - α= 90.0, β= 90, γ= 90.0

Cell volume, U - 2716.0(19) $Å^3$

Cell measurement temperature - 293 K

Symmetry space group - Pbca

Cell formula units (_cell_formula_units_Z) - 8

Total number of measured intensities (_diffrn_reflns_number) - 18717

Total number of reflections (_reflns_number_total) - 2525

Rint (_diffrn_reflns_av_R_equivalents) - 0.0144

wR(F2) (_refine_ls_wR_factor_ref) - 0.1230

Fractional coordinates

Number	Label	SybylType	Xfrac + ESD	Yfrac + ESD	Zfrac + ESD	Symm. op.
1	C11	C.2	0.45748(19)	-0.05576(15)	0.33117(6)	x,y,z
2	C12	C.2	0.4406(2)	-0.17843(15)	0.33161(6)	x,y,z
3	H12	H	0.3716	-0.2137	0.3529	x,y,z
4	C13	C.2	0.5267(2)	-0.24731(18)	0.30038(7)	x,y,z
5	H13	H	0.5143	-0.329	0.3004	x,y,z
6	C14	C.2	0.6309(3)	-0.1961(2)	0.26924(7)	x,y,z
7	H14	H	0.6892	-0.2432	0.2485	x,y,z
8	C15	C.2	0.6484(3)	-0.0752(2)	0.26890(7)	x,y,z
9	H15	H	0.7191	-0.0407	0.248	x,y,z
10	C16	C.2	0.5620(2)	-0.00456(19)	0.29931(6)	x,y,z
11	H16	H	0.5735	0.0772	0.2985	x,y,z
12	C17	C.2	0.3558(2)	0.02433(15)	0.35986(7)	x,y,z
13	O11	O.2	0.3061(2)	0.11292(13)	0.34005(6)	x,y,z
14	C18	C.3	0.31559(18)	-0.00358(14)	0.41167(6)	x,y,z
15	Cl11	Cl	0.16366(6)	0.07830(5)	0.43347(2)	x,y,z
16	C21	C.2	0.39464(19)	-0.07825(13)	0.44012(6)	x,y,z

17	H21	H	0.4762	-0.112	0.4237	x,y,z
18	C22	C.2	0.38126(17)	-0.11819(13)	0.49081(6)	x,y,z
19	C23	C.2	0.4838(2)	-0.20449(15)	0.50613(6)	x,y,z
20	H23	H	0.5572	-0.2297	0.4839	x,y,z
21	C24	C.2	0.4817(2)	-0.25406(16)	0.55248(6)	x,y,z
22	H24	H	0.5517	-0.3118	0.5611	x,y,z
23	C25	C.2	0.3742(2)	-0.21689(17)	0.58611(6)	x,y,z
24	C26	C.2	0.2731(2)	-0.12901(18)	0.57262(7)	x,y,z
25	H26	H	0.2023	-0.1027	0.5954	x,y,z
26	C27	C.2	0.2755(2)	-0.07998(16)	0.52612(6)	x,y,z
27	H27	H	0.2065	-0.0211	0.518	x,y,z
28	O21	O.3	0.36019(16)	-0.25942(14)	0.63276(5)	x,y,z
29	C28	C.3	0.4599(3)	-0.3514(2)	0.64792(8)	x,y,z
30	H281	H	0.4481	-0.4183	0.6265	x,y,z
31	H282	H	0.5622	-0.3236	0.6464	x,y,z
32	H283	H	0.4364	-0.3743	0.6811	x,y,z

(*E*)-2-Chloro-3-(benzofuran-2-yl)-1-phenylprop-2-en-1-one (***E*-202**)

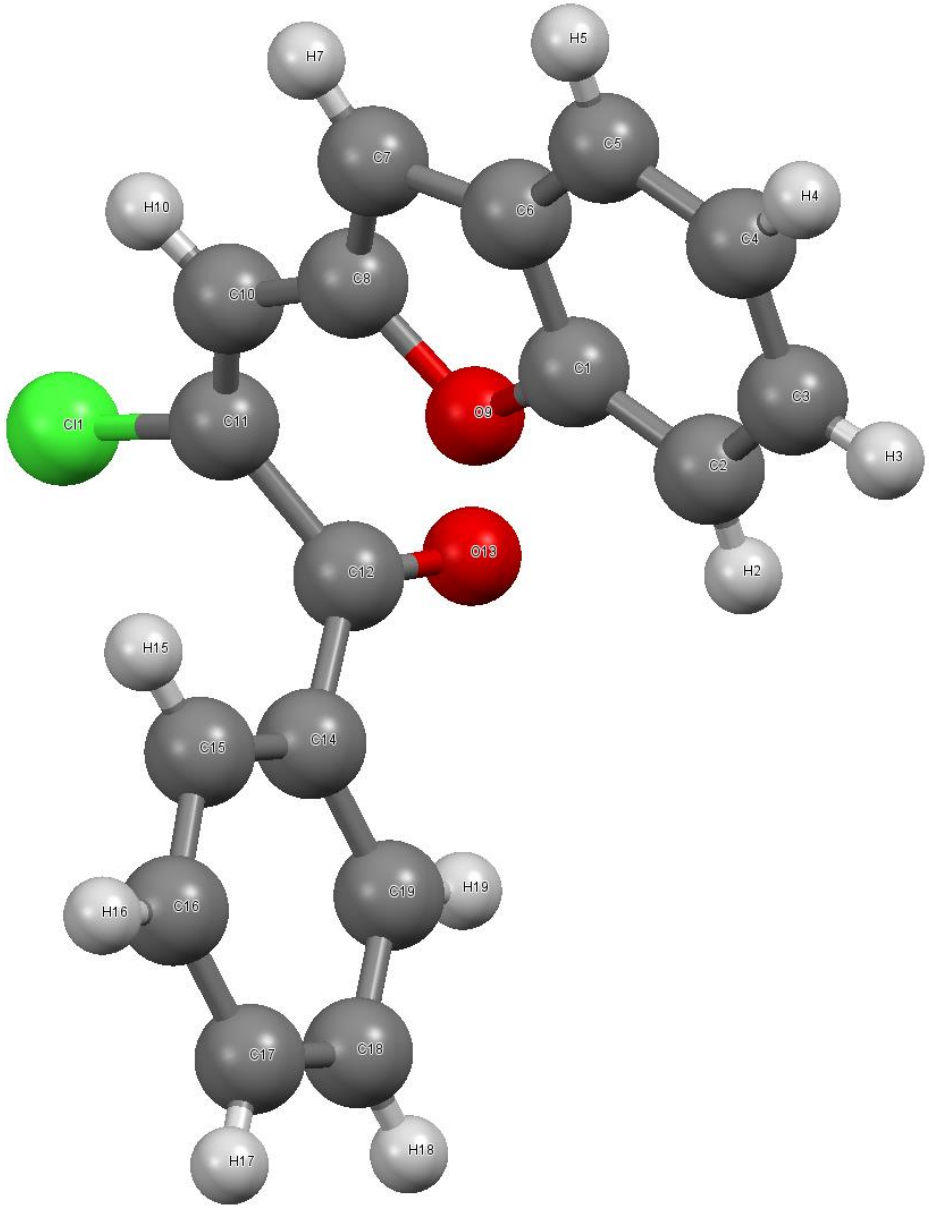

Molecular formula – $C_{17}H_{11}ClO_2$

Molecular Mass - 282.71

Symmetry cell setting - monoclinic

Cell length - a= 8.087(4), b= 6.124(4), c= 13.998(7)

Cell angle - α= 90.0, β= 91.490(9), γ= 90.0

Cell volume, U - 693.0(6) $Å^3$

Cell measurement temperature - 293 K

Symmetry space group – P21

Cell formula units (_cell_formula_units_Z) - 2

Total number of measured intensities (_diffrn_reflns_number) - 5162

Total number of reflections (_reflns_number_total) - 2586

Rint (_diffrn_reflns_av_R_equivalents) - 0.0168

wR(F2) (_refine_ls_wR_factor_ref) - 0.0866

Fractional coordinate

Number	Label	SybylType	Xfrac + ESD	Yfrac + ESD	Zfrac + ESD	Symm. op.
1	Cl1	Cl	-0.49310(8)	-0.00138(11)	-0.42034(4)	x,y,z
2	C1	C.2	-0.2376(3)	0.2621(4)	-0.03643(15)	x,y,z
3	C2	C.2	-0.1523(3)	0.4352(4)	0.00324(17)	x,y,z
4	H2	H	-0.1197	0.5543	-0.033	x,y,z
5	C3	C.2	-0.1180(4)	0.4215(5)	0.1002(2)	x,y,z
6	H3	H	-0.0606	0.5345	0.1306	x,y,z
7	C4	C.2	-0.1668(4)	0.2446(6)	0.1528(2)	x,y,z
8	H4	H	-0.1426	0.2424	0.2181	x,y,z
9	C5	C.2	-0.2500(4)	0.0707(5)	0.11223(19)	x,y,z
10	H5	H	-0.2809	-0.0483	0.1489	x,y,z
11	C6	C.2	-0.2867(3)	0.0783(4)	0.01421(17)	x,y,z
12	C7	C.2	-0.3679(3)	-0.0593(4)	-0.05463(19)	x,y,z
13	H7	H	-0.4141	-0.1954	-0.0429	x,y,z
14	C8	C.2	-0.3654(3)	0.0434(4)	-0.13946(17)	x,y,z
15	O9	O.3	-0.28582(19)	0.2435(3)	-0.13122(10)	x,y,z
16	C10	C.2	-0.4264(3)	-0.0191(5)	-0.23332(17)	x,y,z

17	H10	H	-0.4761	-0.1556	-0.239	x,y,z
18	C11	C.3	-0.4184(3)	0.0991(4)	-0.31192(18)	x,y,z
19	C12	C.2	-0.3555(3)	0.3296(4)	-0.32365(17)	x,y,z
20	O13	O.2	-0.4527(2)	0.4776(3)	-0.31697(14)	x,y,z
21	C14	C.2	-0.1799(3)	0.3635(4)	-0.34690(15)	x,y,z
22	C15	C.2	-0.0617(3)	0.2028(4)	-0.32972(17)	x,y,z
23	H15	H	-0.0924	0.068	-0.3052	x,y,z
24	C16	C.2	0.1019(3)	0.2444(6)	-0.34924(19)	x,y,z
25	H16	H	0.1818	0.1391	-0.3354	x,y,z
26	C17	C.2	0.1473(3)	0.4386(6)	-0.38868(18)	x,y,z
27	H17	H	0.2575	0.4638	-0.4026	x,y,z
28	C18	C.2	0.0302(3)	0.5975(5)	-0.40791(18)	x,y,z
29	H18	H	0.0612	0.7292	-0.4352	x,y,z
30	C19	C.2	-0.1327(3)	0.5609(4)	-0.38660(18)	x,y,z
31	H19	H	-0.2114	0.6687	-0.3988	x,y,z

(*Z*)-2-Chloro-3-(benzofuran-2-yl)-1-phenylprop-2-en-1-one (***Z*-202**)

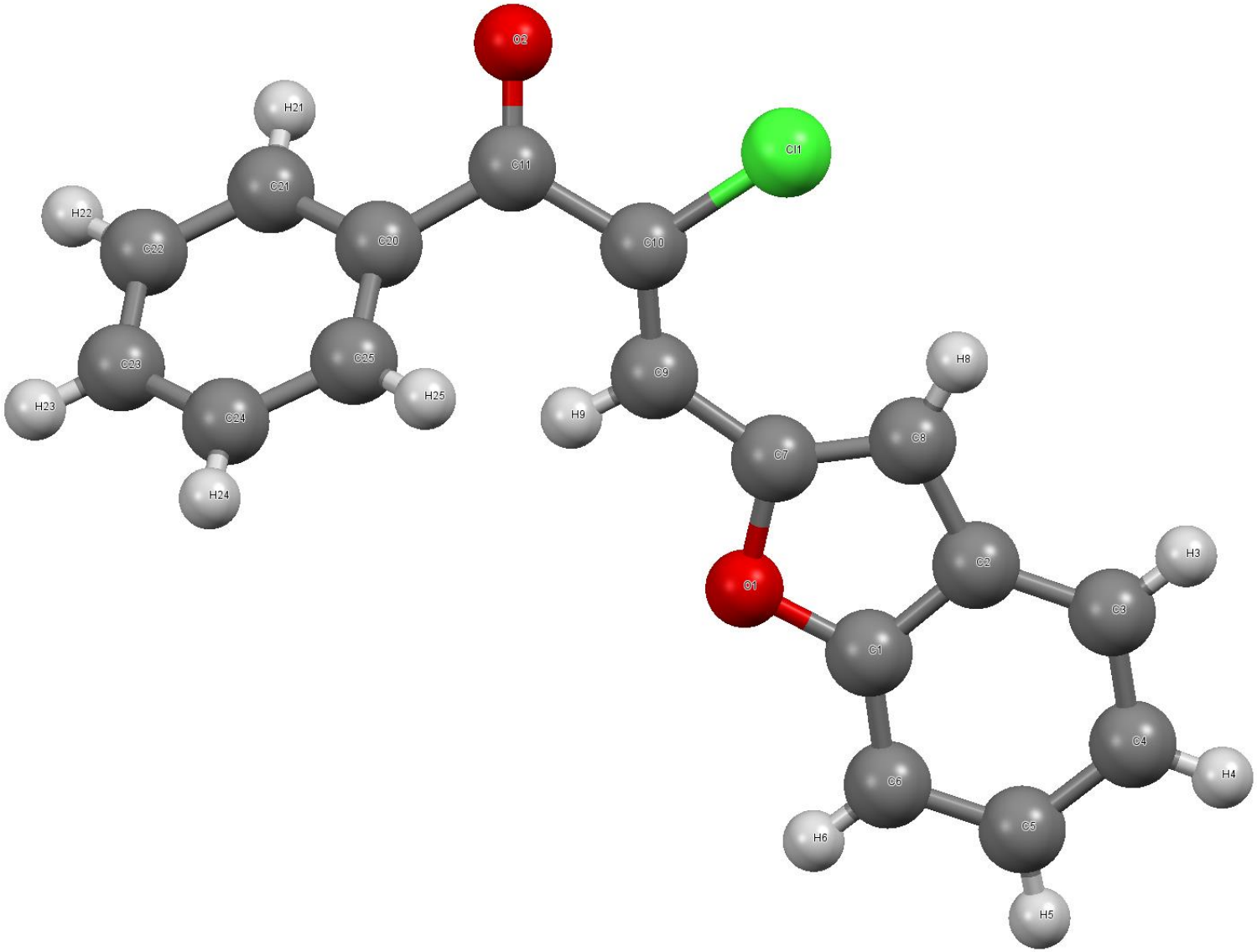

Molecular formula – $C_{17}H_{11}ClO_2$

Molecular Mass - 282.71

Symmetry cell setting - orthorhombic

Cell length - a = 6.1663(8), b= 12.6929(11), c = 17.4233(15) Å

Cell angle - α= 90.0, β= 90.0, γ= 90.0

Cell volume, U - 1363.7(2) $Å^3$

Cell measurement temperature - 293 K

Symmetry space group – P212121

Cell formula units (_cell_formula_units_Z) - 4

Total number of measured intensities (_diffrn_reflns_number) - 10108

Total number of reflections (_reflns_number_total) - 2540

Rint (_diffrn_reflns_av_R_equivalents) - 0.0282

wR(F2) (_refine_ls_wR_factor_ref) - 0.0853

Fractional coordinates

Number	Label	SybylType	Xfrac + ESD	Yfrac + ESD	Zfrac + ESD	Symm. op.
1	Cl1	Cl	-0.92142(9)	-0.46062(4)	-0.23320(3)	x,y,z
2	C1	C.2	-1.6244(3)	-0.31125(14)	-0.10162(11)	x,y,z
3	C2	C.2	-1.4915(3)	-0.25051(15)	-0.14855(11)	x,y,z
4	C3	C.2	-1.5483(4)	-0.14522(16)	-0.16203(12)	x,y,z
5	H3	H	-1.4624	-0.1022	-0.1927	x,y,z
6	C4	C.2	-1.7345(4)	-0.10729(17)	-0.12866(14)	x,y,z
7	H4	H	-1.7752	-0.0377	-0.1373	x,y,z
8	C5	C.2	-1.8641(4)	-0.17114(18)	-0.08198(14)	x,y,z
9	H5	H	-1.9891	-0.1431	-0.0602	x,y,z
10	C6	C.2	-1.8107(4)	-0.27472(17)	-0.06759(14)	x,y,z
11	H6	H	-1.8961	-0.3175	-0.0365	x,y,z
12	O1	O.3	-1.5423(2)	-0.41131(10)	-0.09507(8)	x,y,z
13	C7	C.2	-1.3555(3)	-0.41327(15)	-0.13962(11)	x,y,z
14	C8	C.2	-1.3202(4)	-0.31830(15)	-0.17248(12)	x,y,z
15	H8	H	-1.2055	-0.3006	-0.2047	x,y,z
16	C9	C.2	-1.2456(4)	-0.51276(15)	-0.13755(11)	x,y,z

17	H9	H	-1.3115	-0.564	-0.1074	x,y,z
18	C10	C.3	-1.0626(3)	-0.54314(16)	-0.17245(11)	x,y,z
19	C11	C.2	-0.9551(3)	-0.64613(16)	-0.15818(12)	x,y,z
20	O2	O.2	-0.7643(3)	-0.65772(14)	-0.17286(12)	x,y,z
21	C20	C.2	-1.0830(3)	-0.73458(15)	-0.12480(11)	x,y,z
22	C21	C.2	-0.9840(4)	-0.79891(17)	-0.06984(12)	x,y,z
23	H21	H	-0.8454	-0.7832	-0.0522	x,y,z
24	C22	C.2	-1.0926(5)	-0.88544(18)	-0.04204(14)	x,y,z
25	H22	H	-1.0269	-0.9278	-0.0052	x,y,z
26	C23	C.2	-1.2958(5)	-0.91001(17)	-0.06781(15)	x,y,z
27	H23	H	-1.3679	-0.9684	-0.0481	x,y,z
28	C24	C.2	-1.3940(4)	-0.84854(18)	-0.12281(15)	x,y,z
29	H24	H	-1.5307	-0.8663	-0.1413	x,y,z
30	C25	C.2	-1.2889(4)	-0.76078(17)	-0.15029(12)	x,y,z
31	H25	H	-1.357	-0.7184	-0.1865	x,y,z

Appendix

Computational studies done by Dr. Peter Budzelaar

DFT: Forced rotation around C=C bond

Geometry optimizations for model compounds **A**-**C** were subject to only torsion constraints used to force rotation around the C1=C2 bond: the H-C1-C2-C3 dihedral angle was stepped in increments of 15° from 15° to 165° while at the same time the H-C1-C2-Cl dihedral angle was increased from -165° to -15°. No constraints were put on torsions involving *Z*. In addition to these constrained optimizations, the begin and end points of the rotation profile were obtained from unconstrained optimizations. The resulting energy profiles for rotation are shown in Figure 55, below.

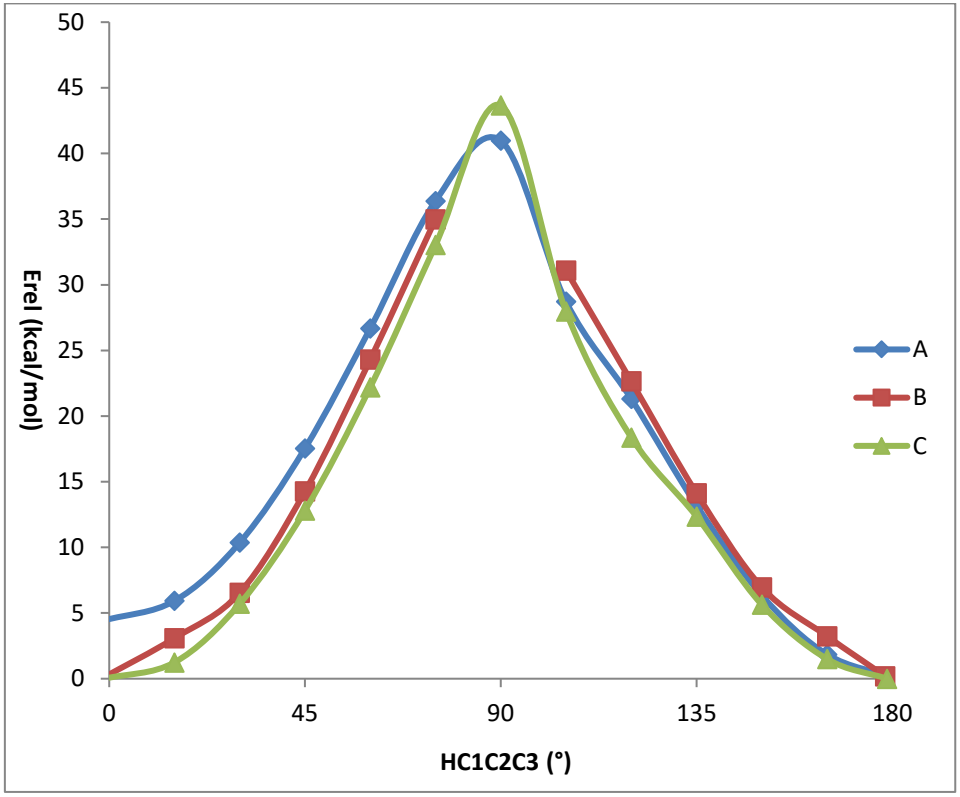

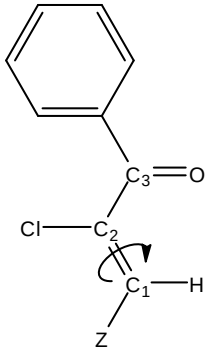

A: Z = *cis*-Pd(PMe$_3$)$_2$Cl
B: Z = *trans*-Pd(PMe$_3$)$_2$Cl
C: Z = H

Figure 55: Energy profiles for forced rotation around C=C bond for species A-C.

Inspection of geometries close to H-C1-C2-C3 = 90° reveals that these constraints do not really enforce rotation around the C=C bond. Instead, all three systems **A-C** "escape" by opening up the H-C1-C2 bond angle to nearly ~140° (and simultaneously reducing Z-C1-C2 to ~100°), at which point the dihedral angle constraints can be satisfied by moving H only a small distance out of the C1C2C3Cl plane. The tables below list energies and relevant geometrical parameters for the rotation profiles of **A-C**. The Figure shows clearly that the Pd atom does not facilitate rotation: distortion costs the same amount of energy for compound **C** (Z = H) as

for the Pd-containing compounds **A** and **B**. The bond lengths in the Tables similarly show no evidence of the shortening of the C1-Pd bond or elongation of the C1-C2 bond that would be expected for a zwitterionic Pd-carbene type structure.

It should be noted that the "top" of the profiles, near 90°, does not correspond to a transition state: as far as we can establish there is no transition state connecting the *cis* and *trans* isomers at the single-determinant DFT level.

Energy profile and geometric details for forced C=C rotation in compound A

	Eelec (h)	**Erel (kcal/mol)**	**HC1C2C3[a] (°)**	**Z-C1 (°)**	**C1-C2 (Å)**	**H-C1-C2 (Å)**	**Z-C1-C2 (°)**
L2PdCl_CCcis (min)	-2392.67804	4.45	-1.05	2.022	1.335	114.5	129.3
L2PdCl_CCtrans15	-2392.67569	5.93	15	2.023	1.336	114.7	127.9
L2PdCl_CCtrans30	-2392.66861	10.37	30	2.030	1.338	116.0	126.6
L2PdCl_CCtrans45	-2392.65718	17.54	45	2.038	1.341	118.6	124.0
L2PdCl_CCtrans60	-2392.64262	26.68	60	2.052	1.342	123.3	120.6
L2PdCl_CCtrans75	-2392.62716	36.38	75	2.093	1.332	134.2	115.3

L2PdCl_CCtrans90	-2392.61984	40.97	90	2.213	1.298	174.6	107.5
L2PdCl_CCtrans105	-2392.63938	28.72	105	2.133	1.300	149.9	107.6
L2PdCl_CCtrans120	-2392.65118	21.31	120	2.068	1.317	130.9	115.4
L2PdCl_CCtrans135	-2392.66409	13.20	135	2.047	1.322	124.4	120.3
L2PdCl_CCtrans150	-2392.67502	6.35	150	2.039	1.323	121.4	122.8
L2PdCl_CCtrans165	-2392.68218	1.85	165	2.034	1.325	119.5	125.2
L2PdCl_CCtrans (min)	-2392.68514	0.00	181.39	2.034	1.326	118.8	126.0

[a] This angle was constrained at the given value, except for the first and last entry.

Energy profile and geometric details for forced C=C rotation in compound B

	Eelec (h)	**Erel (kcal/mol)**	**HC1C2C3[a] (°)**	**Z-C1 (°)**	**C1-C2 (Å)**	**H-C1-C2 (Å)**	**Z-C1-C2 (°)**
LLPdCl_CCcis (min)	-2392.69864	0.00	-1.80	1.995	1.338	113.0	130.0

LLPdCl_CCtrans15	-2392.69372	3.09	15	1.999	1.339	112.6	130.4
LLPdCl_CCtrans30	-2392.68821	6.54	30	2.000	1.339	113.8	129.3
LLPdCl_CCtrans45	-2392.67591	14.26	45	2.005	1.343	116.3	126.7
LLPdCl_CCtrans60	-2392.65991	24.30	60	2.013	1.345	120.8	123.6
LLPdCl_CCtrans75	-2392.64288	34.99	75	2.051	1.333	133.0	117.9
b			90				
LLPdCl_CCtrans105	-2392.64908	31.10	105	2.102	1.308	142.8	109.2
LLPdCl_CCtrans120	-2392.66255	22.65	120	2.053	1.322	127.9	115.9
LLPdCl_CCtrans135	-2392.67612	14.13	135	2.032	1.327	122.2	120.7
LLPdCl_CCtrans150	-2392.68755	6.96	150	2.019	1.331	118.9	124.7
LLPdCl_CCtrans165	-2392.69347	3.24	165	2.012	1.337	116.3	129.1
LLPdCl_CCtrans (min)	-2392.69834	0.19	178.36	2.007	1.336	116.1	129.2

[a] This angle was constrained at the given value, except for the first and last entry. [b] Unstable optimization, "flipping" between <90 and >90 torsion values.

Energy profile and geometric details for forced C=C rotation in compound C

	Eelec (h)	Erel (kcal/mol)	HC1C2C[a] (°)	Z-C1 (°)	C1-C2 (Å)	H-C1-C2 (Å)	Z-C1-C2 (°)
H_CCcis (min)	-882.75249	0.00	-1.06	1.082	1.329	118.7	122.3
H_CCtrans15	-882.75052	1.24	15	1.082	1.331	118.6	122.1
H_CCtrans30	-882.74340	5.71	30	1.084	1.333	119.4	119.9
H_CCtrans45	-882.73207	12.82	45	1.088	1.338	121.2	116.8
H_CCtrans60	-882.71712	22.20	60	1.093	1.343	124.4	112.6
H_CCtrans75	-882.69987	33.03	75	1.101	1.348	130.2	107.5
H_CCtrans90	-882.68294	43.65	90	1.116	1.341	145.9	100.0
H_CCtrans105	-882.70794	27.96	105	1.102	1.347	131.1	106.4

H_CCtrans120	-882.72322	18.37	120	1.094	1.344	126.5	111.0
H_CCtrans135	-882.73281	12.35	135	1.090	1.332	125.3	113.3
H_CCtrans150	-882.74350	5.64	150	1.087	1.332	123.6	116.0
H_CCtrans165	-882.75010	1.50	165	1.083	1.330	122.6	118.0
H_CCtrans (min)	-882.75250	0.00	178.79	1.084	1.329	122.4	118.8

[a] This angle was constrained at the given value, except for the first and last entry.

DFT: Energies for species on enone-enolate isomerization path

General

Final free energies were calculated from (for details see main text, "Computational"):

Thermal corrections (298 K, 1 bar) from the b-lyp /def-SV(P) level vibrational analysis

Single-point energy at TPSSh/def-TZVPP

DFT-D dispersion correction

All relevant conformations of the five stationary points of the isomerization path (Scheme 4) were optimized without constraints, for all combinations of four substrates (acrolein "Acr", **1** "Nav0", **3a**/**4a** "Nav" and methyl maleate/fumarate "FM") and two ligands (DMPE "PE" and DMPE mono-oxide "PO"). The results are summarized in the following Tables. For each species, "c" and "t" in the name indicate cis/cisoid or trans/transoid orientations around C-C or C-O bonds; "x" and "y" refer to the twist of the (DMPE)Pd or (DMPE-O)Pd chelate ring. "TS" indicates the **9**/**10** and **10**/**11** transition states; "Diyl" indicates the enolate cyclic intermediate. The lowest-energy species for each block is highlighted. "rel" lists free energy (kcal/mol) relative to the most stable species on each path; "bind" is the binding free energy of the relevant enone isomer to the LPd fragment.

Total and relative energies for degenerate isomerization of acrolein (298 K, 1 bar)

Name	HCorr	TSCorr	Eelec	Edisp	G	rel	bind

Acr_c	0.06462	0.03175	-191.99283	-0.00237	-191.96232	2.07	
Acr_t	0.06456	0.03166	-191.99629	-0.00223	-191.96562	0.00	
PE_x	0.21745	0.05653	-1049.04011	-0.01892	-1048.89811		
PO_x	0.22254	0.05896	-1124.31645	-0.02163	-1124.17450		
PE_x_AcrDiyl_f	0.28324	0.06809	-1241.07255	-0.02692	-1240.88432	16.98	-29.90
PE_y_AcrDiyl_f	0.28322	0.06824	-1241.07194	-0.02689	-1240.88384	17.28	
PE_x_AcrTS_f	0.28206	0.06889	-1241.05673	-0.02683	-1240.87038	25.73	
PE_y_AcrTS_f	0.28207	0.06875	-1241.05712	-0.02687	-1240.87067	25.55	
PE_x_Acr_fc	0.28410	0.06996	-1241.09596	-0.02701	-1240.90883	1.60	
PE_x_Acr_ft	0.28392	0.06992	-1241.09774	-0.02716	-1240.91089	0.31	
PE_y_Acr_fc	0.28410	0.06977	-1241.09611	-0.02708	-1240.90886	1.58	
PE_y_Acr_ft	0.28390	0.07003	-1241.09786	-0.02740	-1240.91139	0.00	

PO_x_AcrDiyl_b	0.28853	0.07027	-1316.34557	-0.03054	-1316.15785	14.84	-25.96
PO_y_AcrDiyl_f	0.28851	0.07031	-1316.34552	-0.03053	-1316.15785	14.84	
PO_x_AcrTS_f	0.28755	0.07121	-1316.33441	-0.03033	-1316.14840	20.77	
PO_y_AcrTS_f	0.28754	0.07064	-1316.33605	-0.03046	-1316.14961	20.01	
PO_x_Acr_fc	0.28926	0.07267	-1316.36389	-0.02954	-1316.17684	2.92	
PO_x_Acr_ft	0.28906	0.07283	-1316.36552	-0.02932	-1316.17861	1.81	
PO_y_Acr_fc	0.28923	0.07246	-1316.36696	-0.03131	-1316.18150	0.00	
PO_y_Acr_ft	0.28911	0.07138	-1316.36735	-0.03127	-1316.18087	0.39	

Total and relative energies for isomerization of E-1 (298 K, 1 bar)

Name	**HCorr**	**TSCorr**	**Eelec**	**Edisp**	**G**	**rel**	**bind**
Nav0_cc	0.13272	0.05159	-1342.39419	-0.01385	-1342.32691	1.84	

Nav0_ct	0.13269	0.05198	-1342.39431	-0.01409	-1342.32769	1.35	
Nav0_tc	0.13286	0.05072	-1342.39866	-0.01332	-1342.32985	0.00	
Nav0_tt	0.13290	0.05052	-1342.39905	-0.01305	-1342.32971	0.08	
PE_x	0.21745	0.05653	-1049.04011	-0.01892	-1048.89811		
PO_x	0.22254	0.05896	-1124.31645	-0.02163	-1124.17450		
PE_x_Nav0_fcc	0.35200	0.08845	-2391.48819	-0.04592	-2391.27054	0.81	
PE_x_Nav0_fct	0.35180	0.08828	-2391.48935	-0.04600	-2391.27183	0.00	-28.89
PE_y_Nav0_fcc	0.35203	0.08882	-2391.48818	-0.0458	-2391.27084	0.62	
PE_y_Nav0_fct	0.35183	0.08818	-2391.48924	-0.04598	-2391.27157	0.16	
PE_x_Nav0TS_fc	0.35083	0.08649	-2391.47040	-0.04333	-2391.24938	14.08	
PE_y_Nav0TS_fc	0.35081	0.08635	-2391.47015	-0.04331	-2391.24900	14.33	
PE_x_Nav0Diyl_f	0.35237	0.08727	-2391.49278	-0.04291	-2391.27059	0.78	

PE_y_Nav0Diyl_f	0.35247	0.08591	-2391.49407	-0.04351	-2391.27102	0.51	
PE_x_Nav0TS_ft	0.35066	0.08633	-2391.46544	-0.04296	-2391.24408	17.42	
PE_y_Nav0TS_ft	0.35067	0.08581	-2391.46694	-0.04314	-2391.24521	16.70	
PE_x_Nav0_ftc	0.35216	0.08826	-2391.49473	-0.04539	-2391.27621	-2.75	
PE_x_Nav0_ftt	0.35205	0.08856	-2391.49287	-0.04513	-2391.27451	-1.68	
PE_y_Nav0_ftc	0.35222	0.08830	-2391.49497	-0.04534	-2391.27639	-2.86	-30.40
PE_y_Nav0_ftt	0.35204	0.08941	-2391.49263	-0.04512	-2391.27512	-2.07	
PO_x_Nav0_fcc	0.35715	0.09149	-2466.76087	-0.04815	-2466.54336	3.09	
PO_x_Nav0_fct	0.35686	0.09110	-2466.76141	-0.04837	-2466.54401	2.68	
PO_y_Nav0_fcc	0.35714	0.09055	-2466.76392	-0.05095	-2466.54829	0.00	-28.92
PO_y_Nav0_fct	0.35686	0.09109	-2466.75928	-0.04873	-2466.54225	3.79	
PO_x_Nav0TS_fc	0.35613	0.08849	-2466.74632	-0.04602	-2466.52470	14.80	

PO_y_Nav0TS_fc	0.35608	0.08778	-2466.74909	-0.04773	-2466.52852	12.41	
PO_x_Nav0Diyl_f	0.35766	0.08885	-2466.78064	-0.04581	-2466.55765	-5.87	
PO_y_Nav0Diyl_f	0.35777	0.08857	-2466.76867	-0.04615	-2466.54562	1.67	
PO_x_Nav0TS_ft	0.35592	0.08905	-2466.74417	-0.04669	-2466.52399	15.24	
PO_y_Nav0TS_ft	0.35599	0.08798	-2466.74551	-0.04568	-2466.52318	15.75	
PO_x_Nav0_ftc	0.35731	0.09046	-2466.76824	-0.04909	-2466.55048	-1.38	
PO_x_Nav0_ftt	0.35715	0.09113	-2466.76575	-0.04783	-2466.54756	0.45	
PO_y_Nav0_ftc	0.35727	0.09106	-2466.76950	-0.04890	-2466.55220	-2.45	-30.02
PO_y_Nav0_ftt	0.35721	0.09188	-2466.76374	-0.04726	-2466.54567	1.64	

Total and relative energies for isomerization of *E*-199/*Z*-199 (298 K, 1 bar)

Name	HCorr	TSCorr	Eelec	Edisp	G	rel	bind
Nav_cc	0.22440	0.05938	-1113.92441	-0.02070	-1113.78009	2.56	
Nav_cc2	0.22441	0.05936	-1113.92440	-0.02071	-1113.78006	2.58	
Nav_tc	0.22455	0.05937	-1113.92884	-0.02030	-1113.78395	0.14	
Nav_tt	0.22460	0.05915	-1113.92941	-0.02021	-1113.78417	0.00	
PE_x	0.21745	0.05653	-1049.04011	-0.01892	-1048.89811		
PO_x	0.22254	0.05896	-1124.31645	-0.02163	-1124.17450		
PE_x_Nav_fcc	0.44356	0.09700	-2163.01316	-0.05517	-2162.72177	0.62	
PE_x_Nav_fct	0.44291	0.09674	-2163.01207	-0.05685	-2162.72275	0.00	-27.96
PE_y_Nav_fcc	0.44361	0.09709	-2163.01293	-0.05502	-2162.72142	0.83	
PE_y_Nav_fct	0.44287	0.09681	-2163.01174	-0.05667	-2162.72235	0.25	
PE_x_NavTS_fc	0.44205	0.09486	-2162.98861	-0.05330	-2162.69472	17.59	
PE_y_NavTS_fc	0.44211	0.09508	-2162.98832	-0.05301	-2162.69430	17.85	
PE_x_NavDiyl_b	0.44328	0.09435	-2163.00934	-0.05424	-2162.71475	5.08	
PE_y_NavDiyl_f	0.44339	0.09454	-2163.01092	-0.05433	-2162.71640	3.99	
PE_x_NavTS_ft	0.44185	0.09533	-2162.98598	-0.05325	-2162.69271	18.85	
PE_y_NavTS_ft	0.44188	0.09429	-2162.98709	-0.05356	-2162.69306	18.63	
PE_x_Nav_ftt	0.44341	0.09687	-2163.01842	-0.05427	-2162.72615	-2.13	
PE_x_Nav_tc	0.44355	0.09646	-2163.02054	-0.05493	-2162.72838	-3.54	
PE_y_Nav_ftc	0.44360	0.09660	-2163.02103	-0.05500	-2162.72902	-3.94	-29.33
PE_y_Nav_ftt	0.44342	0.09714	-2163.01826	-0.05439	-2162.72638	-2.28	
PO_x_Nav_fcc	0.44853	0.09998	-2238.28573	-0.05757	-2237.99475	1.27	
PO_x_Nav_fct	0.44783	0.10020	-2238.28110	-0.05874	-2237.99221	2.86	

PO_y_Nav_fcc	0.44872	0.09919	-2238.28673	-0.05957	-2237.99677	0.00	-26.47
PO_y_Nav_fct	0.44799	0.09929	-2238.27866	-0.05925	-2237.98921	4.74	
PO_x_NavTS_fc	0.44749	0.09774	-2238.26509	-0.05599	-2237.97134	15.96	
PO_y_NavTS_fc	0.44744	0.09643	-2238.26667	-0.05698	-2237.97264	15.14	
PO_x_NavDiyl_f	0.44876	0.09640	-2238.28207	-0.05711	-2237.98683	6.24	
PO_y_NavDiyl_f	0.44874	0.09653	-2238.28231	-0.05619	-2237.98628	6.58	
PO_x_NavTS_ft	0.44739	0.09753	-2238.26607	-0.05734	-2237.97354	14.58	
PO_y_NavTS_ft	0.44727	0.09714	-2238.26801	-0.05657	-2237.97445	14.01	
PO_x_Nav_ftc	0.44863	0.10016	-2238.29200	-0.05785	-2238.00138	-2.89	
PO_x_Nav_ftt	0.44857	0.09999	-2238.28897	-0.05699	-2237.99738	-0.38	
PO_y_Nav_ftc	0.44868	0.09965	-2238.29435	-0.05848	-2238.00379	-4.41	-28.31
PO_y_Nav_ftt	0.44858	0.10004	-2238.28758	-0.05670	-2237.99574	0.64	

Total and relative energies for isomerization of maleate/fumarate (298 K, 1 bar)

Name	HCorr	TSCorr	Eelec	Edisp	G	rel	bind
FM_cct	0.14549	0.05048	-534.56757	-0.01061	-534.48317	4.71	
FM_cct2	0.14548	0.05051	-534.56754	-0.01061	-534.48318	4.71	
FM_tct	0.14554	0.05152	-534.56562	-0.01111	-534.48271	5.01	
FM_ctc	0.14577	0.04953	-534.57718	-0.00975	-534.49069	0.00	
FM_ctt	0.14581	0.05038	-534.57593	-0.00984	-534.49035	0.21	
FM_ttt	0.14589	0.05057	-534.57505	-0.00993	-534.48967	0.64	
PE_x	0.21745	0.05653	-1049.0401	-0.01892	-1048.89811		
PO_x	0.22254	0.05896	-1124.3165	-0.02163	-1124.17450		
PE_x_FM_fccc	0.36474	0.08890	-1583.66762	-0.03936	-1583.43114	0.53	
PE_x_FM_ftcc	0.36482	0.08725	-1583.66980	-0.03971	-1583.43194	0.02	
PE_x_FM_ftct	0.36485	0.08729	-1583.66831	-0.04017	-1583.43091	0.67	
PE_y_FM_fccc	0.36479	0.08856	-1583.66766	-0.03912	-1583.43056	0.89	
PE_y_FM_ftcc	0.36483	0.08829	-1583.66923	-0.03929	-1583.43198	0.00	-31.81
PE_y_FM_ftct	0.36483	0.08782	-1583.66791	-0.03983	-1583.43073	0.78	
PE_x_FM_TS_fcc	0.36267	0.08622	-1583.62574	-0.04037	-1583.38966	26.56	
PE_x_FM_TS_ftc	0.36298	0.08428	-1583.62987	-0.04088	-1583.39205	25.06	
PE_y_FM_TS_fcc	0.36271	0.08592	-1583.62570	-0.04046	-1583.38937	26.74	
PE_y_FM_TS_ftc	0.36285	0.08545	-1583.62838	-0.04031	-1583.39130	25.53	
PE_x_FMDiyl_fc	0.36357	0.08705	-1583.62965	-0.04060	-1583.39374	24.00	
PE_x_FMDiyl_ft	0.36386	0.08623	-1583.63455	-0.04039	-1583.39731	21.75	
PE_y_FMDiyl_fc	0.36362	0.08649	-1583.62990	-0.04067	-1583.39343	24.19	
PE_y_FMDiyl_ft	0.36422	0.08421	-1583.64033	-0.04103	-1583.40135	19.22	

Name	HCorr	TSCorr	Eelec	Edisp	G	rel	bind
PE_x_FM_TS_bct	0.36275	0.08663	-1583.63226	-0.03966	-1583.39580	22.70	
PE_x_FM_TS_btt	0.36295	0.08601	-1583.63168	-0.03954	-1583.39428	23.65	
PE_y_FM_TS_bct	0.36266	0.08606	-1583.63279	-0.03891	-1583.39510	23.14	
PE_y_FM_TS_btt	0.36285	0.08613	-1583.63116	-0.03940	-1583.39384	23.93	
PE_x_FM_fctc	0.36498	0.08892	-1583.68170	-0.03845	-1583.44409	-7.60	-34.70
PE_x_FM_fctt	0.36510	0.08772	-1583.68092	-0.03895	-1583.44249	-6.60	
PE_x_FM_fttt	0.36515	0.08827	-1583.68040	-0.03896	-1583.44247	-6.59	
PE_y_FM_fctc	0.36500	0.08845	-1583.68179	-0.03849	-1583.44373	-7.37	
PE_y_FM_fttc	0.36509	0.08750	-1583.68111	-0.03882	-1583.44234	-6.50	
PE_y_FM_fttt	0.36513	0.08874	-1583.68068	-0.03895	-1583.44323	-7.06	
PO_x_FM_fccc	0.36986	0.09084	-1658.93465	-0.04176	-1658.69738	4.12	
PO_x_FM_ftcc	0.36989	0.08930	-1658.93939	-0.04230	-1658.70110	1.78	
PO_x_FM_ftct	0.36992	0.08981	-1658.93727	-0.04280	-1658.69995	2.50	
PO_y_FM_fccc	0.36988	0.09044	-1658.93805	-0.04341	-1658.70202	1.21	
PO_y_FM_ftcc	0.36980	0.08886	-1658.94058	-0.04430	-1658.70394	0.00	-29.03
PO_y_FM_ftct	0.36977	0.08990	-1658.93730	-0.04448	-1658.70190	1.28	
PO_x_FM_TS_fcc	0.36810	0.08765	-1658.90379	-0.04385	-1658.66720	23.06	
PO_x_FM_TS_ftc	0.36840	0.08652	-1658.90715	-0.04388	-1658.66915	21.84	
PO_y_FM_TS_fcc	0.36814	0.08648	-1658.90491	-0.0458	-1658.66873	22.09	
PO_y_FM_TS_ftc	0.36827	0.08663	-1658.90714	-0.04522	-1658.67073	20.84	
PO_x_FMDiyl_fc	0.36907	0.08842	-1658.90530	-0.04563	-1658.67028	21.12	
PO_x_FMDiyl_ft	0.36920	0.08754	-1658.90858	-0.04538	-1658.67231	19.85	
PO_y_FMDiyl_fc	0.36897	0.08891	-1658.90523	-0.04416	-1658.66934	21.72	

Name	HCorr	TSCorr	Eelec	Edisp	G	rel	bind
PO_y_FMDiyl_ft	0.36926	0.08736	-1658.91015	-0.04414	-1658.67239	19.80	
PO_x_FM_TS_bct	0.36822	0.08935	-1658.90671	-0.04232	-1658.67016	21.20	
PO_x_FM_TS_btt	0.36843	0.08807	-1658.90712	-0.04213	-1658.66889	22.00	
PO_y_FM_TS_bct	0.36826	0.08854	-1658.90575	-0.04224	-1658.66827	22.39	
PO_x_FM_fctc	0.37007	0.09002	-1658.94969	-0.04253	-1658.71218	-5.17	-29.48
PO_x_FM_fctt	0.37010	0.09092	-1658.94729	-0.04198	-1658.71009	-3.86	
PO_x_FM_fttt	0.37026	0.09040	-1658.94795	-0.04217	-1658.71026	-3.96	
PO_y_FM_fctc	0.37015	0.09006	-1658.94916	-0.04254	-1658.71161	-4.81	
PO_y_FM_fctt	0.37021	0.09010	-1658.94806	-0.04270	-1658.71065	-4.21	
PO_y_FM_fttt	0.37020	0.09030	-1658.94713	-0.04244	-1658.70966	-3.59	